LEABHARLANN CHOLÁISTE NA TRÍONÓIDE, BAILE ÁTHA CLIATH | TRINITY COLLEGE LIBRARY DUBLIN
Ollscoil Átha Cliath | The University of Dublin

Terms and Conditions of Use of Digitised Theses from Trinity College Library Dublin

Copyright statement

All material supplied by Trinity College Library is protected by copyright (under the Copyright and Related Rights Act, 2000 as amended) and other relevant Intellectual Property Rights. By accessing and using a Digitised Thesis from Trinity College Library you acknowledge that all Intellectual Property Rights in any Works supplied are the sole and exclusive property of the copyright and/or other IPR holder. Specific copyright holders may not be explicitly identified. Use of materials from other sources within a thesis should not be construed as a claim over them.

A non-exclusive, non-transferable licence is hereby granted to those using or reproducing, in whole or in part, the material for valid purposes, providing the copyright owners are acknowledged using the normal conventions. Where specific permission to use material is required, this is identified and such permission must be sought from the copyright holder or agency cited.

Liability statement

By using a Digitised Thesis, I accept that Trinity College Dublin bears no legal responsibility for the accuracy, legality or comprehensiveness of materials contained within the thesis, and that Trinity College Dublin accepts no liability for indirect, consequential, or incidental, damages or losses arising from use of the thesis for whatever reason. Information located in a thesis may be subject to specific use constraints, details of which may not be explicitly described. It is the responsibility of potential and actual users to be aware of such constraints and to abide by them. By making use of material from a digitised thesis, you accept these copyright and disclaimer provisions. Where it is brought to the attention of Trinity College Library that there may be a breach of copyright or other restraint, it is the policy to withdraw or take down access to a thesis while the issue is being resolved.

Access Agreement

By using a Digitised Thesis from Trinity College Library you are bound by the following Terms & Conditions. Please read them carefully.

I have read and I understand the following statement: All material supplied via a Digitised Thesis from Trinity College Library is protected by copyright and other intellectual property rights, and duplication or sale of all or part of any of a thesis is not permitted, except that material may be duplicated by you for your research use or for educational purposes in electronic or print form providing the copyright owners are acknowledged using the normal conventions. You must obtain permission for any other use. Electronic or print copies may not be offered, whether for sale or otherwise to anyone. This copy has been supplied on the understanding that it is copyright material and that no quotation from the thesis may be published without proper acknowledgement.

Antimicrobial Peptide Preventing Beer Spoilage

Thesis submitted for the degree of Doctor of Philosophy

Trinity College Dublin

2012

By Joanne Denise Kavanagh

TRINITY COLLEGE
2 2 OCT 2012
LIBRARY DUBLIN

Thesis 9707

Declaration

I, Joanne Denise Kavanagh, certify that the experimentation recorded herein represents my own work, unless otherwise stated in the text and has not been previously presented for a higher degree at this or any other University. This thesis may be lent at the discretion of the Librarian.

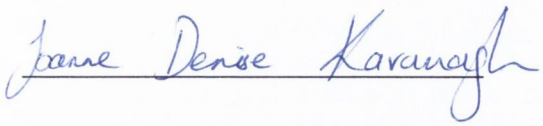

Joanne Denise Kavanagh.

Summary

Beer spoilage micro-organisms (BSMs) are a common threat to Master Brewers worldwide. Numerous studies have been carried out to date to overcome this problem, yet the most common preventative measure is the addition of chemical preservatives to the beverage. The aim of the research outlined in this thesis was to generate a series of *Saccharomyces* yeast strains with antimicrobial ability to minimize or eliminate beer spoilage micro-organisms without affecting the fermentation process. The human defensin, HβD-3, was chosen in this study due to its broad antimicrobial spectrum and nutraceutic potential. HβD-3 was cloned into *Saccharomyces cerevisiae* and *Saccharomyces pastorianus* on low and high copy number plasmids, under the control of a variety of gene promoters such as the inducible galactokinase (*GAL1*) promoter, the inducible α-glucosidase (*AGT1*) promoter, the constitutive translational elongation factor EF-1 alpha (*TEF1*) promoter and the constitutive phosphoglycerate kinase (*PGK1*) promoter. HβD-3 was also integrated directly into the genome of *S. pastorianus*. The variation of inducible and constitutive promoters allowed for the analysis of HβD-3 expression under various environmental conditions, leading to the discovery of the optimum promoter for HβD-3 production. *S. pastorianus* clones were selected by antibiotic resistance to the kanMX marker present on the low copy number pGREG vector or within the integrated strains, or the hphNT1 marker present on the pRS42H high copy vector.

HβD-3 expression was observed in all strains, suggesting that all promoters are functional. Recombinant HβD-3 was detected at low levels in the growth culture spent media for all strains except CM-506hbd3PGK1, suggesting that mature HβD-3 peptide was synthesized and secreted in the majority of strains generated during this study. RP-HPLC analysis of selected *S. pastorianus* HβD-3-encoding yeast strains and subsequent ELISA analysis revealed higher estimated levels of secretory recombinant HβD-3 produced by these strains. Furthermore RP-HPLC and Western immunoblot experiments indicated that recombinant HβD-3 is hyperglycosylated in certain *S. pastorinus* HβD-3-encoding strains.

In vitro and *in vivo* bioassays were carried out to analyse the antimicrobial activity levels of recombinant HβD-3. *In vitro* bioassays indicate that recombinant HβD-3 present in concentrated spent media from growth cultures of CM-505hbd3GAL1 is

active against the BSM *Lactobacillus brevis* at levels similar to synthetic HβD-3 at 0.5μg/mL. Further *in vivo* bioassays revealed that recombinant HβD-3 secreted from the above strains retains antimicrobial activity in a fermentation and is active against Gram-positive BSMs such as *Lb. brevis* and Gram-negative BSMs such as *Pectinatus frisingensis*. During this study, a treatment method was developed to increase the antimicrobial activity of recombinant HβD-3 during fermentation. A "freeze-treatment" at -70°C was carried out on fermentation samples, as the bacterial membrane may become more susceptible to HβD-3 under these conditions. The results indicate that a further decrease in BSM viability is observed in "freeze-treated" fermentation samples compared to samples that are "untreated". *In vivo* bioassays were carried out on all strains generated during this study. CM-505hbd3TEF1 and CM-INT-51 displayed the highest levels of antimicrobial activity, decreasing the viability of *Lb. brevis* by as much as 85-91% respectively before freeze-treatment. Viability was reduced further following freeze-treatment of the samples.

The research presented in this thesis reports that *S. pastorianus* strains expressing HβD-3 have the ability to minimize beer spoilage during lager fermentations. This decrease in BSM viability is observed in HβD-3 producing lager fermentations compared to CMBS-33 wild-type fermentations. This is the first report of the generation of *S. pastorianus* yeast strains expressing and secreting active HβD-3. This principle can potentially be applied to other forms of alcoholic fermentations.

Acknowledgements

I would like to thank my supervisor, Dr. Ursula Bond, for the opportunity to carry out this research and for all of her help, support and advice over the past four years. I would also like to extend a sincere thanks to my second supervisor, "Big" Jimmy, for always answering my questions and providing constant advice and support. A special thank you to my fellow lab members, past and present – Suzanne, my cleaning/organisation partner who always listened to my rants, "Little" Jimmy who always made me laugh and offered encouraging advice, Christina my very first bay-buddy and Will for providing me with much needed coffee during the last year of my PhD. It would have been impossible to get through this without all of you. Thank you for all the laughs, advice and encouragement and for helping me get through bad science days (weeks!).

Thank you to past and present members of the Dorman lab including Dan, Andrew, Shane, Colin and Heather for all their encouragement, laughs and advice, I could always rely on you guys when I needed to "borrow" lab essentials! A big thank you to my friends Fitzy and Kelly, for the endless chats and support on this journey. I look forward to the celebrations that will no doubt follow the completion of this project!

Thank you to everyone in the Moyne Institute including the technical staff Gerry, Dave, Margaret, and Myriam. Thanks to Ronan and Stephen from the prep room for putting up with my endless media orders. I would like to thank our executive officers; Jayne and Noreen. Thank you to Dr. Vincent Kelly and Dr. Coilin Boland in the Biochemistry department for all their help with RP-HPLC experiments. I wish to thank my funding board, The Department of Agriculture. Thank you for making this research possible.

Thank you to all my non-science friends, Louise, Brid, Eilish, Sarah, Monica and Nicola, including my amazing sister, Jennifer. Thanks for the years of friendship and all the laughs we've had. You are all friends for life and I hope I can help you all in the future as much as you'se have helped me in the past. Now that I have emerged from the lab and am officially not a broke student anymore, I can't wait to see a lot more of you! Here's to all the future weddings, christenings and parties as we all finally grow up!

A huge thank you to all of my family for constantly believing in me and supporting me even when you didn't understand exactly what it was I was doing! There's one person that deserves the biggest thank you and that's my Mammy, this is dedicated to you. X

Finally, to my partner in crime and my soul-mate. Mick, I couldn't have done this without you, thank you for absolutely everything, your love and support means the world to me. I love you, and I think you deserve a honorary doctorate yourself after these last five years! Here's to our future together. x

Conference Communications and Patent Status

Conferences attended:

Joanne Kavanagh, T. C. James and Ursula Bond. Antimicrobial Peptide Preventing Beer Spoilage. Poster presentation at the Irish Fungal Meeting, Trinity College Dublin, June 2011.

Joanne Kavanagh, T. C. James and Ursula Bond. Antimicrobial Peptide Preventing Beer Spoilage. Poster presentation at the Irish Fungal Meeting, University College Cork, June 2010.

Joanne Kavanagh, T. C. James and Ursula Bond. Antimicrobial Peptide Preventing Beer Spoilage. Poster presentation at the Irish Fungal Meeting, University College Dublin, June 2009.

Joanne Kavanagh, Jane Usher, T. C. James and Ursula Bond. Antimicrobial Peptide Preventing Beer Spoilage. Poster presentation at S.G.M. Autumn Meeting, Trinity College Dublin, September 2008.

Joanne Kavanagh, Jane Usher, T. C. James and Ursula Bond. Antimicrobial Peptide Preventing Beer Spoilage. Poster presentation at the Irish Fungal Meeting, N.U.I. Galway, June 2008.

Joanne Kavanagh, Jane Usher, T. C. James and Ursula Bond. Antimicrobial Peptide Preventing Beer Spoilage. Poster presentation at the British Yeast Group Meeting, N.U.I. Maynooth, March 2008.

Patent Status:

A priority patent application entitled "Preventing Spoilage in Alcohol Fermentations" was filed with the US patent office [US61/491, 584], July 2011.

Index of Figures

Figure	Title	Page
Chapter 1		
1.1a	Fungal species tree	5
1.1b	A model for the formation of *Saccharomyces pastorinaus*	7
1.2	The mosaic chromosomes of *Saccharomyces pastorianus,* due to recombination of two parental homoeologous chromosomes	10
1.3	Schematic illustration of three models depicting the mode of action of cationic antimicrobial peptides	22
1.4	Schematic representation of amino acid sequences and disulphide linkages in human α- and β-defensins	30
1.5	Schematic illustration of HNP-3	32
1.6	Schematic representation of the structural aspects of native HβD-3 peptide	35
1.7	Schematic representation of HβD-3 gene construct	43
1.8	Schematic representation of regions of interest in pGREG vectors	45
1.9	Schematic representation of HβD-3 gene construct inserted into CMBS-33	47
Chapter 2		
2.1	Graphic of pBlueScript SK- plasmid	62
2.2	Schematic representation of pGREG vectors used in this study	63
2.3	Schematic map of pRS42H plasmid	65

Chapter 3

3.1 Schematic diagram of the *AGT1-MAL12* divergent promoter used in this study 76

3.2 Schematic of HβD-3 primers and gel electrophoresis of HβD-3 and 5.8S RT-PCR products from CMBS-33, CM-INT-37 and CM-INT-51. 78

3.3 Schematic illustration and PCR amplification of regions of interest in pGREG vectors 80

3.4 DNA sequence alignment of newly synthesized pGREG505hbd3GAL1 versus pGREG505GAL1 83

3.5 Schematic diagram of regions of interest surrounding the *GAL1* promoter in pGREG vectors 84

3.6 DNA sequence of the *TEF1* promoter 86

3.7 Schematic representation of pGREG505TEF1 and insertion of the HβD-3 fragment into the linearised plasmid 87

3.8 Gel electrophoresis of digested pGREG505TEF1, HβD-3 fragment and the *TEF1* promoter in CM-505hbd3TEF1 89

3.9 Schematic illustration of non-specific 5'UTR of CM-505hbd3TEF1 and DNA sequence alignment of the non-specific 5'UTR region of CM-505hbd3TEF1 versus CM-505hbd3GAL1 91

3.10 Schematic diagram of the *AGT1* promoter used in this study 95

3.11 Schematic representation the *AGT1* promoter and replacement of the *GAL1* promoter in CM-506hbd3GAL1 97

3.12 Gel electrophoresis of the *AGT1* promoter and restriction digest of

pGREG506hbd3GAL1 99

3.13 Schematic illustration of CM-506hbd3AGT1 plus primers and colony PCR confirmation of the *AGT1* promoter in CM-506hbd3AGT1 100

3.14 Nucleotide sequence alignment of the *AGT1* promoter of CM-506hbd3AGT1 versus *S. cerevisiae* 101

3.15 Schematic representation of the *S. cerevisiae PGK1* promoter 103

3.16 Schematic representation of the *PGK1* promoter inserted into pGREG-506hbd3GAL1 and gel electrophoresis of the *PGK1* promoter 104

3.17 Schematic representation of CM-506hbd3PGK1 and colony PCR of *PGK1* promoter in this strain 106

3.18 Schematic illustration of the GAL1, HβD-3, 6xHis-tag fragment generation and gel electrophoresis of the HβD-3-6xHis-tag fragment.108

3.19 Schematic illustrating the generation of CM-pRShbd3PGK1 and gel electrophoresis of the HβD-3 gene construct and the pRS42H linearised plasmid.....111

3.20 Schematic illustration of CM-pRShbd3PGK1 displaying primers and colony PCR of this strain 113

3.21 Nucleotide sequence alignment of the $PGK1_{SB}$ promoter region in CM-pRShbd3PGK versus pBSK-HβD-3 114

3.22 Nucleotide sequence alignment of the $PGK1_{SB}$ promoter versus $PGK1_{SC}$ promoter 116

3.23 Schematic diagram showing the length of the non-specific 5'UTR regions of all yeast strains containing pGREG vectors 122

Chapter 4

4.1 Semi-quantitative RT-PCR analysis of HβD-3 expression 128

4.2 Expression of YPR159W and YPR160W in CM-INT-51 and CM-INT-37 132

4.3 Synthetic HβD-3 standard curve displaying absorbance values for CM-505hbd3GAL1 and CM-506hbd3GAL1 136

4.4 Reversed phase high-performance liquid chromatography (RP-HPLC) analysis of synthetic HβD-3 140

4.5 Reversed phase high-performance liquid chromatography (RP-HPLC) analysis of supernatant samples from CMBS-33 strains expressing HβD-3 142

4.6 ELISA analysis of RP-HPLC fractions 145

4.7 ELISA analysis of CM-505hbd3GAL1 and CM-506hbd3GAL1 RP-HPLC samples 149

4.8 Reversed phase high-performance liquid chromatography (RP-HPLC) analysis of CM-INT-51 supernatant 153

4.9 ELISA analysis of CM-INT-51 RP-HPLC samples 155

4.10 Reversed phase high-performance liquid chromatography (RP-HPLC) analysis of synthetic HβD-3 in the presence and absence of DTT 158

4.11 Reversed phase high-performance liquid chromatography (RP-HPLC) analysis of CM-INT-51 (-G418) plus Endo H 159

4.12 Reversed phase high-performance liquid chromatography (RP-HPLC) analysis of CM-INT-51 (+G418) plus Endo H 160

4.13 Coomassie stain and Western blot analysis of recombinant and synthetic

HβD-3 164

4.14 Western blot analysis of synthetic HβD-3 and Endo H treated recombinant HβD-3 167

4.15 Western immunoblot analysis of fused HβD-3-6x-His-tag peptide fractions after nickel column purification 169

Chapter 5

5.1 CMBS-33 fermentations with or without *Lb. brevis* 183

5.2 Viability of *Lb. brevis* in CMBS-33 fermentations at 20°C 185

5.3 Treatment of *Lb. brevis* with synthetic and recombinant HβD-3 187

5.4 *Lb. brevis* viability in various fermentative conditions 193

5.5 Antimicrobial activity of recombinant HβD-3 against *Lb.* brevis in YEPGal fermentations 194

5.6 Antimicrobial activity of recombinant HβD-3 against *Lb.* brevis in wort fermentations 196

5.7 *P. frisingensis* viability in various fermentative conditions 199

5.8 Antimicrobial activity of recombinant HβD-3 against *P. frisingensis* in YEPGal fermentations 201

5.9 Antimicrobial activity of recombinant HβD-3 against *P. frisingensis* in wort fermentations 203

5.10 Brix values and percentage alcohol for fermentations at 11°C 207

5.11 Antimicrobial activity of recombinant HβD-3 in fermentations at 11°C. 210

5.12 Brix values and percentage alcohol for fermentations at 20°C 214

5.13 Antimicrobial activity of recombinant HβD-3 in fermentations at 20° 216

Index of Tables

Table **Title** **Page**

Chapter 1

1.1 List of beer spoilage bacteria 16

Chapter 2

2.1 Oligonucleotide primers used to amplify plasmids, integration and genomic DNA 53

2.2 Oligonucleotide primers used for promoter swap, gene swap and HIS-TAG in plasmids 54

2.3 *S. pastorianus* strains generated in study 60

2.4 *S. cerevisiae* strains generated in study 61

Chapter 3

3.1 Summary of mutations/changes in plasmid clones 93

Chapter 4

4.1 Summary of RP-HPLC elution times for 3 independent experiments..143

Contents

Declaration ii

Summary iii

Acknowledgements v

Conference communications and Patent status vii

Index of Figures viii

Index of Tables xiii

Chapter 1 - Introduction

1.1 Introduction to beer fermentation 2

1.2 The genomes of brewing yeast 3

1.2.1 Ale yeasts 3

1.2.2 Lager yeasts 6

1.3 Beer spoilage micro-organisms 11

1.3.1 Introduction to microbial contamination in brews 11

1.3.2 Gram-positive bacteria 15

1.3.3 Gram-negative bacteria 17

1.3.4 Wild yeasts 18

1.4 Prevention of beer spoilage 18

1.4.1 Hops 18

1.4.2 Chemical preservatives 19

1.4.3 Chitosan 19

1.5 Antimicrobial peptides 20

1.5.1 General introduction to antimicrobial peptides (AMP) 20

1.5.2 Microbial antimicrobial peptides 23

1.5.2.1 Introduction to microbial antimicrobial peptides 23

1.5.2.2 Nisin 23

1.5.2.3 Pediocin, Plantaricin and Enterocin 24

1.5.2.4 Colicin and Microcin 25

1.5.3 Mammalian antimicrobial peptides 25

1.5.3.1 Introduction to mammalian AMPs 25

1.5.3.2 Cathelicidins 26

1.5.3.3 Histatins 27

1.5.3.4 Defensins 27

1.5.4 Human defensins 29

1.5.4.1 α-defensins 29

1.5.4.2 β-defensins 34

1.6 Research undertaken prior to Ph.D. 42

1.7 Objectives of this project 49

Chapter 2 - Materials and Methods

2.1 Reagents, strains, media and growth conditions 51

2.1.1 Strains 51

2.1.2 Yeast strains and growth conditions 51

2.1.3 Bacterial strains and growth conditions 52

2.1.4 Monitoring the growth of yeast and bacterial cultures 52

2.2 Polymerase chain reaction (PCR) and gel electrophoresis 52

2.3 Gel extraction and purification 55

2.4 Direct colony PCR 55

2.5 DNA purification 56

2.6 RNA purification 56

2.7 Determination of nucleic acid concentrations 57

2.8 DNase I treatment of RNA 57

2.9 cDNA synthesis and reverse transcriptase PCR (RT-PCR) 57

2.10 Transformations 58

2.10.1 Preparation of electrocompetant *E. coli* XL1-Blue cells 58

2.10.2 Bacterial transformations 58

2.10.3 Yeast lithium acetate tranformations 58

2.11 Isolation of plasmid DNA from bacteria 59

2.12 DNA sequencing 59

2.13 HβD-3 fragment construction 59

2.14 Yeast plasmids 59

2.14.1 pGREG vectors 59

2.14.2 Multi-copy plasmid 64

2.15 Promoter and gene swaps 64

2.15.1 Promoter swaps 64

2.15.2 Gene swaps 64

2.16 His-Tag addition and purification 66

2.16.1 Addition of 6xHis-tag 66

2.16.2 Nickel affinity column purification of fused HβD-3-6xHis-tag peptide from

concentrated supernatant 66

2.17 Yeast fermentations 67

2.18 Seeding of fermentations with beer spoilage micro-organisms 67

2.19 Concentrating supernatant and cell pellet protein extraction 68

2.19.1 Concentration of supernatant via freeze-drying 68

2.19.2 Concentration of supernatant via molecular weight cut off filters 68

2.19.3 Concentration of supernatant via Sep-Pak cartridges 68

2.19.4 Cell pellet protein extraction 68

2.19.5 Bradford assay 69

2.20 Endoglycosidase H treatment 69

2.21 ELISA 69

2.22 SDS-Polyacrylamide Gel Electrophoresis (PAGE) and Western Blotting Analysis 70

2.22.1 SDS-PAGE gel 70

2.22.2 Coomassie stain 70

2.22.3 Western immunoblotting 70

2.23 Reversed-phase high-peformance liquid chromatography (RP-HPLC) 71

2.24 HβD-3 activity assays 71

2.24.1 HβD-3 biossay 71

2.24.2 Defensin activity *in vivo* and freeze-treatment analysis 72

Chapter 3 - Generation of *Saccharomyces pastorianus* Strains to Express Antimicrobial Peptide

3.1 Introduction 74

3.2 Results 77

3.2.1 Plasmids and yeast strains containing HβD-3 77

3.2.1.1 Confirmation of HβD-3 integration via direct colony PCR 77

3.2.1.2 Characterisation of pGREG505hbd3GAL1 and pGREG506hbd3GAL1 plasmids 77

3.2.1.3 Generation of CM-505hbd3TEF1 82

3.2.2 Promoter swaps leading to variants of the pGREG vector series 94

3.2.2.1 Replacement of the inducible *GAL1* promoter, for an inducible *AGT1* promoter 94

3.2.2.2 Replacement of the inducible *GAL1* promoter, for a constitutive *PGK1* promoter 102

3.2.3 Addition of a polyhistidine-tag 107

3.2.4 Formation of a multi-copy plasmid containing HβD-3 110

3.3 Discussion 117

Chapter 4 - Antimicrobial Peptide Expression and Secretion Analysis

4.1 Introduction 125

4.2 Results 127

4.2.1 Analysis and semi-quantification of HβD-3 expression in CMBS-33 via RT-PCR 127

4.2.2 Analysis of YPR159W and YPR160W genes 131

4.2.3 Detection of secreted recombinant HβD-3 134

4.2.3.1 ELISA analysis of recombinant HβD-3 secreted from pGREG vectors 505 and 506 under the control of the *GAL1* promoter 134

4.2.3.2 ELISA analysis of recombinant HβD-3 secreted from various lager strains ... 138

4.2.4 Reversed phase high-performance liquid chromatography (RP-HPLC) of concentrated supernatant samples ... 139

4.2.4.1 RP-HPLC analysis of CM-505hbd3GAL1 and CM-506hbd3GAL1 ... 139

4.2.4.2 ELISA analysis of CM-505hbd3GAL1 and CM-506hbd3GAL1 RP-HPLC samples ... 144

4.2.4.3 RP-HPLC analysis of the integrated strain, CM-INT-51 ... 152

4.2.4.4 ELISA analysis of CM-INT-51 (+G418) RP-HPLC samples ... 152

4.2.4.5 Reduction of the disulphide bonds of HβD-3 and RP-HPLC analysis ... 157

4.2.4.6 Cleavage of potential N-glycans from recombinant HβD-3 using Endo H ... 157

4.2.5 Detection of recombinant HβD-3 via Western blot analysis ... 163

4.2.5.1 Western blot of CM-INT-51 ... 163

4.2.5.2 Western blot of CM-505hbd3HISGAL1 ... 168

4.3 Discussion ... 172

Chapter 5 – Analysis of HβD-3 Antimicrobial Activity

5.1 Introduction ... 180

5.2 Results ... 182

5.2.1 Analysis of BSM survival in fermentations ... 182

5.2.2 Analysis of the antimicrobial activity of recombinant HβD-3 in concentrated supernatant samples ... 186

5.2.3 Detection of antimicrobial activity of recombinant HβD-3 *in vivo* ... 191

5.2.3.1 Analysis of recombinant HβD-3 bactericidal activity against Gram positive

bacteria, under various growth conditions 191

5.2.3.2 Analysis of recombinant HβD-3 bactericidal activity against Gram negative bacteria, under various growth conditions 198

5.2.4 Comparison of the antimicrobial activity of recombinant HβD-3, *in vivo*, expressed from various promoters and under varying fermentation temperatures 206

5.2.4.1 *In vivo*, antimicrobial activity of recombinant HβD-3 expressed from different promoters at a fermentation temperature of 11°C 206

5.2.4.2 *In vivo*, antimicrobial activity of recombinant HβD-3 expressed from different promoters at a fermentation temperature of 20°C 213

5.3 Discussion 220

Chapter 6 – General Discussion

6.1 General Discussion 226

Bibliography 236

Chapter 1: Introduction

This introduction aims to give an overview of the complex *Saccharomyces pastorianus* genome, the process of beer fermentation and problems with brew contamination, and an insight into human defensins, and their broad spectrum of antimicrobial activity.

1.1 Introduction to beer fermentation

Beer is one of the most commonly consumed alcoholic beverages in the world, with approximately 1.8 x 10^{11} L being produced annually worldwide (Barth, 2011), 90% of which is lager (Nakao et al., 2009). The ingredients of pure beer include, malt, hops (*Humulus lupulus L.)* water and brewery yeast. Malt extract, made from malted barley or wheat, provides the essential sugars that are converted into alcohol by the action of added yeasts. In brewers wort, 50-60% of total sugars are maltose, 10-15% are maltotriose and 10-15% are glucose (Zastrow, 2001). Hops improve aroma and add flavour to the beer, while being a natural preservative, helping to prevent beer spoilage. Breweries yeasts are classified as top or bottom fermenters, producing ale and lager respectively. Ale is predominantly fermented using the *Saccharomyces cerevisiae* strain (Dunn and Sherlock, 2008), fermentations are usually carried out at ~20°C, and during fermentation a layer or "crust" develops on top of the beverage due to a portion of yeast cells flocculating to the top of the medium. Lager is fermented predominantly from *Saccharomyces pastorianus* and fermentations are carried out at a lower temperature range of 7°C - 14°C (Dunn and Sherlock, 2008). Unlike ale, flocculation during lager fermentation does not result in the developement of a "crust", as yeast cells flocculate at the bottom of the brewing vessel. Flocculation is regulated by a family of genes, namely the *FLO* genes, which encode cell wall glycoproteins (Halme et al., 2004). Flocculation during fermentation is influenced by other factors such as surface hydrophobicity (Rouxhet, 1997), aerobic and anaerobic conditions (Lawrence, 2009; Lawrence, 2007), medium composition (Claro et al., 2007; Sampermans et al., 2005; Smukalla et al., 2008; Verstrepen et al., 2003) and cell age (Powell et al., 2003; Powell, 2007). The auto-aggregation property of flocculant yeast has been advantageously exploited in many areas of industry including, brewing, wine production and the production of biofuel (Van Holle et al., 2011). Efficiently this yeast sediment, collected at the end of a fermentation, can be repitched into subsequent brews, a technique that is used in breweries worldwide, then reinoculating or repitching is usually carried out up to 8-15 times (Boulton, 1991; Smart, 1996).

The genome of *S. pastorianus* is somewhat unstable and chromosome length polymorphisms are commonly seen in chromosomes containing genes linked to fermentation, including *FLO1* and *MAL4* genes (Casey, 1996). Studies carried out by James et al. (2008) demonstrated that genomes of lager yeasts are quite dynamic under fermentation conditions and undergo genome rearrangements in response to stressful environment conditions (James et al., 2008). In this study lager yeasts were repetitively exposed to severe high temperatures, followed by selection under high specific gravity conditions. A number of stress-tolerant lager yeast isolates were characterised and genome analysis revealed that a number of gross chromosomal rearrangements had occured in the new isolates (James et al., 2008). The majority of these rearrangements occured at "hot spots" of recombination previously identified by Bond et al. (2004) (Bond et al., 2004). Along with genome rearrangements, clusters of gene amplification, particularly near the telomeres, was evident. DNA amplification was also observed on chromosome XII, for genes that flank the rRNA locus (James et al., 2008). Thus, gene mutations in a fermentative environment may be a possibility, particularly under stress-inducing conditions. If these mutations go undetected this may lead to a mixed population, resulting in genetic drift within the culture. To avoid such problems repropagation normally takes place after 8-15 fermentations, however the number of times a strain can be repropagated depends on the individual strain, the quality of the cropped slurry and microbial contamination of the brew. If fermentation conditions are kept constant and are relatively stress free, i.e. ideal temperatures of 7 - 14°C, then it is possible that the lager genome will not undergo chromosomal rearrangements. Studies carried out by Powell and Diacetis (2007) indicated that, if beer spoilage could be avoided, individual lager strains have the ability to be serially repitched for many generations. Over the course of 135 generations, the lager strain used in this study, did not exhibit any detectable genetic changes or alterations in fermentation characteristics (Powell, 2007). Thus, if beer spoilage was eliminated from fermentations and yeast cells were repropagated up to 135 times without any effect on the fermentation, this would financially benefit the brewery industry.

1.2 The genomes of brewing yeast

1.2.1 Ale yeasts

As mentioned above the main yeasts used in the production of ale is *S. cerevisiae*. *S. cerevisiae* originates from oak trees in the Northern Hemisphere (Sniegowski et al., 2002; Sampaio and Goncalves, 2008). The genome of *S. cerevisiae* underwent a whole-

genome duplication (WGD) approximately 100 million years ago, after the divergence of *Saccharomyces* from *Kluyveromyces* (Wolfe et al., 1997) (Fig. 1.1a). This duplication was followed by substantial gene deletion and rearrangement, resulting in a *S. cerevisiae* genome that consists of ~5500 genes, of which ~500 are ohnologs, duplicate genes formed from polyploidization (Wolfe et al., 1997; Wolfe et al., 2000; Wolfe, 2004). This WGD may have contributed to the evolution of *Saccharomyces* yeasts and its ability to ferment sugar to alcohol (Wolfe et al., 1997). *S. cerevisiae* is a member of the *Saccharomyces sensu stricto* complex (Vaughan-Martini and Martini, 1995), which includes other post-duplication species such as *Saccharomyces bayanus, Saccharomyces pastorianus, Saccharomyces paradoxus, Saccharomyces cariocanus* (Naumov et al., 2000), *Saccharomyces mikatae* (Naumov et al., 2000), *Saccharomyces kudriavzevii* (Sampaio and Goncalves, 2008) and *Saccharomyces arboricolus* (Wang and Bai, 2008) (Fig. 1.1a).

S. cerevisiae is the most genetically and biochemically characterised *Saccharomyces* strain. Previously ale strains have been erroneously identified as true *S. cerevisiae,* when in fact they appeared to be hybrids of *S. cerevisiae* and other *Saccharomyces* yeasts. Hybridisation is a common occurence between *Saccharomyces* strains as many strains coexist in the same natural and fermentative environments (Sampaio and Goncalves, 2008; Belloch et al., 2009). Along with ale production, *S. cerevisiae* is commonly used in the production of wine and cider. Wine and cider hybrids consist of hybridisations between *S. cerevisiae* x *S. bayanus var. uvarum* and *S. cerevisiae/S. bayanus var. uvarum/ S. kudriavzevii* x *S. cerevisiae/S. kudriavzevii* (de Barros Lopes et al., 2002; Le Jeune et al., 2007; Masneuf et al., 1998). Gonzalez et al. (2008) recently discovered six new types of *S. cerevisiae* x *S. kudriavzevii* hybrids among brewing strains. Furthermore, three different genome types were identified among wine yeast hybrids, these novel genomes contain putative chimeric chromosomes which may have been generated due to recombination between homeologous chromosomes of different parental origins (Gonzalez et al., 2008). Further studies by Belloch et al. (2009) found that the genomes of several *S. cerevisiae* x *S. kudriavzevii* hybrids were very similar, suggesting that they share the same ancestor and originated from a limited number of hybridization events. Following hybridization, extensive chromosomal rearrangements occurred including the generation of chimeric chromosomes and chromosome losses (Belloch et al., 2009). The resultant *S. cerevisiae* x *S. kudriavzevii* hybrids, like other *S.*

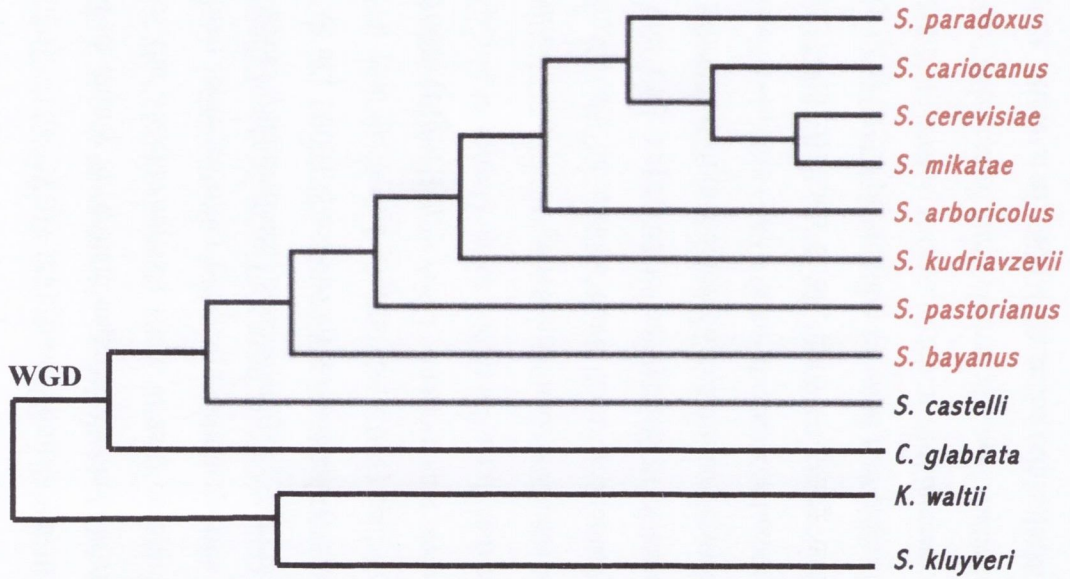

FIG. 1.1a Fungal species tree. Members of the *Saccharomyces* sensu stricto group are highlighted in red. The likely position of the whole genome duplication (WGD) is shown.

Figure adapted from Cornell et al. 2007 and Wang and Bai, 2008.

cerevisiae hybrids, are better adapted to harsh environmental conditions compared to parental species (Belloch et al., 2009).

1.2.2 Lager yeasts

S. pastorianus (syn. *Saccharomyces carlsbergensis*) is the most common yeast used in the production of lager. Unlike the true species *S. cerevisiae*, *S. pastorianus* is a domesticated hybrid species that has never been isolated from the wild (Libkind et al., 2011). It was originally proposed that *S. pastorianus* was a partial amphidiploid, generated by the hybridization of *S. cerevisiae* and *S. bayanus* (Peterson and Kurtzman, 1991). Studies have indicated that all *S. pastorianus* strains are polyploid strains containing complex multi-hybrid genomes, which arose from the natural fusion of two *Saccharomyces* yeast species, one species closely related to *S. cerevisiae* and the other species a non-*S. cerevisiae* species (James et al., 2008; Dunn and Sherlock, 2008). Until recently, the non-*S. cerevisiae* portion of *S. pastorinaus* was defined as a *S. bayanus*-like species (James et al., 2008; Dunn and Sherlock, 2008). However, recent studies by Libkind et al. (2011) proposed that the non-*S. cerevisiae* portion of *S. pastorianus* is the newly identified species, *Saccharomyces eubayanus* sp. nov., (Fig. 1.1b). Nomenclature reflects the resemblance of *S. eubayanus* sp. nov. to *S. bayanus*, which is a complex hybrid species of *S. uvarum, S. eubayanus* and *S. cerevisiae* (Libkind et al., 2011). *S. eubayanus* sp. nov. is a true species that has been isolated from tree bark in Patagonia. It is similar to its sister species, *S. uvarum*, with only ~7% genome-wide sequence divergence between each species. *S. eubayanus* and *S. uvarum* are considered sympatric and exist in natural conditions in forests in Patagonia (Libkind et al., 2011). However, unlike *S. uvarum*, European isolates of *S. eubayanus* have never been discovered since the isolation of pure yeast cultures in the 19th century, suggesting that *S. eubayanus* was imported into Europe during trans-Atlantic trade (Hansen, 1883; Libkind et al., 2011).

Lager beer arose in Bavaria in the 15th century and became extremely popular in the 19th century, following the advent of refrigeration (Corran, 1975; Dunn and Sherlock, 2008). Interspecific hybridisation among the sensu stricto *Saccharomyces* species is a common occurance in industrial and natural settings (Masneuf et al., 1998; Groth et al., 1999; de Barros Lopes et al., 2002; Liti et al., 2005; Gonzalez et al., 2007, 2008; Lopandic et al., 2007). It is proposed that the allotetraploid hybrid, *S. pastorianus,* was created during the 15th century in a lager-brewery environment by "instantaneous

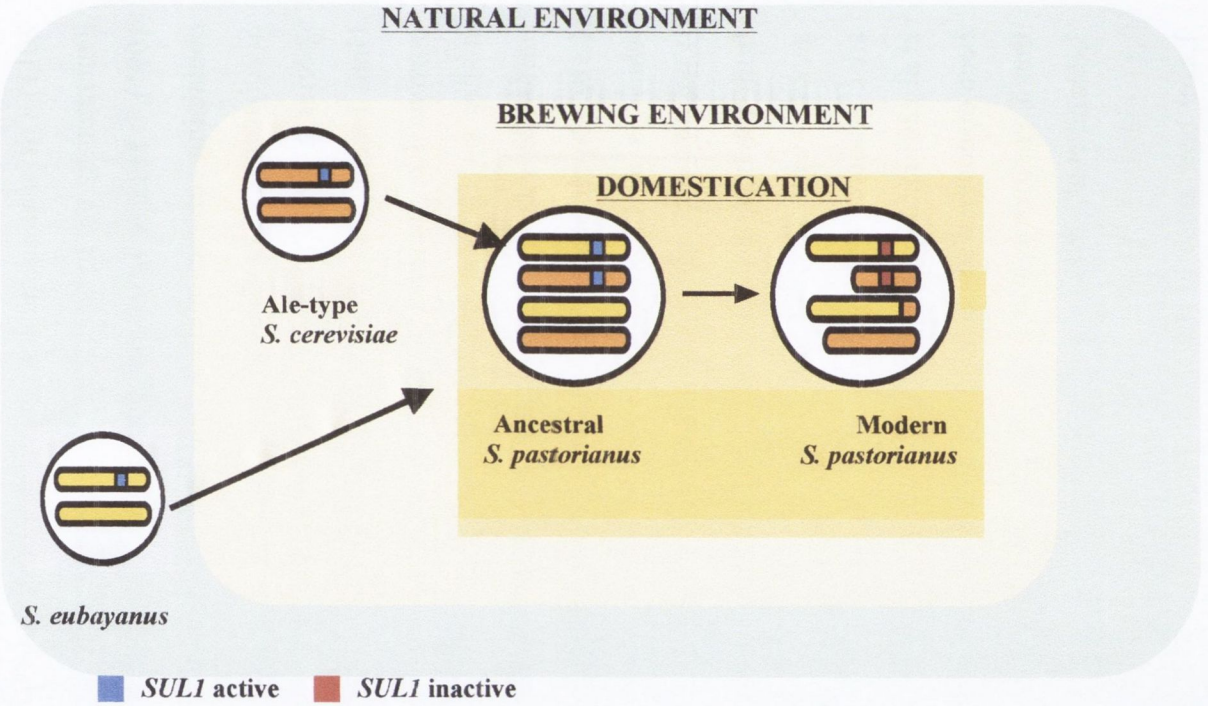

FIG. 1.1b A model for the formation of *Saccharomyces pastorianus*. A model depicting the hybridization of *S. eubayanus* and *S. cerevisiae* genomes to form the hybrid strain, *S. pastorianus*. Ancestral *S. pastorianus* represents a hybrid genome with equal portions of *S. cerevisiae* and *S. eubayanus*, along with active *SUL1* genes. Domestication led to modern *S. pastorianus* which possesses an aneuploid genome with unequal portions of *S. cerevisiae* and *S. eubayanus*, along with inactive *SUL1* genes.

Figure adapted from Libkind et al. 2011.

speciation" due to an interspecific hybridization event between a *S. cerevisiae* ale-yeast and *S. eubayanus* (Martini and Kurztman, 1985; Martini and Martini, 1987; Hornsey, 2003, Libkind et al., 2011) (Fig. 1.1b). It is postulated that at least two interspecific hybridization events occurred (Corran, 1975; Dunn and Sherlock, 2008). Further DNA repair mechanisms, mitotic crossovers and chromosome loss and/or duplication events took place, following the fusion of *S. cerevisiae*-like chromosomes to *S. eubayanus* chromosomes (Dunn and Sherlock, 2008; James et al., 2008; Nakao et al., 2009). The resultant *S. pastorianus* lager yeasts are aneuploid and possess unequal numbers of both *S. cerevisiae*-like and *S. eubayanus* chromosomes.

During domestication of *S. pastorianus,* specific genetic changes occured in response to the cold lager brewing temperatures, resulting in lager yeasts with advantageous brewing properties (Dunn and Sherlock, 2008; Libkind et al., 2011). Maltose metabolism and utilization is a strongly selected trait in *S. pastorianus* (Donalies et al., 2008; Nakao et al., 2009). Furthermore, sulfite formation is important in lager-brewing as sulfite acts as a flavour stabilizer (Donalies et al., 2008). Thus, the less efficient *SUL1* genes have been inactivated in *S. pastorianus* to improve sulfite production through the use of the more efficient *SUL2* genes (Nakao et al., 2009) (Fig. 1.1b). *S. pastorianus* maintains a high metabolic rate at the lower temperatures imposed during lager-brewing conditions. This may be due to the presence of *S. eubayanus* genomes in the hybrid species *S. pastorianus*, as *S. cerevisiae* is a thermotolerant yeast (Sato et al., 2002).

Dunn and Sherlock (2008) characterized 17 *S. pastorianus* strains, all representing different beer types, via competitive genomic hybridization (CGH) studies. From this study, two groups of distinct *S. pastorianus* strains were characterized, based on the number of copies of each parental chromosome, genome rearrangement locations and DNA polymorphisms. The *S. cerevisiae* content between the two groups is almost identical, with a minor 0.3% variation in nucleotides (Querol and Bond, 2009). It was suggested that strains from each group originated from two independent events. Group I strains resulted from interspecific hybridisation between two spores of haploid *S. cerevisiae* and haploid *S. eubayanus*. A large portion of *S. cerevisiae* DNA was lost, thus group I strains contain a maximum of one *S. cerevisiae* genome equivalent and also contain one *S. eubayanus* genome equivalent (Dunn and Sherlock, 2008). Group II strains arose from hybridisation of a diploid *S. cerevisiae* with a haploid *S. eubayanus*,

and contains two *S. cerevisiae* and one *S. eubayanus* genome equivalents (Dunn and Sherlock, 2008). An allotetraploid was then generated due to recombination between homoeologous chromosomes resulting in a lager yeast that contains multiple copies of the three types of chromosomes, *S. cerevisiae*-like, *S. eubayanus* and mosaic chromosomes containing *S. cerevisiae*-like and *S. eubayanus* genes (Fig. 1.2). The nine mosaic chromosomes of *S. pastorianus,* seen in Fig. 1.2, were generated by the recombination between homoeologous chromosomes at specific locations which are proximal to tRNA gene clusters, Ty elements or in regions of highly repetitive DNA sequences (Bond et al., 2004). Chromosome XVI is the only chromosome in *S. pastorianus* that contains a region of *S. eubayanus* alleles alone (Bond et al., 2004) (Fig. 1.2).

The nature of the *S. pastorianus* genome was also analysed via CGH studies by Bond et al. (2004). Two strains, namely CMBS-33 and 6701, were analysed in this study and at least 28 locations were identified where recombination between homoeologous pairs of chromosomes or chromosomal translocations may have occurred (Bond et al., 2004). Some recombination events occured in subtelomeric X elements or within 25kbp of the telomere, while the remaining recombination events took place at unique sites within nine different chromosomes in strains 6701 and CMBS-33 (Fig. 1.2). Interestingly, many of the genes that surround these unique recombination sites play an essential role in fermentation, eg: alcohol dehydrogenase 2 (*ADH2*), responsible for the oxidation of ethanol to acetaldehyde and *ADH4*, responsible for the reduction of acetaldehyde to ethanol (Bond et al., 2004). Another extraordinary finding in this study was the apparent identification of a *S. bayanus*-like specific region on chromosome XVI, as seen in Fig. 1.2, between the genes YPR160 and YPR190. *S. cerevisiae*-like genes are completely absent from this region in both group I and group II lager yeasts. This was further confirmed by the subsequent whole genome sequencing of the *S. pastorianus* strain, Weihenstephan 34/70 (Nakao et al., 2009). The lager strains CMBS-33 and 6701 are members of Group II (Querol and Bond, 2009).

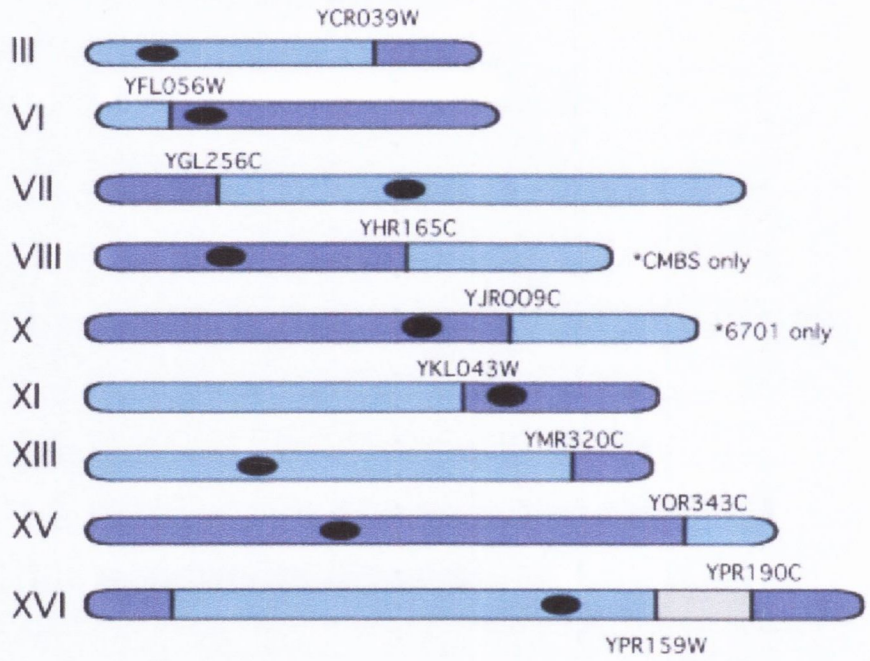

FIG. 1.2 The mosaic chromosomes of *Saccharomyces pastorianus*, due to recombination of two parental homoeologous chromosomes (indicated by blue and purple sections). Recombination locations are depicted in relation to the centromeres (black dots). *Saccharomyces eubayanus* genes are represented by a grey section in chromosome XVI. Chromosomal rearrangements are unique to specific strains.
Figure taken from Querol and Bond, 2009

1.3 Beer spoilage micro-organisms

1.3.1 Introduction to microbial contamination in brews

In a fermentation, the main role of lager yeasts is to rapidly and efficiently catalyse the conversion of wort sugars to ethanol, carbon dioxide and other metabolites, without developing off-flavours. As described previously, *S. pastorianus* strains are highly stress tolerant. It is thought that polyploidization reduces the fitness of an organism overall (Mable and Otto, 2001; Thorpe et al., 2007), however allotetraploid lager yeasts are exposed to numerous stresses during fermentation and have acquired the ability to grow in harsh fermentation conditions. These harsh conditions include high osmotic pressure, high carbon dioxide content, ethanol content, low pH, high hydrostatic pressure, low temperature, high cell density and the presence of compounds derived from hops (Attfield, 1997; Brosnan et al., 2000; Carrasco et al., 2001; Gibson et al., 2008; Zuzuarregui et al., 2005; Zuzuarregui and del Olmo, 2004). This high degree of resistance to various stresses is specifically apparent in allotetraploid strains, while the parental strains *S. cerevisiae* and *S. eubayanus* are less robust in the same environmental conditions, especially in the ability to metabolize available sugars to ethanol (Querol and Bond, 2009).

This harsh environment created during fermentation provides an unsuitable medium for the growth of many organisms, besides *Saccharomyces pastorianus* strains, as it is deficient in amino nitrogen, oxygen, fermentable carbohydrates and vitamins (Fernandez and Simpson, 1994; Rainbow, 1981). However, there are certain beer spoiling micro-organisms (BSMs) that have the ability to grow in this harsh environment, resulting in one of the most serious problems in the brewing industry.

Beer spoilage is a common problem among brewers worldwide, resulting in a loss of stock due to contamination. While medium-sized breweries admit to a loss of approximately €3 million per annum, with a withdrawel of less than one months stock, for commercial reasons, there is very little statistical information published regarding this matter (Personal communication, Dr. Ronald Russell). This loss is due to *Lactobacillus* spoilage alone, however *Pediococcous* spoilage is a major problem amongst brewers also. In the Czech Republic, all BSMs detected in breweries were lactic acid bacteria. Furthermore, between 1980-1990, 58-88% of all spoilage incidents in Germany were caused by lactobacilli and pediococci (K. Sakamoto http:dissertations.ub.rug.nl/FILES/faculties/science/2002/k.sakamoto/thesis.pdf). Dr.

Ronald Russell (senior lecturer, Microbiology department, Trinity College Dublin) has previously been requested to deal with spoilage problems in Coors and other breweries while the Carlsberg brewery have informally quoted "Beer spoilage from *Lactobacillus* spp. is a real and common problem in Breweries".

Many factors contribute to the growth of spoilage organisms, such as oxygen content, pH, concentration of hop bitters, nutrient contents and storage temperatures (Hough et al., 1982). Lindner was the first to report contamination and beer spoilage by Enterobacteriaceae in 1895 (Campbell, 2003). Several contaminating species have subsequently been isolated from breweries, including *Lactobacillus* spp., *Pediococcus* spp., *Pectinatus* spp. and *Saccharomyces* spp. (Jespersen and Jakobsen, 1996). Biofilms containing *Saccharomyces* spp., non-*Saccharomyces* spp. and bacteria are also a major threat to industrial breweries, as biofilms have the ability to accumulate on stainless steel surfaces within niches in the machinery (Timke et al., 2005). In breweries, biofilm species such as the slime producers, Acetobacteraceae, are considered the main primary colonisers (Back, 1994). These Gram-negative, strictly aerobic, acetic acid bacteria have the ability to oxidise ethanol to acetic acid (Dworkin and Falkow, 2006). Furthermore, primary colonisers enable secondary bacteria to become part of a biofilm, thus the Acetobacteraceae provide favourable conditions for *Lactobacillus* spp., *Pectinatus* spp. and *Megasphaera* spp. in brewery biofilms (Timke et al., 2004). The composition of biofilms in breweries varies greatly and Back et al. (1994) had previously shown that there is an increase in problems with BSMs during summer time. Timke et al. (2004 and 2005) carried out studies to analyse the composition of biofilms present in breweries. Biofilm samples were taken from various locations within various breweries during spring, summer and winter. Whole cell fatty acid profiles were different for each biofilm sample indicating variation in microbial composition, thus no typical biofilm community was identified (Timke et al., 2005; Timke et al., 2004). However, each biofilm appeared to be dominated by *Saccharomyces* and non-*Saccharomyces* spp., while half of the samples analysed contained dimethylacetals indicating the presence of strictly anaerobic bacteria including *Pectinatus* spp. (Timke et al., 2005; Timke et al., 2004). Furthermore, studies indicate that a high portion of Gammaproteobacteria, including Enterobacteriaceae and Pseudomondaceae were present in biofilms at different stages of the year (Timke et al., 2004). This data agrees with previous reports from breweries, which state that *Pseudomonas* spp. and Enterobacteriaceae occur in wort but do not multiply in bottled

beer (Lawrence 1988). Finally studies by Timke et al. (2004 and 2005) also indicate that lactic acid bacteria such as *Lactobacillus* spp. were present at very low levels in comparison to other contaminting species in these biofilms (Timke et al., 2005; Timke et al., 2004).

It can be noted that there are two distinct types of spoilage organisms, wort-spoilage organisms and beer spoilage micro-organisms (BSMs) (Jespersen and Jakobsen, 1996). Wort-spoilage organisms cannot multiply in beer and wort-spoilage contamination is primarily caused by low pitching rates or unhealthy yeast (Jespersen and Jakobsen, 1996). This contamination can be prevented by pitching wort with an adequate amount of healthy yeast cells, for example 1-1.5 x 10^7 viable cells/mL. This large quantity of yeast cells promotes quick assimilation of wort to an acidic and anaerobic environment characteristic of beer. Unlike beer spoilage micro-organisms, wort-spoilage organisms such as *Obesumbacterium* spp., *Aerobacter* spp. and *Escherichia* spp. cannot grow in this environment (Jespersen and Jakobsen, 1996). Beer spoilage micro-organisms, on the other hand can become effective during any phase of fermentation, but multiply best after an acidic, anaerobic environment has been created (Schiller, 1993). Examples of beer spoiling micro-organims include *Pediococcus* spp., *Acetobacter* spp. and *Acetomonas* spp. When contamination occurs a range of characteristics are observed, including visible growth of contaminants, extra bubbles, the formation of a haze or "ropiness" (a complex polysaccharide slime) in the brew and an increase in acidification causing sourness, with the latter two characteristics largely due to Gram-positive bacteria (Jespersen and Jakobsen, 1996). Microbial contamination can result in the developement of off-flavours, with the resulting beverage possessing a sour taste or rancid buttery flavour. Disagreeable aromas are often detected depending on the type of contamination, *Obesumbacterium* sp. produce a parsnip like odor while *Zymomonas* sp. promote the developement of a smell similar to that of rotten apples. BSM metabolites produced in the beverage include propionic, acetic and succinic acids, dimethly sulphide, hydrogen sulphide and methyl mercaptan, which are all products of Gram-negative bacteria (Jespersen and Jakobsen, 1996). The secretion of BSM metabolites subsequently decreases the shelf-life of beer. To prevent the growth of beer spoilage micro-organisms, chemical preservatives such as sulphur dioxide are often added to the beverage. Attenuation, the point at which a yeast culture completes the conversion of fermentable sugars to alcohol and diacetyls, may be reached quicker than normal in contaminated brews, resulting in superattenuation. Superattenuation can be an

additional complication associated with contamination, due to the spoilage organisms ability to ferment dextrins and starch, which are not normally fermented by the culture yeast and producing unwanted by-products such as lactic acid (Lawrence, 1988).

The organoleptic characteristics of uncontaminated brews depend on many factors including the aroma-active substances produced by yeast during fermentation, levels of which are crucial to the final complex flavour of the beer (Saerens et al., 2008). Aroma profiles differ from beer to beer, some beers may produce a sweet fruity aroma, while others produce a floral aroma. Genes that are involved in the biosynthesis of these aroma compounds include *BAP2*, *BAT1*, *BAT2*, *ILV5*, *ATF1*, *ATF2*, *IAH1*, *EHT1*, *EEB1* and *ADH1*. The latter is suprisingly repressed at the transcriptional level during days 3 and 8 of a fermentation compared to day 1 (James et al., 2003; Saerens et al., 2008). A direct correlation can be made between the expression levels of these genes and flavour generation (Saerens et al., 2008). The final flavour of the beverage can also be influenced by fermentation in high gravity wort, due to increased acetate ester production, yet increasing fermentation temperature had very limited effect on the overall taste (Saerens et al., 2008).

Beer spoiling micro-organisms are particularly hard to detect, for a number of reasons. Firstly, bacterial contamination is often present in very low numbers, therefore the detection method used must be very sensitive. Secondly, beer-spoilage organisms can be specifically adapted to a fermentative environment, thus growth in other environments such as nutrient rich agar plates, may be difficult, making screening for contamination problematic (Jespersen and Jakobsen, 1996). The use of selective media is an obvious choice to determine contamination, but in some cases selectivity is not possible. Additionally, the conventional plate count method is time consuming, as it can take up to 3 days for spoilage organisms to grow on selective media, and this is an unrealistic identification method in large scale breweries. Finally the contamination of wild yeasts is extremely hard to identify as the majority of wild yeasts belong to the same genus as the culture yeast, these levels are also extremely low and it is impossible to distinguish between one colony of spoilage yeast for every 10^6 colonies of culture yeast (de Angelo and Siebert, 1987; Thurston, 1986). As very low levels of contamination may eventually result in growth and spoilage, a rapid and exceptionally sensitive method would be ideal to diagnose such levels of contamination. Thus, more conventional methods are required to identify low levels of beer contaminants.

Methods used to identify beer contaminants include randomly amplified polymorphic DNA polymerase chain reaction (RAPD-PCR) (Menz et al., 2010) and a HybriScan® Beer kit that can provide reliable results within two hours (Sigma Aldrich).

1.3.2 Gram-positive bacteria

Gram-positive bacteria are regarded as the most hazardous beer spoiling micro-organisms, with bacteria belonging to the genera *Lactobacillus* and *Pediococcus,* being the most frequently isolated Gram-positive bacteria from breweries (Ogden, 1986). Lactobacilli, belonging to the lactic acid bacteria group, are facultative anaerobic rods, that have the ability to convert lactose into lactic acid, glucose and galactose. There are various strains within this species including *L. brevis, L. curvatus, L. lindneri, L. casei, L. coryneformis, L. buchneri, L. plantarum, L. brevismilis, L. malefermentas,* and *L. parabuchneri*, all of which are listed in Table 1.1 (Jespersen and Jakobsen, 1996; Sakamoto and Konings, 2003). While each species is classed as a beer spoilage micro-organism, the level of contamination varies greatly as lactic acid beer spoilage is dependent on the composition of the brew. Furthermore, different organisms have divergent thresholds for growth in a fermentative environment, for example resistance to hops and level of alcohol tolerable. Numerous lactic acid bacteria are resistant to hops, which is considered a multi-gene trait (Fujii et al., 2005). Two genes are thought to be responsible for hop tolerance, *horA* (Sami and Yamashita, 1997; Sami et al., 1997) and *hitA* (Hayashi et al., 2001). *horA* appears to be the central component of hop tolerance in lactic acid bacteria, encoding an ABC transporter gene that has the ability to expel α-acids of hop extracts, such as iso-humulones, from the cell (Sakamoto et al., 2001; Sakamoto et al., 2002). *hitA* encodes a putative divalent cation transporter, and is assumed to contribute to hop resistance in *L. brevis* when manganese is present (Hayashi et al., 2001; Simpson, 1993; Simpson and Hughes, 1993). *Lactobacillus* spp. produce excessive turbidity and off-odours, while each *Lactobacillus* species has a different effect on a fermentation, *L. brevis* has been shown to cause superattenuation while *L. casei* produces increased amounts of diacetyl (Lawrence, 1988; Sakamoto and Konings, 2003).

Pediococci are also classed as lactic acid bacteria (LAB). They are facultative anaerobic cocci and species include *P. damnosus, P. inopinatus and P. dextrinicus,* some of which are also resistant to hop compounds (Table 1.1) (Gil et al., 2004; Jespersen and Jakobsen, 1996). *P. dextrinicus* was recently reassigned to the genus

Species	Growth Restrictions
Lactobacillus brevis *Lactobacillus buchneri* *Lactobacillus lindneri* *Lactobacillus coryneformis* *Lactobacillus curvatus* *Lactobacillus plantarum* *Lactobacillus brevismilis* *Lactobacillus casei* *Lactobacillus malefermentas* *Lactobacillus parabuchneri* *Lactobacillus dextrinicus*	Some of the lactobacilli may be sensitive to hops, although most are resistant
Pediococcus damnosus *Pediococcus inopinatus*	Growth above pH 4.2, Low EtOH, Low Hops
Micrococcus kristinae *Micrococcus luteus*	Sensitive to high EtOH and hops concentrations
Pectinatus cerevisiiphilus *Pectinatus frisingensis*	Growth above pH 4.5 Sensitive to high EtOH and hops concentration
Zymophilus raffinosivorans	n/a
Megasphaera cerevisiae	Sensitive to EtOH
Zymomonas mobilis	Growth above pH 3.4
Acetobacter aceti	Growth in aerobic conditions
Hafnia protea	Growth in aerobic conditions

Table 1.1 List of beer spoilage bacteria

Lactobacillus (Haakensen et al., 2009). The growth of *P. inopinatus* and *P. dextrinicus* is limited to environments with low ethanol concentrations, low hop concentrations and a pH greater than 4.2 (Lawrence, 1988), this does not make them a great threat to brewers as the pH of lager fermentations can be as low as 4. *Pediococcus* species in particular have been linked with honey flavoured brews, and the so-called "sarcina-sickness", which is defined by increased acidity, granular sediments and turbidity (Basanta et al., 2008). Like *L. casei*, *Pediococcus* species are thought to produce extensive amounts of diacetyl (Lawrence, 1988).

Finally, *Micrococcus* species, which are obligate anaerobes, have also been documented as Gram-positive beer spoilage micro-organisms. This species is very sensitive to common fermentation characterisitics such as high ethanol levels (Back, 1981). A couple of *Micrococcus* species that have been isolated from breweries are *M. kristinae* and *M. luteus* (Table 1.1). A typical trait of *M. kristanae* contamination is the development of a fruity atypical aroma (Back, 1981).

1.3.3 Gram-negative bacteria

Gram-negative bacteria are widespread in beer spoilage, with the majority being strict anaerobes. *Pectinatus* beer spoilage species include *P. cerevisiiphilus* and *P. frisingensis* (Table 1.1) (Schleifer et al., 1990; van Vuuren, 1996). Phylogenetically similar to *Pectinatus* species is the genus *Zymophilus,* of which *Z. raffinosivorans* has been isolated from breweries (Table 1.1) (Schleifer et al., 1990). Beer spoiling micro-organsims from both of the above genera produce numerous toxins during growth within a fermentation containing ethanol concentrations below 5% (w/v) and a pH value in the range of 4.3-4.6 (Jespersen and Jakobsen, 1996). While the strictly anaerobic spoilage organism *Megasphaera cerevisiae* is sensitive to low pH levels (< 4.5) and high alcohol content (> 2.8%) (Haikara and Lounatmaa, 1987), the facultative anaerobe, *Zymomonas mobilis* can grow in more harsh conditions including high alcohol concentrations (< 10%) and pH levels above 3.4 (Table 1.1) (van Vuuren, 1996). Aerobic Gram-negative bacteria, such as *Acetobacter aceti*, have been isolated from brews and have the ability to convert ethanol to acetic acid (Table 1.1) (Lawrence, 1988). Due to their aerobic status, they are not considered a great threat as beer spoilage micro-organisms. However there are certain aerobic bacteria that have the ability to survive, but not multiply, in a fermentation. These bacterial cells cosediment

with yeast cells and are repitched into fresh wort eg: *Hafnia protea* (Table 1.1) (Thastum and Jakobsen, 1981).

1.3.4 Wild yeasts

As stated above, biofilms isolated from breweries were shown to be dominated by *Saccharomyces* and non-*Saccharomyces* yeasts (Timke et al., 2005), confirming the ability of wild yeasts to act as beer spoilage micro-organisms. Wild yeasts are defined as yeasts that are not deliberately used in the brewery and are not under full control (Priest, 1981). *Saccharomyces* strains are deemed the most hazardous with regards to beer spoilage (Jespersen and Jakobsen, 1996; van der Aa Kuhle and Jespersen, 1998). Contamination with *Saccharomyces* strains can result in the development of phenolic, acidic, fatty acid and estery off-flavours, in addition to superattentuation of the fermentation and the formation of a rope or haze (Jespersen and Jakobsen, 1996; Lawrence, 1988). Superattenuation occurs in the presence of wild yeast due to the production and secretion of glycoamylases, enabling the wild yeast to ferment dextrins that culture yeast cannot (Jespersen and Jakobsen, 1996). Non-*Saccharomyces* wild yeast include a range of genera including *Brettanomyces, Candida, Kluyveromyces* and *Pichia* (Campbell, 1996; Campbell and Msongo, 1991; Ingledew and Casey, 1982).

1.4 Prevention of beer spoilage

1.4.1 Hops

To eliminate this growing problem of beer spoilage, many methods have been tried and tested over the last 20 years. The most common form of antimicrobial activity in brews is the use of hop-extracts, containing hop oils, alpha acids and beta acids. The agricultural crop, hops, is valued for its high terpenophenolic, polyphenolic, and essential oil levels (Chadwick et al., 2006; Overk et al., 2005; Stevens et al., 1997). Hop polyphenols and terpene oils contribute complex flavours to the beer, including bitterness (Deinzer, 2006; Forster et al., 2003; Taylor et al., 2003). It has recently been indicated that polyphenols also contribute to the foam stability and reduction-oxidation effects that occur during fermentation (Deinzer, 2006). The terpenophenolic compounds, specifically prenylated acylphloroglucinols, also known as α-acids, but which includes some β-acids, are responsible for antimicrobial activity displayed by hop extracts (Kavalier et al., 2011). α-acids or humulones, impart a bitter flavour to the beer (Neve, 1991), but more importantly they function as cell membrane ionophores, transferring ionophoric α-acids and protons, across the plasma membrane and into the

bacterial cell (Sakamoto and Konings, 2003; Simpson, 1993; Simpson and Smith, 1992). This results in the reduction of the intracellular pH, leading to cell death (Simpson, 1993; Simpson and Fernandez, 1994). The bactericidal activity of hop-extracts appears to be pH dependent, and Simpson (1993) has previously shown that its activity decreased 800-fold when the pH was raised from 4 to 7 (Simpson, 1993). Many beer spoilage strains display a degree of resistance towards hops (Table 1.1), for this reason, other methods of antimicrobial activity are required during lager fermentation.

1.4.2 Chemical preservatives

A range of chemical preservatives are often added to a fermentation to help prevent contamination, these include formaldehyde, sulphur dioxide, ethyl para-hydroxybenzoate, sorbic acid, propylparaben and methyl para-hydroxybenzoate. Formaldehyde is often added to brews to improve the clarity of the beer and prolong shelf life, but in all cases the levels of formaldehyde in beer are below the levels considered dangerous by the World Health Organization. Sulphur dioxide occurs naturally in beer as it is a by-product of yeast fermentation, however additional sulphur dioxide is added to the fermentation to exert antimicrobial properties (Ilett, 1995). Ethyl para-hydroxybenzoate, sorbic acid, propylparaben and methyl para-hydroxybenzoate are all antimicrobial agents and as Ethyl para-hydroxybenzoate has anaesthetic properties and may cause numbness to the mouth, this particular additive has been banned in Australia.

The use of chemical substances leads to an increase in the consumer awareness in terms of health risks associated with their consumption. Thus, brewers use alternative methods to prevent the growth of beer-spoilage microorganisms, these are mainly based on extrinsic factors, including refrigeration, pasteurization and filtration (Douglas et al., 2006; Vaughan et al., 2005). The use of natural antimicrobial peptides (AMPs) has also been investigated as another method.

1.4.3 Chitosan

Chitosan is a biopolymer that is derived from chitin deacetylation, and is mainly obtained from crustaceous shells or cell walls of fungi (Gil et al., 2004). A study carried out by Gil et al (2004), describes the activity levels of the natural antimicrobial compound, chitosan, against various lactic acid bacteria and several brewing yeasts (Gil

et al., 2004). Chitosan at 0.1mg/mL inhibits the growth of *Pediococcus* spp. at 10^5 cfu/mL, while at 1mg/mL chitosan inhibits the growth of *Lb. plantarum* at 10^5 cfu/mL. These concentrations of chitosan do not have a significant effect on lager yeast at 1-1.5 x 10^6 cfu/mL, with a 1 log decrease observed at 1mg/mL of chitosan. It was also indicated that chitosan can be added directly to a fermentation, with very little affect on the overall process, thus may be a useful antimicrobial compound during fermentation. This study did not assay the antimicrobial effects of chitosan during a contaminated fermentation. Furthermore, the addition of synthetic chitosan to fermentations would be cost prohibitive to the brewer (Gil et al., 2004). Further studies carried out by Galvagno et al. (2007) found that chitosan has a much greater effect on *Pediococcus* viability and no effect on yeast viability (Galvagno et al., 2007). The addition of chitosan at 0.1mg/mL, inhibits the growth of *Pediococcus* spp. after 2 hr and had no effect on yeast viability (Galvagno et al., 2007).

1.5 Antimicrobial peptides

1.5.1 General introduction to antimicrobial peptides (AMP)

Lysozyme was one of the first antimicrobial proteins discovered by Fleming in 1922 (Fleming, 1922). Today there is approximately 1790 unique peptides listed on the antimicrobial peptide database (http://aps.unmc.edu/AP/statistic/statistic.php). This large group of peptides contains a range of diversity. Antimicrobial peptides contain a number of similar characteristics: the majority are small (< 60 amino acid residues), positively charged (+2 to +11), amphipathic in nature, with activity against a broad spectrum of bacteria (Cederlund et al., 2011; Jenssen et al., 2006). The average length of peptides within the database is 31 amino acids, with an average net charge of 3.8 (http://aps.unmc.edu/AP/statistic/statistic.php).

Antimicrobial peptides can be produced via non-ribosomal peptide synthesis (Maget-Dana and Peypoux, 1994; Storm et al., 1977) or ribosomal peptide synthesis (AMPs) (Jack et al., 1995; Papagianni, 2003). Non-ribosomally synthesized peptides include the well known antibiotics, such as vancomycin and polymyxin B, which are synthesized via peptide synthetases, and form cyclic peptides containing unusual amino acids (Cederlund et al., 2011; Maget-Dana and Peypoux, 1994; Storm et al., 1977). Resistance to these common antibiotics is prevalent in bacterial genera such as Enterococci and Staphlococci. The bacterium, *Bacillus subtilis,* produces AMPs such as subtilin, via ribosome mediated protein synthesis (Banerjee and Hansen, 1988) and

additionally produces the peptide iturin, using the non-ribosomal pathway (Moyne et al., 2001).

Ribosomally synthesized AMPs are more widespread than non-ribosomally synthesized peptides, and are present in many different organisms including plants, insects, reptiles, birds, mammals and microorganisms (Lehmann et al., 2002; Lehrer and Ganz, 2002; Sahl, 1994; Zasloff, 2002). They play a very important role in the host defense system and are produced as the immediate first line of antimicrobial defense against many invading organisms including Gram-negative bacteria, Gram-positive bacteria, fungi, protozoa, enveloped viruses and tumour cells (Jenssen et al., 2006). Furthermore, the unique antimicrobial spectrum of each AMP is influenced by its amino acid sequence and structural composition, and there is little sequence homology between AMPs (Papagianni, 2003). The mechanism of action of AMPs has been thorougly investigated over the last decade, and is known to involve electrostatic interactions between the positively charged peptides and the negatively charged membranes. This primary interaction is subsequently followed by membrane disruption or permeabilization, activation of cell wall lytic enzymes and disruption of membrane bound multienzyme complexes and intracellular events (Nuding et al., 2009). Although the exact mechanism of action is unknown, a number of models have been proposed. The primary model is the carpet-type mechanism, which suggests that the peptide remains parallel to the membrane surface and lawns itself over the surface of the microorganism in a carpet-like manner (Chang et al., 2008) (Fig. 1.3 C). Interaction of the peptide at critical concentrations, with the anionic charges of the lipopolysaccharide (LPS) molecule or the lipoteichoic acid (LTA) polymer, results in the neutralization of the endotoxic activity via its cationic charges (Dhople et al., 2006). This leads to membrane disruption, subsequently leading to micelles or small peptide-lipid aggregates (Chang et al., 2008) (Fig. 1.3 C). The barrel-stave model and "toroidal pore" model suggest that pores are formed within the membrane, through which ion and peptide transport occurs, leading to cell death (Fig. 1.3 A & B) (van der Weerden et al., 2010). All the above models are illustrated in Fig. 1.3.

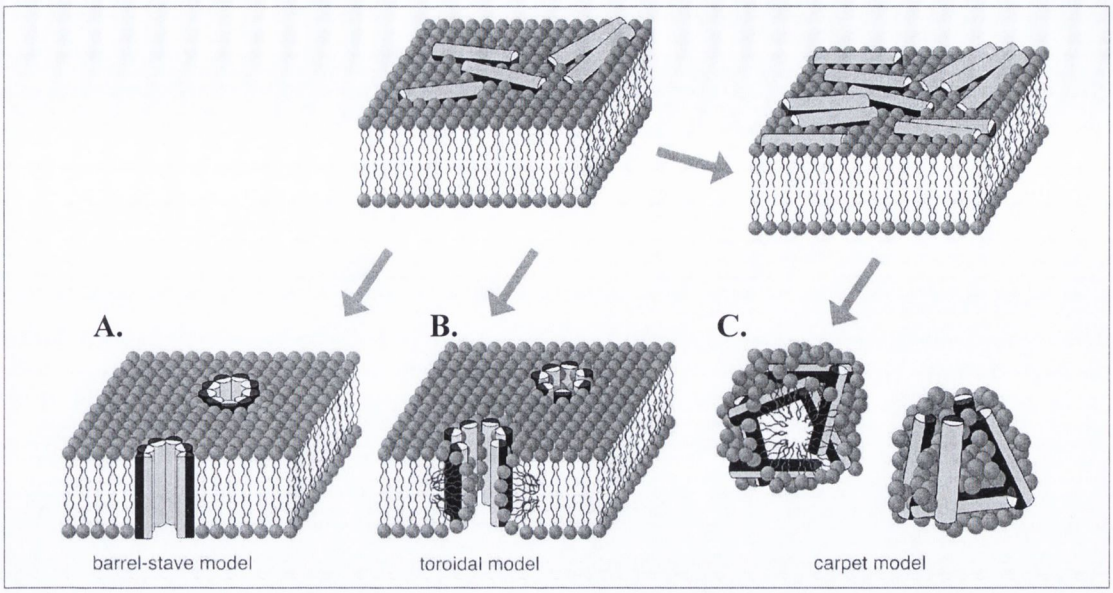

FIG. 1.3 Schematic illustration of three models depicting the mode of action of cationic antimicrobial peptides.

The barrel-stave model (A) and torodial model (B), predict the insertion of the AMP into the lipid bilayer. The carpet-type model (C) proposes a membrane disruption of the cell. Hydrophilic regions are depicted in grey colouring and lipophilic regions are illustrated in black.

(Wiesner and Vilcinskas, 2010).

1.5.2 Microbial antimicrobial peptides

1.5.2.1 Introduction to microbial antimicrobial peptides

Bacterial antimicrobial peptides are generally non-ribosomally synthesized and are referred to as bacteriocins. In general, bacteriocins are considered to have a narrow activity spectrum and inhibit the growth of similar and/or closely related bacterial strains. However, they leave the host bacteria undamaged due to selective killing subject to specific post-transcriptional modification and/or specific immunity mechanisms (Jack et al., 1995). Bacteriocins are produced by both Gram-positive bacteria and Gram-negative bacteria. The lactic acid bacteria (LAB) bacteriocins have a broad range of antimicrobial activity, including activity against spoilage organisms and food-borne pathogenic microorganisms (Cintas et al., 2001; Cleveland et al., 2001; Cotter et al., 2005; Diep and Nes, 2002; Franz et al., 2007; Klaenhammer, 1993; Nes et al., 1996; Nes et al., 2007). LAB bacteriocins are divided into four categories, classes I-IV (Klaenhammer, 1993). Class I and class II are generally small peptides that range from 3-10 kDa, with cationic, amphiphilic and membrane permeabilization properties, representing the lantibiotics and nonlantibiotics respectively (Klaenhammer, 1993; Papagianni, 2003). Class III bacteriocins are defined as heat-labile proteins and are greater than 30 kDa (Papagianni, 2003). Finally class IV bacteriocins contain complex lipid or carbohydrate moieties (Papagianni, 2003).

1.5.2.2 Nisin

Nisin, a class I bacteriocin, is a type of lantibiotic, a lantionine-containing antibiotic. Nisin has been demonstrated as an efficient natural antimicrobial, effective against the lactic acid beer spoilage bacteria (Odgen and Tubb, 1985; Odgen et al., 1988; Sakamoto and Konings, 2003), without affecting intact yeast cells (Dielbandhoesing et al., 1998). Its mechanism of action involves binding to and inhibiting the transglycosylation of lipid II, leading to a decrease in synthesis of peptidoglycan (Jenssen et al., 2006). It is a polycyclic antibacterial peptide composed of 34 amino acids and contains the uncommon amino acids lanthionine (Lan), methyllanthionine (MeLan), didehydroalanine (Dha) and didehydropaminobutyric acid (Dhb). It is produced by *Lactococcus lactis* when grown on natural substrates such as milk or dextrose (Mattick and Hirsch, 1947; Schleifer et al., 1985). Studies carried out by Galvagno et al. (2007) indicate that when nisin is added to a fermentation at 0.2μg/mL, it inhibits the growth of *Pediococcus* spp. after 2 hr, but also reduces the growth of *S. cerevisiae* by 1 log cycle (Galvagno et al., 2007). Furthermore, the addition of nisin (0.1μg/mL) to a

fermentation inoculated with *Pediococcus* spp. (10^6 CFU/mL) resulted in total killing of *Pediococcus* spp. after 28 days at 25°C (Galvagno et al., 2007). Nisin has also been shown to prevent spoilage bacterial contamination in wine and fruit brandies (Henning et al., 1986; Odgen et al., 1988; Radler, 1990a, b). Nisin has been approved as a safe food additive by the Joint FAO/WHO Expert Committee on Food Additives and is used in over 48 countries in various food applications including processed cheese, canned foods and pastuerised milk (Cotter et al., 2005). However, nisin has only been approved in Australia and New Zealand, as a safe biopreservative additive in beer (Delves-Broughton et al., 1996). Overall it is thought that the use of bacteriocins, in conjunction with more traditional methods, including pasteurization and filtration may lead to the development of safer beers (Vaughan et al., 2004).

1.5.2.3 Pediocin, Plantaricin and Enterocin

S. cerevisiae strains have been engineered to secrete bacteriocins, specifically pediocin PA-1, which is produced by *Pediococcus acidilactici*. The resultant strain displayed antibacterial activity against various *Lactobacillus* spp. when tested by an agar plate assay method (Schoeman et al., 1999). Furthermore, the bacteriocin, plantaricin 423, synthesized by *L. plantarum* 423, was introduced into a *S. cerevisiae* strain, on the multicopy shuttle vector YEp352 (Van Reenen et al., 2003). Bactericidal activity against *L. monocytogenes* was demonstrated with the recombinant strain, using an agar plate assay method. The bacteriocin, enterocin L50, which is composed of two antimicrobial peptides, enterocin L50A (EntL50B) and enterocin L50B (EntL50B), is produced by the strain *Enterococcus faecium* L50 (Basanta et al., 2008). Enterocin L50 displays a broad spectrum of antimicrobial activity against various LAB strains when grown on de Man, Rogosa and Sharpe (MRS) media, in wort, and in lager beers (Basanta et al., 2008). To analyse this further, Basanta et al. (2009) modified *S. cerevisiae* strains to express and secrete EntL50A and EntL50B, independently and together, using a series of high copy number expression vectors (Basanta et al., 2009). Each gene was recombined to the α-factor leader sequence from *S. cerevisiae* and was under the control of a galactose inducible promoter. Recombinant *S. cerevisiae* strains displayed antimicrobial activity when grown in yeast extract peptone supplemented with galactose and raffinose (YPGR) or synthetic complete supplemented with galactose and raffinose (SCGR) media (Basanta et al., 2009). ELISA results indicate that after 192hr of growth in SCGR media, recombinant EntL50A and EntL50B were secreted into the supernatant at 10.9ng/mL and 40.5ng/mL respectively. In this study,

antimicrobial activity was never assayed under fermentation conditions, but it is assumed that the strains would need to be further modified as both peptides undergo partial inactivation from oxidation (Basanta et al., 2009).

1.5.2.4 Colicin and Microcin

Gram-negative bacteria produce a range of AMPs, which are larger than Gram-positive bacteriocins, including colicins and microcins. Colicins, produced by strains of *E.coli* that carry colicinogenic plasmids, are greater than 20 kDa and are toxic for closely related strains (Papagianni, 2003). Microcins are produced by Enterobacteriaceae strains, and are separated into three classes based on their mode of action, class A, class, B and class D (Nissen-Meyer and Nes, 1997). Unlike colicins, these are small peptides that are less than 10 kDa, but similar to colicins, these peptides possess antibacterial activity towards strains of a similar phylogenetic makeup (Papagianni, 2003). Colicin V is also classed as a microcin due its smaller size (Papagianni, 2003).

1.5.3 Mammalian antimicrobial peptides

1.5.3.1 Introduction to mammalian AMPs

Bacteriocins have been successfully used as antimicrobials during the fermentation process as stated above, however other types of non-bacterial AMPs may also be beneficial in preventing beer spoilage. Mammalian AMPs have an advantage over bacteriocins, as these AMPs have a broad activity spectrum and are active against Gram-positive bacteria, Gram-negative bacteria, fungi and viruses, unlike bacteriocins which have a narrow spectrum of bactericidal activity. Mammalian AMPs play an important role in the hosts immune system. They are expressed either constitutively or inducibly by infectious/inflammatory stimuli such as bacterial molecules that induce innate immunity (Jenssen et al., 2006). This ability to recognise and neutralize invading organsims quickly and specifically is greatly beneficial to the innate immunity. Furthermore, evidence suggests that AMPs play an important role in regulating the adaptive immune system, as many mammalian peptides are involved in receptor-mediated effector functions in chemotaxis (Dhople et al., 2006; Pag et al., 2004). The degree of AMPs importance in the immune system is reinforced by the fact that the induction pathways of AMPs in all organisms is conserved (Hoffmann et al., 1999). There are three types of AMPs in mammals, cathelicidins, histatins and defensins.

1.5.3.2 Cathelicidins

Cathelicidins/cathelin-associated peptides consist of a preprotein sequence at the N-terminus and an antimicrobial domain at the C-terminus, peptidase cleavage of the C-terminus forms the mature AMP (Papagianni, 2003). The N-terminal proregion is highly conserved and is homologous to the cysteine protease inhibitor, cathelin. The C-terminal region is highly divergent in terms of the number of residues (12-79), sequence and structure, resulting in a wide range of diversity within this group of AMPs. According to Papagianni (2003), cathelicidins can be categorized into three groups. Group 1 peptides possess a high content of repetitive amino acids often proline, for example the peptide PR-39 (Pro-Arg-rich peptide) contains up to 20 repeats of Pro-Arg and is found in the intestine and/or leucocytes of pigs. The bactenecins Bac-5 and Bac-7, are 5 kDa and 7kDa peptides respectively. Bac-5, containing 42 amino acid residues and Bac-7, containing 59 amino acid residues, are both found in neutrophils of cattle, goat and sheep. Group II cathelicidins possess intramolecular disulphide bonds and includes peptides such as dodecapeptide, a 12 amino acid cyclic dodecapeptide found in the neutrophils of bovine species and protegrins (16-18 amino acids) which are found in the leucocytes of porcine species. Group III cathelicidins include the only cathelicidin found in humans, LL-37. These petides are characterized by the presence of amphiphilic regions due to the α-helical structures. The AMP LL-37 is encoded by the *CAMP* gene and is synthesized as a 100 residue proprotein, 37 of which make up the antimicrobial C-terminal region (Agerberth et al., 1995). This cationic, amphipathic, α-helical peptide has a broad antimicrobial spectrum and is active against a range of Gram-positive bacteria, Gram-negative bacteria, fungi and viruses (Kai-Larsen and Agerberth, 2008). The mechanism of action of LL-37 involves the attraction of negatively-charged phospholipids, and the integration into the cell membrane leading to membrane disruption (Cederlund et al., 2011). LL-37 plays different roles in the immune system, examples include: interaction with Formyl Peptide Receptor-Like 1 (FPRL1) which results in the chemoattraction of neutrophils, monocytes and T-cells, and the involvement in a positive feedback loop in neutrophils, whereby LL-37 interacts with the pro-inflammatory lipid mediator leukotriene B4, leading to an increase in the inflammatory process (Agerberth et al., 2000; De et al., 2000; Wan et al., 2011). Analysis of *CAMP* gene expression levels indicates that LL-37 may be involved in numerous autoimmune diseases such as cystic fibrosis and psoriasis (Chen et al., 2004; Frohm et al., 1997).

1.5.3.3 Histatins

Histatins, are histidine-rich cationic peptides that are widespread in saliva (De Smet and Contreras, 2005). Histatins primarily have antifungal activity with modest activity against *S. mutans, S. mitis, Porphyromonas gingivalis* and *Actinobacillus* spp. (MacKay et al., 1984). There are 12 histatin peptides in humans, the parent peptides, histatin 1 (Hst1) and histatin 3 (Hst 3), are encoded by two genes, *HTN1* (*HIS1*) and *HTN2* (*HIS2*), localized on chromosome 4q13 (Sabatini et al., 1993; vanderSpek et al., 1989). Hst 4 – 12 are formed from the proteolytic cleavage of Hst 3, while Hst 2 is similar to Hst 1 (Castagnola et al., 2004). These peptides are linear in structure, have a molecular weight of approximately 3-4 kDa and are composed of 24-37 residues, each containing seven histidine residues (MacKay et al., 1984). They are constitutively secreted by the parotid, submandibular and sublingual glands (vanderSpek et al., 1989). Hst 1, 3 and 5 (Hst1, Hst3 and Hst5) are considered the most important (De Smet and Contreras, 2005). Hst 5 forms a random coil structure in aqueous solvents and an α-helical structure in non-aqueous solvents and has a broad range of potent antimicrobial activity and is active against *C. albicans, A. fumigatus* and *S. mutans* (Raj et al., 1998; Tsai and Bobek, 1997). Interestingly, a small 12 amino acid fragment of Hst5, named P-113, retains the anticandidal activity of the parent compound (Rothstein et al., 2001). Due to its high antifungal activity, this fragment is of great interest as a therapeutic agent. Clinical trials were previously carried out on P-113, for use in a medicinal mouth rinse. The P-113 mouth rinse was shown to be tolerated by humans and effective against gingivitis, gingival bleeing and plaque (Paquette et al., 2002).

1.5.3.4 Defensins

Defensins, like the majority of AMPs, are present in a wide range of organisms including plants, invertebrates and vertebrates. The defensins are effector molecules of the innate host defense system, and primarily possess a broad spectrum of antimicrobial activity against a variety of pathogens (Dhople et al., 2006). They are categorized into three subfamilies based on their molecular weight, disulphide pairings between the six conserved cysteine residues (α-defensins and β-defensins) and their macrocyclic nature (θ-defensins). Defensins are cationic, hydrophobic, amphipathic, small peptides, ranging in size from 3-6 kDa, that carry a positive net charge (Ouellette, 1999).

Studies by Xiao et al., (2004) indicate that all mammalian defensins evolved from an ancestral β-defensin-like gene. The α-defensins were derived from β-defensins, the

most ancient defensins, by gene duplication after the divergence of mammals from other vertebrates. Furthermore, the θ-defensins which are specific to primates, arose from the α-defensins by gene duplication. Mammalian defensins have co-evolved with microbes for millions of years and have undergone positive Darwinian selection at the amino acid level to select for advantageous mutations (Hughes and Yeager 1997; Lynn et al., 2004). Furthermore, Lynn et al. (2004) identified 14 specific amino acid sites that are under positive selection in the active region of α-defensins, indicating that these defensins have evolved to preserve an adaptive phenotype.

Plant defensins are cysteine rich, contain 40-45 residues, and possess four or five disulphide bonds (Lay and Anderson, 2005). The plant defensins such as NaD1 (*Nicotiana alata* defensin 1), synthesized in the flowers of *N. Alata,* possess antifungal activity only (Lay et al., 2003). NaD1's mechanism of action involves three steps, first the interaction with the fungal cell wall, second the permeabilization of the plasma membrane and third the introduction of the peptide into the cytoplasm (van der Weerden et al., 2010).

Invertebrate defensins are open-ended cyclic peptides, with three or four disulphide bridges and include the cecropins (Jenssen et al., 2006). Both cecropin and cecropin-like molecules have been isolated from *Diptera* sp., including *Drosophila* and *Lepidoptera* sp. including *Bomyx* (Bulet et al., 2004). Cecropin A was the first α-helical defensin isolated from *Hyalophora cecropia* (Steiner et al., 1981), and its mode of action involves membrane permeabilization of susceptible bacteria (Gazit et al., 1996). Generally cecropins are 29-42 residues in length, possess a tryptophan in position 1 or 2 and a C-terminal amidated residue (Bulet et al., 2004).

The α- and β-defensins are widespread throughout vertebrates, whereas the θ-defensins, to date, have only been isolated from non-human primates. Up to six θ-defensin pseudogenes containing premature stop codons, have been identified in humans (Seidel et al., 2010). θ-defensins are unique as they are the only known cyclic defensins in the animal kingdom. They are active against a wide range of viruses including herpes simplex virus and human immunodeficiency virus (HIV) (Cole et al., 2002). An example of a θ-defensin is rhesus θ-defensin-1 (RTD-1), found in the neutrophils of the rhesus macaque. RTD-1, along with other θ-defensins, is effective against HIV-1 and

the mode of action towards this virus involves the defensins binding to the HIV-1 surface glycoprotein gp120 and the HIV-1 receptor CD4+, subsequently blocking the entry of HIV-1 into cells (Munk et al., 2003; Seidel et al., 2010). This activity against HIV-1, may indicate that RTD-1 plays a role in the innate immune system of the rhesus macaque against simian immunodeficiency virus (SIV) (Seidel et al., 2010). Recently, Venkataraman et al. (2009) suppressed the stop codon of a θ-defensin pseudogene, in a human cervicovaginal tissue model, and a fully processed, biologically active θ-defensin was produced (Venkataraman et al., 2009). Thus, reawakening the θ-defensin pseudogenes in humans, which may provide a new area for targeting HIV-1 infections.

1.5.4 Human Defensins

The most widely studied vertebral defensins are the human defensins, which represent a major class of antimicrobial peptides in humans. As stated above, the mechanism of action of defensins is known to involve membrane disruption, this disruption depends on the lipid composition (Wilmes et al., 2011). The human defensin genes characterized thus far, are clustered on chromosome eight (Cederlund et al., 2011). There are two distinct classes of human defensins, the α-defensins and the β-defensins (Dhople et al., 2006). These are characterized by their distinct disulphide bridges (Fig. 1.4).

1.5.4.1 α-defensins

Six human α-defensins have been identified to date, four of these are located in the azurophilic granules of neutrophil granulocytes while the other two are present in the granules of Paneth cells in the crypts of the small intestine (De Smet and Contreras, 2005). The four neutrophil defensins are named accordingly HNP-1 to HNP-4 (Human Neutrophil Peptides). HNP-1 to -3 are found at very high concentrations in the neutrophils, making up approximately 50% of the azurophilic proteins levels, while HNP-4 is present at much lower concentrations (Ganz, 1990). HNP-1 to -3 have also been located in T cells and natural killer (NK) cells (Agerberth et al., 2000). There is a high level of homology between these HNP's as HNP-1, -2 and -3 are coded by 2 genes, *DEFA1* and *DEFA3*, from one locus located on chromosome 8p23 (Linzmeier et al., 1999). *DEFA1* and *DEFA3* encode identical peptides differing only the first amino acid, which is alanine in HNP-1, and aspartic acid in HNP-3 (Fig. 1.4 A). HNP-2 is

Box 1

Box 2

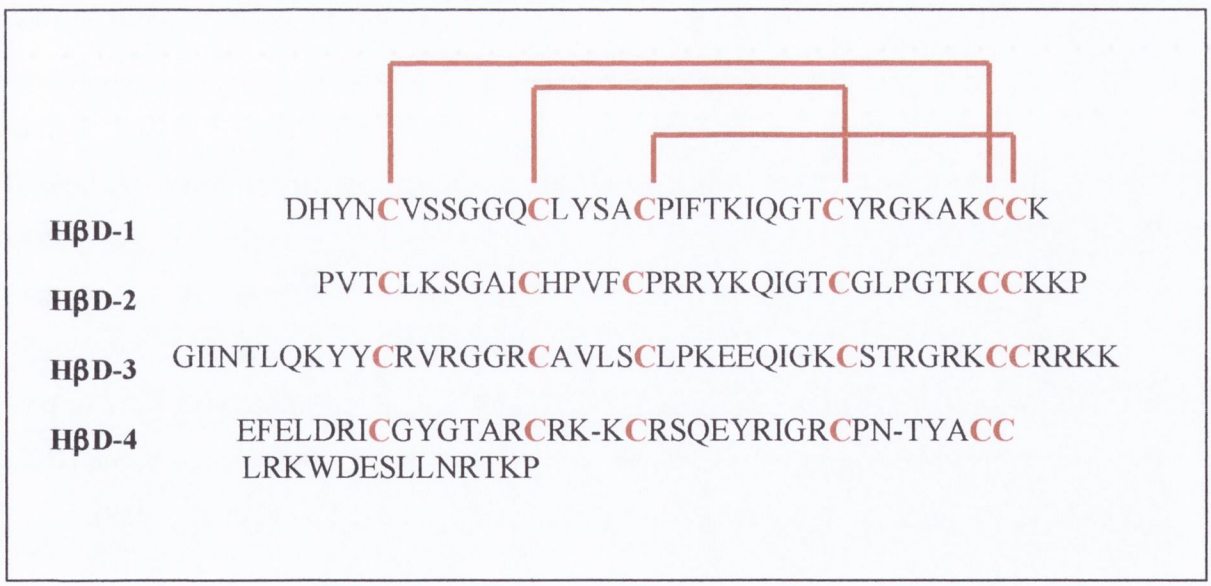

FIG. 1.4 Schematic representation of amino acid sequences and disulphide linkages in human α- and β-defensins

A) Box 1 represents human α-defensin sequences.

B) Box 2 represents human β-defensin sequences.

The conserved cysteine sequences are highlighted in red and the disulphide linkages are represented by red connections.

identical to HNP-1 and HNP-3, but is an N-terminally truncated iso-form lacking the first amino acid (Fig. 1.4 A). HNP-4 is encoded by *DEFA4* and does not share the high sequence similarity seen between HNP-1 to -3 (Fig. 1.4 A). The two remainding α-defensins, HD-5 and HD-6 (Human defensin), which are found in the paneth cells are also located in the epithelial cells of the female urogenital tract and are referred to as enteric defensins (De Smet and Contreras, 2005). These peptides are encoded by the genes *DEFA5* and *DEFA6* respectively.

The α-defensins are short, cationic peptides of 29-35 residues, and contain 3 conserved Cys-Cys disulphide linkages. These disulphide linkages provide structural stability, and stability against proteases. In α-defensins the characteristic disulphide connectivities are Cys1-Cys6, Cys2-Cys4 and Cys3-Cys5 (Fig. 1.4 A). These bridges account for the triple β-sheet, β-hairpin loop structure of the α-defensins (Fig. 1.5). α-defensins are synthesized as preproteins that have no antimicrobial activity. In the case of HD-5 and HD-6, metalloproteinase is responsible for the release of the active peptide (Cederlund et al., 2011; De Smet and Contreras, 2005).

α-defensins have many roles in the immune system of humans and the antimicrobial action follows the standard membrane permeabilization mechanism, although studies on HNP-1 reveal an inhibition on nucleic acid synthesis (Lehrer et al., 1989). Recent studies by De Leeuw et al. (2010), proposed that HNP1 activity is based on lipid II binding, and the ability of HNP-1 to kill *S. aureus* is reduced in cells that have altered lipid II levels (de Leeuw et al., 2010). HNP-1 to -4 contribute to the oxygen-independent killing of phagocytosed microorganisms (De Smet and Contreras, 2005). Furthermore, these HNP's are released via degranulation in response to bacterial or pro-inflammatory stimuli. HNP-1 and -2 are also known to act as chemokines, while HNP-4 inhibits glucocorticoid production (Oppenheim et al., 2003; Territo et al., 1989).

It is indicated that HNP-1 neutralizes herpes simplex virus 1 (HSV-1) in a pH, time and temperature-dependent manner (Jenssen et al., 2006) The expression patterns of some α-defensins are distinctive in individuals with certain diseases, for example Crohn's patients have decreased expression levels (Wehkamp et al., 2004), while patients with coeliac disease displayed increased expression levels (Frye et al., 2000). HNP presence and increased expression levels have also been linked with various types of cancer,

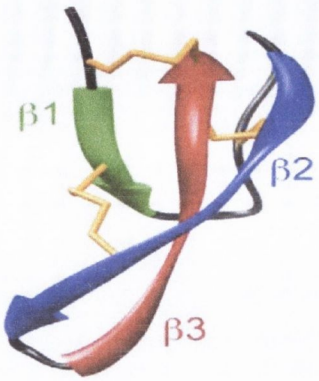

FIG. 1.5 Schematic illustration of HNP-3

The crystal structure of a HNP-3 monomer, illustrating the disulphide bonds, which are represented by orange lines. The three β-sheets are depicted by green, red and blue arrows. (Zhang et al., 2010)

whether this presence hinders or aids tumour proliferation is unclear (Albrethsen et al., 2005). HNP-1 to -3 have been shown to be extremely abundant in colon tumours, with levels being so high that each defensin is also detected in serum (Albrethsen et al., 2005). HNP-1 alone is abundant in lung tumours and is thought to be involved in tumor immunity of oral carcinomas (Bateman et al., 1992; Mizukawa et al., 2000).

As bacterial strains become more resistance to over-used, day-to-day antibiotics such as vancomycin, it is imperative to exploit the use of natural defensins in the fight against disease. In order to achieve this, a sufficient system is required for the successful high yield biosynthesis of active peptides. Hsu et al. (2009) have recently produced active HD-5 in *Pichia pastoris*, in the secretory form (Hsu et al., 2009). HD-5, unlike other defensins, is stored in secretory vesicles as a propeptide and cleaved to form an active peptide. Several forms of proteolytically processed HD-5 can be isolated from the intestinal lumen, where they create a microbicidal environment. HD-5 is active against a range of microorganisms, such as *E. coli* and *Candida albicans*, and therefore has the potential for therapeutic application (Hsu et al., 2009).

On that note it is imperative to point out that the expression of AMPs in eukaryotic systems is a common procedure, and *S. cerevisiae* is the main host strain used. The presence of zwitterionic phospholipids or cholesterol, strongly reduces peptide binding. As these substances are abundant in eukaryotic cells, there is reduced toxicity towards the host cell (Wilmes et al., 2011). However, recent studies carried out by Weghuber et al. (2011), suggest that at high concentrations of cationic amphipathic peptides, the selectivity for bacterial membranes over eukaryotic host membranes is reduced, this may result in detrimental side-effects for the host and difficulties in production in a eukaryotic system (Weghuber et al., 2011). In this study carried out by Weghuber et al. (2011), the application of synthetic cationic AMPs resulted in the accumulation of sialylated proteins and lipids at the plasma membrane of various mammalian cells. Morton et al. (2007) have demonstrated the effect that natural AMPs, such as dermaseptin and magainin, have on yeast cells (Morton et al., 2007a; Morton et al., 2007b). Both dermaseptin S3 and magainin 2 are amphibian-derived α-helical cationic peptides that have been shown to have the ability to interfere with yeast DNA integrity *in vivo,* despite the resistance mechanisms of *S. cerevisiae* which is conferred by genes involved in telomere maintenance, chromosome organization and double-strand break repair. Futhermore, it was hypothesized that dermaseptin S3 may induce cell suicide in

S. cerevisiae, and its anti-fungal mode of action involves the initiation of programmed cell death (Morton et al., 2007a). Therefore, α-defensins may have antifungal activity when expressed in yeasts.

1.5.4.2 β-defensins

The first β-defensin, the tracheal antimicrobial peptide (TAP), was discovered in the bovine tracheal mucosa (Diamond et al., 1991). Bensch et al. (1995) later discovered the first human β-defensin (HβD-1), which was extracted from the blood of renal patients (Bensch et al., 1995). Today there are 31 human β-defensin genes in the human genome, and six of these β-defensin peptides have been isolated from human tissues, of which 4 have been characterized (Pazgier et al., 2006). The most well characterized β-defensins are HβD-1, -2, -3 and -4, encoded by *DEFB1*, *DEFB2*, *DEFB103* and *DEFB104* respectively (Dunsche et al., 2001; Harder et al., 2004). The majority of the human β-defensin genes were identified by Schutte et al (2002), via a genomic computational approach. Using this approach, 28 of the 31 genes were identified however, a portion of these genes represent pseudogenes containing premature stop codons (Schutte et al., 2002). The β-defensin genes are located on five gene clusters, with each cluster containing genes of a similar sequence and organization (Schutte et al., 2002). These five gene clusters are located across 3 chromosomes, 6, 8, and 20, with the genes coding for the well characterized defensins, HβD-1 to -4, located on chromosome 8p23-p22 (Schutte et al., 2002). The coding sequence of these genes contains two exons, the first exon transcribes the 5'UTR sequence and the leader domain of the preproprotein and the second exon transcribes the mature active peptide containing the characteristic six cysteine domain (Schutte et al., 2002). Posttranslational modifications include the proteolytic clevage of the leader sequence and the N-terminal propeptide (Ganz et al., 1993; Valore and Ganz, 1997).

HβD-1 to -4 are highly cationic peptides, consisting of approximately 38-47 amino acids and are between 4 to 5 kDa in size (Dhople et al., 2006). Each defensin contains a high number of arginine and lysine residues, this contributes to the high positive charge, which is between +4 to +11 at neutral pH (Schroder and Harder, 1999). There is little sequence homology between these amphipathic defensins (Fig. 1.4 B). In contrast, the tertiary structure of each characterized defensin is highly similar (Fig. 1.6). β-defensins

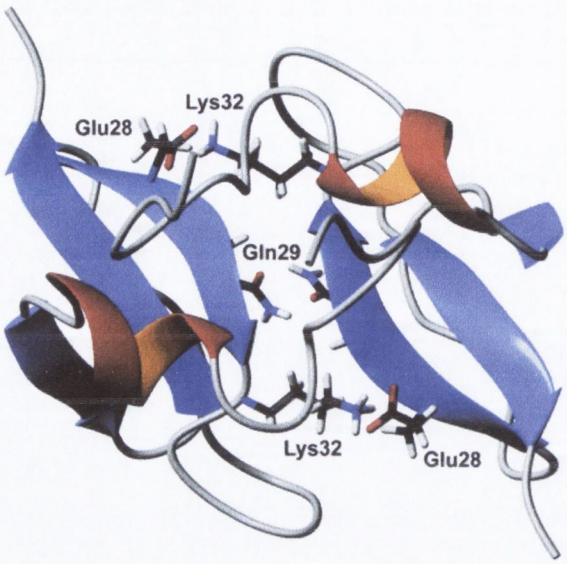

FIG. 1.6 Schematic representation of the structural aspects of native HβD-3 peptide

Tertiary structure of two HβD3 monomers, showing possible orientations for dimer formation. The Glu and Lys residues can be seen (Schibli et al., 2002).

are composed of 3 anti-parallel β-sheets and may be flanked by a short helical loop at the N-terminus. These antiparallel β-sheets are constrained by three intramolecular disulphide bridges, creating the characteristic "defensin-like" topological fold with spatially separated hydrophobic and hydrophilic regions (Pazgier et al., 2006). The cysteine connectivities characterisitic of β-defensins are Cys1-Cys5, Cys2-Cys4 and Cys3-Cys6 (Fig. 1.4, box 2) (Dhople et al., 2006). Furthermore, each β-defensin has a β-bulge in the second β-sheet, involving the highly conserved Gly-X-Cys motif, which is thought to be important for the correct folding and formation of the native structure (Xie et al., 2005). The β-defensin tertiary structure displays the potential to form oligomers (Pazgier et al., 2006).

HβD-1 to -4 are expressed on many epithelial surfaces such as that of the gastrointestinal tract, respiratory tract, reproductive system and the nasal and oral mucosa (Abiko et al., 2003). While HβD-1 is expressed constitutively in epithelial cells, HβD-2 and HβD-3 are inducibly expressed. The latter two defensins are expressed on epithelial surfaces following stimulation via pro-inflammatory cytokines such as interferon-gamma (IFN-γ), IL-1β or tumor necrosis factor-alpha (TNF-α), or exposure to microorganisms (Abiko et al., 2003). HβD-1 and HβD-2 have also been detected in saliva, and are derived from keratinocytes of the oral mucosa, providing the oral epithelium with AMPs (Abiko et al., 2003). Other AMPs, such as lysozyme, histatins and phospholipase, all involved in mediating the immune response, contribute to the antimicrobial protection of the oral cavity (Mandel, 1987). HβD-1 and -2 have been detected in saliva at approximately 150ng/mL, while the mRNA levels of HβD-3 are lower than that of HβD-1 and -2 (Abiko et al., 2003).

Like other human defensins, β-defensins are directly involved in innate immunity. These defensins provide a first line of defense against invading microorganisms, by multiple modes of activity, including directly targetting the invading cells and/or chemoattraction or stimulation of different host immune cells (Ganz, 1999; Pazgier et al., 2006; Pazgier et al., 2007a; Yang et al., 2002; Yang et al., 1999). HβD-1 to -3 act through the chemokine G protein-coupled receptor (GPCR) CCR6 (Pazgier et al., 2007b; Yang et al., 1999). The natural ligand of CCR6 is macrophage inflammatory protein-3 (MIP-3α). Comparisons of the tertiary structures of MIP-3α and HβD-1 and -2 revealed subtle similarities between these proteins, these similarities may mediate

receptor recognition (Hoover et al., 2002; Perez-Canadillas et al., 2001). The chemoattractant activities of β-defensins also involve the attraction of immature dendritic cell and memory T-cells to the site of infection through interaction in CCR6 (Yang et al., 1999). Hoover et al. (2003) have suggested that this chemoattractive ability of β-defensins only occurs when the defensin is correctly folded. The structure of β-defensins, to a certain extent, dictates the mode of action of β-defensins. The charged residues and hydrophobicity are responsible for electrostatic interactions and disruption of the lipid bilayer, respectively, as described in section 1.5.1 (Brogden, 2005; White et al., 1995).

While HβD-1, -2 and -3 have similar tertiary structures, they vary in their antimicrobial spectrum and activity in certain environments. The HβD-1 gene maps to the chromosomal region of 8p23.1 – 23.2, which is close in proximity (within 100 – 150kb) to the gene that encodes HNP-1, both of which are expressed in the salivary ductal cells (Liu et al., 1997). HβD-1 is 36 amino acids in length, with a charge of +4 and a molecular weight of 3.9 kDa (Fig. 1.4 box 2) (Bensch et al., 1995). HβD-1 is monomeric and has the ability to form weak dimers (Hoover et al., 2001). Mutagenesis studies carried out on HβD-1, revealed that the cationic residues at the C-terminus were imperative for activity, while the N-terminal residues were deemed essential for chemotactic activity with CCR6 transfected cells (Pazgier et al., 2007b). Furthermore, the promoter of HβD-1 contains various E-box-like c-Myc binding sites and a PAX2 (paired box gene 2) consensus recognition sequence (Sherman et al., 2006; Bose et al., 2009). Thus, HβD-1 may be upregulated by a non-inflammatory pathway involving c-Myc and can be repressed by the binding of PAX2 to the promoter (Sherman et al., 2006; Bose et al., 2009). HβD-1 has been shown to be particularly active against Gram-negative bacteria and fungi, but is significantly less potent against Gram-positive bacteria (Goldman et al., 1997). This defensin also shows decreased activity levels in an environment containing high salt concentrations (Dale and Krisanaprakornkit, 2001; Jia et al., 2001; Schroder and Harder, 1999; Weinberg et al., 1998). Schroeder et al. (2011) illustrated that the activity of HβD-1 *in vitro* can be increased upon reduction of disulphide bonds, although this effect on *in vivo* activity remains to be determined.

Similar to HβD-1, HβD-2 was first isolated from psoriatic skin lesions and displays preferential activity against Gram-negative bacteria compared to Gram-positive bacteria

(Bals et al., 1998; Harder et al., 1997; Schulz et al., 2005). The peptide has a molecular weight of 4.3 kDa, contains 41 amino acid residues and a net charge of +6 (Fig. 1.4 box 2) (Harder et al., 1997). It is mostly monomeric in bulk solution, with a mildly amphipathic N-terminal helix (Bauer et al., 2001; Hoover et al., 2000; Sawai et al., 2001). Crystallographic studies demonstrated that HβD-2 may form dimers at higher concentrations, and it was the first β-defensin to report that oligomerization can occur from non-covalent bonding of dimers (Hoover et al., 2000). Similar to HβD-1, HβD-2 antimicrobial activity is affected by high salt concentrations and a significant reduction in activity is observed under these conditions (Dale and Krisanaprakornkit, 2001; Jia et al., 2001; Schroder and Harder, 1999; Weinberg et al., 1998). Studies by Hoover et al. (2003) suggest that the α-helical N-terminus of HβD-2 is involved in the antimicrobial activity of this peptide. Furthermore, the HβD-2 promoter contains one AP-1 (Activator Protein-1) binding site and three NF-κB binding sites (Jang et al., 2004; Wehkamp et al., 2004; Wehkamp et al., 2006). Thus, HβD-2 expression is regulated by NF-κB and it is also induced by various proinflammatory stimuli including IL-1α, IL-1β and TNF-α (Moon et al., 2002; Jang et al., 2004; Wehkamp et al., 2006).

Harder et al. (2001) and Garcia et. al (2001) simultaneously reported the identification of HβD-3, which was isolated from human lesional psoriatic scales (Dhople et al., 2006; Garcia et al., 2001; Harder et al., 2001). It has since been isolated from primary keratinocytes and lung epithelial cells (Harder et al., 2001). HβD-3 is a small highly cationic peptide, with a net positive charge of +11 and a molecular weight of 5.1 kDa (Dhople et al., 2006). It consists of 45 amino acids with an asymmetrical distribution of charged residues, clustered mainly at the carboxyl-terminal region (Fig. 1.4 box 2). The peptide can be defined as a β-defensin by its six-cysteine motif spacing (Fig. 1.4, box 2). HβD-3, like HβD-1 and HβD-2, possesses a tertiary structure consisting of 3 antiparallel β-sheets and a short helical loop at the N-terminus (Dhople et al., 2006), stablized by the typical β-defensin intramolecular disulphide bridges (Pazgier et al., 2006). Unlike HβD-1 and -2, this peptide has the ability to form a stable, symmetrical dimer (Fig. 1.6) and higher ordered oligomeric structures (Dhople et al., 2006). Interaction occurs via glu-28 and lys-32 of the β-2 strands promoting the formation of a salt bridge, stabilizing the dimer (Fig. 1.6) (Pazgier et al., 2006). The dimerization, with the ability to oligomerize supports the carpet-type mechanism of action as explained in section 1.5.1 (Pazgier et al., 2006).

HβD-3 is a highly potent endogenous antibiotic and has a very broad spectrum of antimicrobial activity, and is active against Gram-positive and Gram-negative bacteria, fungi and viruses (Harder et al., 2001). It also displays antimicrobial activity against a number of multidrug-resistant clinical isolates of common nosocomial pathogens including *E. faecium* and *P. aeruginosa*, with reduced activity in the presence of human serum (Maisetta et al., 2006). Unlike other β-defensins, the activity of HβD-3 is salt independent (Harder et al., 2001). It is suggested that these HβD-3 specific traits are due to the peptides high cationic charge, along with its ability to form dimers (Schibli et al., 2002). Mutagenesis experiments carried out by Kluver et al. (2005) have shown that the distribution of positively charged amino acids and hydrophobic side chains determines HβD-3 antimicrobial potency (Kluver et al., 2005). Furthermore, studies by Boniotto, et al. (2003) included the formation of a ftkHβD-3 analog, whereby the three residues responsible for dimerization, Lys_{26}-Glu_{27}-Glu_{28}, were replaced by Phe-Thr-Lys, the residues which are present in HβD-1. This analog did not undergo dimerization, yet its antimicrobial activity was comparable to the native HβD-3 against *S. aureus* (Boniotto et al., 2003). Thus, HβD-3 is of specific interest in terms of biological significance and for use in food preservation, or as a therapeutic application.

HβD-3 is inducibly expressed on the surfaces of epithelial cells, and depending on the stimulant and the location of stimulation, induction of peptide expression is carried out by many different pathways (Dhople et al., 2006). HβD-3 is under the control of an inducible, mosaic promoter which contains binding sites for AP-1, NF-κB, NF-IL-6 response elements and IFN-γ interferon response elements (Sperandio et al., 2008; Scharf et al., 2010). HβD-3 expression is induced by multiple factors including interleukin-1, tumor necrosis factor-α, interferon-γ, as well as Gram-negative and Gram-positve bacteria (Dhople et al., 2006), along with covalent expression. It is expressed in various regions of the human body including, the uterus, pharynx, kidney, thymus and placenta (Harder et al., 2001; Jia et al., 2001). Host proteases, cathepsins, are required for HβD-3 regulation (Dhople et al., 2006). Data by Ji, et al. (2009) indicated that, toll-like receptor 2 (TLR2) and pyrin domain-containing protein 2 (NALP2) mediate the induction of human beta-defensins by *Fusobacterium nucleatum* in gingival epithelial cells (Ji et al., 2009). Whilst studying the role of AMPs in the prevention of bacterial bone infection, Varoga et al. (2009) suggest that the bacterial induction of HβD-3 occurs via TLR-2 and -4 in osteoblasts (Varoga et al., 2009).

HβD-3 is known to connect the innate and adaptive immune system due to its role in chemoattraction. It is involved in many different diseases and can impact on these positively or negatively. Steubesand et al. (2009) demonstrated that NF-κB and MAPK signalling pathways contribute to the regulation of HβD-2 in *Candida* esophagitis (Steubesand et al., 2009). Futhermore HβD-3 was classed as a downstream target of a distinct EGFR/MAPK/AP-1 pathway in *Candida* esophagitis infection. HβD-3, from tumorigenic human embryonic kidney 293 cells (HEK293), has been demonstrated to act as a chemoattractant for the recruitment of tumor-associated macrophages (TAMs) (Jin et al., 2010). HβD-3 chemoattracts macrophages/monocytes via the chemokine receptor CCR2, supporting the growth and progression of tumors (Jin et al., 2010). The disulphide topology of HβD-3 may contribute to its chemotactic activity. Various HβD-3 isoforms, with alternative disulphide linkages, have been shown to possess different chemotactic activities against monocytes and CCR6+HEK293 cells (Wu et al., 2003). In some cases, certain isoforms showed enhanced activity compared to that of the natural chemokine ligand of CCR6, which is MIP-3α, while the disulphide deficient HβD-3 variant showed no activity (Wu et al., 2003).

The exact mechanism of action of HβD-3 is still unknown. HβD-3 is believed to disrupt negatively charged membranes and cause leakage of cellular contents, resulting in cell death by osmosis (Dhople et al., 2006). Morgera et al. (2008), suggest that HβD-2 and HβD-3 interact with membranes as cationic β-sheet platforms, presenting amphipathic helices for insertion into the lipid bilayer. The dimeric β-sheet platform, is membrane-stabilised, and presents aligned anti-parallel helices to the membrane for insertion. The β-sheet structure seems to be the key element in antimicrobial activity of HβD-3, while the helical stretch may affect membrane selectivity and/or killing kinetics (Morgera, 2008). These suggested non-specific membrane permeabilising mechanisms subsequently make the resistance of bacteria rare, but not unachievable. HβD-3 activity has been reportedly inhibited by the 31 kDa protein streptococcal inhibitor of complement (Yu et al., 2008), which is predominantly secreted by M1 strains of group A *Streptococci* (Dhople et al., 2006). Futher studies carried out by Sass et al. (2008) proposed a specific mode of action for HβD-3 against *S. aureus*. It was indicated that HβD-3 affects the cytoplasmic membrane of *S. aureus*, but this effect does not contribute greatly to cell death. Results obtained in this study hypothesize that in actual fact, HβD-3 interfers with complex functional membrane-associated processes, through

low-affinity interaction with membrance components,exerting multiple stresses at many sites (Sass et al., 2008). This combination of stresses on important machineries such as the cell wall biosynthesis machinery, subsequently leads to cell death. This hypothesized mode of action, which involves untargetted activities, would also explain why high-level resistance is rare.

Research into HβD-3 is ongoing since isolation of the peptide approximately ten years ago. The exact mode of action of this peptide against various microorganisms is still unclear. Due to the broad antimicrobial spectrum of HβD-3, and its unique stability in harsh environments such as exceedingly high salt concentrations, this AMP may be applied to various scenarios such as therapeutic applications and food preservation. Ito et el. (2009) have been investigating the introduction of HβD-3 into engineered keratinocyte sheets, which exhibited significant antimicrobial activity (12). From these findings, they suggest that the therapeutic introduction of HβD-3 into cell sheets may provide a new gene therapy strategy for infectious diseases. HβD-3 has the ability to perform as an alternative antimicrobial agent for use in food preservation. In this project, we aim to apply HβD-3 to the preservation of beer and use this system to combat the unresolved problem of beer spoilage.

1.6 Research undertaken prior to Ph.D.

Research was carried out prior to this Ph.D. by Dr. Tharappel James.

Many studies have demonstrated the effectiveness of defensins against both Gram-positive and Gram-negative bacteria. As indicated in section 1.4.2, Gram-positive bacteria, specifically the lactobacilli and pediococci species, are major sources of contamination during alcohol fermentation by yeasts. The aim of our research was to determine if AMPs, and in particular HβD-3, are effective at eliminating BSMs during and after yeast fermentations. Ultimately, if we were successful, we wished to engineer yeast strains to express and secrete HβD-3 during fermentation and thus provide prophylactic protection against BSMs during fermentation with additional potential neutraceutic value.

To initiate these studies, the mature HβD-3 peptide was chemically synthesized by GL Biochem (Shanghai) Ltd. HβD-3 is a 67 amino acid peptide in its precursor form, 22 of which form the native signal peptide. The synthetic peptide used in this study contained the 45 amino acids that form the mature HβD-3 peptide. A chimeric gene construct was synthesized to incorporate the *S. bayanus* phosphoglycerate kinase ($PGK1_{SB}$) promoter, a signal sequence of the yeast mating factor pheromone alpha-factor, the HβD-3 gene and the termination sequence in the 3' untranslated region of the alcohol dehydrogenase (*ADH*) gene. The α-factor signal sequence from *S. cerevisiae*, was fused to the HβD-3 gene to ensure direct secretion of the peptide from the yeast cell. The protease necessary to cleave the α-factor signal sequence (KEX2) is present in *S. pastorianus* (Seeboth and Heim, 1991). The amino acid sequences of HβD-3 (NCBI/Genebank, Gene ID: 55894) and the α-factor signal sequence, were reverse translated to DNA sequences, with codon optimisation for yeast protein production. The *ADH* terminator was used as it is akin to fermentation conditions. Thus, the HβD-3 gene construct contains the $PGK1_{SB}$ promoter, the α-factor signal sequence, the HβD-3 gene, and the *ADH* terminator (Fig. 1.7). This DNA fragment (951bp) was synthesized, and inserted into the BamHI site of a pBlueScript SK plasmid (Fig. 2.1) (pBSK-) (Stratagene) in the order displayed in Fig. 1.7. This work was carried out by GenScript, USA INC. The DNA sequence of the gene construct is shown in Appendix I.

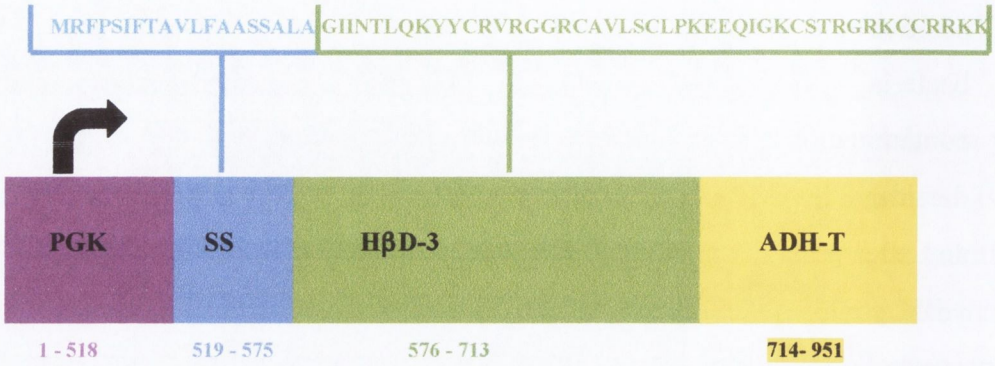

FIG. 1.7 Schematic representation of HβD-3 gene construct.

A HβD-3 gene construct was synthesized and inserted into the multiple cloning site of a pBluescript SK(-) plasmid. *S. bayanus PGK1* promoter: pink. α-factor leader sequence: blue. HβD-3 gene: green. *ADH* terminator: yellow. The amino acid sequence of α-factor signal sequence and HβD-3 is in blue and green respectively.

Note: Diagram not to scale.

Initially the HβD-3 gene construct (Fig. 1.7) was cloned into pGREG vectors, which contain a yeast autonomously replicating sequence (ARS). The pGREG vectors 505 and 506 differ only in auxotrophic markers. pGREG-505 contains a *LEU2* marker while pGREG-506 contains a *URA3* marker (Fig. 2.2) (Jansen et al., 2005). Both of these plasmids contain a *GAL1* promoter (401bp) for the control of inserted genes, a *HIS3* stuffer cassette (1159bp) and a kanamycin resistance (kanMX) cassette (746bp) (Fig. 2.2) (Jansen et al., 2005). The HβD-3 gene constructs were cloned into pGREG-505 and pGREG-506, replacing the *HIS3* cassette. The resultant pGREG-505 plasmid contains the *GAL1* promoter, α-factor signal sequence, the HβD-3 gene, a partial *ADH* terminator and a full length *CYC* terminator (Fig. 1.8 A). This construct will be referred to as pGREG505hbd3GAL1 throughout the rest of this thesis (Fig. 1.8 A). Similarly, the pGREG-506 construct contains the *GAL1* promoter, α-factor signal sequence, the HβD-3 gene, a full length *ADH* terminator and a full length *CYC* terminator (Fig. 1.8 B). This construct will be referred to as pGREG506hbd3GAL1 throughout the rest of this thesis (Fig. 1.8 B). These procedures were accomplished by exploiting homologous recombination in *S. cerevisiae* as outlined in Jansen et al., 2005. HβD-3 gene construct PCR products were generated with regions of homology to the recombination sites in pGREG vectors 505 and 506. The *HIS3* stuffer gene was digested from pGREG-505 and -506 using SalI restriction enzymes and the HβD-3 PCR product and linearised plasmid were recombined in *S. cerevisiae* using lithium acetate transformation. Fig. 1.8 will be referred to throughout the rest of this thesis, in schematics illustrating pGREG505hbd3GAL1 and pGREG506hbd3GAL1.

Following DNA sequence verification and the expression of HβD-3 in these plasmids, the HβD-3 gene construct (Fig. 1.7) was amplified in two overlapping fragments from the pBSK-HβD-3 plasmid. The forward primer amplifying the $PGK1_{SB}$ promoter has sequence homology at its 5' end to the intergenic region between the open reading frames YPR159W and YPR159C-A. The kanMX cassette was amplified from pGREG-505 (Fig. 2.2) using a forward primer which overlaps with the *ADH* termination squence and a reverse primer with sequence homology to YPR160W. Fragments were integrated contiguously by homologous recombination into the genome of *S. pastorianus* CMBS-33 between YPR159C-A and YPR160W, on chromosome XVI (Fig. 1.9). This region contains an uncharacterized hypothetical open reading frame (ORF), YPR159C-A, which interacts with at least five proteins, mostly relevant to the

FIG. 1.8 Schematic representation of regions of interest in pGREG vectors.

A HβD-3 gene construct was synthesized and inserted inbetween the recombination sites of two pGREG plasmids. Gal promoter: red. α-factor signal sequence: blue. HβD-3: green. *ADH* terminator: yellow. *CYC* terminator: orange. The rec 1 and rec 2 sequences are highlighted in pink. The SacI restriction sites of each plasmid, located within a region of untranslated sequence (dark green), are underlined in the dark green text box. The SpeI restriction sites, of each plasmid, located in the non-specific 5'UTR region, are underlined. The SalI restriction sites, of each plasmid are denoted in pink, underlined nucleotides. A. Regions of pGREG505hbd3GAL1 (8537bp), which contains a partial *ADH* terminator and a *CYC* terminator. B. Regions of pGREG506hbd3GAL1 (7613bp), which contains a full *ADH* terminator and a *CYC* terminator.

Note: This diagram is not to scale.

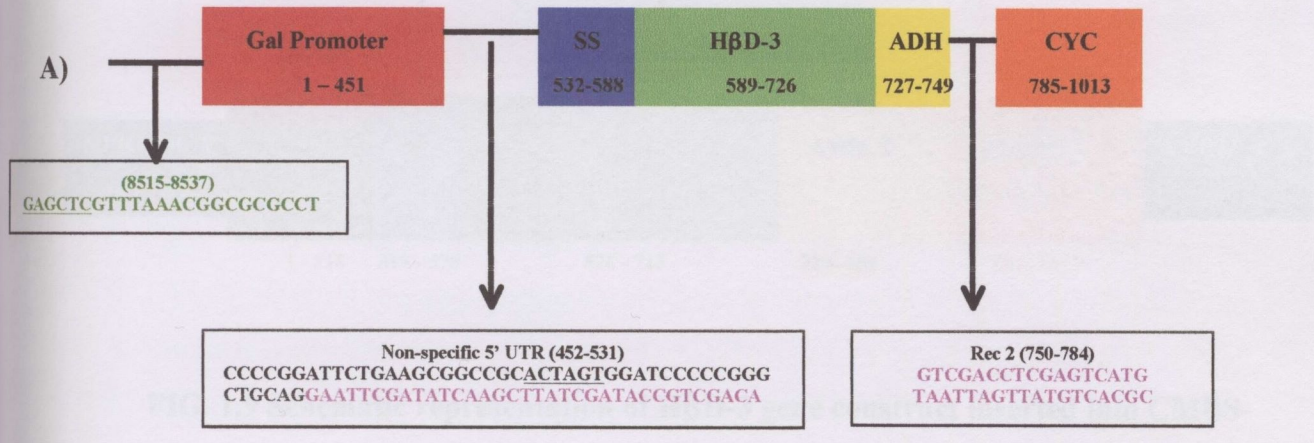
A)
Gal Promoter
1 – 451
SS
532-588
HβD-3
589-726
ADH
727-749
CYC
785-1013
(8515-8537)
GAGCTCGTTTAAACGGCGCGCCT
Non-specific 5' UTR (452-531)
CCCCGGATTCTGAAGCGGCCGCACTAGTGGATCCCCCGGG
CTGCAGGAATTCGATATCAAGCTTATCGATACCGTCGACA
Rec 2 (750-784)
GTCGACCTCGAGTCATG
TAATTAGTTATGTCACGC

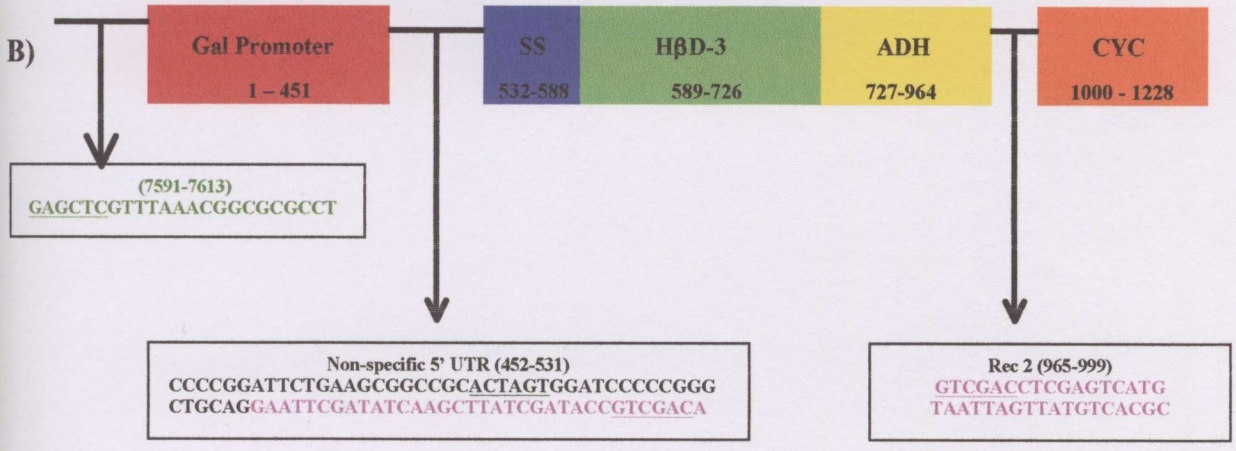
B)
Gal Promoter
1 – 451
SS
532-588
HβD-3
589-726
ADH
727-964
CYC
1000 - 1228
(7591-7613)
GAGCTCGTTTAAACGGCGCGCCT
Non-specific 5' UTR (452-531)
CCCCGGATTCTGAAGCGGCCGCACTAGTGGATCCCCCGGG
CTGCAGGAATTCGATATCAAGCTTATCGATACCGTCGACA
Rec 2 (965-999)
GTCGACCTCGAGTCATG
TAATTAGTTATGTCACGC

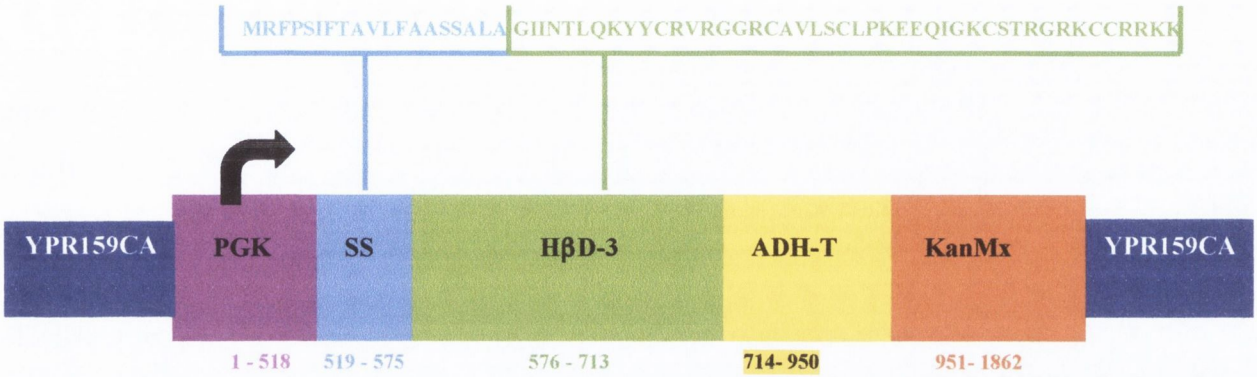

FIG. 1.9 Schematic representation of HβD-3 gene construct inserted into CMBS-33.

A HβD-3 gene construct was synthesized in the above order and inserted into the CMBS-33 genome, in the putative gene of YPR159C-A, located between YPR159W and YPR160W, on chromosome XVI. *S. bayanus PGK1* promoter: pink. α-factor leader sequence: blue. HβD-3 gene: green. *ADH* terminator: yellow. YPR159C-A: navy. The amino acid sequence of α-factor signal sequence and HβD-3 is in blue and green respectively. Note: Diagram not to scale.

endoplasmic reticulum and secretion (Yu et al., 2008). Two separate integration clones were generated creating two unique lager strains, CM-INT-37 and CM-INT-51. The HβD-3 gene construct was integrated 129bp upstream of the start codon of YPR160W. As mentioned in section 1.2.2, *S. pastorianus* is an allotetraploid, containing four copies of chromosome XVI. Three copies contain a *S.cerevisiae*-like YPR159W gene and the fourth copy contains a *S. bayanus*-like YPR159W gene. Furthermore, three copies of chromosome XVI contain a mosaic *S. cerevisiae*-like/*S. bayanus*-like YPR160W gene and the fourth copy contains a *S. bayanus*-like YPR160W gene (Usher and Bond, 2009). Potentially the gene cassette could integrate into any one, or all four, of the putative integration regions. Sequence analysis indicates that one copy of the HβD-3 gene cassette has been integrated into a hybrid copy of chromosome XVI, for CM-INT-37 and CM-INT-51. Microarray analysis of the copy number of the region YPR159C-A to YPR190W indicated that CM-INT-37 has a lower *S. bayanus* copy number for this region compared to CM-INT-51. Preliminary data indicates that CMBS-33, CM-INT-51 and CM-INT-37 have one, two and three copies respectively of *S. cerevisiae* in this region. This current hypothesis does not agree with previous publications which indicate that *S. pastorinaus* has no copies of *S. cerevisiae* in this region (Nakao et al., 2009; James et al., 2008), thus further experimentation is needed to examine this current hypothesis in detail.

1.7 Objectives of this project

The overall aim of this project was to examine the possibility of using HβD-3 in the fermentation process as a natural antimicrobial, to defend against beer spoiling micro-organisms. The co-production of the HβD-3 peptide during the brewing process would be advantagous to the beverage in terms of shelf-life and would also eliminate the need for added perservatives. Secreting HβD-3 throughout the fermentation process may allow pasturization regimes to be omitted, lowering energy costs. The resulting beverage may be regarded as a functional food with therapeutic potential to fight off oral bacterial infections, while the spent yeast with antimicrobial properties could also be used as animal feed. Furthermore, the use of HβD-3, compared to bacteriocins or other AMPs, provides an effector molecule of innate host defense system, as it is a naturally occuring human peptide.

The specific aims of this thesis are:

1. To generate a series of lager yeast strains expressing HβD-3 under the control of a variety of promoters.
2. To analyse the expression levels and secreted levels of HβD-3 from each of the generated strains, and from the strains CM-INT-37 and CM-INT-51, which contain the gene integrated into the genome.
3. To determine the level of antimicrobial activity of recombinant HβD-3 in concentrated supernatant samples of each of the above strains.
4. To examine the antibacterial activity of recombinant HβD-3 *in vivo,* establish if the peptide is active in a fermentative environment and design specific treatment methods to amplify this activity.

Here we report the first expression of HβD-3 from a *S. pastorianus* strain.

Chapter 2: Materials and Methods

2.1 Reagents, strains, media and growth conditions

All chemicals and reagents were of analytical grade and unless otherwise stated were purchased from Sigma-Aldrich (Dublin, Ireland). The water used through out this study was sterile distilled water.

2.1.1 Strains

Saccharomyces cerevisiae strain S150 (Bond Laboratory, Trinity College Dublin) (*Mat* **a**, *leu*2-3, 112 *ura*3-52, *trp*1-289, *his*3) is a haploid laboratory yeast strain. *Saccharomyces pastorianus* is a polyploid yeast strain. The bottom fermenting lager yeast strain CMBS-33 was from the Centre for Malting and Brewing Science (Leuven, Belgium) Lager Strain Collection (kindly provided by Dr. K. Verstrepen). *Lactobacillus brevis* 1268 and *Pectinatus frisingensis* 6306 were obtained from Deutsche Sammlung von Mikroorganismen und Zellkulturen GmbH, Braunschweig, Germany (DSMZ). Plasmid propagation was carried out in *Escherichia coli* XL1-Blue (*recA1*, *endA1m*, *gyrA96*, *thi-1*, *hsdR17*, *supE44*, *relA1*, *lac*[*F'proAB*, *lacIZ_M15*, *Tn10*] (Stratagene, La Jolla, CA, USA).

2.1.2 Yeast strains and growth conditions

Yeast strains were cultured at 30°C for 48 hours unless otherwise stated. The standard growth medium was YEPD (1% (w/v) yeast extract, 2% (w/v) bacto peptone, 2% (w/v) dextrose), or synthetic complete media (SC.; 6.7g litre^{-1} yeast nitrogen base w/o amino acids and ammonium sulfate (Formedium, Norwich, England), 0.5% (w/v) $(NH_4)_2SO_4$, 0.57g litre^{-1} drop out medium (Foremedium, Norwich, England)), 20g litre^{-1} glucose and supplemented with amino acids: 0.2g litre^{-1} adenine, 0.12g litre^{-1} lysine, 0.08g litre^{-1} tryptophan, 0.08g litre^{-1} leucine, 0.02g litre^{-1} histidine, and 0.03g litre^{-1} uracil. Agar plates of the above media were made by addition of 17g litre^{-1} of agar.

For the induction of yeast clones that contained the pGREG vectors with a *GAL1* promoter, a medium containing galactose as a carbon source (YEPGal) was used (1% (w/v) yeast extract, 2% (w/v) bacto peptone, 2% (w/v) galactose) or SC galactose (as described above except containing 2% (w/v) galactose in place of 2% dextrose). For the induction of HβD-3 from cells containing the pGREG vector with an *AGT1* promoter in place of the *GAL1* promoter, SC or YEP media containing 2% maltose as a carbon source. Yeast clones containing the following constitutive promoters *S. cerevisiae*

TEF1, *S. bayanus* $PGK1_{SB}$ and *S. cerevisiae* $PGK1_{SC}$ were also grown in YEPMal or SC-Mal.

All yeast clones containing pGREG vectors were grown in medium containing 0.2 g litre^{-1} of G418 disulphate (geneticin) (Melford, Suffold, UK) aminoglycoside antibiotic. All yeast clones containing pRS vectors were grown in medium containing 0.3g litre^{-1} of hygromycin B.

2.1.3 Bacterial strains and growth conditions

Lactobacillus brevis L1055 was cultured at 37°C overnight in MRS media (10g litre^{-1} universal peptone, 5g litre^{-1} meat extract, 5g litre^{-1} yeast extract, 20g litre^{-1} D(+)-glucose, 2g litre^{-1} K_2HPO_4, 2g litre^{-1} diammonium hydrogen citrate, 5g litre^{-1} NaOAc, 0.1g litre^{-1} $MgSO_4$, 0.05g litre^{-1} $MnSO_4$, final pH 6.5 +/- 0.2 at 37°C) (DeMan, 1960). To prevent yeast growth in combined bacterial and yeast cultures, MRS media was supplemented with cycloheximide at 80μg/mL. *Pectinatus frisingensis* was cultured at 30°C in MRS broth. Culture conditions for strictly anaerobic bacteria were as described by (Miller and Wolin, 1974). *Escherichia coli* XL1-Blue was cultured in L-broth at 37°C, 200rpm overnight. Agar plates of the above media were made by addition of 17g litre^{-1} of agar.

2.1.4 Monitoring the growth of yeast and bacterial cultures

The growth of yeast and bacterial cultures was determined by measuring the optical density of the culture at a wavelength of 600nm. 1mL of culture was aliquoted into a plastic cuvette and the OD_{600} value was measured in an Eppendorf BioPhotometer V1.35.

2.2 Polymerase chain reaction (PCR) and gel electrophoresis

All reagents were suppiled by Yorkshire Bioscience Ltd. (York, UK) unless otherwise stated. Primers were supplied by IDT (San Jose, CA, USA) or Sigma-Aldrich (St. Louis, MO, USA). Primers were manually designed to incorporate sequences of homology to the region of amplification, ensuring each primer in a pair had similar melting temperatures. Oligonucleotide primers used in this study are listed in Tables 2.1 and 2.2. All PCR reactions were carried out in a 25μl reaction mixture, which contained a final concentration of 0.25mM dNTPs, 1X Buffer N (10mM Tris-Cl [pH 8.8], 50mM KCl, 1.5mM $MgSO_4$, 0.1% Triton X-100), 1.5mM $MgCl_2$, 400nM forward primer, 400nM reverse primer and 50-200ng of desired genomic DNA, or 10-30% of

Table 2.1 Oligonucleotide primers used to amplify plasmids, integration and genomic DNA

Primer name	Oligonucleotide sequence (5'-3')[a]
One-4-all_F1	GAATTCGATATCAAGCTTATCGATACC
One-4-all_R	GCGTCCCAAAACCTTCTCAAGCAA
One-4-all_F2	CGATATCAAGCTTATCGATACCG
KanMX_F	CGTTTTCGACACTGGATGGCGGCG
KanMX_R	GGAAAAGACTCACGTTTCGAGGCC
HβD-3_F1	GTTCGCTGCTTCTTCTGCTT
HβD-3_R1	TTTTTCTTCTACAACATTTTCTACCTC
HβD-3_R2	GCTTATTTAGAAGTGGCGCGCCTC
RT-PCR HβD-3_R	GAGGCGCGCCACTTCTAAATAAGC
GAL1_F	TAGTACGGATTAGAAGCCGCCG
GAL1_R	ATCCGGGGTTTTTTCTCCTTGACG
Rec1_F	GAATTCGATATCAAGCTTATCGATACCG
Rec2_R	GCGTGACATAACTAATTACATGACTCGAGG
T3_F	ATTAACCCTCACTAAAGGGA
$PGK1_{SC}$_F1	CAAGGTCCTAGCGACGGCTCACAGG
$PGK1_{SC}$_R1	CCTGTGAGCCGTCGCTAGGACCTTG
$PGK1_{SB}$_F1	GACGAATTTTGTGAAAAGAGCACCC
ADHT_R	CCTAGCGGATCTGCCGGTAGAG
AGT1_F1	CCGGGCTTGAGGGACATACAGAGAC
AGT1_R1	GTCTCTGTATGTCCCTCAAGCCCGG
TEF1_F1	CCTCTAGGGTGTCGTTAATTACCCG
TEF1_R1	CGGGTAATTAACGACACCCTAGAGG
hphNT1_R	CAATGTCAAGCACTTCCGGAA
2μm_F	ACATACAGCTCACTGTTCACGTC
LacO_F	GCGGGCCTCTTCGCTATTACGCC
LacO_R	GGAATTGTGAGCGGATAACAATT
TDH-3_F	CTGTCAAGTTGAACAAGGAAACCAC
TDH-3_R	CAACGTGTTCAACCAAGTCGACAA
Actin_F	CTGAATTAACAATGGATTCTGGTA
Actin_R	AGATACCTCTCTTGGATTGAGCTT
YPR159W_F	GTTCCCCGGATGGTATTTCT
YPR159W_R	TTTGCAAGGATTGAGAGGCTA
YPR160W_F	TTCGTGACAATTTGGTCATTG
YRP160W_R	TGACAGGAATTTGCACTTCG
5.8S_F	CGGATCTCTTGGTTCTCGC
5.8S_R	TGACGCTCAAACAGGCATG
YPR159W_F	GTTCCCCGGATGGTATTTCT
YRP159W_R	TAGCCTCTCAATCCTTGCAAA
YPR160W_F	TTCGTGACAATTTGGTCATTG
YPR160W_R	CGAAGTGCAAATTCCTGTCA

[a] Reverse primers are in reverse complement

Note primers are grouped together based on plasmid template

Table 2.2 Oligonucleotide primers used for promoter[a] swap, gene[b] swap and [c]HIS-TAG in plasmids

Primer name	Oligonucleotide sequence (5'-3')[d]
[a]AGT1_F2	**CAAGCGCGCAATTAACCCTCACTAAAGGGAACAAAAGCT** GTTGTGTGGGGTCCGCGAAAATTTCCGG
[a]AGT1_R2	**CGGTATCGATAAGCTTGATATCGAATTCCTGCAGCCCGG GGGATCC**ATTATACTATTTTTTTAGTTGTTTGATGTTC
[a]PGK1$_{SC}$_F2	**CAAGCGCGCAATTAACCCTCACTAAAGGGAACAAAAGCT** GCCAAGAATTACTCGTGAGTAAGGAAAGAGTGAGG
[a]PGK1$_{SC}$_R2	**CGGTATCGATAAGCTTGATATCGAATTCCTGCAGCCCGG GGGATCC**CCGCGGTGTTTTATATTTGTTGT
[b]PGK1$_{SB}$_F2	**GACTCACTATAGGGCGAATTGGGTACCGGG**GACGAA TTTTGTGAAAAGAGCACCC
[b]ADHT_R1	**AACCCTCACTAAAGGGAACAAAAGCTGGAGCTCCAC CGCG**TATATTACCCTGTTATCCCTAGC
[c]HIS-TAG_R	**GCGTGACATAACTAATTACATGACTCGAGGTCGACT CA***GTGATGGTGATGGTGATG***TTTTTTTCTTCTACAACAT TTTCTACCTC**

[a] Sequences highlighted in bold represents homology to pGREG vectors

[b]Sequences highlighted in bold represents homology to pRS42H

[c]Reverse primers are in reverse complement and sequences highlighted in bold represent homology to pGREG505GAL1

cDNA reaction mix. Either 0.04U Taq polymerase, and/or 1unit of Verizyme™ polymerase was additionally used when required. The PCR cycle used to generate fragments was 95°C for 5 min followed by 20-35 cycles of 95°C for 30 sec, 55-60°C for 45 sec, 72°C for 1 min and a final elongation hold of 72°C for 10 min. PCR was performed using an Applied Biosystems GeneAmp® PCR System 2700.

20-50% of each PCR reaction was mixed with 2µl of sample loading buffer (0.1% Bromophenol blue, 0.1% Xylene Cyanol blue, 50% (w/v) Glycerol and 10mM EDTA, [pH8]). The sample was electrophoresed on 1-2% (w/v) agarose gel in TAE buffer (40 mM Tris, 20 mM glacial acetic acid, 2 mM EDTA [pH 8]), or TBE buffer (89mM Tris, 89mM Boric acid and 2mM EDTA [pH8]) containing ethidium bromide (1.25 µg ml^{-1}). Electrophoresis was carried out at approximately 60V for 1hrs and the gel was visualised on a UV transilluminator at 302 nm. DNA size ladders, either Hyperladder I (200bp-10000bp) or Hyperladder II (50bp-2000bp) (Bioline, Kilkenny, Ireland), were included in each gel,. Alternatively Q-Step 1 Quantitative DNA Ladder (100-1250bp) and Q-Step 4 Quantitative DNA Ladder (100-10,000bp) (Yorkshire Bioscience Ltd, York, UK) were used.

2.3 Gel extraction and purification

Following gel electrophoresis, DNA bands were excised from the agarose gel. The agarose plug fragment was transferred to a centrifuge tube and mixed with 500 µl of gel dissolving solution (5.5 M guanidine thiocyanate, 10 mM Tris-HCl [pH 7.5]). The solution was heated to 55°C until the agarose melted. Following vortexing, the agarose solution was transferred to a silica resin spin column (Epoch LifeScience, Texas, USA). The column was centrifuged at 14,000rpm for 1 min. The column was washed with 500 µl of wash buffer (60% (v/v) ethanol, 60 mM potassium acetate, 10 mM Tris-HCl [pH 7.5]). Following centrifugation at 14,000rpm, the column was transferred to a new collection tube and centrifuged again to dry the column. The column was transferred to a centrifuge tube and the purified DNA was eluted in 20 µl of sterile distilled water.

2.4 Direct Colony PCR

Direct colony PCR was carried out to screen for the presence of recombinant DNA in yeast transformants. Cells were lysed open by incubation in 10µl of 20mM NaOH, at 95°C for 10 min. 1µl of cell lysate was used as a template for PCR reactions as

described in Section 2.2, using primers specific for the cloned fragment and the surrounding sequence (Table 2.1/2.2).

2.5 DNA Purification

Genomic DNA was extracted from *S. pastorianus* as described by Cassago et al., (2002) with the following modifications. Yeast cells were cultured in YEPD media at 30°C, and at 200rpm overnight. 5-10mL of culture was centrifuged at 4,000rpm and the cell pellet was washed twice in sterile distilled water (SDW). The cell pellet was resuspended in 400µl of resuspension buffer (1% (w/v) sodium docecyl sulphate [SDS], 10mM EDTA and 0.1M Tris-HCl [pH8]). Acid-washed glass beads (0.5vol) were added. The solution was vortexed vigourously for 2 min. Tris-HCl buffered-phenol (pH 8) (0.5vol) was added and the solution was vortexed vigourously for 2 min. Chloroform (0.5vol) was added and the solution was vortexed vigourously for 2 min. Following vortexing and centrifugation at 14,000rpm for 5 min, the aqueous layer was transferred to a new tube. Two further extractions were carried out on the aqueous layer, first with one volume of tris-HCl buffered-phenol (pH 8) and chloroform as before, omitting the glass beads. The third extraction was carried out with one volume of chloroform. Following centrifugation as before, the DNA was precipitated by adding 1/10 of the volume of 3M sodium acetate (NaOAc) and 3 volumes of 100% EtOH to the aqueous layer. The mixture was placed at -70°C for a minimum of 45 min. Following centrifugation at 14,000rpm for 30min, the DNA pellet was washed with 70% EtOH. The DNA was then pelleted again and any remnants of alcohol were removed before resuspending the pellet in 50-100µl of SDW.

2.6 RNA Purification

RNA isolation was carried out using the hot-phenol method (Krieg, 1996) with some modifications. Cells were pelleted (10-50ml, OD_{600} 1-4) by centrifugation at 4,000 rpm for 10 min. Cells were washed twice with ice-cold diethyl pyrocarbonate (DEPC)-treated SDW. Collected cells were resuspended in 500µl of AE buffer (10mM EDTA, 50mM sodium acetate, pH 5.3), containing 1% SDS and 550µl of pre-warmed AE buffered-phenol (pH 5.3, 65°C). Acid-washed glass beads were added to half the volume. The solution was vortexed vigourously for 3 min, and then incubated at 65°C for 30 min, vortexing for 10 sec every 5 min. Following centrifugation at 14,000rpm for 5 min, the aqueous layer was transferred to a new tube. Two further extractions

were carried out on the aqueous layer, first with one volume of pre-warmed AE buffered-phenol (pH 5.3, 65°C), and second with one volume of chloroform. The RNA was precipitated as described previously for DNA. The dried pellet was resuspended in 50µl of DEPC-treated SDW. 5µg of RNA was added to 5µl of RNA loading buffer (100µl DEPC-SDW, 350µl formaldehyde, 1mL formamide, 200µl of 10X MOPS (200mM MOPS, 300mM Sodium Citrate [pH7]) and 350µl of sample loading buffer) and denatured at 65°C for 15 mins. The denatured RNA was separated on a 1% TAE agarose gel (Section 2.2).

2.7 Determination of nucleic acid concentrations

RNA and DNA concentration values were obtained by measuring the absorbance at 260nm in a Nanodrop Spectrophotometer ND-1000.

2.8 DNase I treatment of RNA

To further purify RNA samples and remove any contaminating DNA, RNA (30µg) was incubated at 37°C for 1 hr with 1 unit of RQ1 RNase-Free DNase I enzyme (Promega, Madison, WI, USA) and RQ1 DNase 1X Reaction buffer (4mM TrisHCl [Ph 8], 1mM $MgSO_4$, 0.1Mm $CaCl_2$) (Promega). Following digestion, deactivation of the enzyme was carried out at 65°C for 5 min. The RNA was ethanol precipitated as described in section 2.6, and after precipitation the dried pellet was resuspended in 12µl of DEPC-treated SDW.

2.9 cDNA synthesis and reverse transcriptase PCR (RT-PCR)

DNase-treated RNA (2µg) samples were reversed transcribed to cDNA using the one-step High-Capacity cDNA Reverse Transcription Kit from ABI (Applied Biosystems, Foster City, CA, USA) as per manufacturers instructions. The RNA template was added to a reaction mix containing 1X RT buffer, 4mM dNTP, 0.4 µM of gene specific reverse primer and 50U of reverse-transcriptase enzyme in a final volume of 20 µl. The negative control omitted the reverse transcriptase enzyme. Samples were incubated at 25°C for 10 min, and 37°C for 2 hr, followed by inactivation at 85°C for 5 sec. 1-3µl of cDNA was used as template, and amplified under similar conditions as described in Section 2.2. For semi-quantitative RT-PCR, 1µl of cDNA was amplified in a 25µl PCR reaction mix, and the PCR cycle was used to generate fragments was 95°C for 5 min followed by 20 cycles of 95°C for 30 sec, 55-60°C for 45 sec, 72°C for 1 min and a final elongation hold of

72°C for 10 min. Products were separated on TAE or TBE gels (Section 2.2). Actin or ribosomal RNA primers were used as positive controls for synthesis and loading (Table 2.1).

2.10 Transformations

2.10.1 Preparation of electrocompetent E. coli XL1-Blue cells

E. coli XL1-Blue was culured overnight in L-broth as described in Section 2.1.3. 10mL of overnight culture was added to 500mL of L-broth in a 2L flask. Cells were grown to an OD_{600} of approximately 0.5. Cells were centrifuged at 4000rm for 20 min at 4°C, and resuspended in 100mL of ice cold SDW. Cells were pelleted as before and resuspended in 10mL of ice cold SDW. This step was repeated twice and after the final centrifugation, cells were resuspended in 1 volume of SDW. 200µl aliquots were frozen at -70°C and 40µl of cells was used for each electroporation reaction.

2.10.2 Bacterial transformations

Transformations into *E. coli* XL1-Blue were carried out for plasmid propagation as previously described (http://www.fhcrc.org/science/labs/gottschling/yeast/ytrans.html). Cells were prepared as described above. Approximately 50ng of plasmid DNA was added to 40µl of electrocompetant *E. coli.* The mixture was transferred to a chilled electroporation cuvette (height 12mm, gap 2mm) (YorkBio, York, UK) and subjected to a 2.5V charge for a time constant of 4 - 5 sec. The cells were allowed to recover in pre-warmed L-broth at 37°C for 60 min. Transformants were selected for on L-agar plates supplemented with 25µg/ml of carbenicillin at 37°C overnight.

2.10.3 Yeast lithium acetate transformations

Yeast transformations were carried out using the lithium acetate method (Jansen et al., 2005) with the following modifications. *S. pastorianus* (CMBS-33) was grown in YEPD, at 30°C overnight and at 200rpm. 2-5mLs of culture was centrifuged at 14,000rpm. The cell pellet was washed twice with sterile dH20 (SDW) and then twice with 0.1M lithium acetate. The transformation mix (360µl) contained 33% polyethylene glycol (PEG) 3300, 0.1 M lithium acetate and 100 µg of single stranded salmon sperm DNA freshly denatured at 100°C for 10 mins. 0.1-2µg of vector was added to the pelleted cells. Linearised DNA fragments, at a minimum of 20:1 DNA:molar ratio, was added to the mix.

The mixture was incubated at 42°C for 1 hour. Following the incubation, yeast cells were allowed to recover in pre-warmed YEPD media at 30°C for 3-6 hours. Transformants were selected for on YEPD agar plates supplemented with relevant selective antibiotic, for example 200μg/ml of geneticin (G418) at 30°C for 48 hr.

2.11 Isolation of plasmid DNA from bacteria

Plasmid DNA was extracted from an overnight culture of transformed *E.coli* grown in L-broth supplemented with 25μg/mL of carbenicillin, using the Sigma GenElute™ Plasmid Miniprep Kit (Sigma), as per manufacturers instructions. A full list of plasmids and strains generated in this study are presented in Table 2.3 and Table 2.4.

2.12 DNA sequencing

All purified plasmid products and PCR fragments of yeast transformants were sent to GATC (Konstadt, Germany) for automated sequencing. Plasmid DNA was sequenced with plasmid specific primers (Table 2.1). The generated sequence was compared *in silico* to the wildtype sequence using the computer program ApE. A list of all DNA sequences is provided in Appendix 1 (CD attached).

2.13 HβD-3 fragment construction

As stated in the preface to this thesis (section 1.6), the HβD-3 gene construct was synthesized, and inserted into the BamHI site of a pBlueScript SK(-) plasmid (Fig. 2.1) (pBSK-) (Stratagene) in the order displayed in Fig. 1.7. This work was carried out by GenScript, USA INC. The DNA sequence of the gene construct in shown in Appendix I.

2.14 Yeast plasmids

2.14.1 pGREG vectors

As stated in the preface to this thesis (section 1.6) a series of galactose-inducible expression vectors, pGREG-505 and -506 (Fig. 2.2) were used in this study (Jansen et al., 2005). pGREG-505 contains a *LEU2* marker, while pGREG-506 contains a *URA3* marker (Fig. 2.2). Both vectors have a galactokinase, *GAL1* promoter which is flanked by SacI and SpeI restriction sites. Cutting the plasmid with these restriction enzymes releases the *GAL1* promoter. The *HIS3* gene is located downstream of the promoter and is flanked by SalI restriction sites, and 2 recombination sites, rec1 and rec2 (Fig 2.2).

Table 2.3 *S. pastorianus* strains generated in study

Strain name	Plasmid name	Plasmid source
CM-505GAL1	pGREG505GAL1	Jansen *et al.*[a]
CM-506GAL1	pGREG506GAL1	Jansen *et al.*[a]
CM-505TEF1	pGREG505TEF1	Karreman, R.J. and Morrissey, J.P.
CM-505hbd3GAL1	pGREG505hbd3GAL1	James, T.C.
CM-506hbd3GAL1	pGREG506hbd3GAL1	James, T.C.
CM-505hbd3TEF1	pGREG505hbd3TEF1	Present study
CM-506hbd3AGT1	pGREG506hbd3AGT1	Present study
CM-506hbd3PGK1	pGREG506hbd3PGK1	Present study
CM-505hbd3HISGAL1	pGREG505hbd3HISGAL1	Present study
CM-pRS	pRS42H	Taxis and Knop[b]
CM-pRShbd3PGK1	pRS42Hhbd3PGK1	Present study
CM-INT-51	Integrated $PGK1_{SB}$ hbd3	James, T.C.
CM-INT-37	Integrated $PGK1_{SB}$ hbd3	James, T.C.

Note strains grouped together based on presence of HβD-3 gene and type of plasmid

[a] (Jansen et al., 2005)

[b] (Taxis and Knop, 2006)

Table 2.4 *S. cerevisiae* strains generated in study

Strain name	Plasmid name	Plasmid source
S150-505GAL1	pGREG505GAL1	Jansen *et al.*
S150-506GAL1	pGREG506GAL1	Jansen *et al.*
S150-505TEF1	pGREG505TEF1	Karreman, R.J. and Morrissey, J.P.
S150-505hbd3GAL1	pGREG505hbd3GAL1	James, T.C.
S150-506hbd3GAL1	pGREG506hbd3GAL1	James, T.C.
S150-505hbd3TEF1	pGREG505hbd3TEF1	Present study

Note strains grouped together based on presence of HβD-3 gene and type of plasmid

[a] (Jansen et al., 2005)

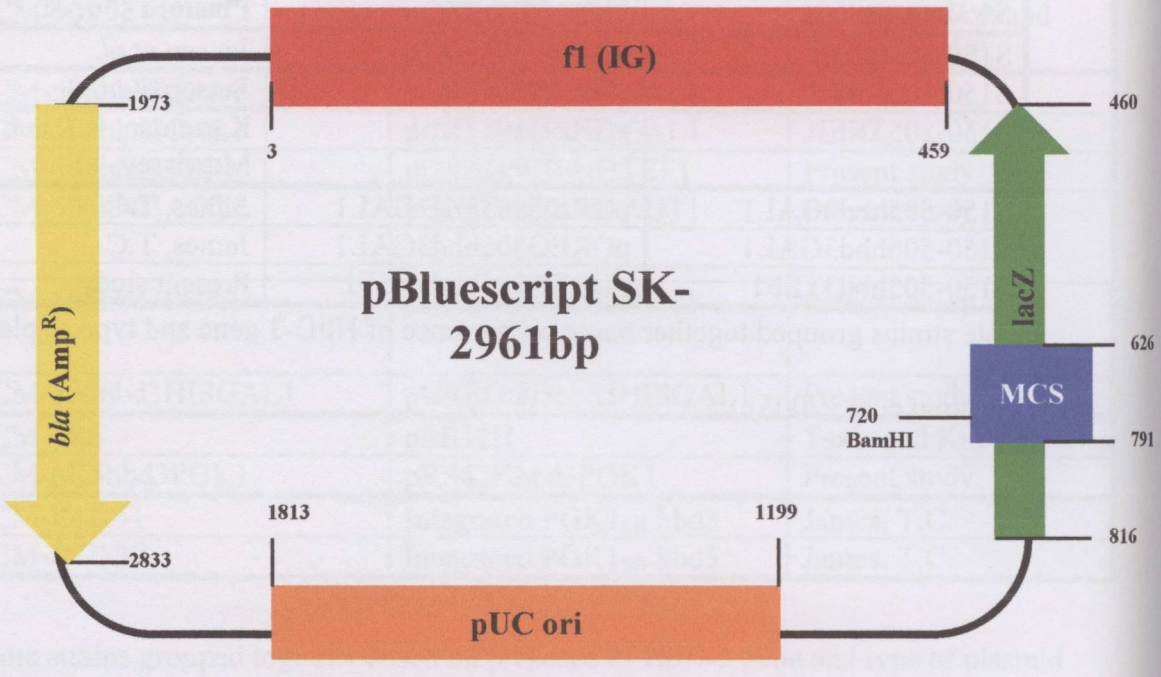

FIG. 2.1 Graphic of pBlueScript SK- plasmid

The 3kb pBlueScript SK plasmid (pBSK) (Stratagene). Note the multiple cloning site (MCS) in blue and the lacZ gene represented by a green arrow. The BamHI site is displayed as 720bp within the MCS (blue). The intergenic region of phage f1 is denoted by a red block f1 (IG), the ampicillin resistance ORF is denoted by a yellow arrow and the origin of replication is denoted by an orange box (pUC ori).

Note: Schematic diagram is not to scale.

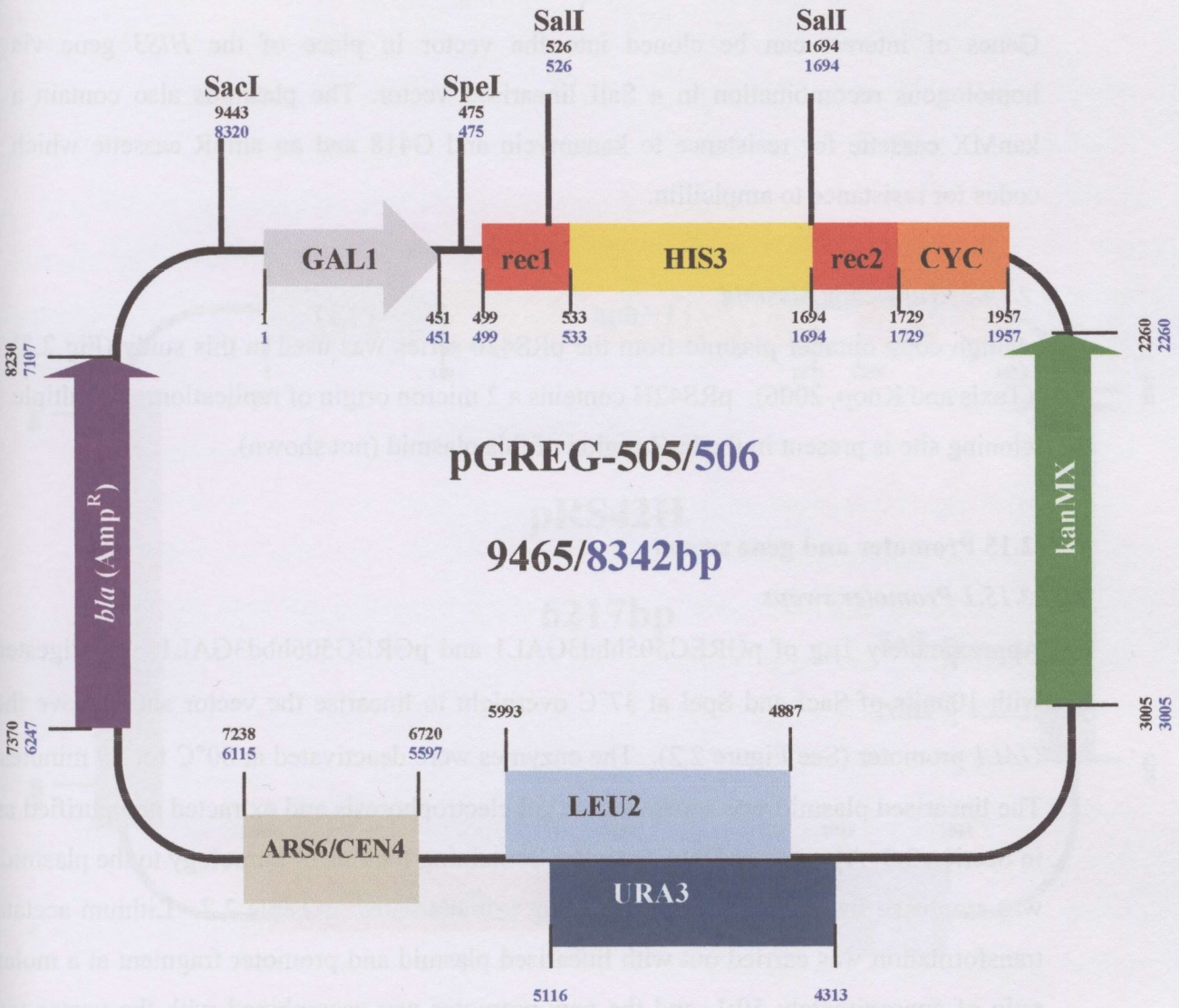

FIG. 2.2 Schematic representation of pGREG vectors used in this study

Schematic diagram showing the key features of pGREG-505 and pGREG-506. The *GAL1* promoter is represented by a grey arrow. The rec1 and rec 2 sites are denoted by red blocks and surround the *HIS3* gene (yellow block) (Jansen et al., 2005). The *CYC* terminator is represented by an orange block. The kanMX cassette is denoted by a green arrow. The auxotrophic markers are denoted by blue blocks, the *LEU2* marker is represented by a light blue block (pGREG -505) while the *URA3* marker is represented by a dark blue block (pGREG-506). ARS/CEN origin of replication: beige box. The ampicillin resistance ORF is represented by a purple arrow. Restriction sites are indicated by black lines. The nucleotide positions of each feature are shown. Black numbers represent nucleotide positions in pGREG-505. Blue numbers represent nucleotide positions in pGREG-506.

Note: schematic diagram is not to scale.

Genes of interest can be cloned into the vector in place of the *HIS3* gene via homologous recombination in a SalI linearised vector. The plasmids also contain a kanMX cassette for resistance to kanamycin and G418 and an ampR cassette which codes for resistance to ampicillin.

2.14.2 Multi-copy plasmid

A high copy number plasmid from the pRS420 series was used in this study (Fig 2.3) (Taxis and Knop, 2006). pRS42H contains a 2 micron origin of replication. A multiple cloning site is present in the lacZ region of this plasmid (not shown).

2.15 Promoter and gene swaps

2.15.1 Promoter swaps

Approximately 1μg of pGREG505hbd3GAL1 and pGREG506hbd3GAL1, was digested with 10units of SacI and SpeI at 37°C overnight to linearise the vector and remove the *GAL1* promoter (See Figure 2.2). The enzymes were deactivated at 80°C for 20 minutes. The linearised plasmid was separated via gel electrophoresis and extracted and purified as in Section 2.3 A promoter DNA fragment containing regions of homology to the plasmid, was amplified by PCR (Section 2.2), using primers listed in Table 2.2. Lithium acetate transformation was carried out with linearised plasmid and promoter fragment at a molar ratio of approximately 50:1, and the new promoter was recombined with the vector via homologous recombination in CMBS-33 (Section 2.10.3). Clones were selected on YPD and G418 plates at 30°C for 48 hr (section 2.1.2). Colonies were screened for the presence of inserted promoter sequence via direct colony PCR (Section 2.4). PCR products were sequenced across the junction as described in Section 2.12. A full list of strains generated is presented in Tables 2.3 and 2.4.

2.15.2 Gene swaps

Approximately 1μg of pGREG505TEF1 was digested with 10units of SalI at 37°C overnight, to remove the *HIS3* stuffer gene (Fig. 2.2). The enzyme was inactivated at 65°C for 20 min. The linearised plasmid was purified as in section 2.15.1. A HβD-3 DNA fragment, with flanking regions of homology to pGREG505TEF1, was amplified with primers Rec1_F and Rec2_R (Table 2.1), as described in section 2.2. The HβD-3 PCR product was purified and cloned into the linearised pGREG505TEF1 plasmid, as carried out for promoter swaps (Section 2.15.1).

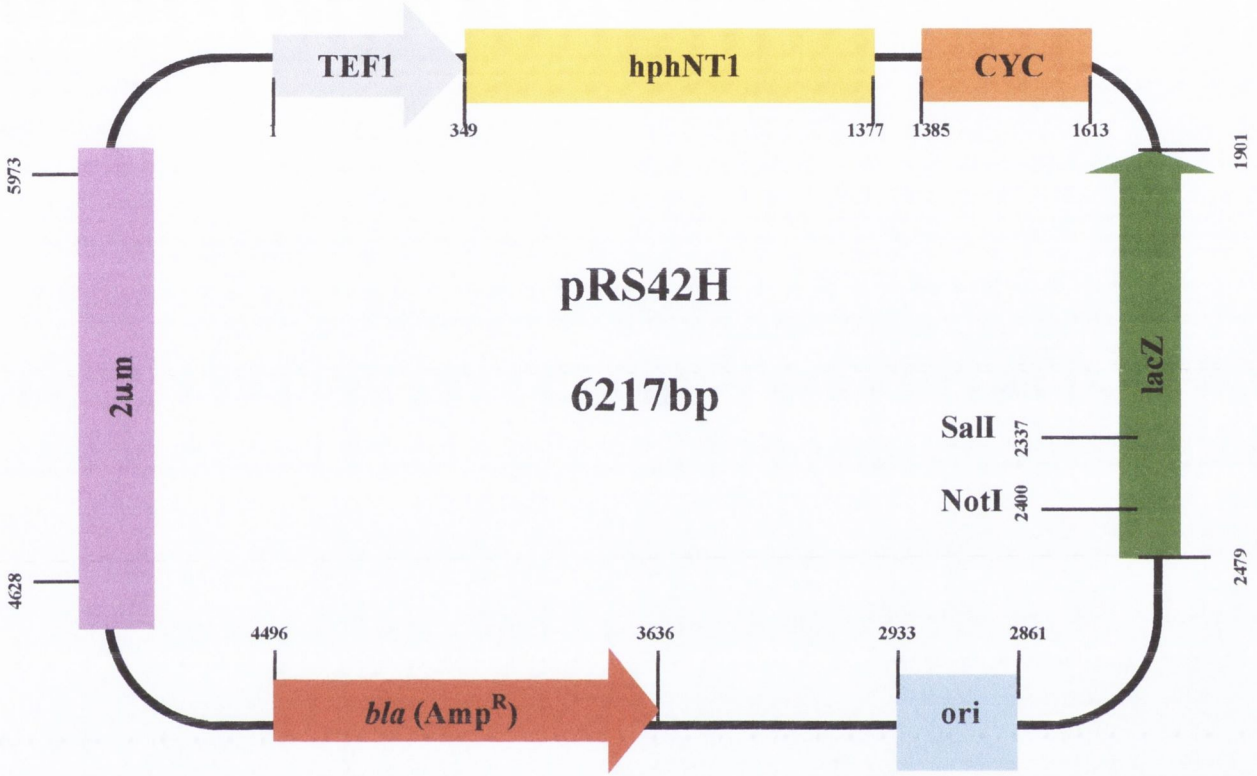

FIG 2.3 Schematic map of pRS42H plasmid

Schematic displaying the key features of the pRS42H plasmid. The *TEF1* promoter is denoted by a grey arrow. A hygromycinB ORF is denoted by a yellow block (hphNT1). A *CYC* terminator is represented by an orange box. A multiple cloning site is present within the lacZ region (green arrow). The origin of replication is denoted by a light blue block. An ampicillin resistance gene is represented by a red arrow. The 2 micron origin of replication is represented by a pink block.

The restriction sites SalI and NotI, used in this study are indicated.

The nucleotide positions of all key features are indicated.

Note: schematic diagram is not to scale.

1µg of pRS42H plasmid was digested with NotI and SalI, at 37°C overnight. The enzymes were inactivated at 65°C for 20 min. The linearised plasmid was purified as in section 2.15.1. The HβD-3 gene construct was amplified from pBSK-HβD-3, using PGK1(sb)_F2 and ADHT_R1 primers (Table 2.2), as described in section 2.2. The PGK1-HβD-3-ADHT fragment was purified and cloned into the linearised plasmid by homologous recombination in yeast (see section 2.15.1), with the following adjustments. Colonies were selected on YPD and hygromycinB plates, at 30°C for 48 hr (section 2.1.2).

2.16 His-Tag addition and purification

2.16.1 Addition of 6xHis-tag

A 6xHis-tag was fused to the C-terminal of HβD-3 in pGREG505hbd3GAL1. A GAL1-HβD-3 fragment was amplified with GAL_F and HIS-TAG_R (Table 2.1/2.2), as described in section 2.2. The HIS-TAG_R primer was designed to fuse 6xHis repeats to the 3'end of HβD-3, immediately before the stop codon. This fragment was cloned into SalI cut pGREG505GAL1 as previously described for gene swaps, section 2.15.2.

2.16.2 Nickel affinity column purification of fused HβD-3-6xHis-tag peptide from concentrated supernatant

CM-505hbd3HISGAL1 was grown in SC-Gal plus G418 (section 2.1.2). Supernatant was concentrated via molecular weight cut-off filters as described in section 2.19.2). 1mL of 50X supernatant was mixed constantly with 300µl of buffer A (200mM sodium phosphate, 2M sodium chloride, pH 8) and 700µl of Ni-NTA His-Bind® Resin (Novagen), at 4°C overnight. A spin column was equilibrated with 5 column volumes (cv) of buffer B (50mM sodium phosphate, 500mM sodium chloride, pH 8). The supernatant/resin mix, was loaded onto the column and allowed to flow through at a rate of 5mL/min, and was collected in a 1.5mL microtube. The column was then washed with 10 cv of buffer B, the first cv was collected in a separate 1.5mL microtube, and the remaining cv were pooled together and discarded. The bound peptide was then eluted in 8 cv of buffer C (50mM sodium acetate, 50mM sodium chloride, pH 4.5). Each elution was collected in a separate 1.5mL microtube. The column was stripped with 3 cv of buffer D (50mM Tris, 500mM sodium chloride, 50mM EDTA, pH 8). Each cv was collected in a separate microtube. All samples were concentrated via freeze-drying (2.19.1), and resuspended in approximately 60µl of SDW.

2.17 Yeast fermentations

Fermentations were carried out with the following modifications (James et al., 2008). Wort was prepared from dried spray malt, (Spraymalt, Brewferm, Amber 18 EBC, Brouland, Belgium). Stock wort was made from powder resuspended in distilled water (dH_2O) and stirred overnight to a final concentration of 40% (w/v). The solution was steamed for 4 hours and cooled to room temperature. Insoluble materials were removed by centrifugation and the degrees Brix (°Bx, sugar content) value was measured using a portable refractometer. Prior to starting the fermentation, the wort was diluted to the required concentration of 12 – 16°Bx, with sterile dH_2O. Fermentations were carried out either in 10, 12 or 200mL volumes in 15mL glass tubes and 250mL sterile glass cylinders respectively. Wort was aerated a couple of times with compressed air, bubbling from the bottom of the vessel, at the start of the fermentation. Anaerobic fermentations were overlaid with mineral oil. Fermentations were pitched at cell densities of 1.5x10^7 cells/mL. Flasks were incubated at a 45° angle, either at room temperature or at 11°C. Fermentation sterility was observed by incubating wort without yeast and checking for contaminants. Degrees Brix values were observed throughout the fermentation and measured using a portable refractometer. These values were converted to specific gravity (the density of a liquid in relation to that of pure water) values using a formula described by James et al. (2008). The specific gravity values were then converted to percentage alcohol using the following formula:

% alcohol=((initial specific gravity-final specific gravity)*(0.1281)*1000))

2.18 Seeding of fermentations with beer spoilage micro-organisms

To analyse beer spoilage micro-organism (BSM) survival in a fermentative environment, fermentations were set up as above. Between days 0 and 7, the brews were seeded with the desired number of beer spoiling micro-organism. When required, samples were taken from the fermentation via a long sterile rubber tube that was inserted into the bottom of the fermentation vessel at the start of the fermentation, this was attached to a 50mL syringe outside the vessel through an airtight stopper, or via a plastic Pasteur pipette. BSM viability was assayed via colony growth on MRS plates containing cycloheximide at 80μg/mL. Cycloheximide will inhibit protein biosynthesis in eukaryotic organisms, preventing yeast growth, enabling the bacterial counts to be obtained. Bacterial colonies were identified based on colony morphology and occasionally analysed microscopically. Glycerol was added to the remainder of the

sample at a final concentration of 20% and placed at -70°C overnight. The sample was thawed on ice and colony counts were obtained after freeze-treatment.

2.19 Concentrating supernatant and cell pellet protein extraction

2.19.1 Concentration of supernatant via freeze-drying

Yeast strains (Table 2.3) were grown overnight, in YEPD supplemented with G418 or hygromycin as described in Section 2.1.2, until an OD_{600} of 1-2 was obtained. Cells were centrifuged at 4000rpm, for 15 min and washed twice in SDW to remove all traces of glucose. Cells were resuspended in 10 times the volume of SC-Gal or SC-Mal media (50mL – 1L) supplemented with G418 or hygromycin and incubated for 48-120 hr, or until an OD_{600} of 1-2 per mL was reached. Cells were centrifuged (4000rpm, for 15min) and the supernatant was seperated. The supernatant was frozen in 250mL - 2L conical flasks at -75°C overnight. Supernatant samples were freeze-dried within a range of 5 to 500-fold concentrate (5-500X) and passed through 25mm syringe filter with 0.45μm PVDF membrane (VWR International). In some cases the supernatant was further concentrated via molecular weight cut off filters as described below.

2.19.2 Concentration of supernatant via molecular weight cut off filters

Cells were cultured and the supernatant was obtained as described above (section 2.19.1). The supernatant was concentrated to a final 10-1000X concentrate via filtration (Ultracel 3K Amicon Ultra Centrifugal Filters, Millipore), at 4000rpm, 4°C for 4-48 hr. Supernatant samples containing proteins greater than 3K were collected and the concentrated supernatant was stored at -20°C.

2.19.3 Concentration of supernatant via Sep-Pak cartridges

Cells were cultured and supernatants were obtained as described above (section 2.19.1). The supernatant was concentrated via Sep-Pak Cartridges (Sep-Pak Plus Short tC18 Cartridges, Waters). The eluate was collected using 80% acetonitrile. The eluate samples were frozen at -75°C overnight, then freeze-dried and filter sterilized via 0.45μm filters to 5-750X concentrate.

2.19.4 Cell pellet protein extraction

Cell pellets, equivalent to 1-10mL of culture, were lysed using 1 volume of 2.0mm Zirconia Beads (BioSpec Products, Inc.) and 2 volumes of CelLytic™-Y Yeast Cell Lysis/Extraction Reagent, with constant shaking until at least 95% of cells were lysed.

Zirconia beads and debris were pelleted by centrifugation at 14,000rpm for 15 mins and the cell pellet protein extract was transferred to a fresh eppendorf and stored at -20°C.

2.19.5 Bradford assay

Total protein in concentrated supernatant samples and cell lysates was analysed by the bradford assay. Bradford reagent was allowed to come to room temperature. 200µl was added to 700µl of SDW and 100µl of total cell pellet protein (at 1/500 dilution) or concentrated supernatant. Total protein values were read at OD_{595}.

2.20 Endoglycosidase H treatment

Endo H treatment was carried out per manufacturers instructions (New England BioLabs®$_{Inc}$, Herts, UK), with the following changes. 1-20µg of total protein or 50µl of 10X concentrated supernatant was combined with 1X glycoprotein denaturing buffer and denatured at 100°C for 10 mins. The total reaction volume was doubled, 1X G5 reaction buffer and 1µl of Endo-H was added and incubated at 37°C for 1hr.

2.21 ELISA

An Enzyme-Linked Immunosorbent Assay was carried out on supernatants using the Human βD-3 ELISA Development Kit, Peprotech, as per manufacturers instructions, with the following exceptions. 96 well flat-bottom plates were used through-out this study (Nunc MaxiSorp® flat-bottom 96 well plate). The standard volume used continuously was 40-60µl/well, and this was tripled when necessary. Capture antibody was diluted in 1X phosphate-buffer saline (PBS) (50mM KH_2PO_4 and 150mM NaCl [pH7.4]) to the recommended concentration of 3µg/mL in a volume of 40-60µl and added to wells and the plate was left at room temperatire overnight. Wells were washed 4 times in 120µl of wash buffer (0.05% Tween-20 in PBS). 180µl of blocking buffer (1% BSA in PBS) was added to each well and incubated at room temperature for 1-2 hr. Wells were washed 4 times in 120µl of wash buffer. Synthetic HβD-3 synthesized by GL Biochem (Shanghai) Ltd, was used as the assay standard at 0.03 - 2µg in a volume of 40-60µl. A standard curve was used to directly compare detection with activity in the concentrated supernatant samples. HβD-3 was diluted in diluent (0.05% Tween-20, 0.1% BSA in PBS). 40-60µl of concentrated supernatant samples (10 – 1000X) or RP-HPLC fractions were added to duplicate wells. The plate was then incubated at 4°C overnight. Wells were washed 4 times in 120µl of wash buffer. Biotinylated detection

antibody was added to the wells at the recommended concentration of 0.25μg/mL in a volume of 40-60μl. The plate was incubated at room temp for 2 hr. Wells were washed 4 times in 120μl of wash buffer. Avidin-HRP conjugate was diluted 1:2000 in diluent and 60μl was added to each well and incubated at room temperature for 30 min. The wells were washed 4 times as before and 120μl of TMB (3,3'5,5'-Tetramethylbenzidine (TMB) Liquid Substrate System) (Sigma) was added to each well at room temperature. The developed blue colour was read at OD_{595} using a Labsystems Original Multiskan EX plate reader.

2.22 SDS-Polyacrylamide Gel Electrophoresis (PAGE) and Western Blotting Analysis

2.22.1 SDS-PAGE gel

Standard 12% SDS-PAGE gels were prepared as follows: running gel; 25% (v/v) 1.5M Tris pH8.8, 0.1% (v/v) SDS, 12% (v/v) acrylamide/bis, 0.04% (v/v) TEMED, and 0.1% (v/v) ammonium persulfate (APS) (Fisher Bioreagents ®), and stacking gel; 25% (v/v) 0.5M Tris pH6.8, 0.1% (v/v) SDS, 5% (v/v) acrylamide/bis, 0.1% (v/v) TEMED, and 0.1% (v/v) APS. One volume of concentrated supernatant sample was added to one volume of 2X Concentrate Sample Buffer, Laemmli, (Sigma), and the sample was boiled at 100°C for 15mins. 40μl aliquots of protein samples were separated on duplicate 12% SDS-PAGE gels. 10μl of Ultra-low Range Molecular Weight Marker (M.W. 1060-26,000) (Sigma) was loaded alongside the samples. The gels were electrophoresed at 80V in 1X running buffer (0.1% (w/v) SDS, 3.02g $litre^{-1}$ Tris, and 14.4g $litre^{-1}$ glycine, pH 8.8), until the dye front reached the bottom of the gel.

2.22.2 Coomassie stain

One of the duplicate gels was stained in Coomassie stain (50% (v/v) methanol, 10% acetic acid, 0.1% Coomassie blue) overnight and de-stained in 10% acetic acid and 50% methanol for approximately 24 hours.

2.22.3 Western immunoblotting

The second gel was prepared for Western blot analysis. Proteins were transferred to an Immobilion-P Transfer Membrane (PVDF), 0.45μm (Millipore, USA), at 45V for 75 min in 1X transfer buffer (2.93g $litre^{-1}$ glycine, 5.82g $litre^{-1}$ tris and 20% (v/v) methanol). PVDF membrane was methanol pretreated as per manufacturers

instructions. The membrane was blocked with 5% Marvel (Original Dried Skimmed Milk, Less than 1% fat) in PBS (10 - 20mL) at 4°C overnight, and then washed three times with 0.05% Tween PBS (15 - 20mL). Either Anti-β-Defensin-3 Polyclonal Antibody (Sigma), at a 1:5000 dilution, or monoclonal mouse anti-poly HIS (Sigma) at 1:3000 in PBS, were added to the membrane and incubated for 2hr at room temperature. The membranes were washed three times with 0.05% Tween PBS. Two secondary antibodies were used in this study, bovine anti-rabbit IgG-HRP conjugated secondary antibody (Santa Cruz Biotechnology) at 1:5000, or goat anti-mouse IgG-HRP conjugated secondary antibody (Santa Cruz Biotechnology) at 1:10,000. Secondary antibody incubations were similar to those above for primary antibody. The membranes were washed three times with 0.05% Tween PBS following secondary antibody incubation. The membrane was incubated with Chemiluminescent peroxidase substrate (Sigma) at room temperature for 5min and exposed to X-ray film. The following positive peptide/protein controls were used, 0.5-10μg of synthetic HβD-3 in a total volume of 10μl, and 10ng-1μg of C-reactive protein (CRP) in a total volume of 10ul. Positive protein samples were prepared as above.

2.23 Reversed-phase high-peformance liquid chromatography (RP-HPLC)

10X concentrated yeast culture supernatant samples and synthetic HβD-3 were applied to a C-18 RP-HPLC column [(C18 column, Zorbax 300SB-C18-Agilent) (150 x 4.6mm, 5μm)]. The column was equilabrated in aqueous buffer (0.1% trifluoroacetic acid (TFA)). 50-100μl of supernatant was reconstituted in an equal volume of aqueous buffer to maximize binding to the column. The sample was filtered via 0.45μm low protein binding columns. The sample was loaded onto the column and run at a gradient which starts at near 100% aqueous buffer (2% acetonitrile) and ramps to 60% organic buffer (Acetonitrile, 0.1% TFA) in 60min. Fractions were collected for every minute at a flow rate of 1mL/min. The total 1mL samples were pooled when necessary, freeze-dried and resuspended in 120μl of SDW. These samples were analysed by ELISA analysis as described in Section 2.21.

2.24 HβD-3 activity assays

2.24.1 HβD-3 bioassay

Lactobacillus brevis L1055 was cultured in MRS media overnight, at 37°C. OD_{600} values were taken and dilutions were carried out, to give 10^2 cells in 100μl total

volumes. As a positive control, cells were treated with varying concentrations of synthetic HβD-3, from 10μg/ml to 0.5μg/ml in 100μl volumes. Cells were also treated with concentrated CMBS-33, CM-505hbd3GAL1 and CM-506hbd3GAL1 supernatant in 100μl volumes. All samples were incubated at 37°C for 2 or 2.5hrs, and colony counts were determined following incubation of lawned (20μl) MRS plates at 37°C, for 48 hrs.

2.24.2 Defensin activity in vivo and freeze-treatment analysis

To analyse HβD-3 activity *in vivo*, fermentations were set up as described in Section 2.17, with HβD-3 containing strains listed in Table 2.3. On days 0 or 2, fermentations were seeded with 10^3 cfu/mL of beer spoilage micro-organisms as described in section 2.18. 1mL samples were taken from the fermentations on various days. To analyse BSM viability samples was lawned onto MRS plates containing cycloheximide (80μg/mL). Fermentation samples (0.4 – 1mL) taken on various days were freeze-treated at -70°C overnight in 20% glycerol. Following thawing on ice samples were lawned onto MRS plates containing cycloheximide (80μg/mL).

Chapter 3:

Generation of *Saccharomyces pastorianus* Strains to Express Antimicrobial Peptide

3.1 Introduction

The aim of the research outlined in this chapter was to determine the most suitable promoter for the expression of HβD-3 in *S. pastorianus*. This was achieved by generating a series of vectors in which the HβD-3 gene is expressed from a variety of inducible and constitutive promoters. Once HβD-3 expression is achieved, the long-term goal was to determine if such strains can minimize or eliminate bacterial contamination during fermentation, without affecting the quality of the brew. HβD-3 was cloned into a series of low and high-copy number plasmids, under the control of a variety of promoters, through exploiting the natural homologous recombination machinery in *S. pastorianus*. As mentioned in the preface to this thesis (section 1.6), the HβD-3 gene, under the control of a $PGK1_{SB}$ promoter, has been integrated directly into the *S. pastorianus* genome at a hypothetical open reading frame, YPR159C-A, partially deleting it (Dr. T.C. James., Unpublished). YPR159C-A is located between the genes YPR159W and YPR160W on chromosome XVI.

The HβD-3 gene was initially cloned into the pGREG-505 and 506 low copy number plasmids, under the control of the *GAL1* promoter, which is highly induced in the presence of galactose and repressed in the presence of glucose, offering very tight expression regulation (section 1.6). In an ideal lager fermentation, yeast are inoculated in sweet wort, in which galactose is absent (Gibson et al., 2008). Maltose and maltotriose account for approximately 60% of the total fermentable sugars available in wort, therefore for this study the HβD-3 gene was placed under the control of a maltose inducible promoter, as maltose is the preferred carbohydrate for *S. pastorianus* strains. *S. cerevisiae* contains 5 unlinked *MAL* loci (*MAL1* to *4* and *MAL6*). Each *MAL* locus contains up to 3 genes, *MALx1, MALx2* and *MALx3,* where x refers to 1 to 4 or 6. *MALx1* genes encode α-glucosidase transporters with high affinity for maltose, *MALx2* genes encode a maltase and *MALx3* genes encode a transcriptional activator of the other two genes (Barnett, 1981; Charron and Michels, 1988; Charron et al., 1989; Goldenthal et al., 1987). The HβD-3 gene was placed under the control of the maltose inducible *AGT1 S. cerevisiae* promoter. In *S. cerevisiae* the *AGT1* gene (α-glucosidase transporter) replaces the *MALx1* gene on the *MAL1* locus (Alves et al., 2008; Chang et al., 1989; Han et al., 1995; Salema-Oom et al., 2005). Studies have shown that both *S. cerevisiae* and *S. pastorianus* strains contain the *AGT1* gene, however lager strains encode a non-functional truncated protein (Nakao et al., 2009; Vidgren et al., 2005).

The *AGT1* promoter is a 785bp divergent promoter of *AGT1* and *MAL12* (Fig. 3.1) (Hong and Marmur, 1987). Recent studies by Vidgren et al. (2011) revealed that the *AGT1* promoter of laboratory yeast strains was extremely divergent compared to the *AGT1* promoter in brewer's yeast strains, where the promoters share a high degree of homology. This divergence in promoters may be due to the evolution of laboratory strains in laboratory conditions (Vidgren et al., 2011). The first 315bp of the *S. cerevisiae AGT1* promoter, are 99% identical to brewer's yeast promoters, while the remaining 470bp are distinctly divergent (Fig. 3.1). This 470bp region is almost identical to the conventional *MALx1-MALx2* divergent promoters found in other MAL loci in *S. cerevisiae* strains (Fig. 3.1) (Vidgren et al., 2011). The sequence divergence starts within the 147bp tandem repeat (Fig. 3.1 black oval), whereby the last 47bp of the 147bp tandem repeat are located in the region homologous to *MALx1-MALx2* promoters (Vidgren et al., 2011) and the first 100bp are located in the region homologous to brewer's yeast *AGT1* promoters. To my knowledge, the introduction of a *S. cerevisiae AGT1* promoter into a *S. pastorianus* strain is a novel approach, and may provide high levels of expression of a gene from this maltose inducible promoter.

Additionally the gene was placed under the control of two constitutive promoters of *S. cerevisiae*, a phosphoglycerate kinase, *PGK1*, promoter and a translational elongation factor EF-1 alpha (*TEF1*) promoter, both of which have been used previously for gene expression studies in *S. cerevisiae*. The $PGK1_{SC}$ promoter drives the expression of phosphoglycerate kinase which is expressed under most environmental conditions. The *S. cerevisiae TEF1* gene belongs to a large family of ribosomal protein genes (RPG), which encode components of the translation machinery (Shore 1994). The *TEF1* promoter has been shown to be one of the stronger constitutive promoters (Gatignol et al., 1990). Studies by Partow et al. (2010) compared the activity of various promoters during YEPD and YEPGal fermentations of *S. cerevisiae* and determined that the *TEF1* promoter displayed the most constant activity (Partow et al., 2010). Thus the use of *TEF1* promoter in this study may result in constant levels of HβD-3 during *S. pastorianus* fermentations. The HβD-3 gene was also cloned into the multi-copy number plasmid, pRS42H, under the control of a *PGK1 S. bayanus* promoter, to increase the levels of expression of HβD-3.

The overall aim is to determine an optimum method for the expression of HβD-3 in *S. pastorianus*.

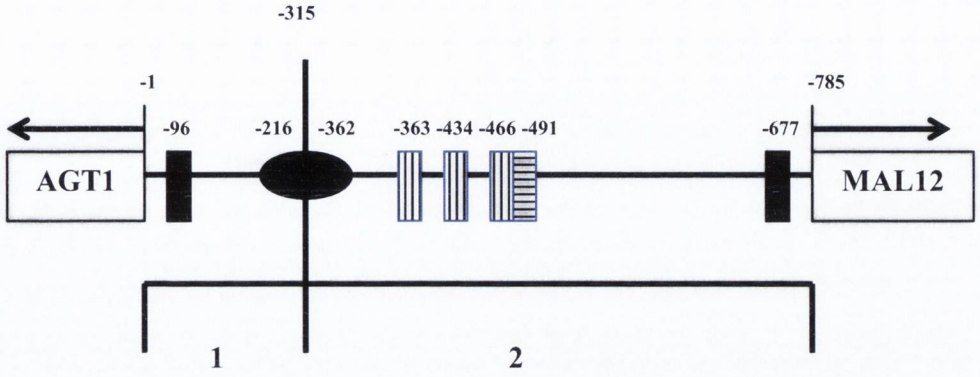

FIG. 3.1 Schematic diagram of the *AGT1-MAL12* divergent promoter used in this study

Schematic diagram illustrating the regulatory elements of the *AGT1-MAL12* divergent promoter of *S. cerevisiae*, from positions -1 to -785 upstream of *AGT1*. TATA boxes (black boxes) are identified at positions -96 to -102 and -677 to -684, upstream from the ATG of the *AGT1* gene. A 147bp repeat element is located from -216 to -362 (black oval). Three *MAL* activator binding sites are located at positions -363-395, -434-452 and -466-490 (vertical lines). A Mig1 binding site is positioned at -491-506 (horizontal lines). Section 1 of the divergent promoter has 99% homology to the *AGT1* promoters of brewer's yeast strains. Section 2 of the divergent promoter has approximately 99% homology to other *MALx1-MALx2* divergent promoters in *S. cerevisiae* (Vidgren et al., 2011).

Note: Diagram is not to scale.

3.2 Results

3.2.1 Plasmids and yeast strains containing HβD-3

3.2.1.1 Confirmation of HβD-3 integration via direct colony PCR

Strains CM-INT-37 and CM-INT-51, in which the HβD-3 gene construct has been cloned into chromosome XVI of the *S.pastorianus* genome, were kindly provided by Dr. T. C. James. The generation of these strains is discussed in section 1.6. To confirm the presence of HβD-3, PCR analysis was carried out on each strain. DNA was amplified using HβD-3_F1 and HβD-3_R1 primers (Table 2.1). A band for HβD-3 (158bp) was detected in DNA extracted from CM-INT-37 and CM-INT-51, while no band of the expected size is seen in CMBS-33 indicating that HβD-3 is not present in wild-type CMBS-33 (data not shown). Furthermore, the expression of HβD-3 was confirmed by RT-PCR. cDNA was amplified using HβD-3_F1 and HβD-3_R1 primers (Table 2.1). As a positive control for the RT-PCR, cDNA was amplified with 5.8S_F and 5.8S_R primers (Table 2.1). As before, a band for HβD-3 (158bp) was detected in DNA extracted from CM-INT-37 and CM-INT-51 (Fig. 3.2 B, lanes 2 and 3 respectively), while no band of the expected size is seen in CMBS-33 cDNA (Fig. 3.2 B, lane 1). The 5.8S cDNA is amplified in all three strains producing the expected size band (150bp) (Fig. 3.2 C).

3.2.1.2 Characterisation of pGREG505hbd3GAL1 and pGREG506hbd3GAL1 plasmids

As described in section 1.6, a series of pGREG vectors, containing a HβD-3 gene construct were generated (Fig. 1.8). The presence of the α-factor signal sequence, the HβD-3 gene and the *ADH* terminator, in each of these plasmids, was confirmed by PCR. 100ng of pGREG505hbd3GAL1 and pGREG506hbd3GAL1 plasmid was used as a template for amplification. The α-factor signal sequence, HβD-3 ORF and part of the *ADH* terminator, were all PCR amplified using One-4-all_F2 and HβD-3_R2 primers (Fig. 3.3 A, Table 2.1), yielding a 246bp product (Fig. 3.3 C, lanes 1 & 2). One-4-all_F1 and One-4-all_R primers (Fig. 3.3 A/B, Table 2.1) were used to amplify the region surrounding the HβD-3 gene construct. pGREG505hbd3GAL1 yielded a 494bp band and pGREG506hbd3GAL1 a 709bp band. The size difference seen between PCR products is due to the additional nucleotides of the *ADH* terminator in pGREG506hbd3GAL1 (Fig. 1.8 A & Fig 3.3 D lanes 1 and 2 respectively). As stated in the preface to this thesis, regions of the HβD-3 gene construct replaced the *HIS3* stuffer cassette (1159bp) in pGREG vectors 505 and 506 (section 1.6). The PCR results

FIG. 3.2 Schematic of HβD-3 primers and gel electrophoresis of HβD-3 and 5.8S RT-PCR products amplified from CMBS-33, CM-INT-37 and CM-INT-51

RT-PCR was performed on CMBS-33, CM-INT-37 and CM-INT-51 amplified with HβD-3 specific primers and 5.8S primers. **A)** Position of HβD-3_F1 and HβD-3_R1 primers relative to the α-factor signal sequence and the HβD-3 ORF in CM-INT-37 and CM-INT-51. Primers are denoted by arrows. Nucleotide positions are denoted by numbers for the schematic diagram and primers. Note: schematic diagram not to scale. **B)** HβD-3 RT-PCR products amplified with HβD-3 specific primers (Table 2.1). Lane 1: CMBS-33. Lane 2: CM-INT-37. Lane 3: CM-INT-51. The latter two samples are positive for HβD-3, with bands seen 158bp. **C)** 5.8S RT-PCR products amplified with specific primers (Table 2.1), to give an expected band size of 150bp. Samples as above. 5μl of hyperladder II molecular weight marker is loaded at the start of each gel. Band sizes are denoted by numbers above each band. All products were separated on 1% TBE agarose.

A)

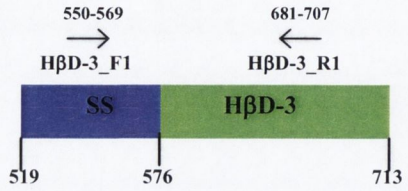
550-569
681-707
HβD-3_F1
HβD-3_R1
SS
HβD-3
519
576
713

B)

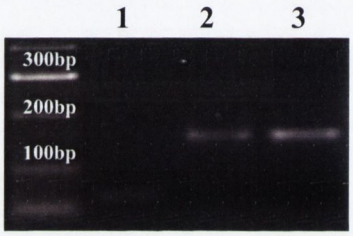
1
2
3
300bp
200bp
100bp

C)

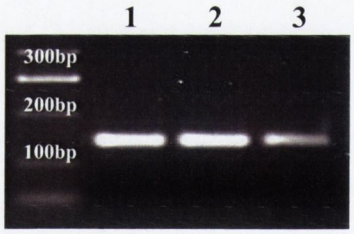
1
2
3
300bp
200bp
100bp

FIG. 3.3 Schematic illustration and PCR amplification of regions of interest in pGREG vectors

100ng of pGREG505hbd3GAL1 and pGREG506hbd3GAL1 plasmids were PCR amplified with plasmid specific primers. **A)** Schematic illustration of regions of interest in pGREG505hbd3GAL1. The positions of One-4-all_F2, HβD-3_R2, One-4-all_F1 and One-4-all_R primers are shown. Primers are denoted by arrows. This represents the position of One-4-all_F2 and HβD-3_R2 primers for pGREG506hbd3GAL1 also. Nucleotide positions are shown for the schematic diagram and primers. Note: Schematic diagrams are not to scale. **B)** Schematic illustration of regions of interested in pGREG506hbd3GAL1. The positions of One-4-all_F1 and One-4-all_R primers are shown. **C)** Amplification of plasmid templates amplified with One-4-all_F2 and HβD-3_R2 primers, giving an expected band size of 246bp. Lane 1: 100ng of pGREG505hbd3GAL1. Lane 2: 100ng of pGREG506hbd3GAL1. **D)** Amplification of plasmid templates amplified with One-4-all_F1 and One-4-all_R, giving an expected band size for pGREG505hbd3GAL1 of 494bp and for pGREG506hbd3GAL1 of 709bp. Samples in each lane are the same as above. 5μl of Hyperladder II molecular weight marker was loaded at the start of the gel. Band sizes are denoted by lines. All of the above PCR products were separated on 1% TBE. All primers are listed in Table 2.1.

A)

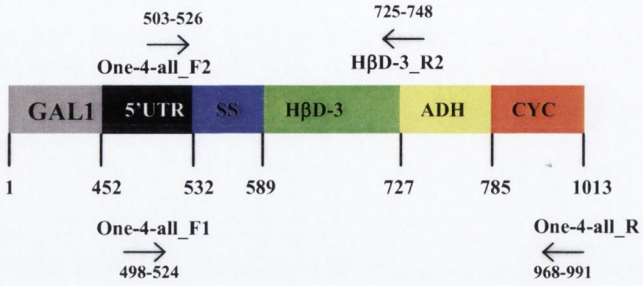
503-526
One-4-all_F2
725-748
HβD-3_R2
GAL1
5'UTR
SS
HβD-3
ADH
CYC
1
452
532
589
727
785
1013
One-4-all_F1
498-524
One-4-all_R
968-991

B)

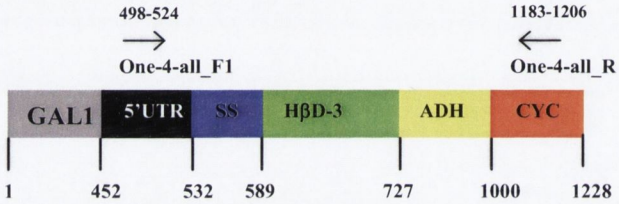
498-524
One-4-all_F1
1183-1206
One-4-all_R
GAL1
5'UTR
SS
HβD-3
ADH
CYC
1
452
532
589
727
1000
1228

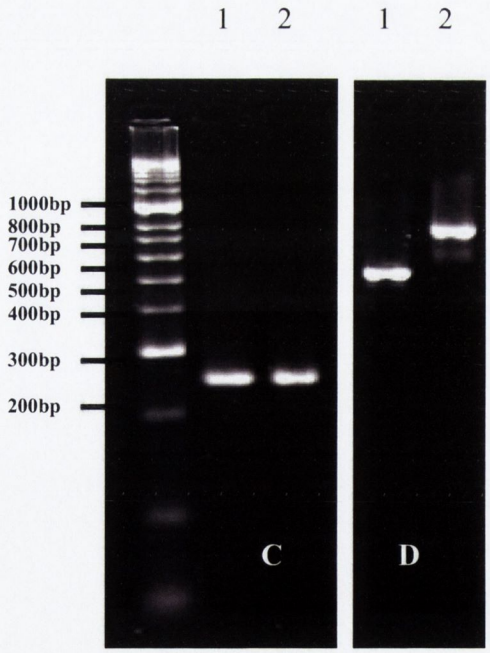
1
2
1
2
1000bp
800bp
700bp
600bp
500bp
400bp
300bp
200bp
C
D

obtained during this study further confirm the replacement of the *HIS3* cassette by the HβD-3 gene construct, as the presence of *HIS3* would result in a 1437bp band in both vectors when amplified with One-4-all_F1 and One-4-all_R primers. Plasmids were sequenced by GATC as described in section 2.12. Sequences obtained revealed that identical mutations were present in both plasmids (Fig. 3.4). A single nucleotide deletion occurred at position 447, in which an adenine (A) nucleotide was deleted, in the promoter specific 5'UTR of the *GAL1* promoter (Fig. 3.4). Two additional mutations occurred at positions 463/464, whereby an adenine-guanine (AG) was replaced by a guanine-adenine (GA) in the non-specific 5'UTR region (Fig. 3.4). The non-specific 5'UTR is determined as the nucleotides that are present in the original pGREG plasmid located between the promoter and the gene. This region contains the SpeI restriction site, the SalI restriction site and the rec1 site (Fig. 2.2). Finally an insertion of an adenine (A) occurred at position 531 in the non-specific 5'UTR (Fig. 3.4).

Each plasmid was transformed into a *S. cerevisiae* strain S150 and a *S. pastorianus* strain CMBS-33. Colonies were selected on YEPD & G418 plates (Section 2.1.2) and all newly transformed strains were screened via direct colony PCR (data not shown). All strains generated in this study are listed in Tables 2.3 and 2.4. Appendix 1 contains sequences for each plasmid.

3.2.1.3 Generation of CM-505hbd3TEF1

pGREG505TEF1 was kindly provided by Dr. R. Karreman, UCC. In this vector, the *GAL1* promoter of pGREG505GAL1 was replaced by a *S. cerevisiae* translational elongation factor EF-1 alpha (*TEF1*) promoter, which is a highly expressed gene (Gatignol et al., 1990). The *TEF1* promoter was previously cloned into the vector using a traditional restriction digest and ligation method, whereby the *GAL1* promoter was digested from the pGREG505GAL1 vector by restriction digest with SacI and SpeI restriction enzymes. The *TEF1* promoter was then ligated into the SacI/SpeI digested pGREG505 (Dr. R. Karreman, unpublished). The positions of these restriction digest sites relative to the *GAL1* promoter can be seen in Fig. 3.5. Digesting the plasmid with these restriction enzymes results in the removal of 23bp upstream of the *GAL1* promoter and a further 28bp downstream of the *GAL1* promoter (Fig. 3.5). The *TEF1* ORF in *S. cerevisiae* is located on chromosome XVI from 700594 to 701970. The *TEF1* promoter region was denoted as 401bp located upstream of the start codon of the ORF, from

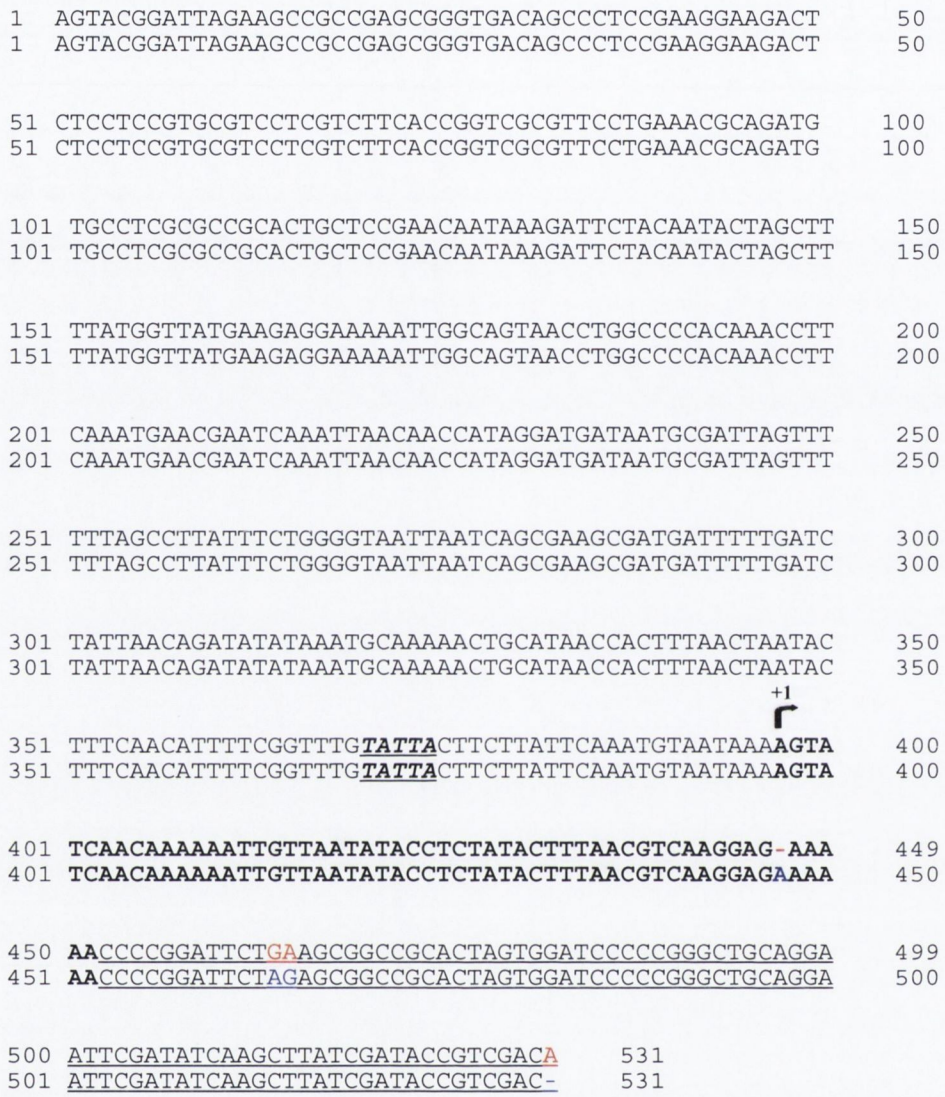

FIG. 3.4 DNA sequence alignment of newly synthesized pGREG505hbd3GAL1 versus pGREG505GAL1

Comparison of the DNA sequence of the *GAL1* promoter region and the non-specific 5'UTR in plasmids pGREG505hbd3GAL1 (top) and pGREG505GAL1 (bottom). The black letters denote similar nucleotides, blue letters denote wildtype nucleotides, and red letters denote mutant nucleotides. The promoter specific 5'UTR of the *GAL1* promoter is defined by bold nucleotides and the TATA box is denoted by bold, underlined italics (Johnston and Davis, 1984). The transcription start site (TSS) is denoted by +1. The non-specific 5'UTR region is underlined.

The sequence alignment for pGREG506hbd3GAL1 and pGREG506GAL1 was identical.

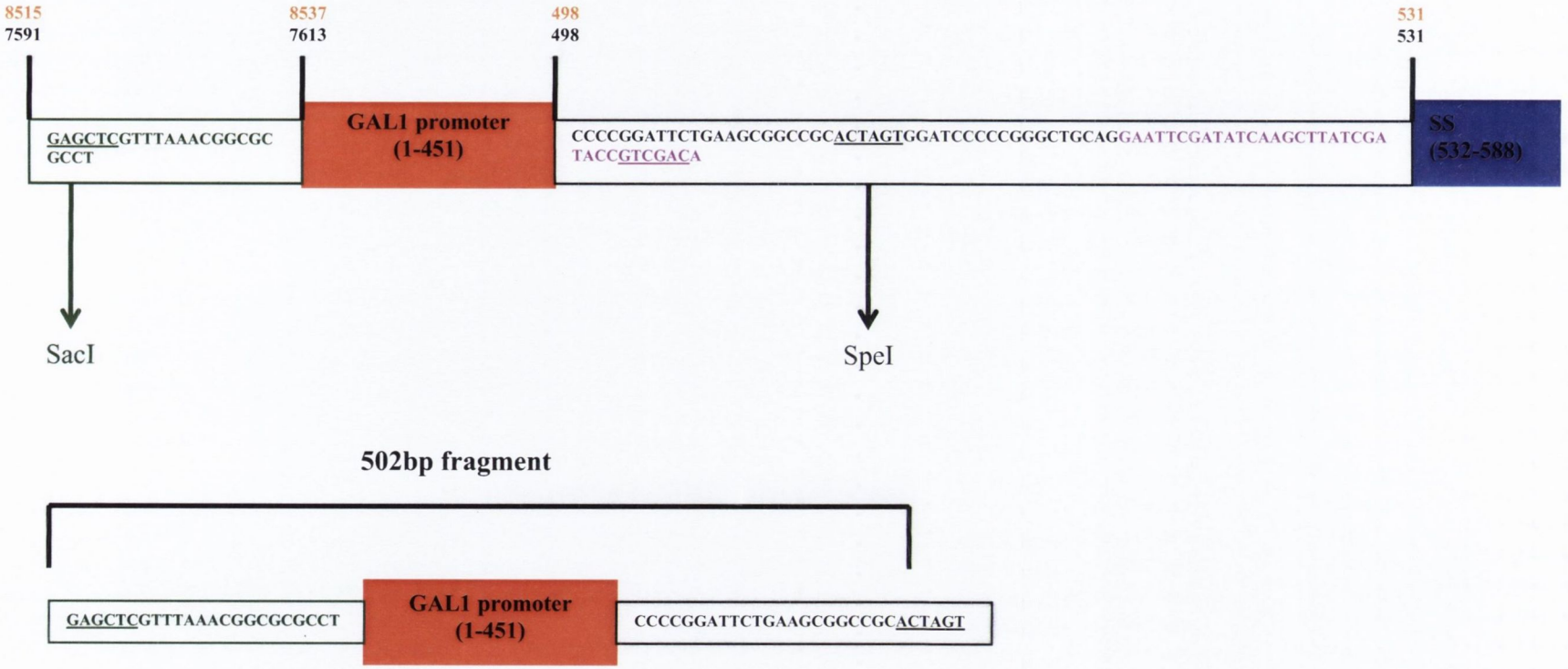

FIG. 3.5 Schematic diagram of regions of interest surrounding the *GAL1* promoter in pGREG vectors

This schematic illustrates the location of the SacI [green] and SpeI [black] restriction sites, seen underlined, in relation to the *GAL1* promoter of the vectors, pGREG505hbd3GAL1 and pGREG506hbd3GAL1. When these plasmids are digested with SacI and SpeI, a 502bp fragment containing the 451bp promoter and additional untranslated nucleotides, is released from the plasmid. The SalI site, located in the rec1 site (pink) is underlined. Note: *GAL1* promoter: red, rec 1 nucleotide sequence: pink, α-factor signal sequence: blue. Schematic is not to scale.

Coordinates of pGREG505hbd3GAL1 and pGREG506hbd3GAL1, are represented by orange and black numbers respectively.

coordinates 700192 to 700592. This is a constitutive promoter and will express during normal growth in rich medium such as YEPD. Studies carried out by Miura et al. (2006) indicate that the promoter specific 5'UTR of the *TEF1* promoter is between 26-49 nucleotides long (Fig. 3.6) (Miura et al., 2006).

The *HIS3* stuffer cassette (1159bp) was digested from pGREG505TEF1 with SalI restriction enzymes, to release the *HIS3* cassette, along with 2bp of non-specific 5'UTR as illustrated in Fig. 3.7 A (section 2.15.2). The first SalI restriction site is located at 454-459bp and the second SalI site is located at 1622-1627bp (Fig. 3.7 A). The released 1159bp fragment and linearised plasmid were separated on 1% TAE agarose (Fig 3.8 A, lane 1). A fragment containing the α-factor signal sequence, the HβD-3 gene and a short *ADH* terminator were amplified by PCR, from pGREG505hbd3GAL1 using Rec1_F and Rec2_R primers listed in Table 2.1 (Fig. 3.7 B), yielding a 287bp product (Fig. 3.8 A, lane 2). This PCR fragment contains 28bp of homology to the non-specific 5'UTR region of pGREG505TEF1 and 30bp of homology to the rec2 site, located directly upstream of the *CYC* terminator in pGREG505TEF1 (Fig 3.7 C). The signal sequence/HβD-3/ADH fragment was inserted into pGREG505TEF1 in the following manner. The linearised plasmid (Fig. 3.8 A, lane 1) and the signal sequence/HβD-3/ADH PCR fragment (Fig. 3.8 A, lane 2) were extracted from the gel and purified as described in section 2.3. After purification, an aliquot of each sample was visualised on 1% TAE agarose, to quantify each sample (data not shown). The linearised plasmid and purified HβD-3 fragment were combined by homologous recombination in CMBS-33 via lithium acetate transformation, as described in section 2.10.3.

Colonies were cultured on YEPD&G418 media and screened for the presence of HβD-3 via direct colony PCR, using TEF_F1 and HβD-3_R1 (Fig. 3.8 B), primers and a product at the expected size of 544bp was obtained (Fig. 3.8 C, lane 3). Direct colony PCR products were sequenced (Appendix 1) which confirmed the presence of the fragment containing HβD-3. This resulted in the generation of the strain CM-505hbd3TEF1 (Table 2.3).

DNA sequence analysis of CM-505hbd3TEF1 indicated a single nucleotide mutation at position 402 in the non-specific 5'UTR, whereby a cytosine (C) nucleotide was substituted by an adenine (A) nucleotide (Fig. 3.9). Furthermore, during the generation

```
  1 AATGTTTCTACTCCTTTTTTACTCTTCCAGATTTTCTCGGACTCCGCGCA      50
 51 TCGCCGTACCACTTCAAAACACCCAAGCACAGCATACTAAATTTCCCCTC     100
101 TTTCTTCCTCTAGGGTGTCGTTAATTACCCGTACTAAAGGTTTGGAAAAG     150
151 AAAAAAGAGACCGCCTCGTTTCTTTTTCTTCGTCGAAAAAGGCAATAAAA     200
201 ATTTTTATCACGTTTCTTTTTCTTGAAAATTTTTTTTTTTGATTTTTTTC     250
251 TCTTTCGATGACCTCCCATTGATATTTAAGTTAATAAACGGTCTTCAATT     300
301 TCTCAAGTTTCAGTTTCATTTTTCTTGTTCTATTACAACTTTTTTTACTT     350
351 CTTGCTCATTAGAAAGAAAGCATAGCAATCTAATCTAAGTTTTAATTACAA    401
```

FIG. 3.6 DNA sequence of the *TEF1* promoter

The above DNA sequence represents the 401bp *TEF1* promoter of *S. cerevisiae,* coordinates 700192-700592 on chromosome XVI. The estimated 5'UTR is underlined (Miura et al., 2006). The Gcr1 binding sites are denoted by bold nucleotides. The upstream activation sequence of ribosome binding genes (UAS_{RPG}) is denoted by bold italic nucleotides (Bi and Broach, 1999).

FIG. 3.7 Schematic representation of pGREG505TEF1 and insertion of the HβD-3 fragment into the linearised plasmid

A) Schematic representation of pGREG505TEF1 containing the *HIS3* cassette. Black block: *TEF1* promoter. Purple block: non-specific 5'UTR. Yellow block: *HIS3* stuffer cassette. Lilac block: Rec 2. Orange block: *CYC* terminator. The nucleotide sequence of the non-specific 5'UTR is displayed above this region. The nucleotide sequence of the Rec2 site is displayed above this region. The SalI sites are denoted by red underlined italics. **B)** Schematic diagram of pGREG505hbd3GAL1 showing the position of Rec1_F and Rec2_R primers. Primers are denoted by arrows. These primers are based at positions 498bp and 755bp, relative to the HβD-3 gene (black arrows). These primers were used to amplify this fragment from pGREG505hbd3GAL1. Grey block: *GAL1* promoter. Black block: non-specific 5'UTR. Blue block: α-factor signal sequence. Green block : HβD-3 ORF. *ADH* terminator: yellow block. Rec2 site: lilac block. Orange block: *CYC* terminator. **C)** Schematic illustration of the insertion of the fragment containing the α-factor signal sequence, HβD-3 and *ADH* terminator into pGREG505TEF1, replacing the *HIS3* stuffer fragment. The purple line represents homology to the non-specific 5'UTR and the lilac line represents homology to the rec2 site. Black block: *TEF1* promoter.

Nucleotide positions are shown for each schematic diagram and primer.

Note: Schematic diagrams are not to scale.

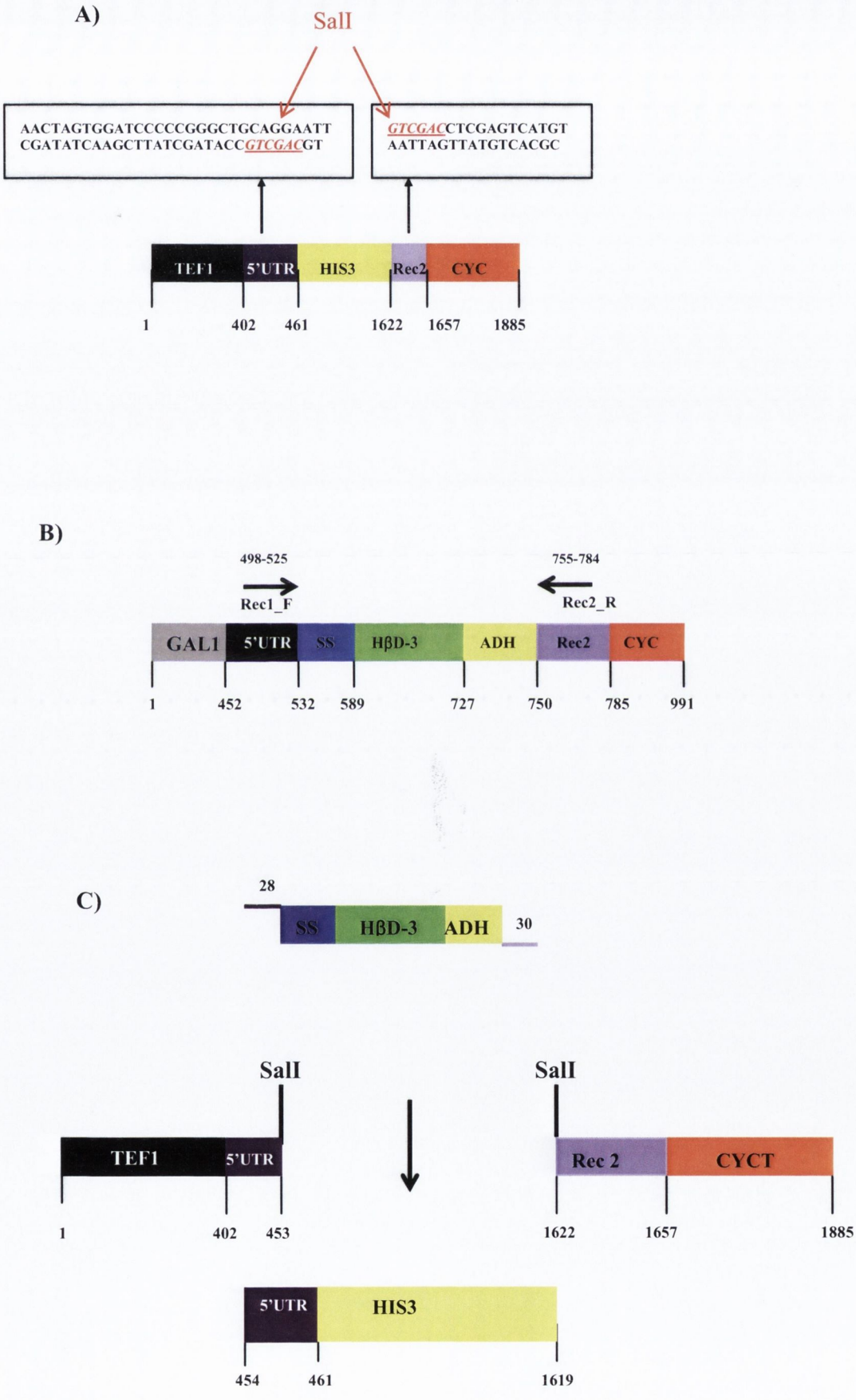
A)
SalI
AACTAGTGGATCCCCCGGGCTGCAGGAATT
CGATATCAAGCTTATCGATACCGTCGACGT
GTCGACCTCGAGTCATGT
AATTAGTTATGTCACGC
TEF1
5'UTR
HIS3
Rec2
CYC
1
402
461
1622
1657
1885
B)
498-525
Rec1_F
755-784
Rec2_R
GAL1
5'UTR
SS
HβD-3
ADH
Rec2
CYC
1
452
532
589
727
750
785
991
C)
28
SS
HβD-3
ADH
30
SalI
SalI
TEF1
5'UTR
Rec 2
CYCT
1
402
453
1622
1657
1885
5'UTR
HIS3
454
461
1619

FIG. 3.8 Gel electrophoresis of digested pGREG505TEF1, HβD-3 fragment and the *TEF1* promoter in CM-505hbd3TEF1

pGREG505TEF1 was digested to remove the *HIS3* stuffer gene. The α-factor leader sequence, HβD-3 and *ADH* terminator fragment was amplified from pGREG505hbd3GAL1. Following recombination direct colony PCR was carried out on pGREG505hbd3TEF1 amplified with a promoter specific forward primer and a HβD-3 specific reverse primer. **A)** pGREG505TEF1 was digested with SalI, to cut out the *HIS3* stuffer fragment. The linearised plasmid can be seen in lane 1, along with the *HIS3* stuffer fragment at 1159bp. HβD-3 was amplified from pGREG505hbd3GAL1, with overhanging regions homologous to pGREG505TEF1, resulting in a 283bp band seen in lane 2. 5μl of Hyperladder I molecular weight marker was loaded at the start of the gel. Band sizes are denoted by lines. **B)** Schematic illustration of CM-505hbd3TEF1 displaying the position of the TEF1_F1 primer and the HβD-3_R1 primer. Primers are denoted by arrows. *TEF1* promoter: black. Non-specific 5'UTR: purple. α-factor signal sequence: blue. HβD-3: green. *ADH* terminator: yellow. Rec2: lilac. *CYC* terminator: orange. Nucleotide positions are shown for regions in the schematic and primers. Note: schematic diagram not to scale. **C)** Amplification of the *TEF1* promoter in CM-505hbd3TEF1 using TEF1_F1 and HβD-3_R1. Lane 1:CM-505hbd3GAL1 and lane 2: CM-506hbd3GAL1 negative controls. Lane 3: CM-505hbd3TEF1, a band at the expected size of 544bp is evident. 5μl of Hyperladder I of molecular weight marker was loaded at the start of the gel. Band sizes are denoted by numbers to the left.

All of the above products were separated on 1% TAE agarose.

A)

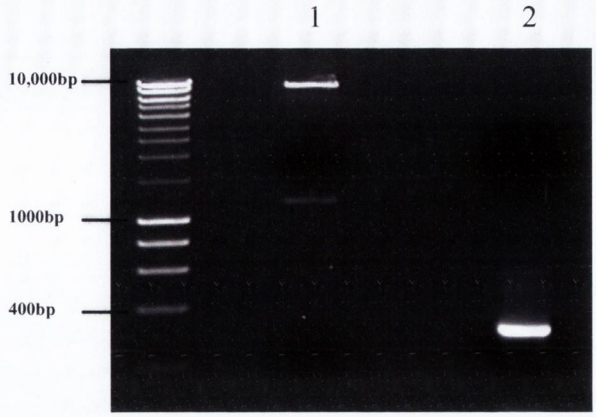
1
2
10,000bp
1000bp
400bp

B)

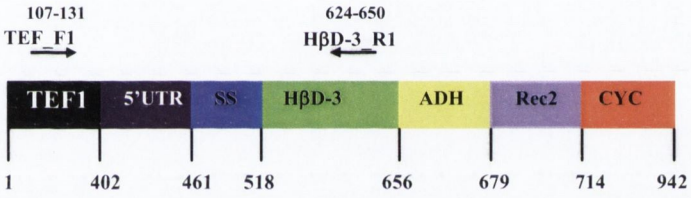
107-131
TEF_F1
624-650
HβD-3_R1
TEF1
5'UTR
SS
HβD-3
ADH
Rec2
CYC
1
402
461
518
656
679
714
942

C)

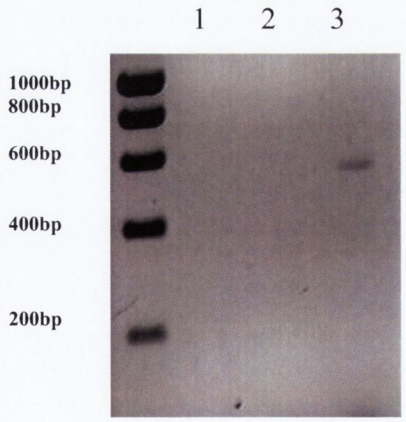
1
2
3
1000bp
800bp
600bp
400bp
200bp

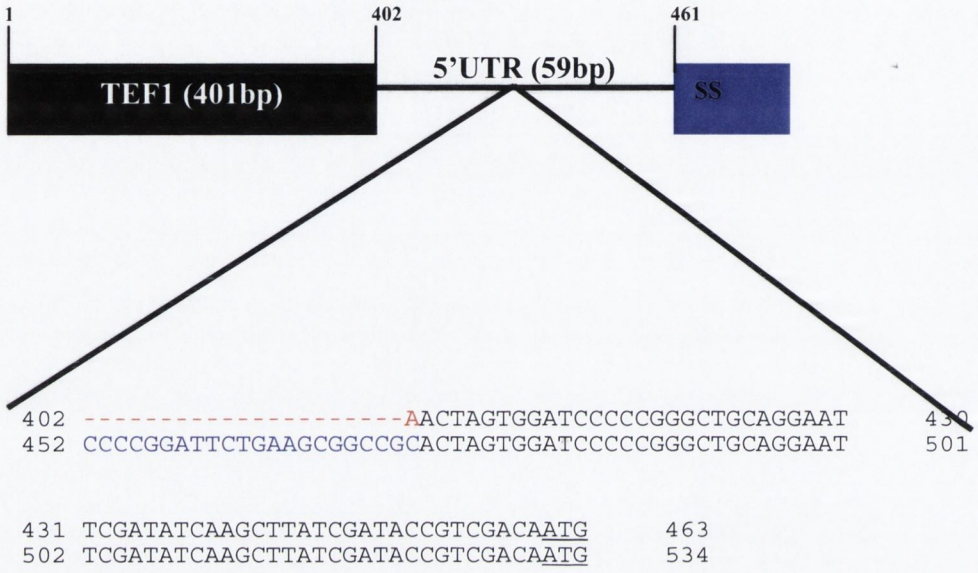

FIG. 3.9 Schematic illustration of non-specific 5'UTR of CM-505hbd3TEF1 and DNA sequence alignment of the non-specific 5'UTR region of CM-505hbd3TEF1 versus CM-505hbd3GAL1

DNA sequence alignment of the non-specific 5'UTR of CM-505hbd3TEF1 (top line) and CM-505hbd3GAL1 (bottom line). The black letters denote similar nucleotides, blue letters denote wild-type nucleotides, red letters denote mutant nucleotides and gaps are represented by dashes. The start codon of HβD-3 is underlined. *TEF1* promoter: black block. α-factor signal sequence: blue block. Note: Schematic diagram is not to scale.

of the construct, nucleotides were deleted from the non-specific 5'UTR at position 401 during the restriction digestion (Fig. 3.9). As stated above, the *TEF* promoter was inserted into pGREG505GAL1 by digesting the *GAL1* promoter from the plasmid via restriction digest with SacI and SpeI restriction enzymes, removing 28bp from the non-specific 5'UTR including the SpeI restriction site (Fig 3.5). This was followed by the ligation of the *TEF1* promoter into the linearised plasmid, which incorporated 7 nucleotides into the non-specific 5'UTR, including the SpeI site (Dr. R. Karreman, unpublished). The resultant non-specific 5'UTR region of CM-505hbd3TEF1, was reduced by 21 nucleotides to 59 nucleotides (Fig. 3.9 & 3.23). A summary of modifications is seen in Table 3.1.

Table 3.1 Summary of mutations/changes in plasmid clones

Strain	Location of mutation	Nature of mutation/change	Region of mutation/change
CM-505hbd3TEF1	401	Nucleotide deletion (21bp)	N/S 5'UTR
	402	Base pair change (C to A)	N/S 5'UTR
CM-506hbd3AGT1	184	Base pair change (T to A)	Promoter
	500	Nucleotide deletion (28bp)	N/S 5'UTR
	547	Nucleotide deletion (TCGA)	N/S 5'UTR
	7608	Nucleotide deletion (23bp)	UTR
CM-506hbd3PGK1	719	Nucleotide deletion (28bp)	N/S 5'UTR
	7830	Nucleotide deletion (23bp)	UTR
CM-pRShbd3PGK1	26	Base pair change (A to G)	Promoter
	262	Base pair change (A to G)	Promoter
	454	Nucleotide deletion (T)	5'UTR
CM-505hbd3HISGAL1	745	Nucleotide deletion (23bp)	ADH terminator

UTR: Untranslated region

N/S 5'UTR: Non-specific 5'UTR

3.2.2 Promoter swaps leading to variants of the pGREG vector series

The *GAL1* promoter in the vectors pGREG505hbd3GAL1 and pGREG506hbd3GAL1, is flanked by the restriction sites, SacI and SpeI, as seen in Fig. 3.5. The *GAL1* promoter can be removed from the plasmid by restriction digestion with SacI and SpeI enzymes. As seen in Fig. 3.5, the SacI restriction site, is located 23bp upstream of the *GAL1* promoter and the SpeI restriction site is located 28bp downstream of the *GAL1* promoter (underlined sequences in dark green and black text respectively). Digesting with these restriction enzymes results in the removal of the *GAL1* promoter (451bp) and additionally the removal of untranslated nucleotides from the plasmid (Fig. 3.5). This results in the removal of a 502bp fragment, eliminating some untranslated nucleotides and shortening the overall length of the non-specific 5'UTR (Fig. 3.5).

3.2.2.1 Replacement of the inducible *GAL1* promoter, for an inducible *AGT1* promoter

To create a lager strain that has the ability to express HβD-3 during fermentation, the gene was placed under the control of a maltose inducible promoter. As stated in section 3.1, maltose is the preferred substrate of *S. pastorianus*, it also constitutes approximately 60% of the fermentable sugars available in wort. The inducible *GAL1* promoter was replaced by a maltose inducible *S. cerevisiae* promoter (*AGT1*). *AGT1* (YGR289C) encodes a high affinity maltose transporter (α-glucosidase transporter) in *S. cerevisiae*, and is located on the MAL1 locus (Cheng, 1990). The *AGT1* (*MAL11*) gene location in *S. cerevisiae*, was identified using the SGD BLAST program. This was confirmed as chromosome VII, coordinates 1073963 to 1075813. The *AGT1* promoter was defined as 500bp upstream of the ATG start codon with the coordinates 1075814 to 1076313 (Fig. 3.10). This 500bp promoter includes all the relevant regulatory elements for *AGT1* expression (Fig. 3.10). The only truncated element was that of the Mig1 binding site. This regulatory element is a 16 nucleotide sequence in the original promoter (TCTTAA**TTGTGTGGGG**), and our 500bp promoter contains the last 10 nucleotides of this sequence (**TTGTGTGGGG**). Mig1p is a zinc finger protein that mediates glucose repression in *S. cerevisiae*, by binding to a GCGGGG motif. Lundin et al. (1994) found that mutating the second C to T in the GC box, does not affect Mig1 binding (Lundin et al., 1994). Furthermore, binding of Mig1 is associated with DNA bending within an AT rich box, upstream of the GC box. The nature of the AT rich box is crucial and is not sequence specific (Lundin et al., 1994). Overall the alterations to the *AGT1* promoter may affect the functionality. This will be examined in chapter 4.

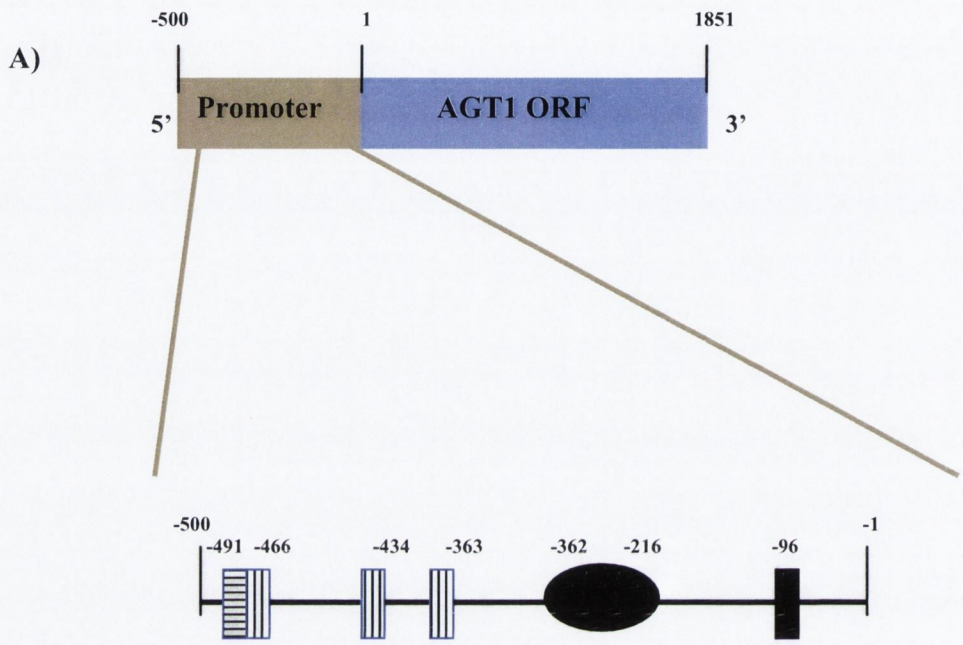

FIG. 3.10 Schematic diagram of the AGT1 promoter used in this study

The schematic diagram illustrates the regulatory elements of the *S.cerevisiae* AGT1 promoter used in this study. AGT1 promoter: beige box. AGT1 ORF: blue box. The TATA box (black box) is located at positions -96 to -102, upstream from the ATG of the AGT1 gene. A 147bp repeat is located between -216 to -362 (black oval). Three MAL activator binding sites are located at positions -363 to -395, -434 to -452 and -466 to -490 (vertical lines). A truncated Mig1 binding site is positioned at -491 to -500 (horizontal lines).

Note: Diagram is not to scale.

Numerous studies have been carried out to date to identify the 5' UTR's of *S. cerevisiae* genes, but such studies have failed to identify the transcription start site (TSS) or the 5'UTR of *AGT1* (*MAL11*) (David et al., 2006; Miura et al., 2006). Steinmetz et al. (2006) maps PolII to 14 sites within the divergent promoter, but other than this no further work as been carried out to identify these regulatory elements (Steinmetz et al., 2006).

Genomic DNA was extracted from *S. cerevisiae* (Section 2.5). The *AGT1* promoter was amplified from total DNA, using primers AGT1_F2 and R2 (Fig. 3.11 A, Table 2.2). These primers were designed to contain flanking regions of homology to the areas surrounding the *GAL1* promoter in pGREG506hbd3GAL1 (Fig 3.11 A, red lines). This resulted in a 586bp PCR product that included the 500bp promoter, plus 40bp of homology upstream and 46bp of homology downstream of the promoter region (Fig 3.12 A, lane 1). pGREG506hbd3GAL1 was digested with SacI and SpeI restriction enzymes, to remove the *GAL1* promoter. This digestion also resulted in the removal of untranslated nucleotides surrounding the promoter (Fig. 3.5). The restriction enzyme digested plasmid was separated on 1% TAE agarose (Fig 3.12 B, lane 1). The linearised plasmid as well as the 502bp fragment containing the *GAL1* promoter was evident (Fig. 3.12 B, lane 1). The *AGT1* promoter was inserted into the linearised plasmid by homologous recombination (Fig. 3.11 A/B). This resulted in the propagation of the strain CM-506hbd3AGT1 (Table 2.3). This was confirmed by direct colony PCR amplifying across the junction using a plasmid specific T3_F primer and a promoter specific AGT1_R primer (Fig. 3.13 A). A band at the expected size of 353bp was obtained (Fig. 3.13 B, lane 1).

Nucleotide sequencing verified the removal of untranslated nucleotides by restriction digestion. 28 nucleotides including the SpeI restriction site, were removed from the non-specific 5'UTR, shortening this region (Table 3.1). Sequencing of this plasmid further revealed a single nucleotide mutation in the *AGT1* promoter. A thymine (T) base was substituted for an adenine (A) nucleotide, at position 184 (Fig. 3.14, Table 3.1). Furthermore, a deletion event occurred at position 547 in the non-specific 5'UTR, in which 4bp (TCGA) were deleted (Table 3.1). This resulted in the loss of a SalI site and a further reduction in the non-specific 5'UTR (Fig. 3.11 C & 3.23). The final non-specific 5'UTR is 48bp long (Fig. 3.11 C & 3.23).

FIG. 3.11 Schematic representation the *AGT1* promoter and replacement of the *GAL1* promoter in CM-506hbd3GAL1

A) Schematic demonstrating the position of the AGTl_F2 and R2 primers relative to the *AGT1* promoter in *S. cerevisiae*. Primers are denoted by arrows. Beige areas of each primer represent areas of homology to the *AGT1* promoter and the length of these regions is denoted by beige numerical values below the arrow. Red regions of each primer represent homology to pGREG506hbd3GAL1 and the length of these regions is denoted by red numerical values below the arrow. *AGT1* promoter: beige. *AGT1* ORF: blue. **B)** Schematic illustration of the insertion of the *AGT1* promoter into pGREG506hbd3, replacing the *GAL1* promoter. The black line represents untranslated regions of the pGREG506hbd3 plasmid upstream from the *GAL1* promoter. Grey block: *GAL1* promoter. Black block: non-specific 5'UTR. Blue block: α-factor signal sequence. Green block: HβD-3. Yellow block: *ADH* terminator. Orange block: *CYC* terminator. Beige block: *AGT1* promoter. Black lines surrounding the *AGT1* promoter represent homology to the plasmid. **C)** Schematic illustration of the *AGT1* promoter (500bp) in CM-506hbd3AGT1, relative to the non-specific 5'UTR sequence (48bp) and the signal sequence (57bp). *AGT1* promoter: beige block. α-factor signal sequence: blue block.

Nucleotide positions are shown for all schematic diagrams and primers.

Note: schematic diagrams are not to scale.

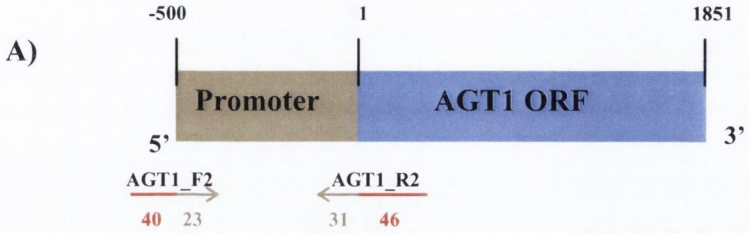
A)
-500
1
1851
Promoter
AGT1 ORF
5'
3'
AGT1_F2
AGT1_R2
40
23
31
46

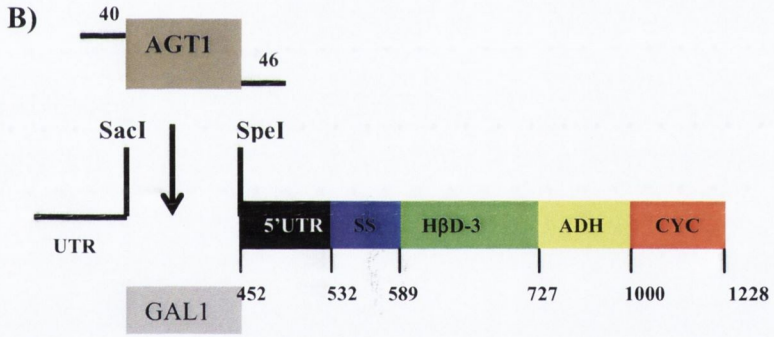
B)
40
AGT1
46
SacI
SpeI
UTR
5'UTR
SS
HβD-3
ADH
CYC
GAL1
452
532
589
727
1000
1228

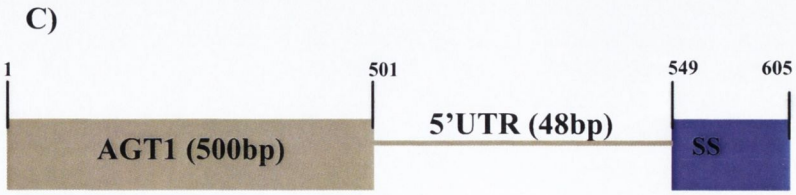
C)
1
501
549
605
AGT1 (500bp)
5'UTR (48bp)
SS

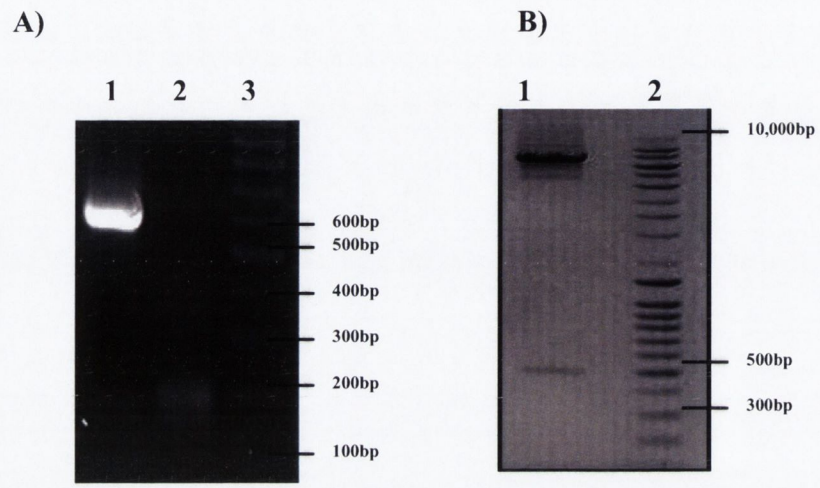

FIG. 3.12 Gel electrophoresis of the *AGT1* promoter and restriction digest of pGREG506hbd3GAL1

Genomic DNA was extracted from *S. cerevisiae* and PCR amplified with *AGT1* promoter specific primers. The *GAL1* promoter from pGREG506hbd3GAL was removed via restriction digest with SacI and SpeI enzymes. **A)** Amplification of the *AGT1* promoter with AGT1_F2 and AGT1_R2 primers gave the expected band size of 586bp including homologous overhangs to pGREG506hbd3GAL1 (lane 1). Lane 2: a H20 negative control. Lane 3: 5µl of Q-Step 1 molecular weight marker. **B)** SacI/SpeI linearised pGREG506hbd3GAL1. A 502bp band shown in lane 1 contains the *GAL1* promoter. Lane 2: 5µl of Q-Step 4 molecular weight marker. All products were electrophoresed on a 1% TAE agarose gel. Band sizes are denoted by lines.

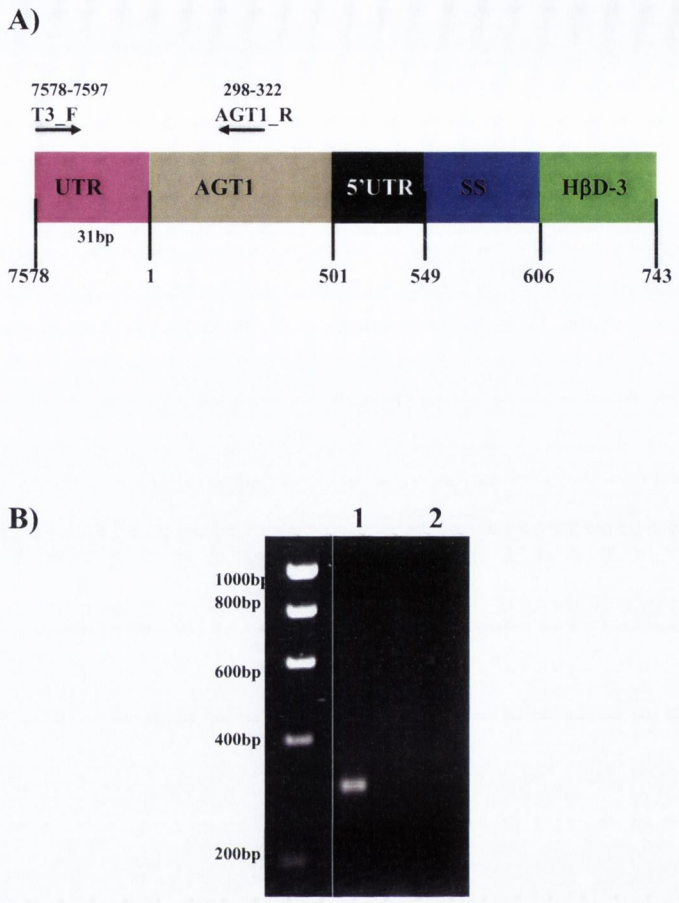

FIG. 3.13 Schematic illustration of CM-506hbd3AGT1 plus primers and colony PCR confirmation of the *AGT1* promoter in CM-506hbd3AGT1

Direct colony PCR of CM-506hbd3AGT1 amplified with a plasmid specific forward primer and an *AGT1* promoter specific reverse primer. **A)** Schematic illustration of CM-506hbd3AGT1 displaying the location of the T3_F and AGT1_R primers. Primers are denoted by arrows. The untranslated region directly upstream of the *AGT1* promoter is denoted by a pink block. *AGT1* promoter: beige block. Non-specific 5'UTR: black block. α-factor signal sequence: blue block. HβD-3: green. Nucleotide positions are shown for regions of the schematic diagram and primers. Note: schematic diagram is not to scale. **B)** Amplification of CM-506hbd3AGT1, across the junction of the *AGT1* promoter, using a plasmid specific T3_F primer and AGT1_R1. The expected band at 353bp was obtained, lane 1. Lane 2: CM-506hbd3PGK1 negative control. 5μl of Hyperladder I molecular weight marker was loaded at the start of the gel. Band sizes are denoted by numbers to the left.

```
1 TTGTGTGGGGTCCGCGAAAATTTCCGGATAAATCCTGTAAACTTTAACTT      50
1 TTGTGTGGGGTCCGCGAAAATTTCCGGATAAATCCTGTAAACTTTAACTT      50

51 AAACCCCGTGTTTAGCGAAATTTTCAACGAAGCGCGCAATAAGGAGAAAT     100
51 AAACCCCGTGTTTAGCGAAATTTTCAACGAAGCGCGCAATAAGGAGAAAT     100

101 ATTATCTAAAAGCGAGAGTTTAAGCGAGTTGCAAGAATCTCTACGGTACA    150
101 ATTATCTAAAAGCGAGAGTTTAAGCGAGTTGCAAGAATCTCTACGGTACA    150

151 GATGCAACTTACTATAGCCAAGGTCTATTCGTAATACTATGGCAGCGAAA    200
151 GATGCAACTTACTATAGCCAAGGTCTATTCGTATTACTATGGCAGCGAAA    200

201 GGAGCTTTAAGGTTTTAATTACCCCATAGCCATAGATTCTACTCGGTCTA    250
201 GGAGCTTTAAGGTTTTAATTACCCCATAGCCATAGATTCTACTCGGTCTA    250

251 TCTATCATGTAACACTCCGTTGATGCGTACTAGAAAATGACAACGTACCG    300
251 TCTATCATGTAACACTCCGTTGATGCGTACTAGAAAATGACAACGTACCG    300

301 GGCTTGAGGGACATACAGAGACAATTACAGTAATCAAGAGTGTACCCAAC    350
301 GGCTTGAGGGACATACAGAGACAATTACAGTAATCAAGAGTGTACCCAAC    350

351 TTTAACGAACTCAGTAAAAAATAAGGAATGTCGACATCTTAATTTTTTATAT   400
351 TTTAACGAACTCAGTAAAAAATAAGGAATGTCGACATCTTAATTTTTTATAT   400

401 ATAAAGCGGTTTGGTATTGATTGTTTGAAGAATTTTCGGGTTGGTGTTTC    450
401 ATAAAGCGGTTTGGTATTGATTGTTTGAAGAATTTTCGGGTTGGTGTTTC    450

451 TTTCTGATGCTACATAGAAGAACATCAAACAACTAAAAAAATAGTATAAT     500
451 TTTCTGATGCTACATAGAAGAACATCAAACAACTAAAAAAATAGTATAAT     500
```

FIG. 3.14 Nucleotide sequence alignment of the *AGT1* promoter of CM-506hbd3AGT1 versus *S. cerevisiae*

The above nucleotide sequence compares the *AGT1* promoter in CM-506hbd3AGT1 (top line) with the original *AGT1* promoter sequence in *S. cerevisiae* (bottom line). A single base mutation is seen at position 184, whereby a thymine (T) [blue] was substituted for an adenine (A) [red]. This occurred within the 147bp repeat element (underlined). The truncated Mig1 binding site is denoted by bold nucleotides. The *MAL* activator binding regions, UAS_{MAL}, are denoted by italic nucleotides. The TATA box is represented by bold, underlined, italics.

3.2.2.2 Replacement of the inducible *GAL1* promoter, for a constitutive *PGK1* promoter

In addition to examining the expression of HβD-3 from inducible promoters, we also wanted to determine the level of expression from a constitutive promoter, which may produce more sustained production over the course of the fermentation. For this, the promoter of the 3-Phosphoglycerokinase gene, *PGK1*, was chosen. *PGK* is a highly expressed glycolytic enzyme in yeast (Hitzeman et al., 1980). The *PGK1* promoter, like the *TEF1* promoter, allows constitutive expression during normal growth in rich medium such as YEPD. The *PGK1* promoter from *S. cerevisiae* was identified in the same manner as the *AGT1* promoter (Section 3.2.2.1). The ORF, YCR012W is located on chromosome III, from coordinates 137746 to 138996. The *PGK1* promoter region was identified as a 712bp fragment, upstream of the start codon ATG (coordinates 137034 to 137745) as seen in Fig. 3.15 A. David et al. (2006) indicated that the 5'UTR of the *PGK1* promoter of *S. cerevisiae,* is 82 nucleotides long (Fig. 3.15 A). $PGK1_{SC}$_F2 and $PGK1_{SC}$_R2 primers were designed to amplify the promoter region and to add flanking regions on either side, with 40-46bp of homology to pGREG506hbd3GAL1 (Table 2.2, Fig 3.15 B, red lines). An additional 6bp was added to the PGK1_R2 primer, to increase the GC content of the primer. These additional nucleotides have no effect on the *PGK1* promoter activity (Dr. J. Fitzpatrick, Unpublished). The PCR amplification products were electrophoresed on 1% TAE agarose and a band at the expected size (798bp) was evident (Fig. 3.16 C, lane 2). pGREG506hbd3GAL1 was digested with SacI and SpeI restriction enzymes, to remove the *GAL1* promoter as before (Fig. 3.16 A). This digestion results in the removal of a 502bp band as before (Fig. 3.12 B, lane 1). The *PGK1* promoter was inserted into the linearised plasmid by homologous recombination (section 3.2.1.3). The strain CM-506hbd3PGK1 was generated (Table 2.3). Direct colony PCR using a plasmid specific T3_F primer and a promoter specific $PGK1_{SC}$_R1 primer (Fig. 3.17 A), yielded a band of the expected size (357bp) (Fig. 3.17 B, lane 2).

The insertion of the *PGK1* promoter, into CM-506hbd3PGK1 was confirmed by DNA sequencing (Appendix 1). The elimination of non-specific nucleotides, by restriction digest, was also confirmed by sequencing (Table 3.1) (Appendix 1). The removal of 28 nucleotides, including the SpeI restriction site, reduces the non-specific 5'UTR by 28 nucleotides (Table 3.1) (Fig. 3.16 B & 3.23). The final non-specific 5'UTR is 58bp (Fig. 3.16 B & 3.23).

A)

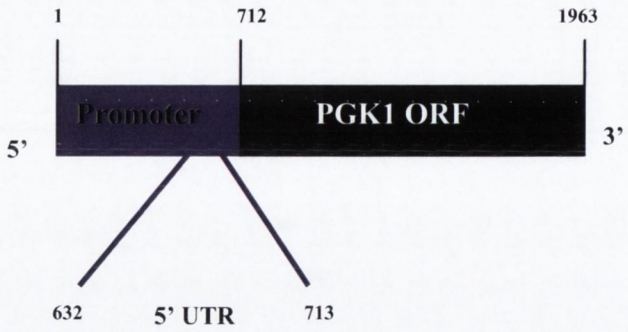

CCAAGAATTACTCGTGAGTAAGGAAAGAGTGAGGAACTATCGCATACCTGCATTTAAAGAT
GCCGATTTGGGCGCGAATCCTTTATTTTGGCTTCACCCTCATACTATTATCAGGGCCAGAAA
AAGGAAGTGTTTCCCTCCTTCTTGAATTGATGTTACCCTCATAAAGCACGTGGCCTCTTATCG
AGAAAGAAATTACCGTCGCTCGTGATTTGTTTGCAAAAAGAACAAAACTGAAAAAACCCAG
ACACGCTCGACTTCCTGTCTTCCTATTGATTGCAGCTTCCAATTTCGTCACACAACAAGGTCC
TAGCGACGGCTCACAGGTTTTGTAACAAGCAATCGAAGGTTCTGGAATGGCGGGAAAGGGT
TTAGTACCACATGCTATGATGCCCACTGTGATCTCCAGAGCAAAGTTCGTTCGATCGTACTG
TTACTCTCTCTCTTTCAAACAGAATTGTCCGAATCGTGTGACAACAACAGCCTGTTCTCACAC
ACTCTTTTCTTCTAACCAAGGGGGTGGTTTAGTTTAGTAGAACCTCGTGAAACTTACATTTAC
ATATA***TATAAA***CTTGCATAAATTGGTCAATGCAAGAAATACATATTTGGTCTTTTCTAATTCG
TAGTTTTTCAAGTTCTTAGATGCTTTCTTTTTCTCTTTTTTACAGATCATCAAGGAAGTAATTA
TCTACTTTTTACAACAAATATAAAACA**CCGCGG**

B)

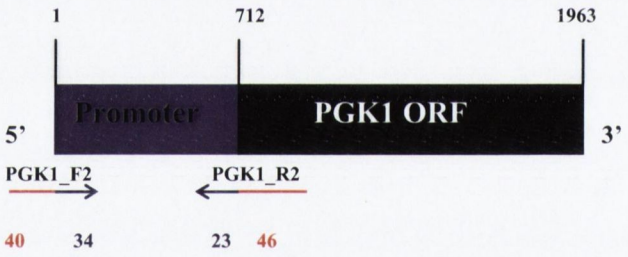

FIG. 3.15 Schematic representation of the *S. cerevisiae PGK1* promoter

A) Schematic diagram illustrating the *S. cerevisiae PGK1* promoter, promoter specific 5' UTR and the ORF. The 712bp promoter sequence is illustrated below the schematic. The 5'UTR region is underlined. The GC anchor is denoted by bold nucleotides. The TATA box is represented by bold, underlined, italics. **B)** Schematic diagram showing the position of the PGK1_F2 and PGK1_R2 primers in relation to the *PGK1* promoter. The primers are denoted by arrows. The purple region represents regions of the primer that have homology to the promoter, and the length of these regions are denoted by purple numerical values below the arrow. The red region represents regions of the primer with homology to the promoter region of pGREG506hbd3GAL1, and the length of these regions is denoted by red numerical values below the arrow. *PGK1* promoter: purple. *PGK1* ORF: black. Nucleotide positions are shown for regions of the schematic diagram and primers. Note: schematic diagrams are not to scale.

FIG. 3.16 Schematic representation of the *PGK1* promoter inserted into pGREG506hbd3GAL1 and gel electrophoresis of the *PGK1* promoter

Genomic DNA was extracted from *S. cerevisiae* and amplified with *PGK1* promoter specific primers. **A)** Schematic illustration of the insertion of the *PGK1* promoter into pGREG506hbd3GAL1, replacing the *GAL1* promoter. Grey block: *GAL1* promoter. Purple block: *PGK1* promoter. Black block: non-specific 5'UTR. Blue block: α-factor signal sequence. Green block: HβD-3. Yellow block: *ADH* terminator. Orange block: *CYC* terminator. Black lines surrounding the *PGK1* promoter represent homology to the plasmid. **B)** Schematic illustration of the *PGK1* promoter (712bp) in CM-506hbd3PGK1, relative to the non-specific 5'UTR sequence (58bp) and the signal sequence. *PGK1* promoter: purple block. α-factor signal sequence: blue block. **C)** Amplification of the *PGK1* promoter from *S. cerevisiae*. Lane 1: 5μl of Q-Step 1 molecular weight marker. Lane 2: *PGK1* promoter amplified from *S. cerevisiae* total genomic DNA. The expected size is 798bp. Products were amplified on 1% TAE agarose. Band sizes are denoted by arrows.

Nucleotide positions are shown for regions of the schematic diagrams and primers. Note: Schematic diagrams not to scale.

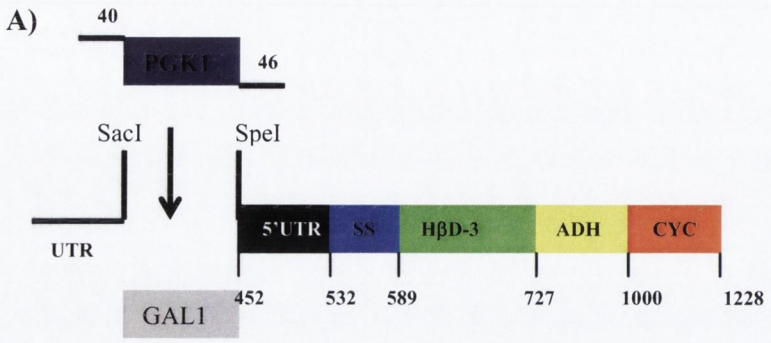
A)
40
PGK1
46
SacI
SpeI
UTR
5'UTR
SS
HβD-3
ADH
CYC
GAL1
452
532
589
727
1000
1228

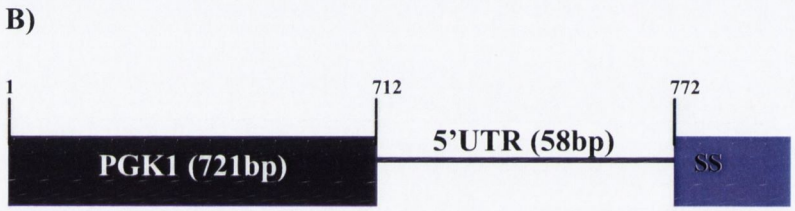
B)
1
712
772
PGK1 (721bp)
5'UTR (58bp)
SS

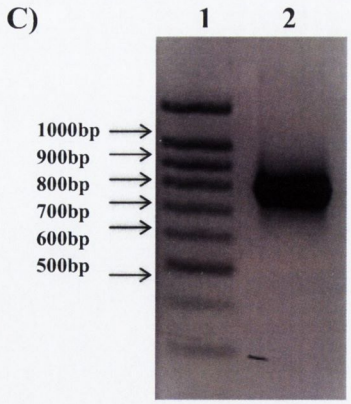
C)
1
2
1000bp
900bp
800bp
700bp
600bp
500bp

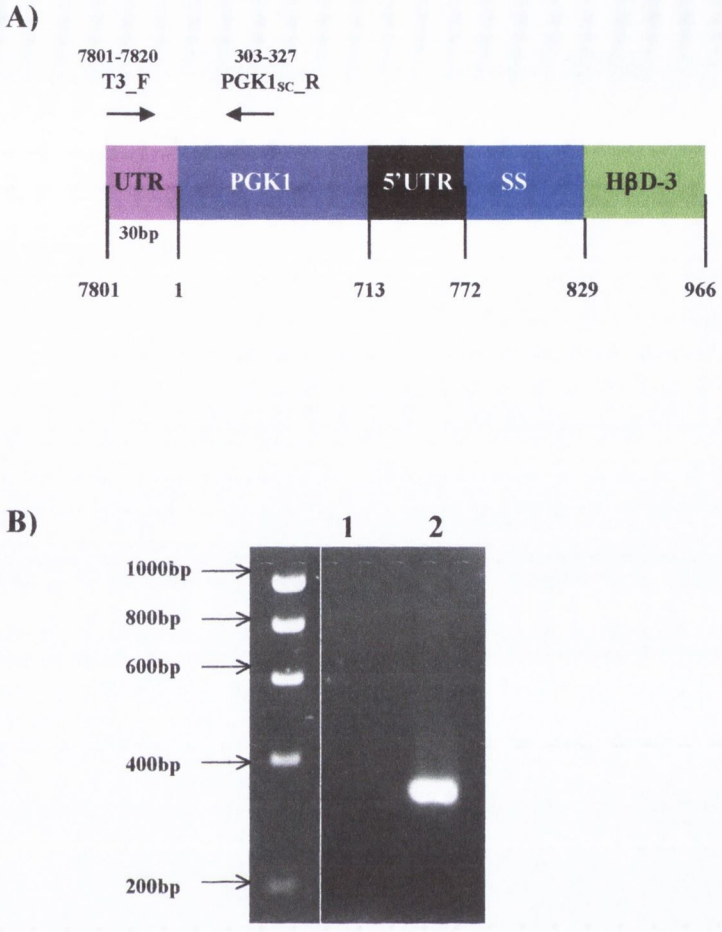

FIG. 3.17 Schematic representation of CM-506hbd3PGK1 and colony PCR of *PGK1* promoter in this strain

Direct colony PCR of CM-506hbd3PGK1 amplified with a plasmid specific forward primer and a *PGK1* promoter specific reverse primer. **A)** Schematic representation of CM-506hbd3PGK1 displaying the location of the plasmid specific T3_F primer and the PGK1$_{SC}$_R1 primer. Primers are denoted by arrows. The plasmid region directly upstream of the *PGK1*$_{SC}$ promoter is represented by a pink block. *PGK1*$_{SC}$ promoter: purple block. Non-specific 5'UTR: black block. α-factor signal sequence: blue block. HβD-3: green. Nucleotide positions are shown for regions of the schematic diagram and primers. Note: Schematic diagram is not to scale. **B)** Amplification across the junction of the *PGK1* promoter in CM-506hbd3PGK1. DNA was amplified using a plasmid specific T3_F primer and a PGK1$_{SC}$_R1 primer. The expected sized product is 357bp. Lane 1: CM-506hbd3AGT1 negative control. Lane 2: CM-506hbd3PGK1. 5μl of Hyperladder I molecular weight marker was loaded at the start of the gel. Band sizes are denoted by arrows.

3.2.3 Addition of a polyhistidine-tag

To detect secreted HβD-3 via Western immunoblotting, a 6xHis-tag was added to the 3' end of the gene, directly before the stop codon, TGA, of the HβD-3 ORF (Fig 3.18). A reverse primer was designed with 29bp of homology to the 3' end of the HβD-3 ORF, followed by a 18bp 6xHis-tag sequence, homology to the stop codon TGA, and a further 35bp of homology to the rec2 site of pGREG505hbd3GAL1 (Fig. 3.18 A, Table 2.2). This primer was designed to remove the 23bp *ADH* terminator present in pGREG505hbd3GAL1, which is located upstream of the rec2 site, as this plasmid already contains a fully functioning *CYC* terminator (Fig. 1.8 A). The primers Gal1_F and HIS-TAG_R (Tables 2.1 and 2.2) were used to amplify a 779bp fragment, which included the *GAL1* promoter, α-factor signal sequence, HβD-3 gene and 6xHis-tag sequence, from pGREG505hbd3GAL1 (Fig 3.18 B and C). This fragment was visualized following electrophoresis on 1% TAE agarose (Fig. 3.18 D, lane 1). The pGREG505GAL1 plasmid was digested with SalI, to remove the 1159bp *HIS3* stuffer cassette, as described section 3.2.1.3 (Fig 3.7 & 3.8 A, lane 1). The HβD-3, 6xHis-tag fragment was inserted into the linearised plasmid by homologous recombination, to generate the strain CM-505hbd3HISGAL1 (Table 2.3).

The addition of the 6xHis-tag was confirmed by DNA sequencing, as was the removal of the truncated *ADH* terminator sequence (Appendix 1).

FIG. 3.18 Schematic representation of the GAL1, HβD-3, 6xHis-tag fragment generation and gel electrophoresis of the HβD-3-6xHis-tag fragment

100ng of pGREG505hbd3GAL1 was PCR amplified with a plasmid specific forward primer and a HIS-TAG_R primer. **A)** DNA sequence of the 85bp HIS-TAG_R primer (top) aligned to the region of amplification in CM-505hbd3GAL1 (bottom). The ORF of HβD-3 is denoted by bold nucleotides. The 6xHis-tag is underlined. The truncated *ADH* terminator sequence in CM-505hbd3GAL1 is denoted by red nucleotides. This region was excluded in the primer (blue dashes). **B)** Illustration of the primers used to amplify the GAL1, HβD-3, 6xHis-tag fragment, from pGREG505hbd3GAL1. Primers are denoted by arrows. Red block: *GAL1* promoter. Black block: non-specific 5'UTR. Blue block: α-factor leader sequence. Green block: HβD-3. Yellow block: *ADH* terminator. Lilac block: rec 2. Red arrow: homology to the *GAL1* promoter. Green arrow/line: homology to HβD-3. Pink line: 6xHis-tag. Lilac line: homology to rec 2. **C)** A schematic diagram illustrating the addition of a 6xHis-tag to the HβD-3 ORF in CM-505hbd3GAL1, directly before the stop codon (TGA). The HβD-3 ORF is illustrated in green, along with the amino acid sequence. 6xHis-tag: pink. The stop codon is denoted by a black asterisk *. All of the remaining regions are the same as above. **D)** Amplification of the GAL1, HβD-3, 6xHis-tag fragment. The gene construct was amplified with the primers Gal1_F and HIS-TAG_R. The resultant PCR products were electrophoresed on a 1% TAE agarose gel. Lane 1: DNA amplified using plasmid pGREG505hbd3GAL1. A band of the expected size (779bp) is evident. Lane 2: H20 negative control. 5μl of hyperladder II molecular weight marker was loaded on the end of the gel. Band sizes are denoted by lines.

Nucleotide positions are shown for regions of the schematic diagrams and primers. Note: Schematic diagrams are not to scale.

A)

```
1  GAGGTAGAAAATGTTGTAGAAGAAAAAAACATCACCATCACCATCACTGA 50
1  GAGGTAGAAAATGTTGTAGAAGAAAAAAA----------------TGA 32

51 ----------------------GTCGACCTCGAGTCATGTAATTAGTTATGTCACGC 85
33 GGCGCGCCACTTCTAAATAAGCGGTCGACCTCGAGTCATGTAATTAGTTATGTCACGC 90
```

B)

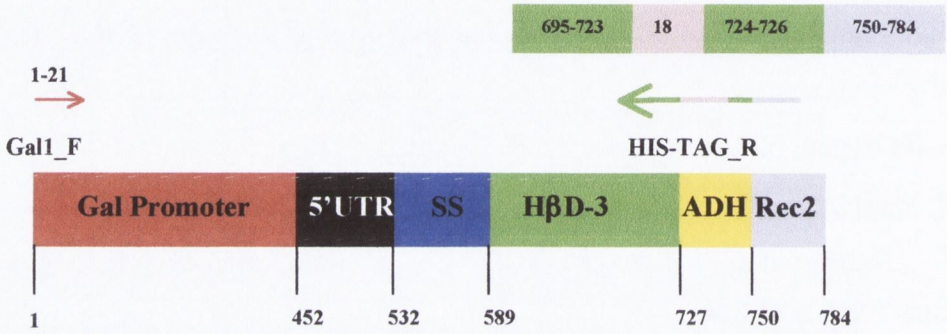

C)

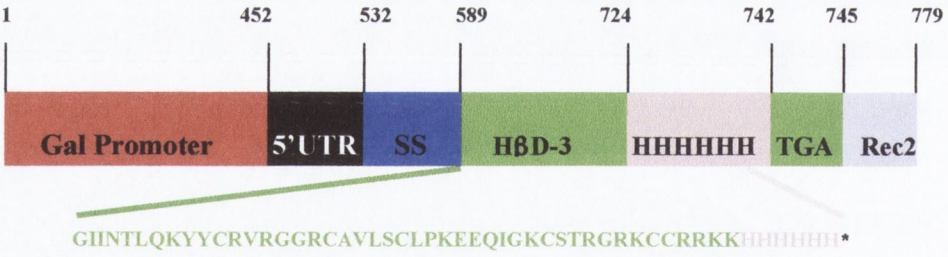

D)

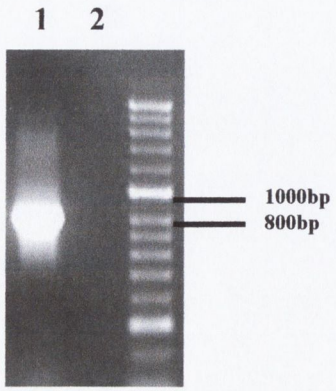

3.2.4 Formation of a multi-copy plasmid containing HβD-3

To increase the levels of HβD-3 expression, a copy of the gene was cloned into a multicopy plasmid, under the control of a constitutive *PGK1*$_{SB}$ promoter from *S. bayanus*. A yeast episomal plasmid (pRS42H) was chosen for this study (Christianson et al., 1992; Sikorski and Hieter, 1989). pRS42H contains a hygromycin B phosphotransferase-encoding gene (hph) with a *CYC1* terminator (NT1) (Fig. 2.3). This plasmid has a copy number of approximately 20 plasmid molecules per cell (Christianson et al., 1992). The PGK1$_{SB}$-HβD-3 gene construct was synthesized and cloned into the BamHI site of a pBSK- plasmid as described in section 1.6 (GenScript, USA INC, Dr. T. C. James unpublished). The HβD-3 gene construct was PCR amplified from the pBSK-HβD-3 plasmid, using PGK1$_{SB}$_F2 and ADHT_R1 primers (Fig. 3.19 A, Table 2.2). These primers have 30-40bp of homology to the lacZ region of pRS42H (Fig. 3.19 A/B). PCR amplification resulted in a 1021bp band (Fig. 3.19 C, lane 1). pRS42H was digested with the restriction enzymes SalI and NotI, these restriction sites are located in the multiple cloning site of LacZ (Fig. 2.3). The digestion yielded a linearised plasmid of 6153bp and an excised fragment of 64bp, which is too small to visualise on a 1% TAE agarose gel (Fig 3.19 D, lane 1). The HβD-3 gene construct was inserted into the linearised plasmid by homologous recombination (section 3.2.1.3), to generate the strain CM-pRShbd3PGK (Table 2.3). Following homologous recombination, 13bp was deleted from the lacZ region upstream of the SalI restriction site and 9bp was deleted downstream of the NotI restriction site.

Colonies were selected on YEPD plates containing hygromycinB (section 2.1.2) and screened using a plasmid specific forward primer LacO_F and an insert specific reverse primer HβD-3_R1, via direct colony PCR (Fig. 3.20 A & B, lane 2). A PCR product of the expected size of 883bp was obtained (Fig. 3.20 B, lane 2). DNA sequencing confirmed the presence of the insert (Appendix 1).

Sequencing of the plasmid revealed that a number of base mutations had occured during cloning. Two single nucleotide mutations occured in the *PGK1*$_{SB}$ promoter region, one at position 26 and the other at position 262 (Fig. 3.21, Table 3.1). In both cases an adenine (A) is replaced by an guanine (G). A further single nucleotide deletion occured at position 454 in the *PGK1*$_{SB}$ promoter region, removing a thymine (T) nucleotide (Fig. 3.21, Table 3.1). As described in section 3.2.2.2, the 5'UTR of the *PGK1*$_{SC}$ promoter is 82bp long (Fig. 3.15 A). The 517bp *PGK1*$_{SB}$ promoter is 76% identical to the *PGK1*$_{SC}$

FIG. 3.19 Schematic illustrating the generation of CM-pRShbd3PGK1 and gel electrophoresis of the HβD-3 gene construct and the pRS42H linearised plasmid

The PGK1-HβD-3 construct was amplified from pBSK-HβD-3. The pRS42H plasmid was linearised with SalI and NotI restriction enzymes. **A)** Schematic diagram showing the position of the primers $PGK1_{SB}$_F2 and ADHT_R1 relative to the HβD-3 gene construct in pBSK-HβD-3. The primers are denoted by arrows. The black regions of the arrow refer to regions of homology to the construct, the length of this region is denoted by a black number. The orange regions of the arrow represent regions of homology to the lacZ region in pRS42H, the length of this region is denoted by orange numbers. Pink block: $PGK1_{SB}$ promoter. Blue block: α-factor signal sequence. Green block: HβD-3. Yellow block: *ADH* terminator. **B)** Diagram of HβD-3 gene construct insertion into pRS42H linearised with SalI and NotI, with 30-40bp of homology to LacZ (orange lines). All features of the HβD-3 gene construct are noted in A. Orange blocks: Lac Z. **C)** Amplification of $PGK1_{SB}$-HβD-3 separated on 1% TAE agarose. The gene construct was amplified from plasmid pBSK-HβD-3 using the primers $PGK1_{SB}$_F2 and ADHT_R1 (lane 1). A band of the expected size (1021bp) is evident. Lane 2: 5μl of Q-Step 4 molecular weight marker. Band sizes are denoted by arrows. **D)** 1% TAE agarose gel of SalI/NotI digested pRS42H. A linearised band is seen at 6153bp in lane 1. Lane 2: 5μl of Q-Step 4 molecular weight marker. Band sizes are denoted by arrows.

Nucleotide positions are shown for regions of the schematic diagrams and primers. Note: Schematic diagrams are not to scale.

A.

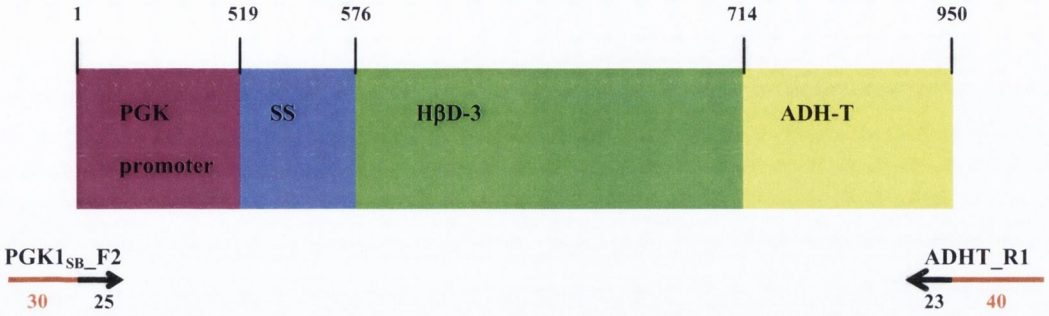
1
519
576
714
950
PGK
promoter
SS
HβD-3
ADH-T
PGK1SB_F2
30
25
ADHT_R1
23
40

B)

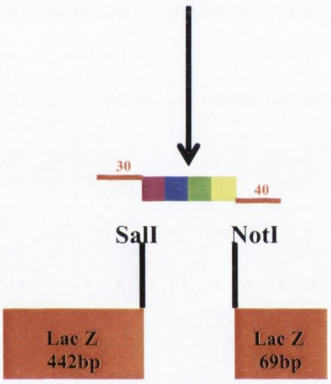
30
40
SalI
NotI
Lac Z
442bp
Lac Z
69bp

C)

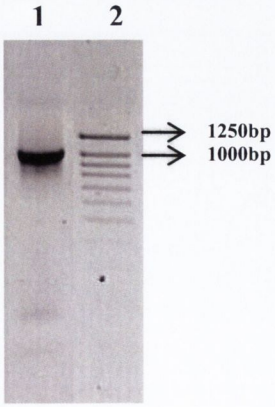
1
2
1250bp
1000bp

D)

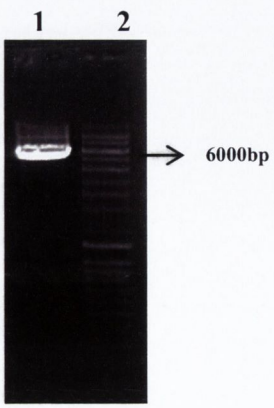
1
2
6000bp

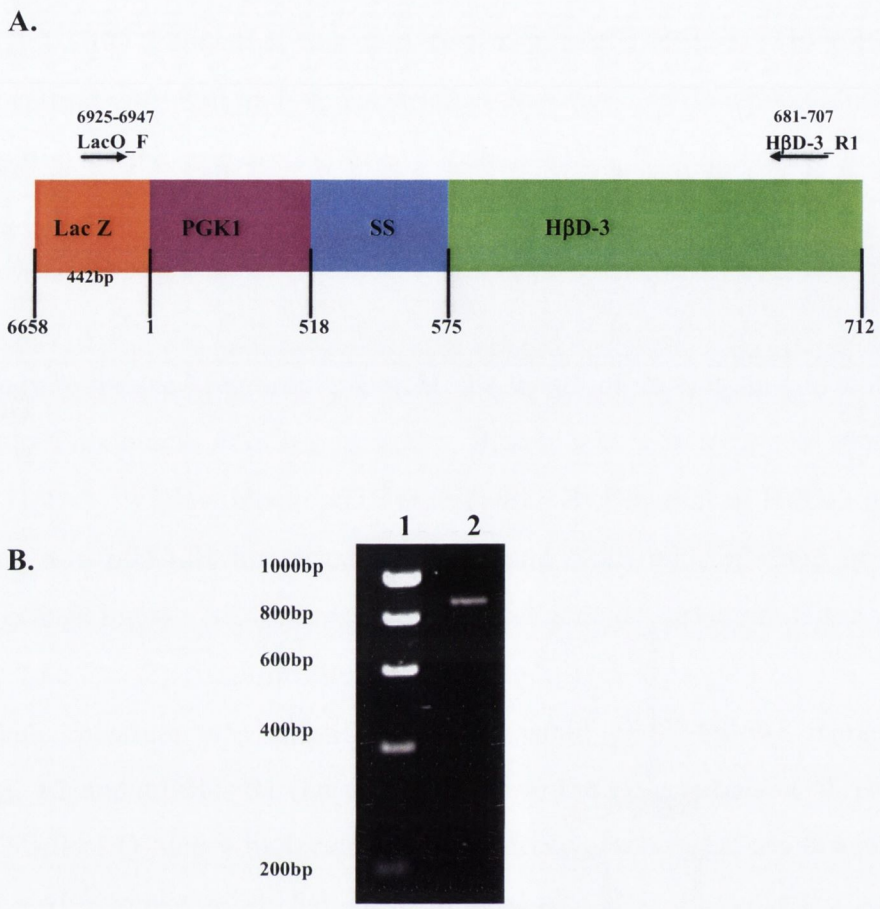

FIG. 3.20 Schematic illustration of CM-pRShbd3PGK1 displaying primers and colony PCR of this strain

Direct colony PCR of CM-pRShbd3PGK1 amplified with a plasmid specific forward primer and a HβD-3 specific reverse primer. **A)** Schematic illustration of CM-pRShbd3PGK1 displaying the position of the LacO_F primer and the HβD-3_R1 primer. Primers are denoted by arrows. Lac Z: orange block. *PGK1*$_{SB}$ promoter: purple block. α-factor signal sequence: blue block. HβD-3: green block. Nucleotide positions are shown for regions of the schematic diagram and primers. Note: Schematic diagrams are not to scale. **B)** Amplification of CM-pRShbd3PGK1, across the junction of the insert, using a plasmid specific LacO_F primer and HβD-3_R1. A band of the expected size (883bp) was obtained (lane 2). Lane 1: 5μl of Hyperladder I molecular weight marker. Band sizes are denoted by numbers to the left.

```
1   GACGAATTTTGTGAAAAGAGCACCCGGACACGCTCGACTTCCTGTCTTCC      50
1   GACGAATTTTGTGAAAAGAGCACCCAGACACGCTCGACTTCCTGTCTTCC      50

51  AGTCTGGAGTCGGCTTCCAATTTCGTCACACAACAAGATTTCTAGCAGCG     100
51  AGTCTGGAGTCGGCTTCCAATTTCGTCACACAACAAGATTTCTAGCAGCG     100

101 GCCTTCAGGCTTGAAACAAAGAATCGAAGGTTCTGGAATGGTGGGAATCA     150
101 GCCTTCAGGCTTGAAACAAAGAATCGAAGGTTCTGGAATGGTGGGAATCA     150

151 GTTTACTACCACATGCTATGATGTCTACCGCACTCTCCAGAGCAAAAGTT     200
151 GTTTACTACCACATGCTATGATGTCTACCGCACTCTCCAGAGCAAAAGTT     200

201 TCGTTCAATCACACTCTTACACTCTCTCTCACACAATTGTTCGAATCGTG     250
201 TCGTTCAATCACACTCTTACACTCTCTCTCACACAATTGTTCGAATCGTG     250

251 TGACAACAGCAGCTTGTTCTCACACAGTCTCTTTTCTTCTAACCAAGGGG     300
251 TGACAACAGCAACTTGTTCTCACACAGTCTCTTTTCTTCTAACCAAGGGG     300

301 TTGTTTGGGCTAGTAAAGCTTTGTGGAAACTTAGATTTACATATATATAA     350
301 TTGTTTGGGCTAGTAAAGCTTTGTGGAAACTTAGATTTACATATATATAA     350

351 AGTTGAACGAATTAGTGAATGCTAAAGAAATATATAATTGACCTTTTTCT     400
351 AGTTGAACGAATTAGTGAATGCTAAAGAAATATATAATTGACCTTTTTCT     400

401 CTAGATAGTTTTTTGAACTTGTTAGATGTATTTTAATTCTTTCTCTGTTT     450
401 CTAGATAGTTTTTTGAACTTGTTAGATGTATTTTAATTCTTTCTCTGTTT     450

451 TTTT-ATTTCTTCTTTTCACAGATCATCAAGGAAGTAATTATCTACTTTT     499
451 TTTTTATTTCTTCTTTTCACAGATCATCAAGGAAGTAATTATCTACTTTT     500

500 TGCAACAAATATAAAACA    517
501 TGCAACAAATATAAAACA    518
```

FIG. 3.21 Nucleotide sequence alignment of the *PGK1*$_{SB}$ promoter region in CM-pRShbd3PGK versus pBSK-HβD-3

Nucleotide sequence alignment of the *PGK1*$_{SB}$ promoter of CM-pRShbd3PGK1 (top line) and pBSK-HβD-3 (bottom line). A single nucleotide mutation is evident at position 26, an adenine (A) [blue] is replaced by a guanine (G) [red]. The same nucleotide mutation is evident at position 262. The estimated promoter specific 5'UTR is underlined. A single nucleotide deletion (red dash) occurred at position 454, within the estimated 5' UTR, whereby a thymine (T) (blue) was deleted.

promoter (Fig. 3.22). Furthermore the 82bp 5'UTR of the *PGK1*$_{SC}$ promoter shares high sequence homology to this region in the *PGK1*$_{SB}$ promoter (Fig. 3.22), but contains a 10bp deletion at position 454bp in the *PGK1*$_{SC}$ promoter. The estimated length of the 5' UTR of the *PGK1*$_{SB}$ promoter is 82bp. The deletion of a T nucleotide occurred at position 454 (Fig. 3.21). This is located within the estimated promoter specific 5'UTR.

```
 2 ACGAATTTTGTGAAAAGAGCACCCGGACACGCTCGACTTCCTGTCTTCCA      51
26 AAAAGAACAAAACTGAAAAAACCCAGACACGCTCGACTTCCTGTCTTCCT      75


52 GTCTGGAGTCGGCTTCCAATTTCGTCACACAACAAGATTTCTAGCAGCGG     101
76 AT-TGATTGCAGCTTCCAATTTCGTCACACAACAAGGTC-CTAGCGACGG     123


102 CCTTCAGGCTT-GAAACAAAGAATCGAAGGTTCTGGAATGGTGGGAATCA    150
124 CTCACAGGTTTTGTAACAAGCAATCGAAGGTTCTGGAATGGCGGGAAAGG    173


151 GTTTACTACCACATGCTATGATGTCTACCGCACTCTCCAGAGCAAAAGTT    200
174 GTTTAGTACCACATGCTATGATGCCCACTGTGATCTCCAGAGCAAAG--T    221


201 TCGTTCAATCACACTCTTACACTCTCTCT--CACACA--ATTGTTCGAAT    246
222 TCGTTCGATCGTACTGTTACTCTCTCTCTTTCAAACAGAATTGTCCGAAT    271


247 CGTGTGACAACAGCAGCTTGTTCTCACACAGTCTCTTTTCTTCTAACCAA    296
272 CGTGTGACAACAACAGCCTGTTCTCACACA--CTCTTTTCTTCTAACCAA    319


297 GGGGTTG-TTTGGGCTAGTAAAGCTTTGTGGAAACTTAGATTTACATATA    345
320 GGGGGTGGTTTAGTTTAGTAGAACCTCGTG-AAACTTACATTTACATATA    368


346 TATAAAGTTGAACGAATTAGTGAATGCTAAAGAAATATATAATTGACCTT    395
369 TATAAACTTGCATAAATTGGTCAATGC--AAGAAATACATATTTGGTCTT    416


396 TTTCTCTAGATAGTTTTTTGAACTTGTTAGATGTATTTTAATTCTTTCTC    445
417 TTCTAATTCGTAGTTTTTC-AAGTTCTTAGATG----------CTTTCT-    454


446 TGTTTTTTTATTTCTTCTTTTCACAGATCATCAAGGAAGTAATTATCTAC    495
455 ---------TTTTCTCTTTTTTACAGATCATCAAGGAAGTAATTATCTAC    495


496 TTTTTGCAACAAATATAAAACA    517
496 TTTTTACAACAAATATAAAACA    517
```

FIG. 3.22 Nucleotide sequence alignment of the *PGK1*$_{SB}$ promoter versus *PGK1*$_{SC}$ promoter

The above nucleotide sequence alignment represents the *PGK1*$_{SB}$ promoter (top line) and *PGK1*$_{SC}$ promoter (bottom line). The 517bp of the *PGK1*$_{SB}$ promoter shares 76% identity with the *PGK1*$_{SC}$ promoter. Similar nucleotides are black, different nucleotides are red and a gap is denoted by a dash. The 5'UTR or *PGK1*$_{SC}$ is underlined and the estimated 5'UTR of *PGK1*$_{SB}$ is also underlined.

3.3 Discussion

The aim of the research described in this chapter was to generate a series of yeast strains that encode HβD-3. Initially, HβD-3 was cloned into a bacterial pBSK- shuttle vector, under the control of a *S. bayanus* constitutive *PGK1* promoter as described in section 1.6. A hydrophobic, 19 amino acid α-factor leader sequence was employed at the N-terminal region, to facilitate the secretion of the peptide from the interior of the yeast cell to the surrounding culture medium (Fig. 1.6). This signal peptide is subsequently cleaved off by specific peptidases during the secretion process, but it has been noted in previous studies that some heterologous proteins may be retained in the periplasmic space, secreted at very low levels or not secreted from the cell at all when they are fused to the α-factor leader sequence (Chaudhuri et al., 1992). The $PGK1_{SB}$ promoter, α-factor leader sequence and HβD-3, were cloned into pBSK-, along with an *ADH* terminator, as described previously (section 1.6, section 2.13). This shuttle vector was the basis for subsequent cloning experiments described in this chapter.

Cells expressing genes from episomal plasmids need to be maintained under constant selective conditions, to prevent plasmid loss. Such selective pressures are not feasible in fermentation conditions. Thus, HβD-3 was stably introduced into the chromosome of *S. pastorianus*. *S. pastorianus* contains a complex polyploid genome with a general tetraploid DNA content, which is believed to have arisen from the natural fusion of two different haploid species followed by a genome duplication event or alternatively from the fusion of two diploid yeast species (Bond, 2006; Caesar et al., 2007; Kielland-Brandt, 1995; Rainieri et al., 2006). Therefore *S. pastorianus* can have as many as four copies of the same gene. Thus, inserting the HβD-3 gene within the intergenic region of YPR159W-YPR160W, should not have a detrimental phenotypic affect on the strain. HβD-3 was ultimately cloned into this region of redundancy, which contains the hypothetical gene YPR159C-A, (section 1.6) and its presence was verified by PCR analysis (Fig. 3.2).

Previously the HβD-3 gene has been introduced into various *E. coli* strains on plasmids, and soluble HβD-3 expression with antimicrobial activity have been achieved (Huang et al., 2006; Huang L, 2007; SI Li-gang, 2007). *S. cerevisiae* has successfully been used as a host for the production of HβD-1, under the control of an *ADH1* promoter (Cipáková, 2005). However, the introduction of HβD-3 into an *S. pastorianus* strain

has not been attemped before. Along with integration of HβD-3 into the chromosome of CMBS-33, a series of vectors were synthesized to encode HβD-3, as described in section 1.6. pGREG505hbd3GAL1 and pGREG506hbd3GAL1 were previously generated in the lab (section 1.6). Sequencing of these plasmids confirmed that identical mutations occured in both plasmids during insertion of the HβD-3 gene construct into each plasmid, as described in section 3.2.1.2. A single nucleotide deletion occured in the promoter specific 5'UTR of the *GAL1* promoter in pGREG505hbd3GAL1 and pGREG506hbd3GAL1 (Fig 3.4). Furthermore two nucleotide mutations and the addition of an extra nucleotide occured the non-specific 5'UTR of pGREG505hbd3GAL1 and pGREG506hbd3GAL1 (Fig 3.4). As mentioned in the above text, the non-specific 5'UTR is determined in this study as the region of the plasmid located between the promoter and the gene. The non-specific 5'UTR is transcribed along with the promoter specific 5'UTR and the ORF of HβD-3.

We wanted to compare the strength of several other promoters and thus the *GAL1* promoter was replaced with two different constitutive promoters and a maltose-inducible promoter. The *S. cerevisiae PGK1* and *TEF1* promoters will allow for constitutive expression of HβD-3 during the fermentation process. Additionally the *S. cerevisiae* inducible *AGT1* promoter was also chosen for analysis. This promoter is regulated by maltose induction and glucose repression. In brewer's wort 50-60% of total sugars are maltose, 15-10% maltotriose and 10-15% glucose (Zastrow, 2001). Once all of the glucose has been utilized, maltose is the preferred substrate for yeast (Day et al., 2002). *AGT1* is present in both ale and lager yeast. Studies by Vidgren et al. (2005) have indicated that *AGT1* is abundantly expressed in ale strains while lager strains do not express significant amounts of *AGT1*. While ale strains encode a full-length protein, lager strains encode truncated polypeptides due to a premature stop codon (Vidgren et al., 2005). Analysis of the *AGT1* promoter of brewer's ale strains and laboratory *S. cerevisiae* strains indicate that these promoters are identical in the first 315bp, after which they differ distinctly in the last 470bp which contains the upstream activator sequences (UAS_{MAL}) (Fig. 3.1). As stated in section 3.1, this sequence divergence occurs within the 147bp tandem repeat element (Vidgren et al., 2011). Thus, the 147bp tandem repeat of conventional *MALx1-MALx2* divergent promoters is different to the 147bp tandem repeat of *S. cerevisiae AGT1-MALx2* divergent promoter. The first 100bp of the tandem repeat element are located within the first 315bp of the promoter, relative to the start codon of *AGT1*, thus these nucleotides are homologous to

the *AGT1* promoter of brewer's lager yeasts (Fig. 3.1) (Vidgren et al., 2011). The remaining 47bp are located from 316bp to 362bp and are homologous to the *MALx1-MALx2* promoter (Vidgren et al., 2005). In general very little is known about the composition of promoters in brewer's yeast strains. Studies by Vidgren et al. (2011) identified regulatory elements of the *AGT1* promoters of brewer's yeast strains. However little information was obtained during this study with regards to the 147bp tandem repeat elements of brewer's yeast *AGT1* promoters. Thus, the *AGT1*-MAL21 divergent promoter of *S. cerevisiae* may contain a unique or truncated 147bp tandem repeat. Studies by Bell et al. (1997) indicated that decreased expression of *AGT1* was correlated with an increase in the number of tandem repeats present in the promoter. Some promoters have as many as 5 copies of the 147bp tandem repeat (Bell et al. 1997). As mentioned above, studies by Vidgren et al. (2005) have shown that *AGT1* is abundantly expressed in brewer's ale strains and *S. cerevisiae* laboratory strains when grown in 2% maltose. Thus, the differing 147bp tandem repeat sequences of each of these promoters does not have an affect on expression levels of *AGT1*. In this study, alterations were made to the *AGT1* promoter, whereby the 785bp divergent promoter was shortened to a 500bp promoter to eradicate the diverging characteristic. This resulted in the truncation of the Mig1 binding site. The affect these alterations may have had on the functionality of the promoter will be examined in chapters 4 and 5.

To increase the levels of HβD-3 further, the gene was cloned into a high copy number plasmid, pRS42H, under the control of a constitutive *S. bayanus PGK1* promoter, and including an *ADH* terminator (Fig. 3.19). The fragment cloned into pRS42H is >99% identical to the fragment integrated directly into the chromosome, therefore comparisons of the expression of HβD-3, can be made between the strains CM-INT-51 and CM-pRShbd3PGK1 (Table 2.3). Furthermore, as mutations occurred in the $PGK1_{SB}$ promoter of CM-pRShbd3PGK1, further studies may identify regions of importance in the promoter.

Further mutations were evident in the DNA nucleotide sequencing of the strains generated during this study. Nucleotide mutations occurred in the promoter regions of CM-506hbd3AGT1 (Fig. 3.14) and CM-pRShbd3PGK1 (Table 3.1). A single nucleotide mutation occurred in the non-specific 5'UTR of CM-505hbd3TEF1 (Fig. 3.9, Table 3.1). A deletion event occurred in the N/S 5'UTR of CM-506hbd3AGT1, along with a deletion event that occurred in the 5'UTR of the *PGK1* promoter of CM-

506hbd3PGK1 (Table 3.1). All fragments prepared for cloning were amplified with a mixture of the enzymes Taq polymerase and Verizyme DNA polymerase (Section 2.2). Taq polymerase ensures a high yield of PCR product while the addition of the proofreading enzyme, Verizyme DNA polymerase, increases the fidelity of PCR approximately 3-6 times more than Taq polymerase alone. Verizyme polymerase catalyses the synthesis of DNA in a 5' to 3' orientation, while it possesses no 5' to 3' exonuclease activity and has a 3' to 5' proof-reading function. The enzyme has the highest fidelity known, with a low error rate of ~1-6x10^{-5}/bp, when used alone. In a Taq/Verizyme mixture, the rate of error increases (~2.8x10^{-3}). Therefore the above missense mutations may be due the probability of error occurring during PCR and may also be due to cloning by homologous recombination in *S. pastorianus,* however the latter is highly unlikely. The deletion mutations may have been caused by errors during homologous recombination and/or sudden/spontaneous changes in the cell during homologous recombination.

Intentional modifications were initiated during the generation of CM-506hbd3AGT1 and CM-506hbd3PGK1 to reduce the number of non-specific untranslated nucleotides. These deletions were carried out during the restriction digest of the original plasmids pGREG505hbd3GAL1 and pGREG506hbd3GAL1. Each plasmid was cut with SacI and SpeI to remove the *GAL1* promoter (Fig. 3.5). Along with the removal of the *GAL1* promoter, nucleotides in the non-specific 5'UTR were removed from the plasmid, resulting in the loss of the SpeI sites (Fig. 3.5). 28 nucleotides at position 498, located in the non-specific 5'UTR of pGREG505hbd3GAL1 and pGREG506hbd3GAL1 were deleted (Fig. 3.5). This resulted in the truncation of the non-specific 5'UTR of CM-506hbd3AGT1 and CM-506hbd3PGK1, when compared to CM-505hbd3GAL1 (Fig. 3.23, Table 3.1). Furthermore, 21 of the 28 nucleotides located in the non-specific 5'UTR of pGREG505hbd3GAL1, were also deleted during the generation of CM-505hbd3TEF1 (Fig. 3.23, Table 3.1). As stated above, the *TEF1* promoter was previously cloned into pGREG505GAL1 via the removal of the *GAL1* promoter by restriction digest with SacI and SpeI restriction enzymes, followed by ligation of the *TEF1* promoter into the linearised plasmid (Dr. R. Karreman, unpublished). Like the above experiments, the non-specific 5'UTR sequence in pGREG505TEF1 was shortened during the digestion of the plasmid. The *TEF1* promoter was ligated into the plasmid whereas the *AGT1* and $PGK1_{SC}$ promoters were inserted into the plasmid via homologous recombination. Thus, the non-specific 5'UTR of CM-505hbd3TEF1 was

only reduced by 21bp in total, as 7bp including the SpeI site, were reincorporated into the plasmid during the ligation process. CM-505hbd3TEF1 contains a shorter non-specific 5'UTR compared to CM-505hbd3GAL1 (Fig. 3.23, Table 3.1). Reducing the size of the non-specific 5'UTR's of these strains will result in a shorter 5'UTR overall. The effect this will have on the translation of HβD-3 is unclear as yet. The work carried out in the next two results chapters will analyze the expression levels of HβD-3 and the activity levels of the mature peptide.

Finally, an epitope tag (6xHis-Tag) was fused to the C-terminal of HβD-3. As mentioned in section 3.2.3, 23bp of *ADH* terminator sequence, located upstream of the rec2 site (Fig. 1.8 A), were deleted from CM-505hbd3HISGAL1, at position 727 (Table 3.1). The HIS-TAG_R primer was designed to eliminate this short *ADH* terminator sequence (described in section 1.6), as a fully functioning *CYC* terminator in present in this plasmid already. The detection of this 6xHis-tag will be examined in the next results chapter.

The variety of strains generated in this chapter provides us with the opportunity to compare HβD-3 expression and activity, from a plasmid and directly from the genome, under the control of various promoters. The mutations that arose during generation, can be used to identify regions of importance in each promoter region. Furthermore, the effect that 5'UTR length has on translation can be analysed. In the following chapter, HβD-3 expression and secretion was analysed in each strain, to help determine which of these strains may is the most suitable.

FIG. 3.23 Schematic diagram showing the length of the non-specific 5'UTR regions of all yeast strains containing pGREG vectors

Schematic diagram illustrating the length of the non-specific 5'UTR of each gene construct generated during this study. The non-specific 5'UTR sequence for each gene construct is denoted below each schematic. The rec1 site of each non-specific 5'UTR is underlined. The SpeI restriction sites are denoted by red nucleotides. The SalI restriction sites are denoted by italics within the rec1 site. The non-specific 5'UTR is the same length for all strains containing the *GAL1* promoter, which is depicted by a red block. *AGT1* promoter: beige block. *TEF1* promoter: black block. $PGK1_{SC}$ promoter: purple block. Due to the length of the non-specific 5'UTR, the position of ATG (green) is different in each strain.

Note: Schematic diagram is not to scale.

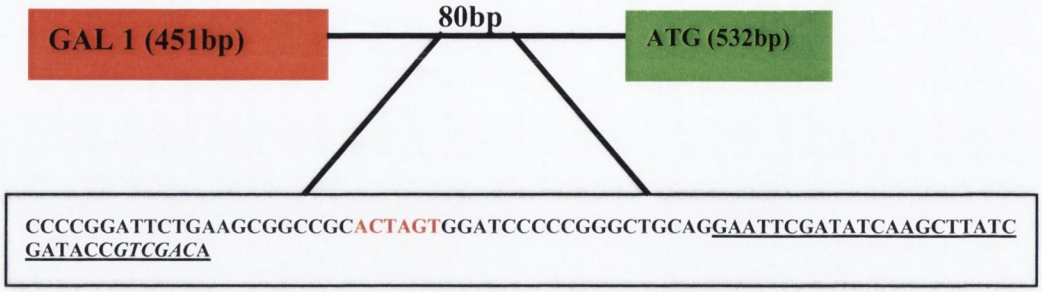
GAL 1 (451bp)
80bp
ATG (532bp)
CCCCGGATTCTGAAGCGGCCGCACTAGTGGATCCCCCGGGCTGCAGGAATTCGATATCAAGCTTATC
GATACCGTCGACA

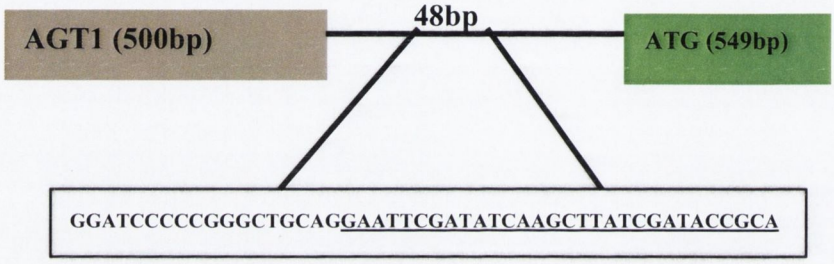
AGT1 (500bp)
48bp
ATG (549bp)
GGATCCCCCGGGCTGCAGGAATTCGATATCAAGCTTATCGATACCGCA

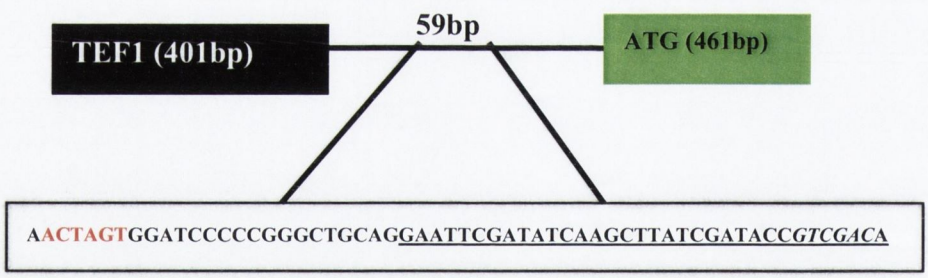
TEF1 (401bp)
59bp
ATG (461bp)
AACTAGTGGATCCCCCGGGCTGCAGGAATTCGATATCAAGCTTATCGATACCGTCGACA

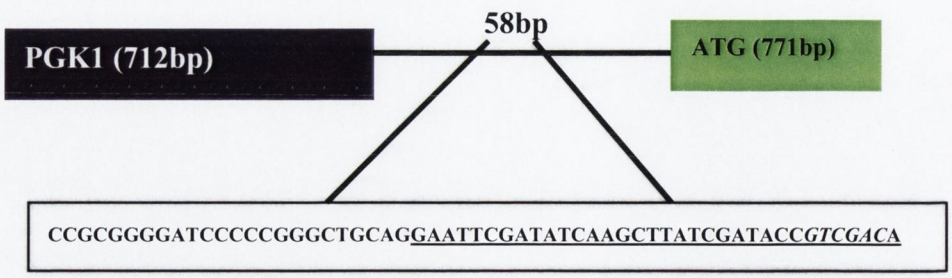
PGK1 (712bp)
58bp
ATG (771bp)
CCGCGGGGATCCCCCGGGCTGCAGGAATTCGATATCAAGCTTATCGATACCGTCGACA

Chapter 4:

Antimicrobial Peptide Expression and Secretion Analysis

4.1 Introduction

Various CMBS-33 *S. pastorianus* strains were generated to encode the antimicrobial peptide, HβD-3. As described in chapter 3, the introduction of HβD-3 into each of these strains included the use of low copy number plasmids such as pGREG vectors, or the pRS42H vector which is a high copy number plasmid, as well as direct integration of the HβD-3 gene into the chromosome. In order to generate an efficient HβD-3-lager yeast system, HβD-3 was introduced into CMBS-33 under the control of various different promoters including $GAL1_{SC}$, $TEF1_{SC}$, $PGK1_{SC}$, $PGK1_{SB}$ and $AGT1_{SC}$ (described in chapter 3). Semi-quantitative reverse-transcriptase PCR (RT-PCR) analysis was carried out for each strain to determine if HβD-3 is expressed in CMBS-33, and which promoter is the most efficient for the expression of HβD-3.

HβD-3 was integrated into the chromosome of CMBS-33, in the region of the putative YPR159C-A gene, located between YPR159W and YPR160W (section 1.6). YPR159C-A represents an uncharacterized open reading frame (Kumar et al., 2002). YPR159W/*KRE6* is a type II integral membrane protein required for beta-1,6 glucan biosynthesis (Roemer and Bussey, 1991). YPR160W/*GPH1* encodes for the non-essential enzyme glycogen phosphorylase and is required for the mobilization of stored glycogen through its conversion into glucose-1-P (Hwang et al., 1989). It is imperative to examine whether the latter two genes have been affected by the introduction of the HβD-3 gene cassette, especially *GPH1*, which lies downstream of the integration site. As described in section 1.2.2, *S. pastorianus* is believed to have arisen from a hybridisation between two *Saccharomyces* species. Subsequent recombination events at specific chromosome locations generated a series of hybrid chromosomes (Libkind et al., 2011). Recent data published during this study suggests that the parental species are *S. cerevisiae*-like, and the newly discovered *S. eubayanus* (Libkind et al., 2011). The DNA content of *S. pastorianus* suggests an allotetraploid genome which contains some hybrid chromosomes. The recombination events occured at specific "hot-spots" in the genome, and the ORF of YPR160W represents one of these "hot-spots" (Usher and Bond, 2009). YPR160W is located on chromosome XVI. The CMBS-33 strain contains four copies of chromosome XVI, three of which are hybrid chromosomes and one additional *S. eubayanus*-like chromosome. The three hybrid chromosomes contain a YPR160W hybrid gene, in which the first ~330bp of this gene are *S. cerevisiae*-like and the remaining 2375bp are *S.eubayanus*-like (Usher and Bond, 2009). Furthermore, recombination at the 5' end of the YPR160W hybrid ORF, led to an insertion of specific

bases, resulting in a frameshift within the ORF, and subsequently a loss of function of *GPH1* in CMBS-33 hybrid chromosomes. CMBS-33 now contains only one functioning *GPH1* gene in the *S. eubayanus*-like chromosome XVI (Usher and Bond, 2009). If this one functioning copy of *GPH1* is affected by the integration of the HβD-3 cassette, it can have detrimental consequences. Previous work has shown that the deletion of *GPH1* leads to stress intolerance and decreased survival in stationary phase (Favre et al., 2008). Thus, analyzing the expression of the YPR160W ORF, along with the YPR159W ORF, is imperative in CM-INT-37 and -51.

Once HβD-3 expression is evaluated, the secretion of this peptide from CMBS-33 must be analysed. The levels of HβD-3 secreted from each of these strains is crucial to the survival of the host cell, because at high concentrations of AMPs, selectivity for bacterial membranes over eukaryotic membranes is reduced (Weghuber et al., 2011). Likewise, if the levels of HβD-3 are too low, then antibacterial activity will be compromised. It is known that β-defensins are not easily detected, the lack of effective expression systems seriously compromises progress in this area (Corrales-Garcia et al., 2011; Valore and Ganz, 1997). HD-5 expressed in *P. pastoris*, was detected in supernatant samples by Western blot analysis. In this study, two distinct HD-5 specific bands were obtained, indicating the possibility of O-glycosylation of the peptide, due to its richness in serine and threonine residues (Hsu et al., 2009). O-glycosylation of HβD-3 may make it difficult to detect the recombinant peptide via Western blot analysis. Thus, various detection methods including enzyme-linked immunosorbent assay (ELISA) and reversed phase high-performance liquid chromatography (RP-HPLC), were used throughout this study.

4.2 Results

4.2.1 Analysis and semi-quantification of HβD-3 expression in CMBS-33 via RT-PCR

To compare the expression of HβD-3 from the various gene promoters described in chapter 3, semi-quantitative RT-PCR was carried out. The recombinant strains CM-505hbd3GAL1, CM-506hbd3GAL1, CM-506hbd3AGT1, CM-505hbd3TEF1, CM-506hbd3PGK1, CM-pRShbd3PGK1, CM-INT-37 and CM-INT-51, as well as wild-type CMBS-33 and a negative control strain CM-pRS, were cultured in YEPD media at 30°C overnight. Yeast strains containing pGREG vectors were cultured in the presence of G418, while strains containing the multi-copy number plasmid, pRS42H, were cultured in the presence of hygromycin B (section 2.1.2). Following overnight incubation, the cells were pelleted by centrifugation at 4,000 rpm, washed twice and fresh cultures were inoculated at a density of 1.5 x 10^7 cfu/mL, into the appropriate media. The high inoculum was used to reflect standard fermentation conditions. Yeast strains containing HβD-3 under the control of a *GAL1* promoter, were cultured in YEP-Gal media at the optimal temperature of 30°C, to facilitate the induction of the *GAL1* promoter. Yeast strains containing HβD-3 under the control of all other promoters mentioned above, were cultured in YEPM media, as maltose is the preferred carbohydrate for *S. pastorianus* strains. Samples (10mL) were taken from each culture at 4 hr intervals, for 24 hrs and cells were pelleted by centrifugation at 4,000 rpm. Total RNA was isolated from the cell pellet using the RNA purification method described in section 2.6. Total RNA (5μg) was separated on 1% TAE agarose gel, to determine the quality of the extracted RNA. A representative gel displaying RNA from CM-505hbd3GAL1 is shown (Fig. 4.1 A). The presence of the 25S and 18S rRNA subunits demonsrates that the RNA is intact (Fig. 4.1 A). Total RNA extracted from all other strains was of the same quality shown in Fig. 4.1 A (data not shown). The total RNA samples were DNase I treated to remove any contaminating DNA (section 2.8), and 2μg of DNase I-treated RNA was reverse transcribed to cDNA, as described in section 2.9. The quality of the extracted RNA was further determined by analysis of the expression levels of the 5.8S ribosomal RNA (5.8s rRNA) gene by semi-quantitative RT-PCR, using the 5.8S_F1 and 5.8S_R1 primers (Table 2.1). A band of the expected size (150bp) was evident in each sample in CM-505hbd3GAL1 (Fig. 4.1 B). The 5.8S ribosomal RNA semi-quantitative RT-PCR products appear to be saturated, therefore analysis of

FIG. 4.1 Semi-quantitative RT-PCR analysis of HβD-3 expression

RNA was extracted from *S. pastorianus* CMBS-33, expressing HβD-3 from different promoters. cDNA samples were prepared using HβD-3 specific primers and/or 5.8S specific primers and the products amplified as described in the text. **A.** CM-505hbd3GAL1 RNA samples from cells grown in YEP-Gal. Lanes labeled 0-24 represent samples taken at 0, 4, 8, 12 and 24 hrs, respectively. The 25S and 18S rRNA subunits are indicated by arrows for each sample. **B.** 5.8S rRNA RT-PCR products of CM-505hbd3GAL1. Lanes labeled 0 - 24 represent samples that were taken at 0, 4, 8, 12 and 24 hrs, respectively. **C – J.** HβD-3 RT-PCR products from HβD-3 encoding yeast strains. Lanes labeled 0 - 24 represent samples that were taken at 0, 4, 8, 12 and 24 hrs, respectively. C: CM-505hbd3GAL1, D: CM-506hbd3GAL1, E: CM-506hbd3AGT1, F: CM-505hbd3TEF1, G: CM-506hbd3PGK1, H: CM-pRShbd3PGK1, I: CM-INT-37, and J: CM-INT-51. The first lane in each panel contains 5µl of Q-Step 1 molecular weight marker. The 100bp and 200bp bands are indicated by numbers above the band.

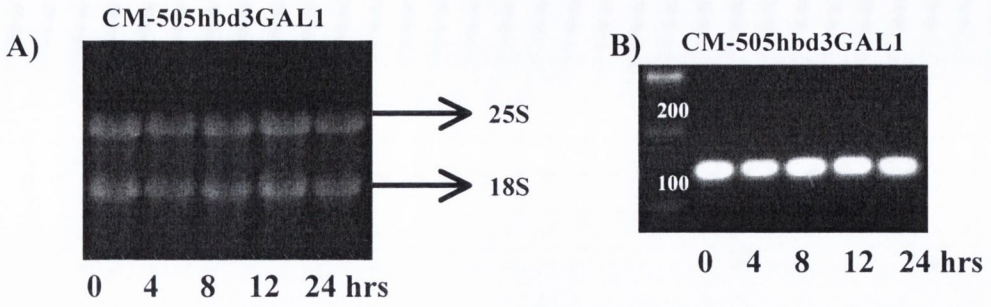
A)
CM-505hbd3GAL1
25S
18S
0 4 8 12 24 hrs
B)
CM-505hbd3GAL1
200
100
0 4 8 12 24 hrs

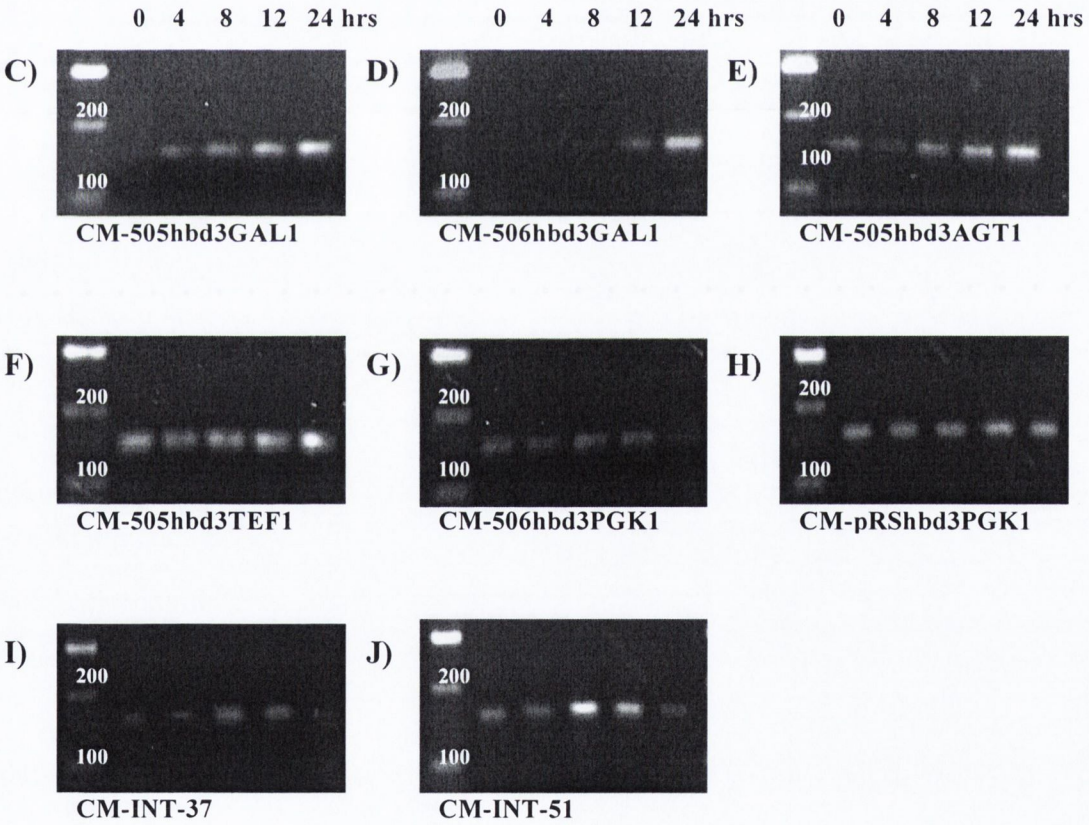
0 4 8 12 24 hrs
C)
200
100
CM-505hbd3GAL1
0 4 8 12 24 hrs
D)
200
100
CM-506hbd3GAL1
0 4 8 12 24 hrs
E)
200
100
CM-505hbd3AGT1
F)
200
100
CM-505hbd3TEF1
G)
200
100
CM-506hbd3PGK1
H)
200
100
CM-pRShbd3PGK1
I)
200
100
CM-INT-37
J)
200
100
CM-INT-51

this gene was not possible under these experimental conditions. Further experiments are needed to determine the optimal experimental conditions for semi-quantitative analysis of this gene. However, the clear amplification of 5.8S rRNA indicated that each RNA sample was of sufficient quality for RT-PCR amplification.

DNase I-treated RNA was reverse transcribed to cDNA using a HβD-3_R1 primer (Table 2.1). 5% of the synthesized cDNA was used as a template for PCR amplification (section 2.2/2.9), using the primers HβD-3_F1 and HβD-3_R1 (Table 2.1). The HβD-3 RT-PCR products were visualised on 2% TBE agarose gel (Fig 4.1 C-J). A band at the expected size (158bp) was obtained in all samples tested. As the HβD-3 semi-quantitative RT-PCR products appear to be unsaturated, analysis of HβD-3 was possible under these experimental conditions. CM-505hbd3GAL1 and CM-506hbd3GAL1 appear to display maximum expression at 24hrs, with the latter strain exhibiting lower levels at earlier time points (Fig. 4.1 C & D). CM-506hbd3AGT1 also appears to display maximum expression at 24hrs (Fig. 4.1 E). Results suggest that CM-505hbd3TEF1 exhibits constitutive expression (Fig. 4.1 F), while the $PGK1_{SC}$ constitutive promoter of CM-506hbd3PGK1 also exhibits constitutive expression with low levels at 24hrs (Fig. 4.1 G). CM-pRShbd3PGK1 appears to display slightly higher expression levels of HβD-3 from the $PGK1_{SB}$ constitutive promoter (Fig. 4.1 H). Results indicate that both CM-INT-37 and CM-INT-51 display maximum HβD-3 expression at 8 hrs (Fig. 4.1 I & J). Thus, the *TEF1* promoter appears to be the strongest constitutive plasmid promoter, with HβD-3 RT-PCR samples appearing slightly more intense for CM-505hbd3TEF1, compared to CM-506hbd3PGK1 and CM-pRShbd3PGK1 (Fig. 4.1 F-H). The HβD-3 levels appear higher in CM-INT-51 compared to CM-INT-37 (Fig. 4.1 I & J).

RT-PCR amplification using the HβD-3 primers, HβD-3_F1 and HβD-3_R1 (Table 2.1), and RNA extracted from CMBS-33 and CM-pRS, did not yield any products (data not shown), while 5.8S primers produced the correct sized products (data not shown). No HβD-3 or 5.8S RT-PCR products were obtained in the absence of reverse transcriptase (data not shown).

4.2.2 Analysis of YPR159W and YPR160W genes

The integrated strains, CM-INT-37 and CM-INT-51, have now been shown to produce HβD-3 mRNA transcripts (section 4.2.1). As described in section 1.6, this HβD-3 gene construct was integrated into the YPR159C-A putative gene between the genes YPR159W and YPR160W. To determine if the integration of HβD-3 affected the expression of YPR159W and YPR160W, the yeast strains were cultured in YEPD, at 30°C overnight, total RNA was extracted (section 2.6) and the total RNA samples were DNase I treated (section 2.8). High quality RNA was obtained as indicated by the presence of 28S/18S rRNAs in each sample (Fig. 4.2 C). cDNA was synthesized from the DNase I treated RNA, as described in section 2.9, and RT-PCR analysis was carried out using YPR159W and YPR160W gene specific primers (Table 2.1). YPR159W_F and YPR159W_R primer positions relative to the YPR159W gene are shown in Fig. 4.2 A and the YPR160W_F and YPR160W_R primers relative to the YPR160W gene are shown in Fig. 4.2 B. As stated in section 4.1, CMBS-33 contains two types of YPR160W genes, one represents a mosaic gene with *S. cerevisiae*-like and *S. bayanus*-like regions while the other is a *S. bayanus*-like gene (Usher and Bond, 2009). The primers used in this study should only amplify the *S. bayanus*-like copy of YPR160W, as this combination of primers will not amplify the mosaic copy of YPR160W due to the position of the forward and reverse primer.

RT-PCR products of the expected sizes (YPR159W: 171bp, YPR160W: 461bp) were produced in all three strains CMBS-33, CM-INT-37 and CM-INT-51, indicating that the presence of HβD-3 does not affect the expression of these genes (Fig 4.2 D & E). In the absence of reverse transcriptase no RT-PCR products were obtained (Fig. 4.2, lane 4 D-F). The expression levels of the *ACT1* gene were analysed alongside HβD-3 expression, as a positive, internal control. The Actin_F and Actin_R primers produced an RT-PCR product of 300bp, as demonstrated in Fig. 4.2 F (Table 2.1).

FIG. 4.2 Expression of YPR159W and YPR160W in CM-INT-51 and CM-INT-37
RNA was extracted from CMBS-33, CM-INT-51 and CM-INT-37. cDNA samples were prepared using YPR159W and YPR160W specific primers and/or *ACT1* specific primers and the products amplified as described in the text. **A)** YPR159W gene [black] showing nucleotide positions of YPR159W_F and YPR159W_R primers. **B)** YPR160W *S. bayanus*-like gene [grey] showing nucleotide positions of YPR160W_F and YPY160W_R primers. **C)** Total RNA (5μg) from strains CMBS-33, CM-INT-51 and CM-INT-37, in lanes 1-3 respectively. The 25S and 18S rRNA are indicated by arrows. **D)** Amplification of YPR159W from CMBS-33, CM-INT-51 and CM-INT-37 (lanes 1-3 respectively). Lane 4 in gels D-F represent CMBS-33 negative controls. The reaction was carried out in the absence of reverse transcriptase prior to PCR amplification. **E)** Amplification of YPR160W from CMBS-33, CM-INT-51 and CM-INT-37 (lanes 1-3 respectively). **F)** Amplification of actin from CMBS-33, CM-INT-51 and CM-INT-37 (lanes 1-3 respectively). The first lane in each panel contains 5μl of Q-Step ladder 4 or hyperladder II molecular weight marker. The band sizes are indicated by lines.

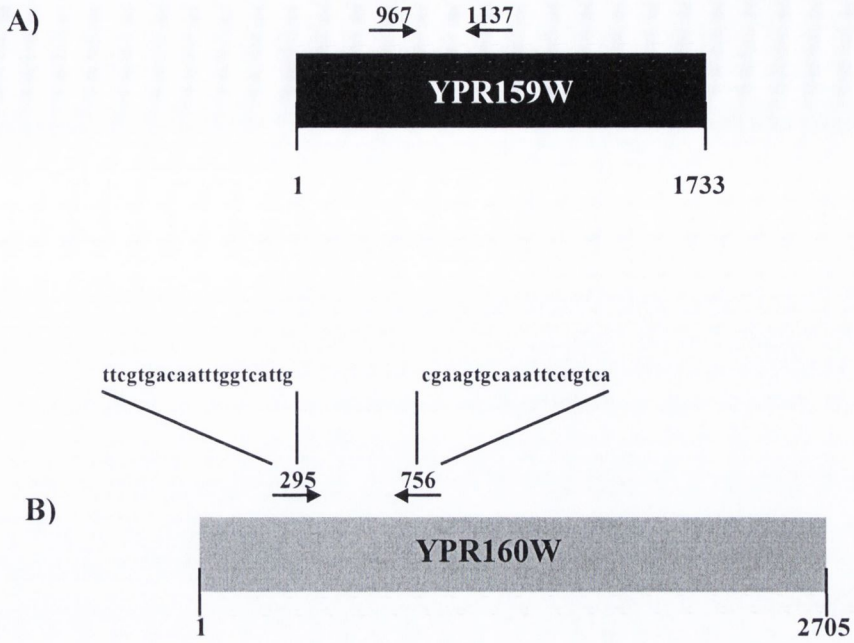
A)
967
1137
YPR159W
1
1733
ttcgtgacaatttggtcattg
cgaagtgcaaattcctgtca
295
756
B)
YPR160W
1
2705

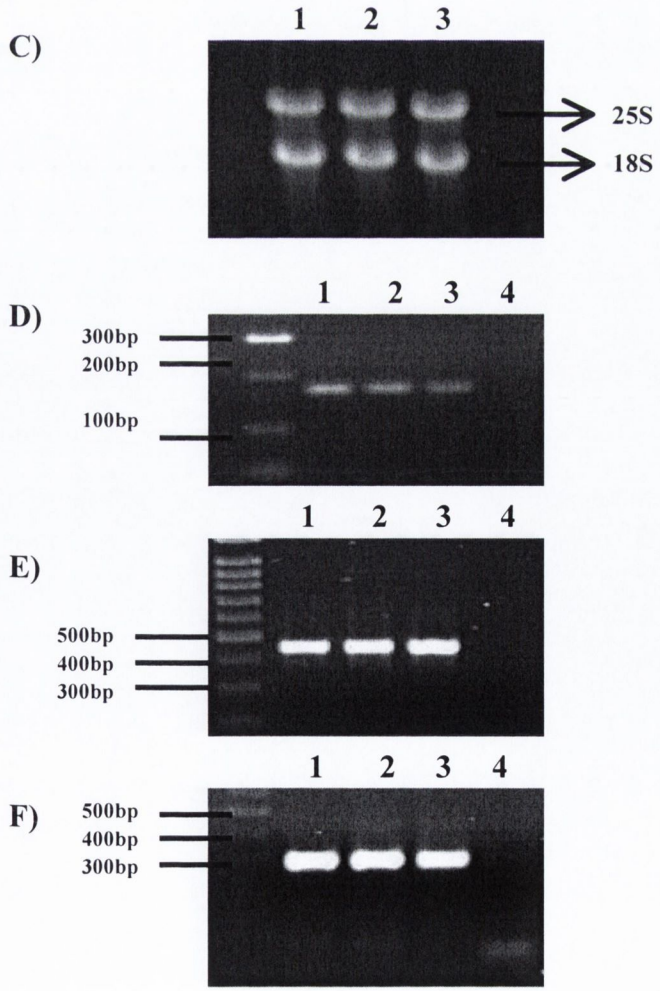
C)
1 2 3
25S
18S
D)
1 2 3 4
300bp
200bp
100bp
E)
1 2 3 4
500bp
400bp
300bp
F)
1 2 3 4
500bp
400bp
300bp

4.2.3 Detection of secreted recombinant HβD-3

All lager strains generated in this study have been shown to successfully produce HβD-3 mRNA transcripts. Ideally, for antimicrobial activity to occur during the fermentation process, the recombinant HβD-3 peptide must be secreted from the cell into the medium. To detect secreted recombinant HβD-3, yeast strains were cultured in synthetic complete (SC) minimal media containing 2% sugar. Minimal media (SC) was used to allow concentration of the supernatant (medium) at the end of a fermentation, as rich media such as YEPM, is too viscous to concentrate due to the presence of yeast extract and peptone. Various methods were used to quantify HβD-3 secretion into the medium, including enzyme-linked immunosorbent assay (ELISA), reversed phase high-performance liquid chromatography (RP-HPLC) and Western immunoblotting.

Yeast strains were first cultured in YEPD media, at 30°C overnight. Yeast strains containing pGREG vectors were cultured in the presence of G418, while those containing the multi-copy number plasmid, pRS42H, were cultured in the presence of hygromycin B. The cells were pelleted by centrifugation at 4,000 rpm and washed twice in SDW. Strains containing HβD-3 under the control of a *GAL1* promoter, were inoculated into SC media supplemented with 2% galactose, while yeast strains containing HβD-3 under the control of all other promoters, were inoculated into SC-Mal (2% maltose) media. The cells were grown for 1-5 nights at 30°C and then pelleted by centrifugation at 4,000 rpm for 15 min. The separated supernatant (spent medium) was first concentrated via freeze-drying and the dried supernatant was resuspended as a 5 - 500-fold concentrate (5X – 500X) (section 2.19.1). The concentrated supernatant sample was filtered via a 0.45μm filter (section 2.19.1), and then concentrated further using a 3kDa molecular weight cut off filter as described in section 2.19.2. The final concentration of supernatant samples were in the range of 10 - 1000X.

4.2.3.1 ELISA analysis of recombinant HβD-3 secreted from pGREG vectors 505 and 506 under the control of the *GAL1* promoter

HβD-3 levels were first monitored in concentrated medium from strains CM-505hbd3GAL1 and CM-506hbd3GAL1, using a sandwich ELISA-based assay containing an antigen-affinity purified rabbit anti-HβD-3 capture antibody and a biotinylated antigen-affinity purified rabbit anti-HβD-3 detection antibody, as described in section 2.21. Yeast strains were cultured in 1L of SC-Gal media at 30°C, for 5 nights,

until an OD_{600} value of approximately 1.2 – 1.4 was obtained. The supernatant was concentrated as described above and this concentrated supernatant (100X) was assayed in two independent experiments. Supernatant from CMBS-33 cells was used as a negative control in these experiments. Absorbance values were read at an optical density of 595nm after 20 – 30mins (experiment 2 and 1 respectively). A standard curve was generated using the synthetic HβD-3 peptide (section 1.6) (experiment one: Fig. 4.3 A, experiment two: data not shown). Under the experimental conditions used (section 2.21), saturation was reached at approximately 25μg/mL of synthetic HβD-3 for each experiment (experiment one: Fig. 4.3 A, experiment two: data not shown).

To accurately quantify the recombinant HβD-3 values in CM-505hbd3GAL1 and CM-506hbd3GAL1 concentrated supernatant, the linear region of the standard curve was expanded. A linear relationship, with a squared correlation coefficient (R^2) value of 0.95527 was achieved for synthetic HβD-3 concentrations at 0.75 – 6.25μg/mL (Fig. 4.3 B). At 100X concentrate, CM-505hbd3GAL1 and CM-506hbd3GAL1, produced absorbance values of 0.757 and 0.657 respectively (Fig. 4.3 B). These absorbance values correspond to recombinant HβD-3 concentrations of 4.65μg/mL and 3.6μg/mL for CM-505hbd3GAL1 and CM-506hbd3GAL1 respectively (Fig. 4.3 B). Taking into account that the supernatant samples are concentrated 100X, the final values indicate that CM-505hbd3GAL1 secretes recombinant HβD-3 into the supernatant at a concentration of approximately 46.5ng/mL, likewise CM-506hbd3GAL1 secretes recombinant HβD-3 into the supernatant at a concentration of approximately 36ng/mL. CMBS-33, which lacks a plasmid, gave negative values, suggesting no HβD-3 is present in this sample as expected (data not shown). These secretion levels cannot be directly compared to expression levels, as expression levels of HβD-3 were analysed after growth in YEPM while secretion levels were analysed after growth in SC-Mal.

Similar results were obtained for experiment two (data not shown). However, as absorbance values were read after 20mins, these concentration values differed slightly. CM-505hbd3GAL1 and CM-506hbd3GAL1 produced absorbance values equivalent to 6.1μg/mL and 2.4μg/mL of synthetic HβD-3 respectively (data not shown). Taking into account that these supernatant samples are concentrated 100X, the final values indicate that CM-505hbd3GAL1 secretes recombinant HβD-3 into the supernatant at a concentration of approximately 61ng/mL, likewise CM-506hbd3GAL1 secretes

FIG. 4.3. Synthetic HβD-3 standard curve displaying absorbance values for CM-505hbd3GAL1 and CM-506hbd3GAL1

CM-505hbd3GAL1 and CM-506hbd3GAL1 were cultured in SC-Gal and HβD-3-specific ELISA analysis was carried out on supernatants (100X). **A)** Absorbance values from ELISA analysis of various concentrations of synthetic HβD-3 at OD_{595} (30mins). **B)** Linear region of synthetic HβD-3 standard curve showing absorbance values from ELISA analysis of CM-505hbd3GAL1 and CM-506hbd3GAL1 concentrated supernatant samples (100X) at OD_{595} (30mins). The absorbance values for CM-505hbd3GAL1 (pink) and CM-506hbd3GAL1 (yellow) are plotted on the Y-axis. The squared correlation coefficient (R^2) value is displayed. The error bars represent standard deviation from duplicate or triplicate values.

A.

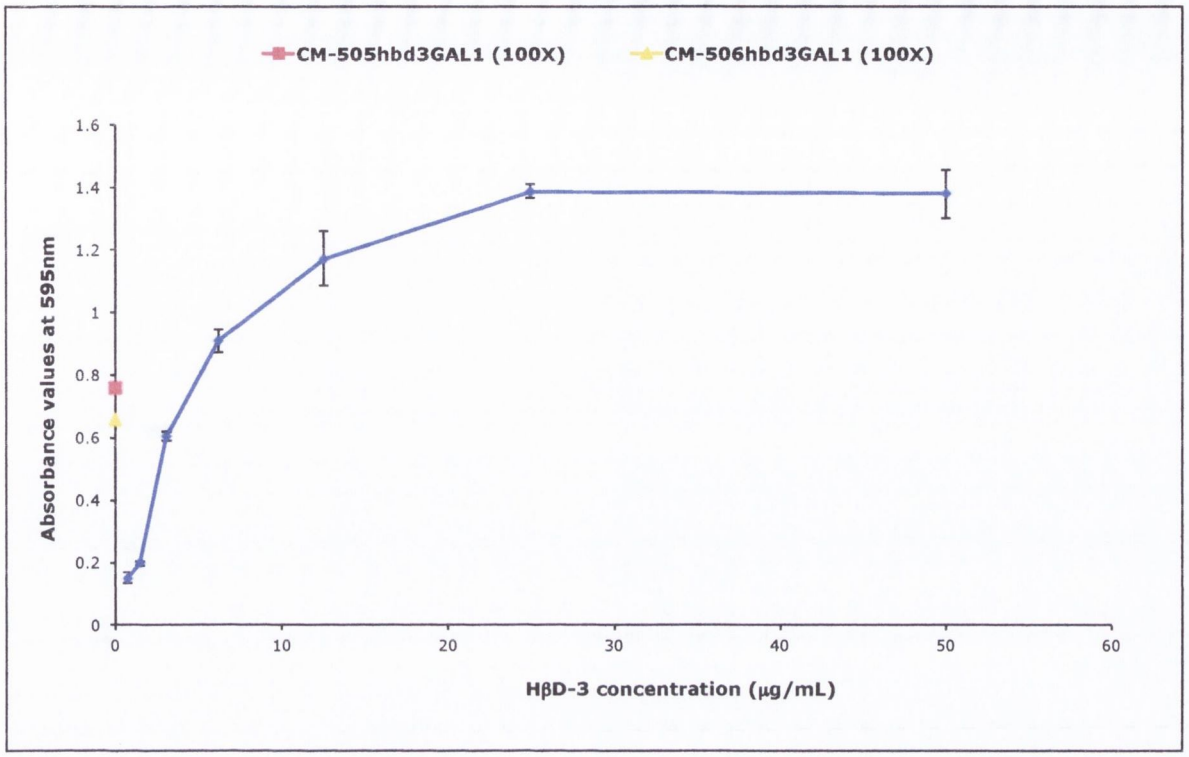
CM-505hbd3GAL1 (100X)
CM-506hbd3GAL1 (100X)
Absorbance values at 595nm
1.6
1.4
1.2
1
0.8
0.6
0.4
0.2
0
0
10
20
30
40
50
60
HβD-3 concentration (μg/mL)

B.

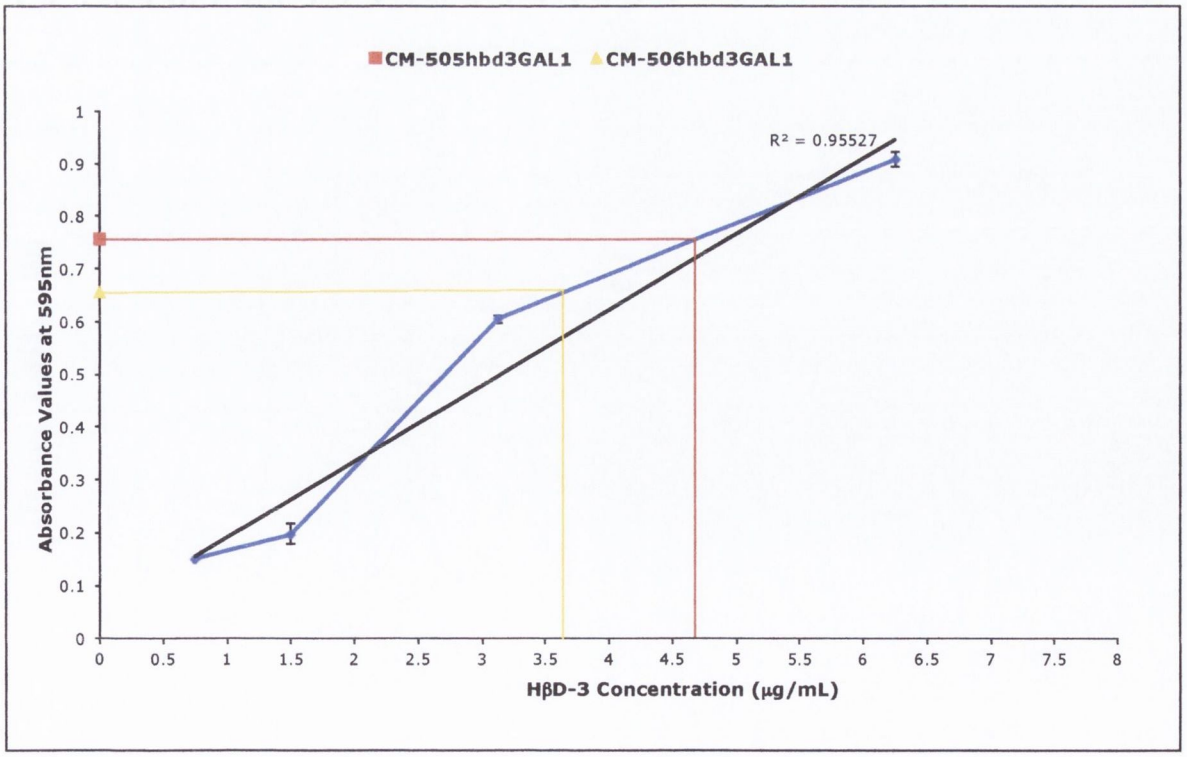
CM-505hbd3GAL1
CM-506hbd3GAL1
R² = 0.95527
Absorbance Values at 595nm
1
0.9
0.8
0.7
0.6
0.5
0.4
0.3
0.2
0.1
0
0
0.5
1
1.5
2
2.5
3
3.5
4
4.5
5
5.5
6
6.5
7
7.5
8
HβD-3 Concentration (μg/mL)

recombinant HβD-3 into the supernatant at a concentration of approximately 24ng/mL. HβD-3 levels in CM-505hbd3GAL1 and CM-506hbd3GAL1 yeast strains were analysed using ELISA in two independent experiments, results indicate that HβD-3 is present in spent medium at 54±7ng/mL and 30±6ng/mL for each strain respectively.

4.2.3.2 ELISA analysis of recombinant HβD-3 secreted from various lager strains

The results described in section 4.2.3.1, indicate that secretory recombinant HβD-3 was detected via ELISA analysis, in CM-505hbd3GAL1 and CM-506hbd3GAL1 using concentrated supernatant samples of cultures grown in SC-Gal media. Under selective conditions, as little as 40µl of sample was required to obtain reliable absorbance values, which is equivalent to 4mL of culture. To quantify the levels of recombinant HβD-3 secreted from all other HβD-3-encoding yeast strains (chapter 3), the yeast strains were cultured in 70mL of SC-Mal media and supernatant was concentrated as described in section 4.2.3. HβD-3-specific ELISA analysis was carried out whereby concentrated supernatant samples (28X) were analysed in 60µl aliquots, via sandwich ELISA (section 4.2.3.1). Preliminary results indicate that HβD-3 is secreted from all strains in the ng/mL range, with the exception of CM-506hbd3PGK1, which does not appear to secrete detectable levels of recombinant HβD-3 (data not shown). Since this experiment was only carried out once, with a single supernatant fraction from each culture, the data is considered preliminary in nature and must be confirmed by additional experimentation.

4.2.4 Reversed phase high-performance liquid chromatography (RP-HPLC) of concentrated supernatant samples

The ELISA results outlined in section 4.2.3.1/4.2.3.2, indicate that HβD-3 is produced and secreted from the majority of recombinant lager yeast strains. To purify the recombinant HβD-3 and examine possible isoforms of HβD-3, the concentrated supernatant samples were analysed via RP-HPLC. RP-HPLC is based on the separation of compounds according to their hydrophobicity, thus the more hydrophobic a compound is, the longer it is retained on the column. Therefore, peptides that co-elute share similar hydrophobic characteristics. The experimental procedures used for RP-HPLC are outlined in section 2.23.

First, 10μg of synthetic HβD-3 was analysed by RP-HPLC to determine a standard elution profile. Three various batches of HβD-3 were compared, each of which came from the same master stock. Each batch was taken from the master stock at different stages, reconstituted in SDW, stored at -20°C and the samples were freeze-thawed numerous times. The three samples of HβD-3 eluted from the column between 3.7 – 5 mins (Fig. 4.4). Maximum peak elutions were between 4 – 4.2 mins, thus the average elution time of synthetic HβD-3 is 4.1 ± 0.1 mins (at 6% acetonitrile).

4.2.4.1 RP-HPLC analysis of CM-505hbd3GAL1 and CM-506hbd3GAL1

CM-505hbd3GAL1 and CM-506hbd3GAL1 were inoculated into SC-Gal (150mL) at 30°C, for 3 nights, until an OD_{600} value of approximately 1.2 – 1.3 was obtained. The supernatants were concentrated 10-fold (10X) as previously described (section 4.2.3). In a separate experiment CMBS-33 was inoculated into SC-Gal (1L) at 30°C, for 5 nights, and an OD_{600} value of 1.4 was obtained. The concentrated supernatant was prepared as above. 50μl of each of the concentrated supernatants (equivalent to 500μl of spent medium) was applied to a C18 RP-HPLC column (section 2.23). As a positive control, 10μg of synthetic HβD-3 was also applied to the column. The column was washed as described in section 2.23 and bound peptides/proteins eluted in 1mL fractions using a gradient of acetonitrile (2 – 60% over 60 mins). Fractions were pooled together according to peak profiles and were initially stored at -70°C, and then freeze-dried and resuspended in 120μl of SDW.

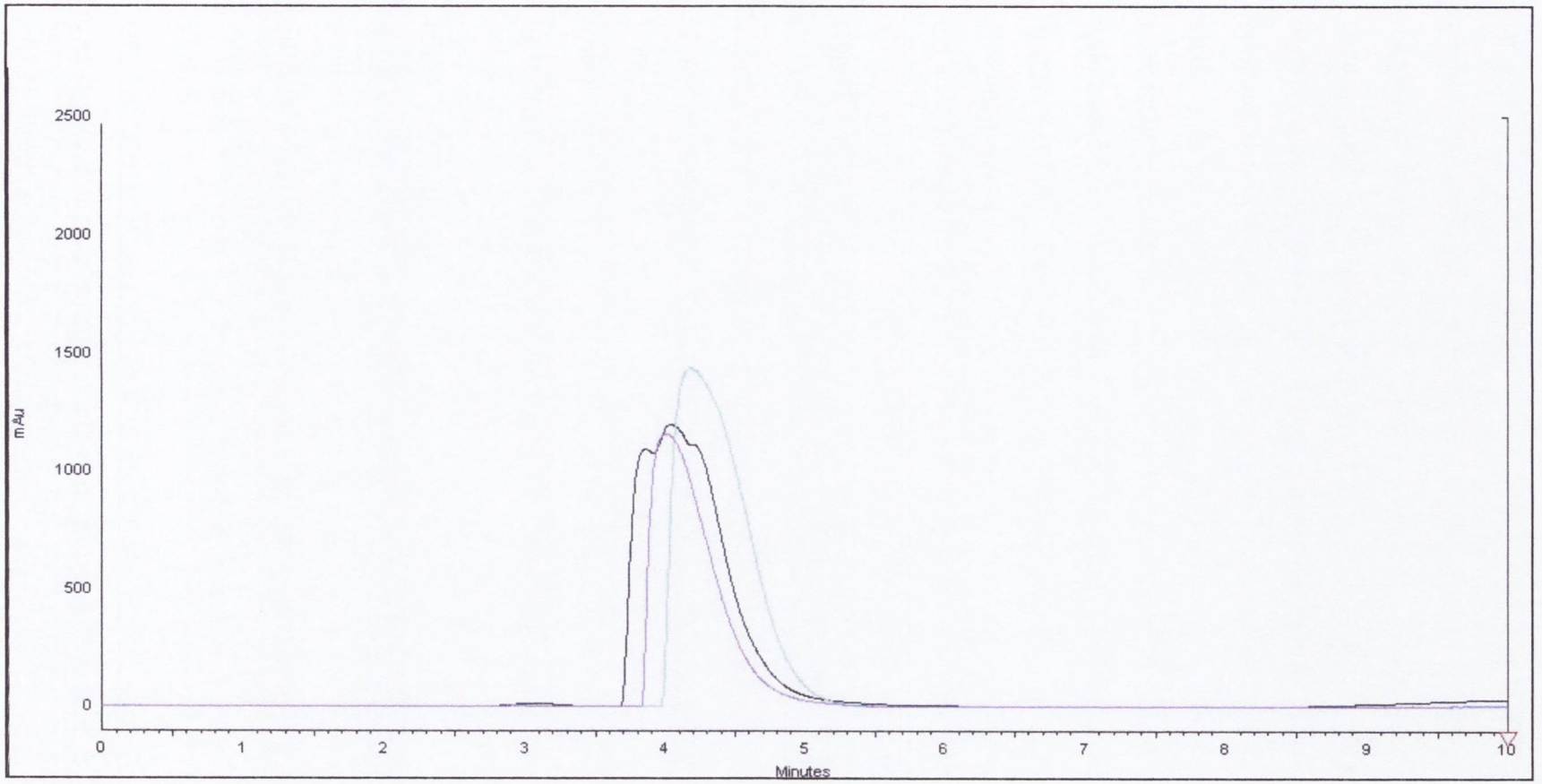

FIG. 4.4 Reversed phase high-performance liquid chromatography (RP-HPLC) analysis of synthetic HβD-3

RP-HPLC fractionation of three individual samples of synthetic HβD-3 (10μg). Each sample was loaded onto a C18 column and eluted using a gradient of acetonitrile (2-11%). The milli-absorbance units (mAu) measured at 215nm are shown in the y-axis.

Consistent with the results shown in Fig. 4.4, synthetic HβD-3 (10μg) showed a maximum peak elution at 4 minutes (Fig. 4.5, black peak). Recombinant HβD-3 secreted from CM-505hbd3GAL1 and CM-506hbd3GAL1, produced narrow and broad peaks respectively and eluted from the column between 2.8 - 3.8 minutes, as shown in Fig. 4.5 (dark green and pink respectively). The maximum peak elution for both CM-505hbd3GAL1 and CM-506hbd3GAL1 was 3.3mins (Fig. 4.5). The supernatant from the CMBS-33 culture produced no peaks with absorbance of 215nm, indicating that there is little or no peptide/proteins present in the same region as the HβD-3 peak elution (Fig. 4.5, pale green). No further peaks were obtained from fractions taken up to 60 mins (data not shown).

The RP-HPLC was performed once or twice on concentrated supernatant samples from three independent experiments (Table 4.1). All supernatants were 10X concentrated but each experiment differed in the volume of the cultures, which ranged from 150mL – 1L. Furthermore, supernatant from one of the CMBS-33 cultures was first concentrated via Sep-pak columns (as opposed to freeze-drying, section 2.19.3). Following concentration, supernatants (50-75μl) were loaded onto a RP-HPLC C18 column as before and each sample displayed a similar elution profile with the recombinant HβD-3 eluting slightly ahead of the synthetic HβD-3 (data not shown). Combining RP-HPLC data from each independent experiment indicates that recombinant HβD-3 has an average elution time of 3.3 mins (Table 4.1). The faster elution of recombinant HβD-3 from the column may indicate reduced hydrophobicity and/or variation in disulphide linkages and/or secondary structure between the synthetic HβD-3 and the recombinant HβD-3 or may result from interference from other contaminating substances such as any remnant of the growth media. The addition of synthetic HβD-3 to CMBS-33 supernatant may help address this problem.

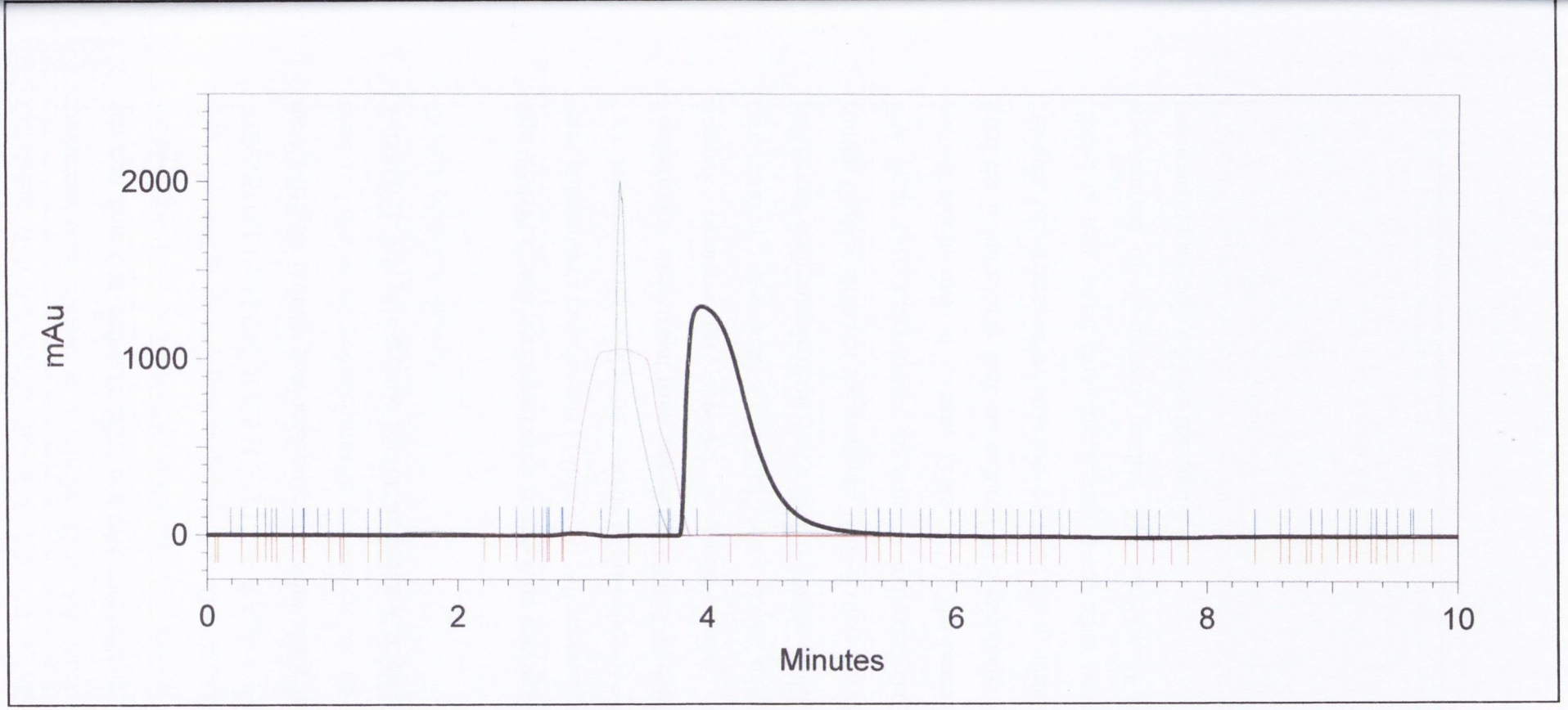

FIG. 4.5 Reversed phase high-performance liquid chromatography (RP-HPLC) analysis of supernatant samples from CMBS-33 strains expressing HβD-3

Synthetic HβD-3 (10μg) (black peak), CM-505hbd3GAL1 10X supernatant (dark green) and CM-506hbd3GAL1 10X supernatant (pink) were applied to a C18 column. Concentrated supernatant from a CMBS-33 culture grown independently but analysed on the same day (pale green). The bound proteins/peptides were eluted using an acetonitrile gradient (2-11%). The milli-absorbance units (mAu) measured at 214nm are shown on the y-axis.

Table 4.1 Summary of RP-HPLC elution times for 3 independent experiments

	Experiment 1	**Experiment 2**	**Experiment 3**
CMBS-33	N/A	No peak	No peak
CM-505hbd3GAL1	3.3mins 3.3mins	3.3mins	N/A
CM-506hbd3GAL1	3.3mins 3.3mins	3.4mins	N/A

N/A: No sample

4.2.4.2 ELISA analysis of CM-505hbd3GAL1 and CM-506hbd3GAL1 RP-HPLC samples

The RP-HPLC analysis demonstrated that peptides/proteins eluted in fractions 3-6 (Fig. 4.5). Therefore, fractions 1-10, 11-20 and 21-30 were pooled together and the presence of HβD-3 was quantitated by ELISA (section 2.21). The experimental design resulted in an approximate 0.1min delay when collecting fractions, thus the first 0.1min for each sample were not collected or analysed. Each fraction was numbered according to its elution time, thus fraction 1 eluted between 0.1mins – 1.1mins. Recombinant HβD-3 activity above background levels was observed in fractions 1-10 for CM-505hbd3GAL1 and CM-506hbd3GAL1, while only background values were obtained in fractions 11-20 and 21-30 (Fig. 4.6 A). When the spurious CMBS-33 background values of fractions 1-10 (no peptide present in these fractions based on mAu at 215nm, Fig. 4.5) are subtracted from the CM-505hbd3GAL1 and CM-506hbd3GAL1 absorbance values, the average concentration of recombinant HβD-3 in these fractions (1-10) can be quantified by HβD-3 specific ELISA analysis (Fig. 4.6 B and C). As stated in section 4.2.4.1, 1mL fractions were collected, these were pooled, concentrated and resuspended in 120μl of SDW. ELISA analysis was carried out on 60μl duplicate samples, which is equivalent to 250μl of supernatant, thus fractionated supernatant is concentrated 4.16-fold. Extrapolating the concentration of recombinant HβD-3 from the standard curve for synthetic HβD-3, estimated concentrations of 6.2μg/mL and 6.9μg/mL were obtained for CM-505hbd3GAL1 and CM-506hbd3GAL1 respectively (Fig. 4.6 C). Taking into account that the fractionated supernatant samples are concentrated 4.16X, the final values indicate that CM-505hbd3GAL1 secretes recombinant HβD-3 into the supernatant at a concentration of approximately 1.49μg/mL, likewise CM-506hbd3GAL1 secretes recombinant HβD-3 into the supernatant at a concentration of approximately 1.66μg/mL.

The same CM-505hbd3GAL1 and CM-506hbd3GAL1 supernatants were reapplied to the HPLC column and fractionated as above. Additionally a second set of independent CM-505hbd3GAL1 and CM-506hbd3GAL1 supernatant cultures were applied to the RP-HPLC column. As an additional control a sample of CMBS-33 concentrated supernatant was also applied to the RP-HPLC column and fractionated as above. As before, 50μl of all 10X supernatants were loaded onto the column, with the exception of one CM-506hbd3GAL1 sample, for which 75μl was loaded. Since HβD-3 activity was

FIG. 4.6 ELISA analysis of RP-HPLC fractions

RP-HPLC fractions were obtained for 10X concentrated supernatant of CMBS-33 [black], CM-505hbd3GAL1 [grey] and CM-506hbd3GAL1 [checked]. The CMBS-33 sample was cultured on a separate day but all samples were fractionated and analysed in a single experiment. Fractions 1-10, 11-20 and 21-30 were pooled together and assayed by HβD-3 specific ELISA. **A)** ELISA values obtained for RP-HPLC fractions. **B)** ELISA values for fractions 1-10 from CM-505hbd3GAL1 and CM-506hbd3GAL1 with the background absorbance values from CMBS-33 subtracted. **C)** Standard curve of synthetic HβD-3. The absorbance values for the pooled fractions (1-10) from CM-505hbd3GAL1 [red] and CM-506hbd3GAL1 [green] minus CMBS-33 background are shown. The error bars represent the standard deviation from duplicate values.

A.

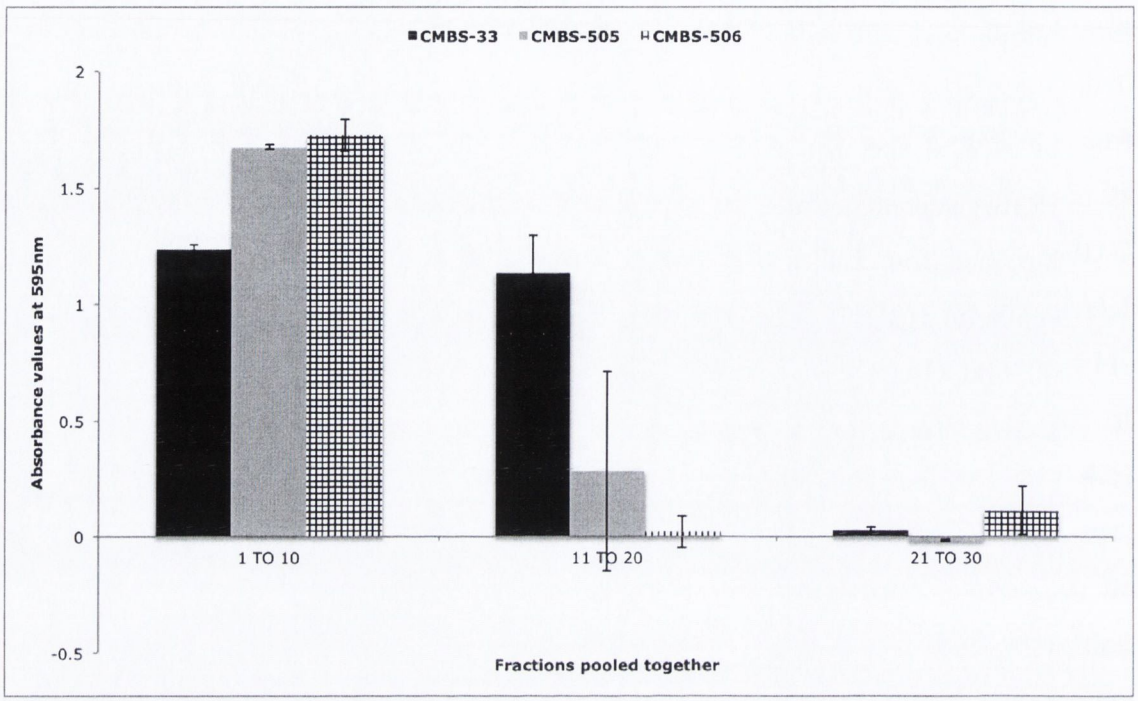
CMBS-33
CMBS-505
CMBS-506
2
1.5
1
0.5
0
-0.5
Absorbance values at 595nm
1 TO 10
11 TO 20
21 TO 30
Fractions pooled together

B.

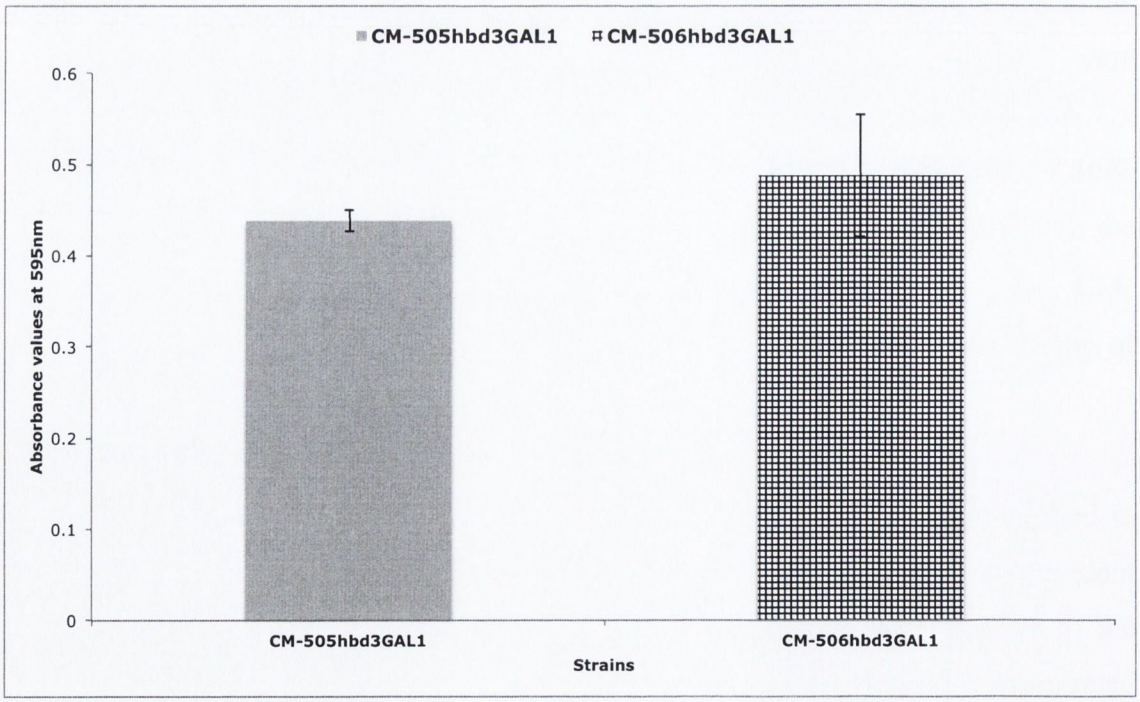
CM-505hbd3GAL1
CM-506hbd3GAL1
0.6
0.5
0.4
0.3
0.2
0.1
0
Absorbance values at 595nm
CM-505hbd3GAL1
CM-506hbd3GAL1
Strains

C.

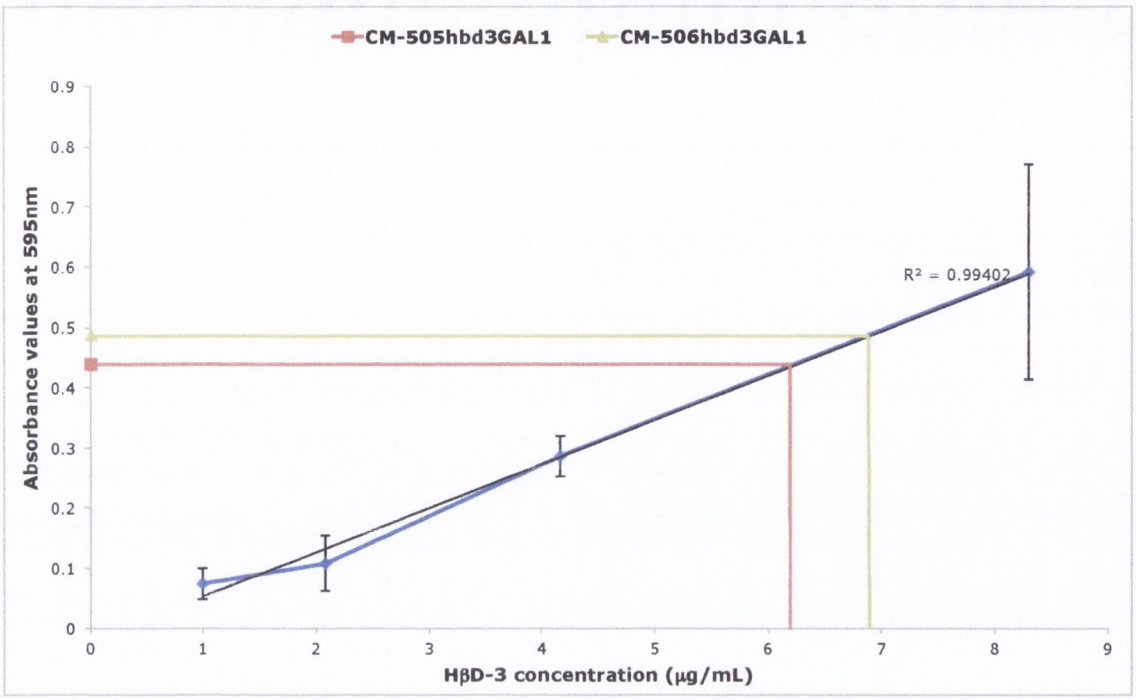
CM-505hbd3GAL1
CM-506hbd3GAL1
Absorbance values at 595nm
0.9
0.8
0.7
0.6
0.5
0.4
0.3
0.2
0.1
0
R² = 0.99402
0
1
2
3
4
5
6
7
8
9
HβD-3 concentration (µg/mL)

observed in fractions 1-10 in the first analysis and peak peptide elution was found in fractions 3-6, fractions 3-6 were pooled together to ensure total capture of HβD-3 and pooled fractions were analysed by ELISA. Synthetic HβD-3 (7μg) was also re-fractionated and fractions 3-6 were collected and pooled.

Both synthetic HβD-3 and recombinant HβD-3 were detected in the pooled fractions from the two independent experiments (3-6) (Fig. 4.7 A). Little activity above background was detected in similar fractions isolated from CMBS-33 supernatant (Fig. 4.7 A, green column). A slightly higher level of HβD-3 activity was detected in CM-506hbd3GAL1 compared to CM-505hbd3GAL1. As stated in section 4.2.4.1, 1mL fractions were pooled, concentrated and resuspended in 120μl of SDW. ELISA analysis was carried out on 60μl duplicate samples, equivalent to 250/375μl of fractionated supernatant, thus fractionated supernatant is concentrated 4.16-fold or 6.25-fold respectively. Extrapolating the concentration of recombinant HβD-3 from the standard curve for synthetic HβD-3, and taking into account the fold concentration of the supernatant, an estimated concentration of 0.84±0.31μg/mL was obtained for CM-505hbd3GAL1. As the absorbance values for CM-506hbd3GAL1 are above the linear range, the HβD-3 concentration values for these samples cannot be accurately measured. However, analysis of the absorbance values for CM-506hbd3GAL1 in two independent experiments indicate that recombinant HβD-3 is present at concentrations higher than 8.3μg/mL (Fig. 4.7 B). CM-506hbd3GAL1 supernatants from two independent experiments were loaded (the equivalent of 500 - 750μl respectively) onto the C18 column. Taking into account the fold concentration of the fractionated supernatant, an estimated minimum concentration of 1.59±0.31μg/mL was obtained for CM-506hbd3GAL1.

As shown in Fig. 4.6 C, the pooled fractions 1-10 from CM-505hbd3GAL1 and CM-506hbd3GAL1 concentrated supernatants were shown to contain HβD-3 at concentrations of 1.49 – 1.66μg/mL respectively. The data from ELISA analysis of fractions 3-6 from the same sample and an independent sample are in broad agreement. The amount of HβD-3 in concentrated supernatants was estimated from the volume originally loaded onto the RP-HPLC column. Therefore it is difficult to accurately quantify these samples as one cannot be certain of the percentage of sample eluted from

FIG. 4.7 ELISA analysis of CM-505hbd3GAL1 and CM-506hbd3GAL1 RP-HPLC samples

10X concentrated supernatants from CMBS-33, CM-505hbd3GAL1 and CM-506hbd3GAL1 were analysed by RP-HPLC. As a positive control synthetic HβD-3 (7μg) was also fractionated by RP-HPLC. The fractions were collected, fractions 3-6 were pooled and analysed by ELISA. **A)** Synthetic HβD-3: blue. CM-505hbd3GAL1 and CM-506hbd3GAL1 10X concentrated supernatants from two independent experiments (red and yellow). Absorbance values from ELISA analysis of fractions 3-6 of 10X concentrated supernatant from a CMBS-33 culture (green). **B)** Standard curve of synthetic HβD-3. Absorbance values for RP-HPLC pooled fractions (3-6) are shown. Synthetic HβD-3: dark blue. CM-505hbd3GAL1: experiments 1 and 2, red and purple. CM-506hbd3GAL1: experiments 1 and 2, green and light blue. The error bars represent the standard deviation of duplicate values.

A.

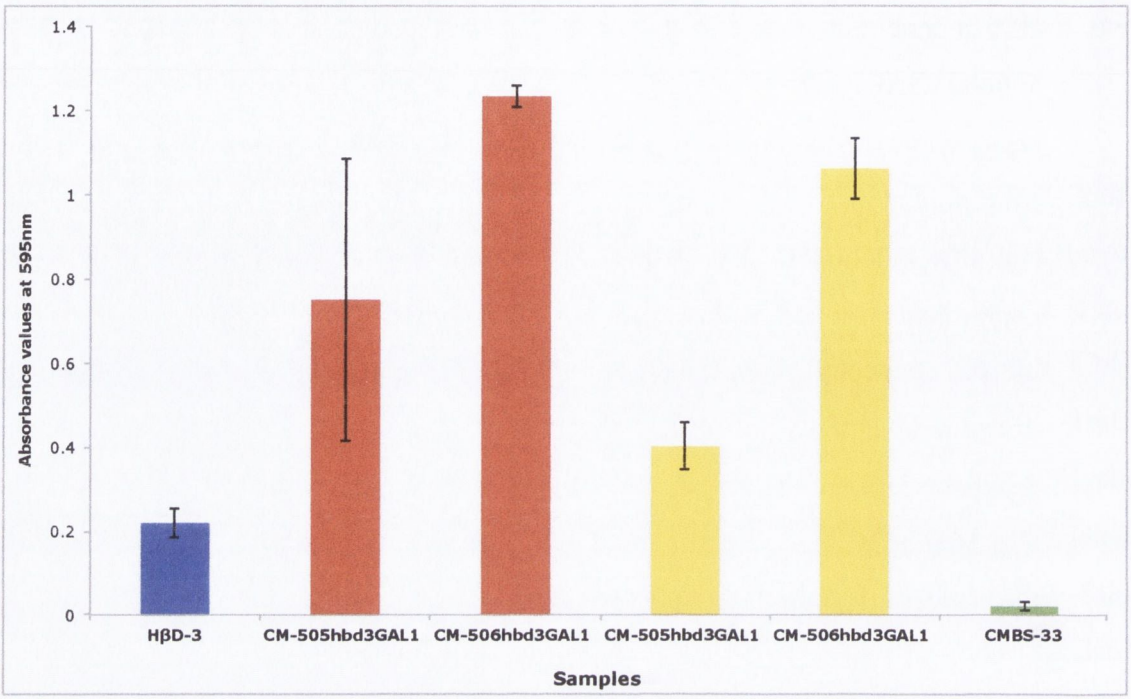
1.4
1.2
1
0.8
0.6
0.4
0.2
0
Absorbance values at 595nm
HβD-3
CM-505hbd3GAL1
CM-506hbd3GAL1
CM-505hbd3GAL1
CM-506hbd3GAL1
CMBS-33
Samples

B.

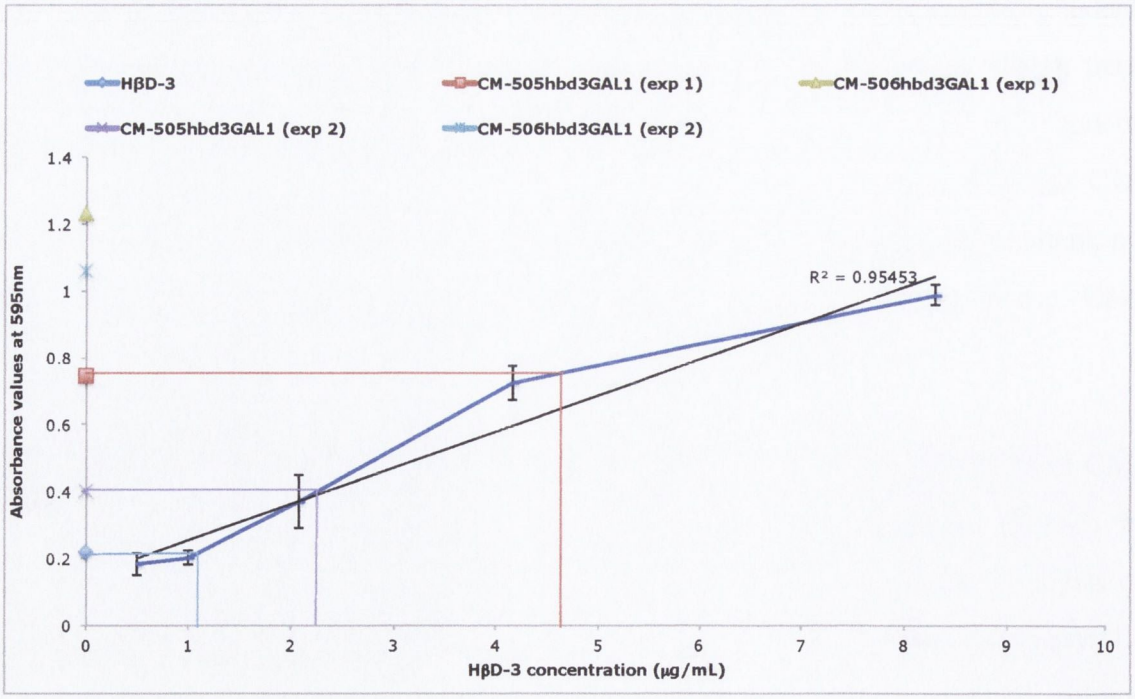
HβD-3
CM-505hbd3GAL1 (exp 1)
CM-506hbd3GAL1 (exp 1)
CM-505hbd3GAL1 (exp 2)
CM-506hbd3GAL1 (exp 2)
R² = 0.95453
Absorbance values at 595nm
HβD-3 concentration (µg/mL)

the column and present in each fraction. For example, 7μg of synthetic HβD-3 was loaded onto the C18 column yet only 0.12μg was retrieved in fractions 3 - 7 (Fig. 4.7 B, blue marker). Furthermore, high background values may affect the absorbance values obtained during HβD-3-specific ELISA analysis. Thus, these preliminary values are estimates of the concentration of recombinant HβD-3.

Overall, ELISA results indicate that recombinant HβD-3 was successfully co-fractionated, within less than 1 minute, of synthetic HβD-3. While results vary from experiment to experiment, the same trend is observed. Additionally, ELISA analysis of fractionated supernatant (10X) samples, indicate that when purified, recombinant HβD-3 is detected at higher levels compared to crude supernatant samples.

4.2.4.3 RP-HPLC analysis of the integrated strain, CM-INT-51

Having demonstrated the detection of recombinant HβD-3 by RP-HPLC analysis, the same analysis was carried out using the CM-INT-51 strain to determine if the integrated strain was also capable of producing secreted HβD-3. CM-INT-51 was cultured in SC-Mal (100mL) media at 30°C for approximately 2-3 nights, to an OD_{600} value of approximately 1 – 2. Since CM-INT-51 contains a kanMX cassette, cells were grown in the presence (+ G418) or absence (- G418) of antibiotic for comparative analysis. The cell pellet and supernatant were separated and the supernatant was concentrated 10-fold as described in section 4.2.3. Synthetic HβD-3 (10μg) was examined as a positive control. 100μl of the concentrated supernatant was loaded onto a C18 column, and 1mL fractions were collected. Each fraction was initially stored at -70°C, and then freeze-dried and resuspended in 120μl of SDW. CMBS-33 was not analysed again as a negative control as previous experiments indicate that this strain does not produce peaks in the same region as HβD-3 (section 4.2.4.2).

As before the synthetic HβD-3 (10μg) eluted from the column, with a maximum peak elution of 4.1 minutes (Fig. 4.8, black peak). The recombinant HβD-3 secreted from CM-INT-51 produces three major peaks with maximum peak elutions at approximately 3.3, 4.6 and 6mins for CM-INT-51 (-G418) (Fig. 4.8, pink peaks), while CM-INT-51 (+G418) produces maximum peak elutions of 3.4, 4.8 and 6.3mins (Fig. 4.8, blue peaks). Thus, the elution profile of recombinant HβD-3 from CM-INT-51 differs from the elution profile of recombinant HβD-3 from CM-505hbd3GAL1 and CM-506hbd3GAL1, where peptides eluted as a single peak at 3.3 mins (Fig. 4.5). Furthermore, these samples display peaks at higher milli-absorbance units (mAu) compared to CM-505hbd3GAL1 and CM-506hbd3GAL1 sample (Fig. 4.8 and 4.5 respectively). These CM-INT-51 supernatant samples were reapplied to the RP-HPLC column and the same trend was obtained (data not shown).

4.2.4.4 ELISA analysis of CM-INT-51 (+G418) RP-HPLC samples

To determine if the RP-HPLC peptide peaks observed in the CM-INT-51 (+G418) sample correspond to HβD-3, fractions representing peptide peaks were analysed by HβD-3-specific ELISA analysis (section 4.2.4.2). Each fraction was numbered according to its elution time, thus fraction 1 represents samples eluted between 0.1 and

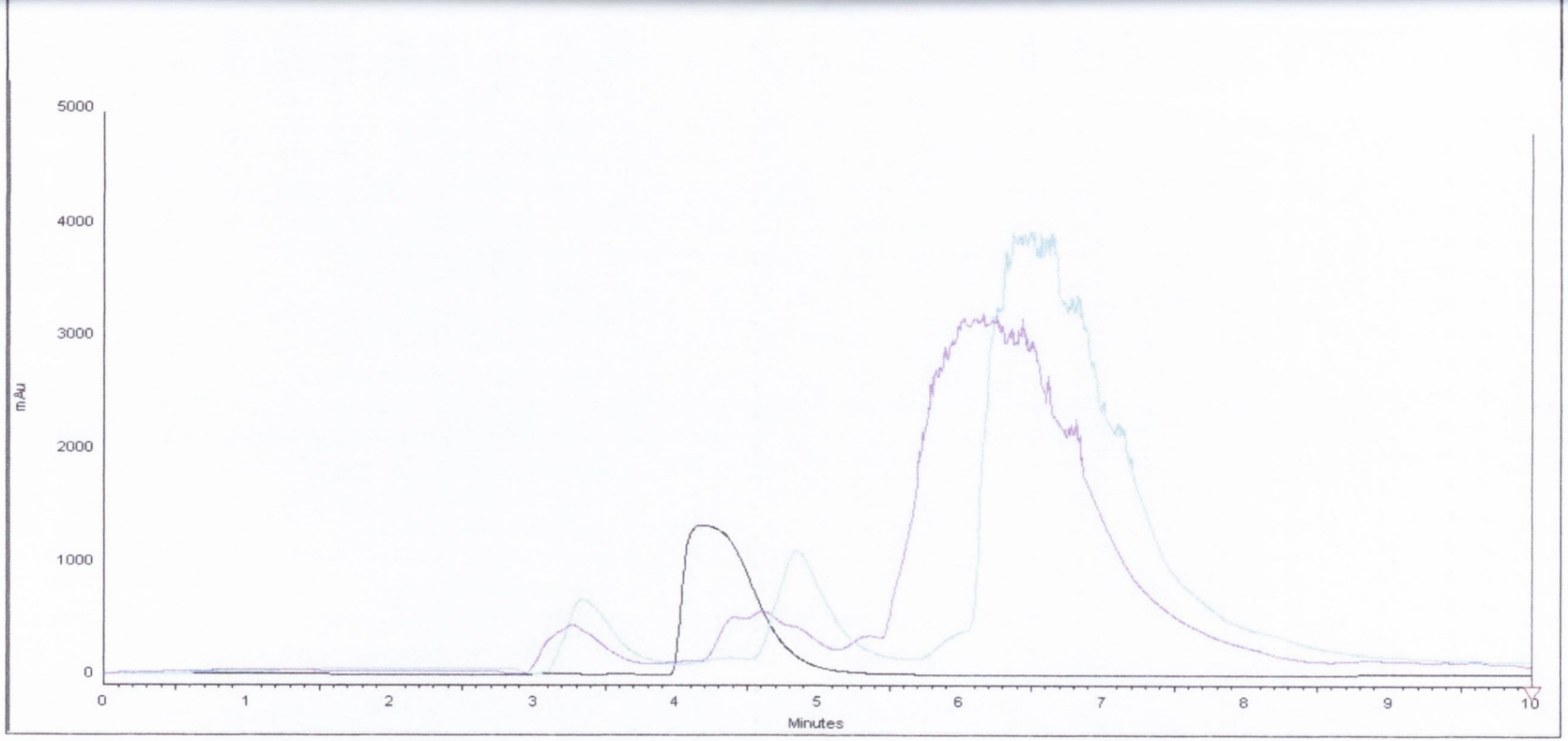

FIG. 4.8 Reversed phase high-performance liquid chromatography (RP-HPLC) analysis of CM-INT-51 supernatant

Synthetic HβD-3 (10μg) [black], CM-INT-51 10X supernatant (cultured plus G418) [blue], CM-INT-51 10X supernatant (cultured minus G418) [pink] were applied to a C18 RP-HPLC column. The bound proteins/peptides were eluted using a gradient of acetonitrile (2-11%). The milli-absorbance units (mAu) measured at 215nm are shown on the y-axis.

1.1mins. The experimental design resulted in a 0.1min delay when collecting fractions, thus the first 0.1min for each sample were not collected or analysed. The RP-HPLC trace indicated that recombinant HβD-3 from CM-INT-51 (+G418) produced maximum peak elutions in fractions 4, 5 and 7 (Fig. 4.8, blue peaks). Therefore fractions 4, 5 and 7 were quantitated by HβD-3-specific ELISA analysis (section 4.2.4.2).

Recombinant HβD-3 was detected in fractions 4, 5 and 7 (Fig. 4.9 A, navy green and grey respectively). Fraction 4 represents the smallest peak obtained by CM-INT-51, yet significant amounts of HβD-3 were detected in this fraction (Fig. 4.9 A, navy column). This correlates well with the elution profile of HβD-3 from CM-505hbd3GAL1 and CM-506hbd3GAL1, which both show a peak elution of HβD-3 at 3.3mins. Preliminary results obtained indicate that fraction 5 displays low absorbance values (Fig. 4.9 A, green column). This value represents data for one RP-HPLC sample, thus further experiments are needed to verify this. The presence of HβD-3 in significant proportions in fraction 7 suggests that CM-INT-51 may secrete various isoforms of the peptide (Fig. 4.9 A, grey column). While the same trend was obtained for RP-HPLC and ELISA analysis of CM-INT-51 (+G418) supernatant on two occasions, one set of RP-HPLC fractions produced lower absorbance values, thus the standard error between duplicate experiments is high.

A standard curve using synthetic HβD-3 was generated (Fig. 4.9 B). The linear region of the standard curve was used to calculate the concentrations of recombinant HβD-3 in fractions displaying activity via ELISA analysis. CM-INT-51 fractions 4, 5 and 7 displayed absorbance values of 0.4, 0.08 and 0.58 respectively (Fig. 4.9 A, navy, green and grey columns respectively). These values correspond to 10.4μg/mL and 13.4μg/mL of HβD-3 in fractions 4 and 7 respectively, while the absorbance value for fraction 5 is too low to measure (Fig. 4.9 B). The estimated concentration of recombinant HβD-3 cannot be measured for individual fractions as it is not possible to estimate the volume of original sample eluted in each fraction. Analysis of pooled fractions 3-9, would provide a better estimation of the concentration of recombinant HβD-3 in CM-INT-51 (+G418) supernatants. A CMBS-33 negative control is required to estimate the levels of background that may be present in these samples. Further ELISA analysis is required to verify the levels of recombinant HβD-3 in CM-INT-51 (-G418) RP-HPLC fractions.

FIG. 4.9 ELISA analysis of CM-INT-51 RP-HPLC samples

Concentrated supernatants (equivalent to 1mL) from CM-INT-51 grown in SC-Mal plus G418 were fractionated by RP-HPLC. The levels of HβD-3 were detected by HβD-3-specific ELISA analysis. **A)** Absorbance at OD_{595} of RP-HPLC fractions detected by HβD-3-specific ELISA. RP-HPLC fractions 4, 5 and 7 (navy, green and grey respectively) from CM-INT-51 (+G418) concentrated supernatant (10X). **B)** Standard curve in the linear range (0.5-16.66μg/mL) of synthetic HβD-3 as detected by ELISA. Absorbance values for CM-INT-51 fractions 4, 5 and 7 are shown on the y-axis (green, pink and red respectively). The error bars represent either the standard error from duplicate experiments (*) or the standard deviation from duplicate values from a single experiment (+).

A.

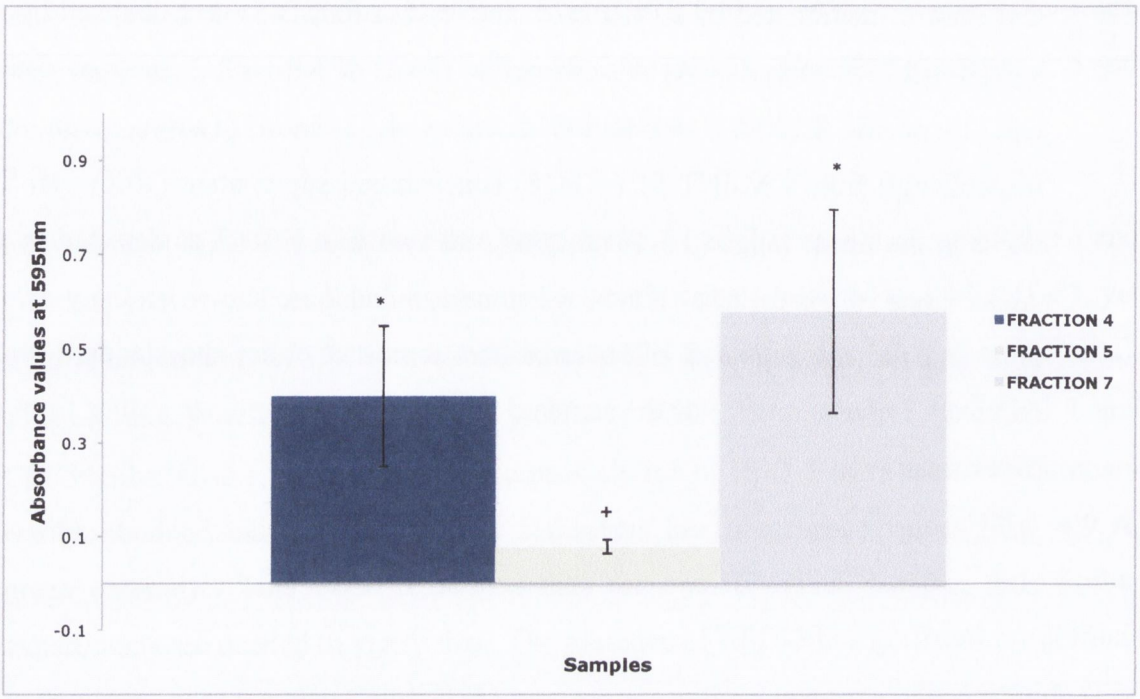
Absorbance values at 595nm
0.9
0.7
0.5
0.3
0.1
-0.1
*
+
*
Samples
FRACTION 4
FRACTION 5
FRACTION 7

B.

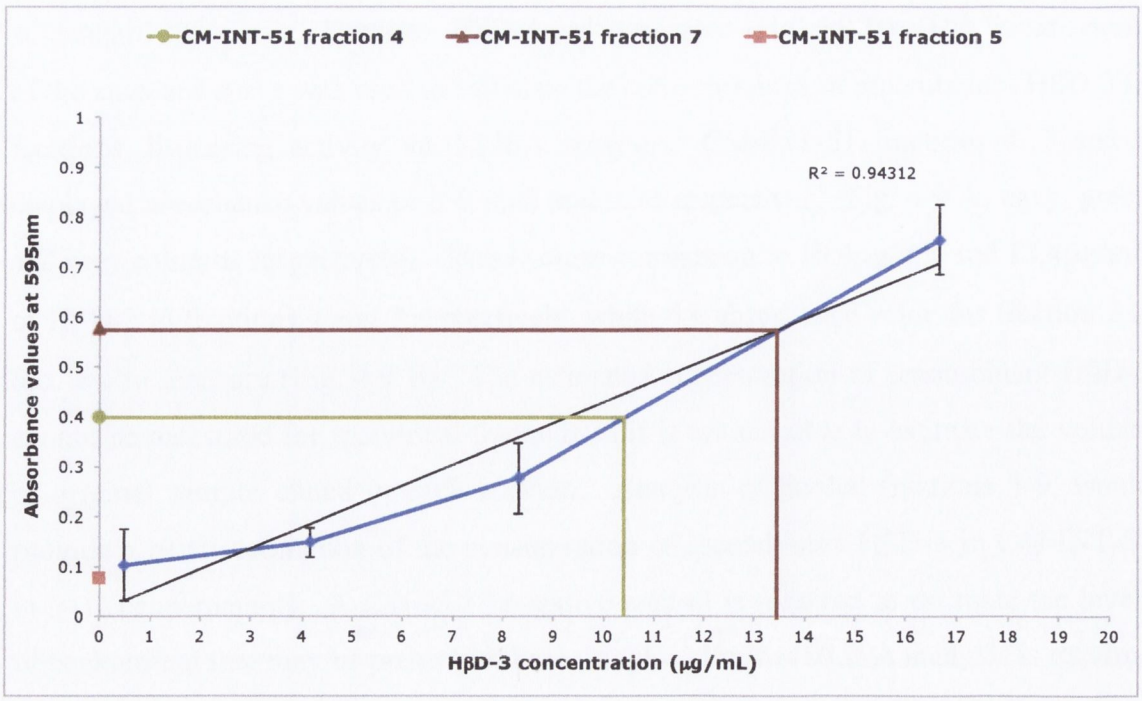
CM-INT-51 fraction 4
CM-INT-51 fraction 7
CM-INT-51 fraction 5
R² = 0.94312
Absorbance values at 595nm
1
0.9
0.8
0.7
0.6
0.5
0.4
0.3
0.2
0.1
0
0 1 2 3 4 5 6 7 8 9 10 11 12 13 14 15 16 17 18 19 20
HβD-3 concentration (µg/mL)

4.2.4.5 Reduction of the disulphide bonds of HβD-3 and RP-HPLC analysis

The data so far suggests that recombinant HβD-3 displays a different elution pattern than synthetic HβD-3. The greatest difference was observed for recombinant HβD-3 secreted by CM-INT-51, which eluted in three fractions, with the majority being retained on the column until 6.3 mins. This longer retention time may indicate that recombinant HβD-3 is a reduced form of HβD-3, and thus the surface area is more hydrophobic than that of synthetic HβD-3. To test this hypothesis, 10 μg of synthetic HβD-3 was treated with 5mM of the reducing agent, dithiothreitol (DTT). In the reduced state, HβD-3 eluted 0.1mins later than the oxidized peptide (Fig. 4.10), thus reducing all the disulphide bonds of HβD-3 does not drastically change the elution profile of synthetic HβD-3.

4.2.4.6 Cleavage of potential N-glycans from recombinant HβD-3 using Endo H

Another hypothesis that may explain the different elution profiles of recombinant HβD-3 compared to synthetic HβD-3 is that recombinant HβD-3 may have undergone glycosylation during maturation and secretion of the peptide. To test this, CM-INT-51 supernatant (10X) samples described in section 4.2.4.3 (+/-G418), were treated with the enzyme Endoglycosidase H (Endo H) (section 2.20), a highly specific endoglycosidase that cleaves asparagine-linked mannose rich oligosaccharides. Thus, if N-glycosylation of recombinant HβD-3 has occurred during post-translational modification of the peptide, the additional N-glycans will be cleaved off by Endo H. The Endo H-treated CM-INT-51 supernatant (10X) samples (+/-G418) were analysed by RP-HPLC. 10μg of synthetic HβD-3 was examined as a positive control and produced a maximum peak elution of 4mins (Fig. 4.11 and 4.12, black peaks).

The RP-HPLC analysis indicates that upon treatment of CM-INT-51 supernatant (10X) (-G418) with Endo H, the pattern of peaks produced by this sample differs significantly to untreated CM-INT-51 supernatant (10X) (-G418) (Fig. 4.11, pink and blue peaks respectively). The peak profile for untreated CM-INT-51 supernatant (10X) (-G418) is the same profile displayed in Fig. 4.8 (pink peaks). CM-INT-51 supernatant (10X) (-G418) treated with Endo H produces 2 peaks, the first eluting in fractions 3 and 4, and

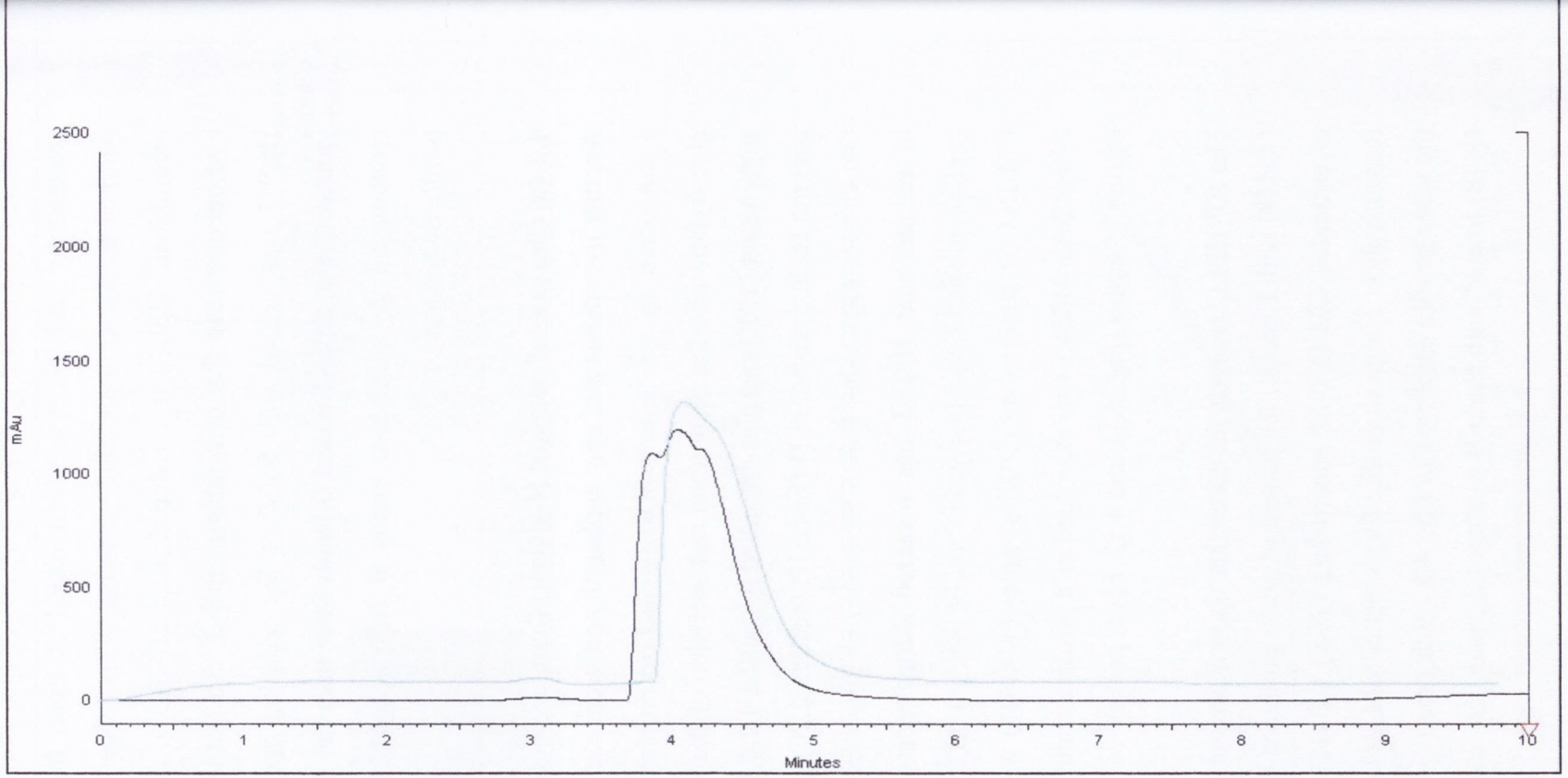

FIG. 4.10 Reversed phase high-performance liquid chromatography (RP-HPLC) analysis of synthetic HβD-3 in the presence of absence of DTT.

Synthetic HβD-3 was treated with 5mM DTT [blue] prior to fractionation on a C18 column. An untreated sample was also fractionted. Synthetic HβD-3 (10μg) [black] and synthetic HβD-3 (10μg) treated with 5mM DTT [blue]. The bound proteins/peptides were eluted using an acetonitrile gradient (2-11%). The milli-absorbance units (mAu) measured at 215nm are shown on the y-axis.

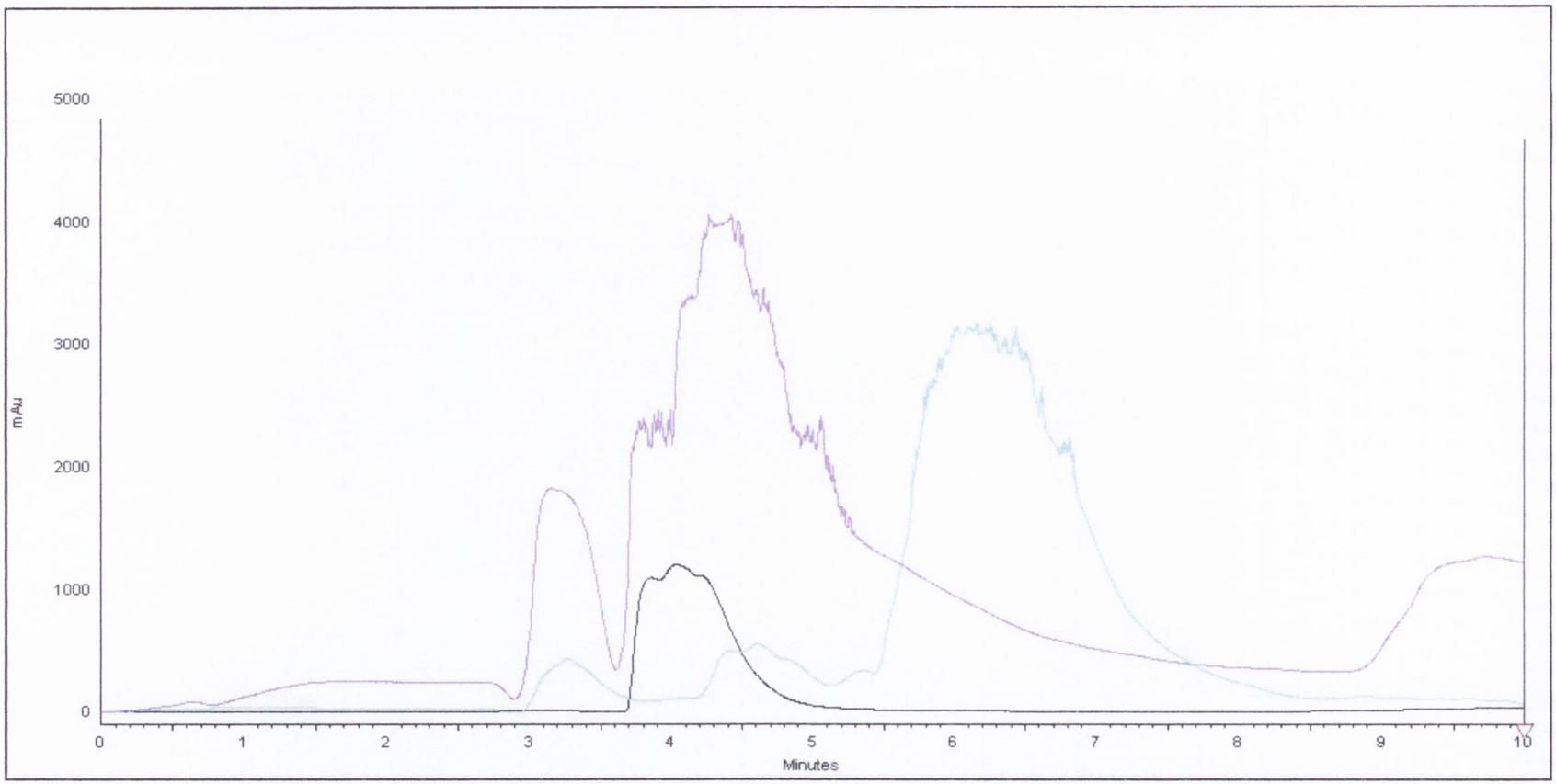

FIG. 4.11 Reversed phase high-performance liquid chromatography (RP-HPLC) analysis of CM-INT-51 (-G418) plus Endo H

CM-INT-51 (-G418) was treated with Endo H prior to fractionation. Synthetic HβD-3 (10μg) [black], CM-INT-51 10X supernatant (-G418) [blue], and CM-INT-51 10X supernatant (-G418) treated with Endo H [pink] were applied to a C18 column. The bound proteins/peptides were eluted using an acetonitrile gradient (2-11%). The milli-absorbance units (mAu) measured at 215nm are shown on the y-axis.

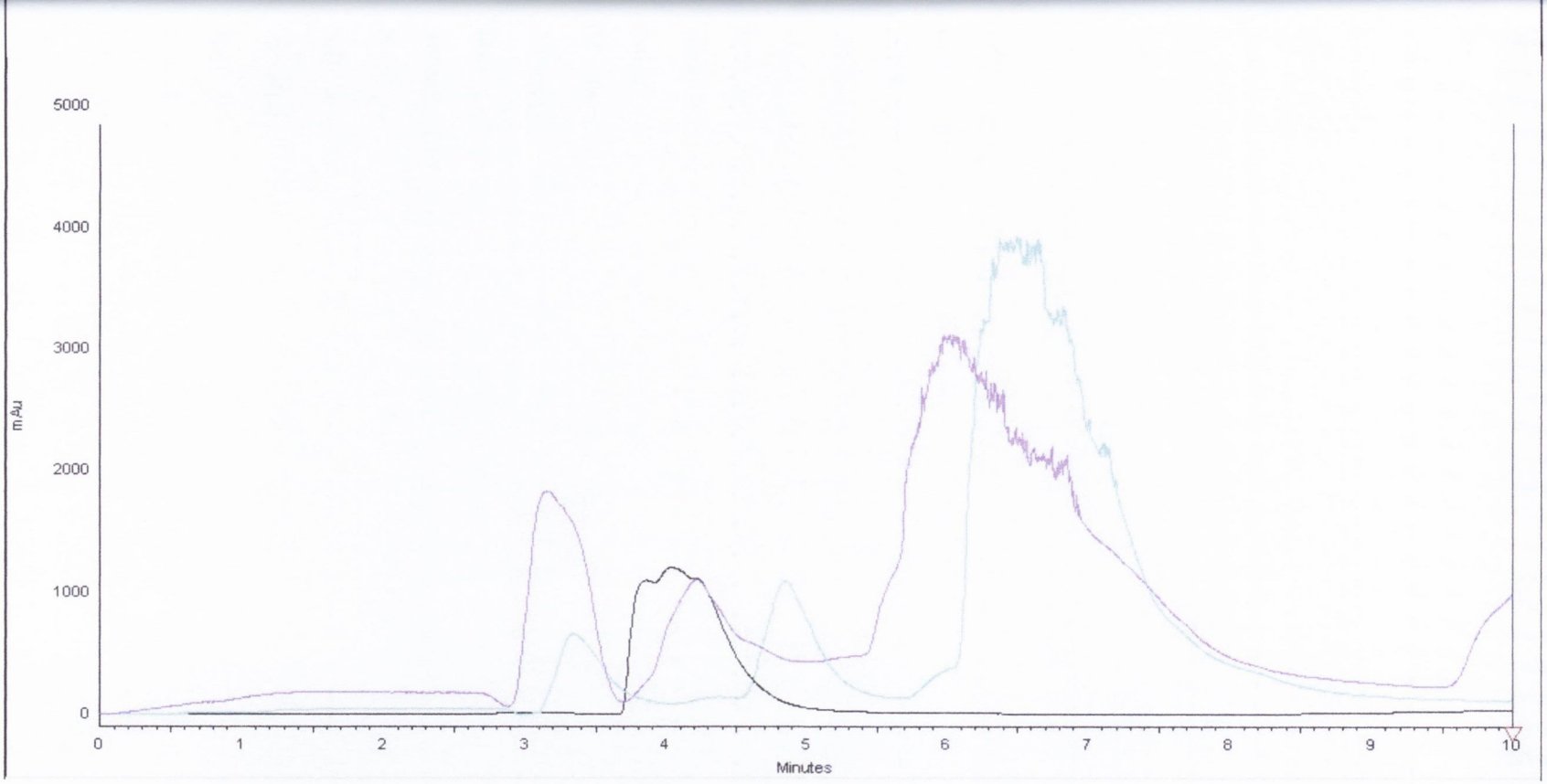

FIG. 4.12 Reversed phase high-performance liquid chromatography (RP-HPLC) trace of CM-INT-51 (+G418) plus Endo H

CM-INT-51 (+G418) was treated with Endo H prior to fractionation. Synthetic HβD-3 (10μg) [black], CM-INT-51 10X supernatant (+G418) [blue], and CM-INT-51 10X supernatant (+G418) treated with Endo H [pink] were applied to a C18 column. The bound proteins/peptides were eluted using an acetonitrile gradient (2-11%). The milli-absorbance units (mAu) measured at 215nm are shown on the y-axis.

the second in fractions 4 - 6, with maximum peak elutions of 3.1 mins and 4.2 mins respectively (Fig. 4.11, pink peaks). This dramatic shift in CM-INT-51 peaks upon Endo H treatment indicates that recombinant HβD-3 has undergone a certain degree of deglycosylation. The deglycosylated recombinant HβD-3 produces a variant of recombinant HβD-3 that mimics the elution profile of CM-505hbd3GAL1 and CM-506hbd3GAL1, which show a maximum peak elution of 3.3 mins (Fig. 4.5). This may represent a higher oxidized form of recombinant HβD-3. Furthermore, the second peak observed in the deglycosylated recombinant HβD-3 from CM-INT-51 (-G418) co-elutes with synthetic HβD-3. The generation of a third peak is visible at approximately 9mins. This may represent an isoform of HβD-3 with higher hydrophobicity that is not visible before Endo H treatment.

RP-HPLC results indicate that upon treatment of CM-INT-51 supernatant (10X) (+G418) with Endo H, the pattern of peaks produced by this sample again is different to the peaks observed for untreated CM-INT-51 supernatant (10X) (+G418) (Fig. 4.12, pink and blue peaks respectively). The peak profile for untreated CM-INT-51 supernatant (10X) (-G418) is the same profile displayed in Fig. 4.8 (blue peaks). CM-INT-51 supernatant (10X) (+G418) treated with Endo H produces 3 peaks, the first eluting in fractions 3 and 4, the second eluting in fractions 4 and 5, and the third peak eluting in fractions 6-8, with maximum peak elutions of 3.1, 4.4 and 5.9 mins respectively (Fig. 4.12, pink peaks). This shift in CM-INT-51 peaks upon Endo H treatment indicates that recombinant HβD-3 has undergone a certain degree of deglycosylation. The deglycosylated recombinant HβD-3 produces a variant that mimics the elution pattern of CM-505hbd3GAL1 and CM-506hbd3GAL1, which shows a maximum peak elution of 3.3 mins (Fig. 4.5). This may represent a more oxidized form of recombinant HβD-3. Furthermore, the second peak observed in the deglycosylated recombinant HβD-3 from CM-INT-51 co-elutes with synthetic HβD-3. As before, the generation of a third peak is visible at approximately 9mins. This may represent an isoform of HβD-3 with higher hydrophobicity that is not visible before Endo H treatment.

Taken together, the same pattern of elution, albeit with minor variations was observed in concentrated supernatants of CM-INT-51 grown in the presence or absence of G418. Furthermore in both samples treatment with Endo H produced HβD-3 variants with

peak elution profiles identical to CM-505hbd3GAL1 and CM-506hbd3GAL1 and synthetic HβD-3. Thus, production of HβD-3 from a gene integrated into the *S. pastorianus* genome produces glycosylated forms of HβD-3. Further ELISA analysis is required to verify the levels of recombinant HβD-3 in these fractions.

4.2.5 Detection of recombinant HβD-3 via Western blot analysis

Data from Endo H treatment of supernatant from CM-INT-51 suggests that the recombinant HβD-3 produced from this strain is glycosylated. To examine the glycosylated forms of recombinant HβD-3, preliminary Western blotting was carried out using a primary human βD-3 polyclonal capture antibody and a bovine anti-rabbit IgG-HRP conjugated secondary antibody, as described in detail in section 2.22.

4.2.5.1 Western blot of CM-INT-51

In this experiment cell pellets rather than cell supernatants were examined, to ensure that viable amounts of recombinant HβD-3 were present for detection by Western blotting. Both CMBS-33 and CM-INT-51 strains were cultured in 100mL of YEP media supplemented with 2% maltose (YEPM). Since CM-INT-51 contains a kanMX cassette, cells were grown in the presence (+ G418) or absence (- G418) of antibiotic for comparative analysis. One tenth of the culture (10mL) was removed and the cell pellet was obtained by centrifugation. The total proteins were extracted from the cell pellet as described in section 2.19.4, and the protein concentration of the sample determined by a Bradford assay (section 2.19.5). Total protein concentrations for each sample ranged from 7.4 – 8.8 μg/mL. Protein samples (0.3μg) were separated on 12% SDS-PAGE and synthetic HβD-3 was used as a positive control. Coomassie staining revealed the detection of a band at 5kDa for synthetic HβD-3 (10μg), representing a HβD-3 monomer (Fig. 4.13 A, Lane 2). A band at approximately 35kDa was detected for CM-INT-51 (-/+ G418) (Fig. 4.13 A, Lanes 4 & 5). This band was not detected for CMBS-33 (Fig. 4.13 A, Lane 6). Western blot analysis revealed the detection of a band at 5kDa for synthetic HβD-3 (0.25μg), representing a HβD-3 monomer (Fig. 4.13 B, Lane 2). A band at approximately 35kDa was detected for CM-INT-51 (+ G418) (Fig. 4.13 B, Lane 5). No band was detected in the CM-INT-51 sample grown in the absence of G418 (Fig. 4.13 B, Lane 4). Furthermore, no band was detected in the CMBS-33 sample (Fig. 4.13 B, Lane 6).

The detection of a band at approximately 35kDa with anti-HβD-3 antibody in the recombinant strain suggests that the intracellular pool of HβD-3 is possibly glycosylated. To test this Endo H treatment was performed on cell lysates (0.1μg) of CMBS-33, CM-INT-51 (-G418) and CM-INT-51 (+G418), as described in section 2.20. Treated

FIG. 4.13 Coomassie stain and Western blot analysis of recombinant and synthetic HβD-3

All cultures were grown in YEPMal. CM-INT-51 was cultured in YEPMal in the presence (+G418) or absence (-G418) of G418. Proteins were extracted from the cell pellet. **A)** Coomassie stain of a 12% SDS-PAGE gel. Lane 1: 10μl of Ultra-low range molecular weight marker. Lane 2: synthetic HβD-3 (10μg), lane 3: blank, lane 4: CM-INT-51 (- G418) cell lysate (0.3μg), lane 5: CM-INT-51 (+ G418) cell lysate (0.3μg) and lane 6: CMBS-33 cell lysate (0.3μg). Bands at approximately 35kDa unique for CM-INT-51 (- G418) and CM-INT-51 (+ G418) are boxed in red (lanes 4 and 5). The sizes of proteins are indicated to the left of the gel. **B)** Western blot analysis with anti-HβD-3 antibody. The same samples shown in A were electrophoresed on a 12% SDS-PAGE gel in the same order. The gel was transferred to PVDF membrane and probed with anti-β-defensin-3 antibody (1:5000). Antibody binding was detected using a HRP conjugated secondary antibody (1:10,000). The membrane was incubated in Chemiluminescent peroxidase substrate (Sigma) and exposed to X-ray film. The 5kDa (lane 2) and 35kDa (lane 5) bands are indicated by arrows.

A.

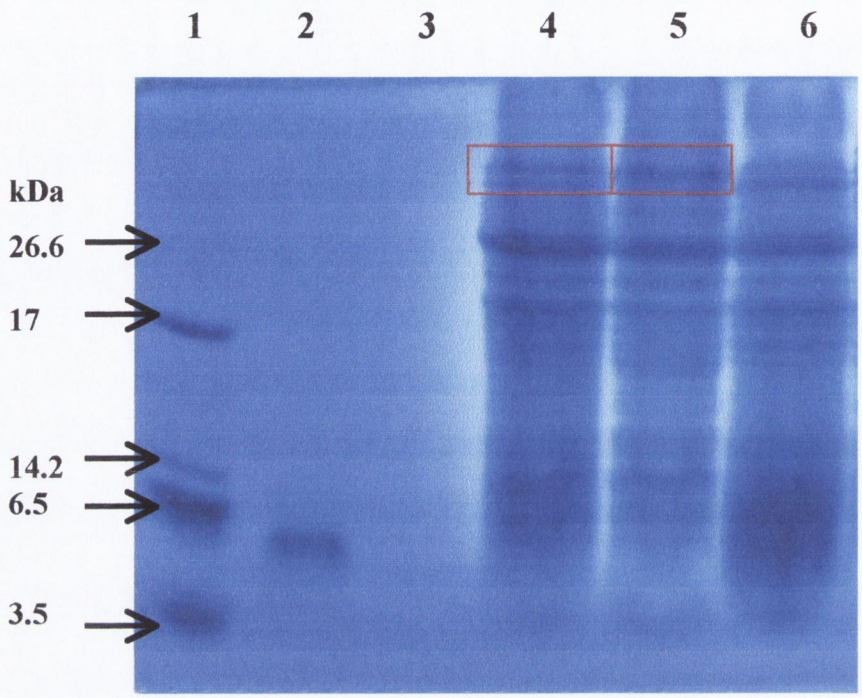

B.

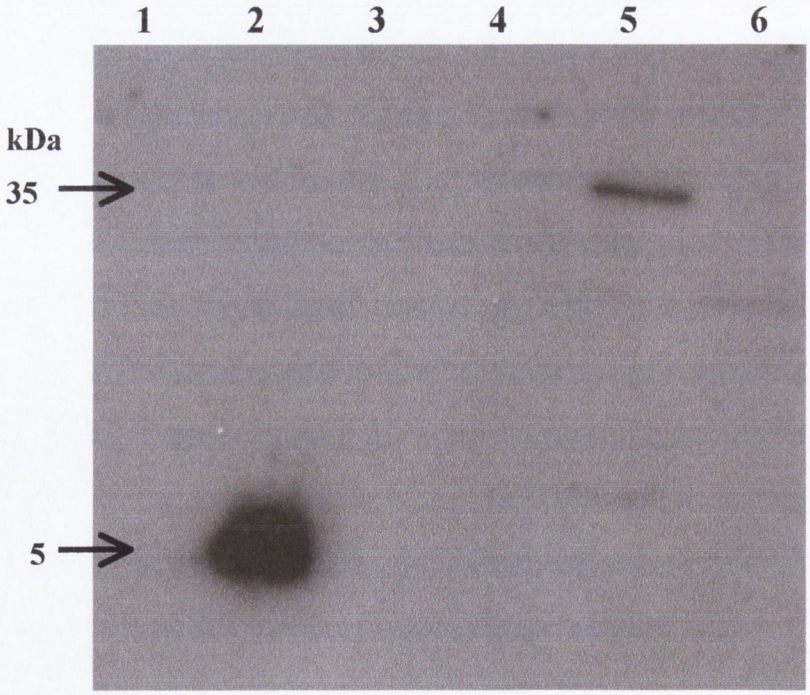

protein samples were analysed by Western blot analysis. Synthetic HβD-3 (0.25μg), not treated with Endo H, was used a positive control, and a band at 5kDa was visualised with the anti-HβD-3 antibody (Fig. 4.14, Lane 1). Three bands at approximately 15, 16 and 22kDa were observed in the CM-INT-51 (-/+ G418) cell pellet samples (Fig. 4.14, Lanes 4 & 5 respectively). This reduction in size of recombinant HβD-3, after Endo H treatment suggests that intracellular recombinant HβD-3 is N-glycosylated and to a certain extent deglycosylation can be obtained via Endo H treatment. A fainter band is evident at approximately 22kDa for CMBS-33, this may be due to slight overloading of the sample in lane 4.

To examine secreted recombinant HβD-3 via Western immunoblot, CMBS-33 and CM-INT-51 were cultured in 100mL of SC-Mal media. As mentioned earlier in the thesis, the necessity for culturing in minimal media arises from the fact that rich medium is highly viscous and insoluble when concentrated. The caveat of using SC-Mal is that much lower cell growth is obtained, compared to growth in rich media. Again CM-INT-51 was cultured in the presence and absence of G418 for comparative analysis. Cells were pelleted as before and the separated supernatant was concentrated 100X, via freeze-drying and the use of molecular weight cut off filters, as described in section 2.19.2. The samples were treated with Endo H as described in section 2.20 and Western immunoblot was performed on the equivalent of 4mL of treated or untreated supernatant samples. As a positive control synthetic HβD-3 (0.25μg) was included. A band corresponding to the 5kDa synthetic HβD-3 peptide was evident as before, however no bands were evident in concentrated supernatant samples (data not shown).

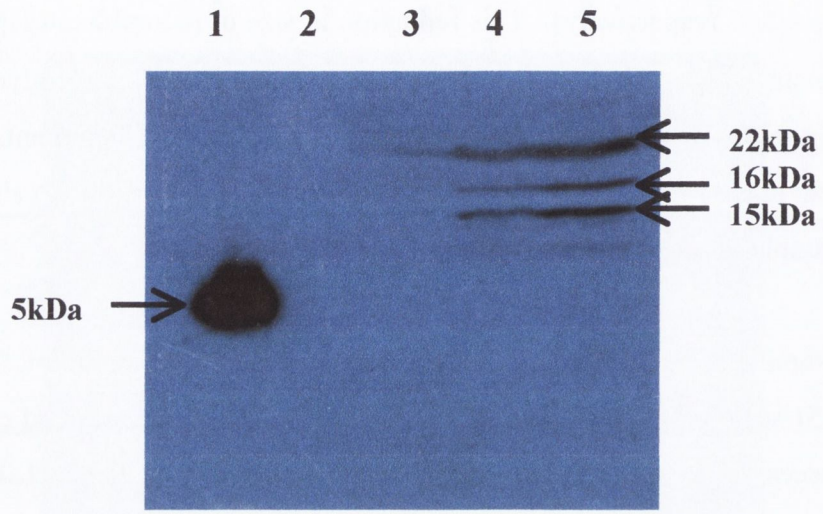

FIG. 4.14 Western blot analysis of synthetic HβD-3 and Endo H treated recombinant HβD-3

Western blot analysis of CM-INT-51 cell lysates treated with Endo H. Cell lysates from CM-INT-51 cultures grown in YEPMal were treated with Endo H (0.1U). The samples were electrophoresed on 12% SDS-PAGE. Following transfer to PVDF membrane, the membrane was probed with anti-β-defensin-3 antibody (1:5000). Antibody binding was detected using a HRP conjugated secondary antibody (1:10,000). The membrane was incubated in Chemiluminescent peroxidase substrate (Sigma) and exposed to X-ray film. The 5kDa (lane 2) and 15, 16 and 22kDa (lanes 4 and 5) bands are indicated by arrows. Lane 1: Synthetic HβD-3 (0.25μg), lane 2: blank, lane 3: CMBS-33 lysate (0.1μg), lane 4: CM-INT-51 (- G418) cell lysate (0.1μg) and lane 5: CM-INT-51 (+ G418) cell lysate (0.1μg). The major bands and approximate sizes are indicated by arrows.

4.2.5.2 Western blot of CM-505hbd3HISGAL1

Recombinant HβD-3 could not be detected in concentrated supernatants of CM-INT-51 cultures grown in SC-Mal by Western immunoblot. This may be due to lower growth levels of cultures in minimal medium. As mentioned above HβD-3 cannot be extracted from supernatant of cells grown in rich medium due to the high viscosity of this medium which contains high levels of peptone and yeast extract. To overcome this problem, a 6xHis-tag was fused to HβD-3, generating CM-505hbd3HISGAL1 (section 3.2.3). This strain was cultured in 70mL of SC-Mal and the supernatant was concentrated 50-fold (50X), as described in section 2.19. A nickel column purification step was performed on 1mL of supernatant samples (50X) as described in section 2.16.2. The flow-through fractions were collected and the column was then washed with buffer B (section 2.16.2). Finally the bound peptide was eluted from the column by buffer C and collected in 4 fractions (section 2.16.2). All fractions were concentrated and loaded onto 12% SDS-PAGE gels. As a negative control the supernatants from CM-505hbd3GAL were processed in the same manner. The majority of protein from CM-505hbd3GAL1, is present in the wash fraction sample (Fig. 4.15 A, lane 5), and a small amount of protein was retained on the column and eluted in fraction 2 of the eluate (Fig. 4.15 A, lane 7). Likewise, the wash fraction of CM-505hbd3HISGAL1 supernatant (50X), contains the majority of the protein (Fig. 4.15 A, lane 11), but a large amount of the protein sample was retained on the column and eluted in fraction 2 of the eluate suggesting that the HβD-3-6xHis-tag peptide bound to the column (Fig. 4.15 A, lane 13). The Coomassie stain indicates that two bands are obtained for CM-505hbd3HISGAL1, one at 8kDa and one at approximately 20kDa (Fig. 4.15, lane 13). As a positive control the bacterial protein CRP containing a C-terminal HIS-tag was included. The levels of which were too low to be detected by coomassie stain (Fig. 4.15 A, lane 2).

A Western immunoblot was performed on all fractions from the nickel column purification of CM-505hbd3GAL1 and CM-505hbd3HISGAL1, using a monoclonal mouse anti-poly HIS primary antibody and goat anti-mouse IgG-HRP conjugated secondary antibody, as described in section 2.22.3. A band corresponding to the 25kDa CRP protein was evident (Fig 4.15 B, lane 2), however no bands were evident in any of the examined supernatant samples (Fig 4.15 B, lanes 3-15).

FIG. 4.15 Western immunoblot analysis of fused HβD-3-6x-His-tag peptide fractions after nickel column purification

CM-505hbd3GAL1 and CM-505hbd3HISGAL1 were cultured in SC-Mal. Supernatants were concentrated 50-fold and purified via nickel column purification as described in the text. **A)** Coomassie blue stain of proteins fractionated by nickel column fractions. Lane 1: 10μl of Ultra-low range molecular weight marker. The size of the major bands are shown to the left of the gel. Lane 2: 0.25μg of CRP, lanes 3-9: CM-505hbd3GAL1 supernatant (50X) fractions, lane 3: flow-through 1, lane 4: flow-through 2, lane 5: wash, lanes 6-9: eluted fractions 1-4, lanes 10-15: CM-505hbd3HISGAL1 supernatant (50X) fractions, lane 10: flow-through 1, lane 11: wash, lanes 12-15: eluted fractions 1-4. The two most prominant bands at 8kDa and 20kDa, evident in the CM-505hbd3HISGAL1 elute fraction 2, are indicated by arrows. **B)** Western blot analysis of nickel column samples. The same samples shown in A were electrophoresed on a second 12% SDS-PAGE gel, with the exception of CM-505hbd3HISGAL1 elute fraction 4. Lane 1: 10μl of Ultra-low range molecular weight marker. Lane 2: 0.25μg of CRP, lane 3: blank, lanes 4-10: CM-505hbd3GAL1 supernatant (50X) fractions, lane 4: flow-through 1, lane 5: flow-through 2, lane 6: wash, lanes 7-10: eluted fractions 1-4, lanes 11-15: CM-505hbd3HISGAL1 supernatant (50X) fractions, lane 11: flow-through 1, lane 12: wash, lanes 13-15: eluted fractions 1-3. The gel was transferred to PVDF membrane and probed with anti-HIS antibody (1:3000). Antibody binding was detected using a HRP conjugated secondary antibody (1:10,000). The membrane was incubated in Chemiluminescent peroxidase substrate (Sigma) and exposed to X-ray film. The CRP protein at 25kDa is indicated by an arrow.

A.

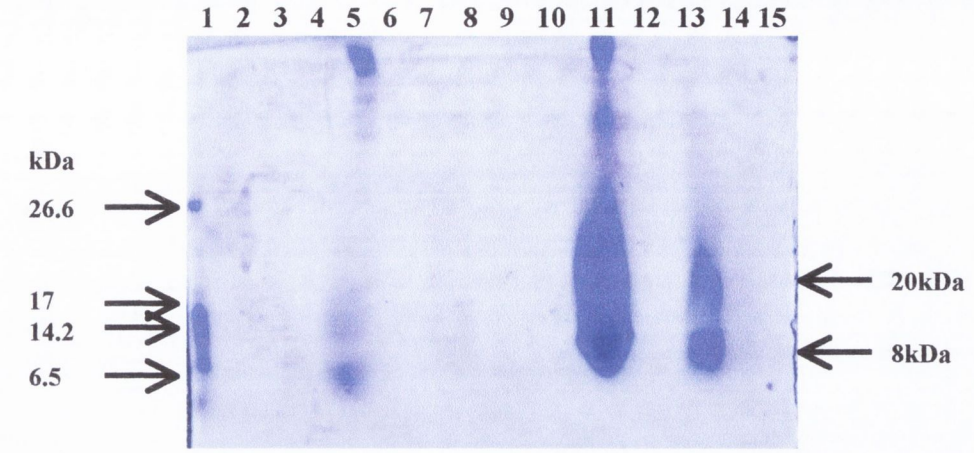
1 2 3 4 5 6 7 8 9 10 11 12 13 14 15
kDa
26.6
17
14.2
6.5
20kDa
8kDa

B.

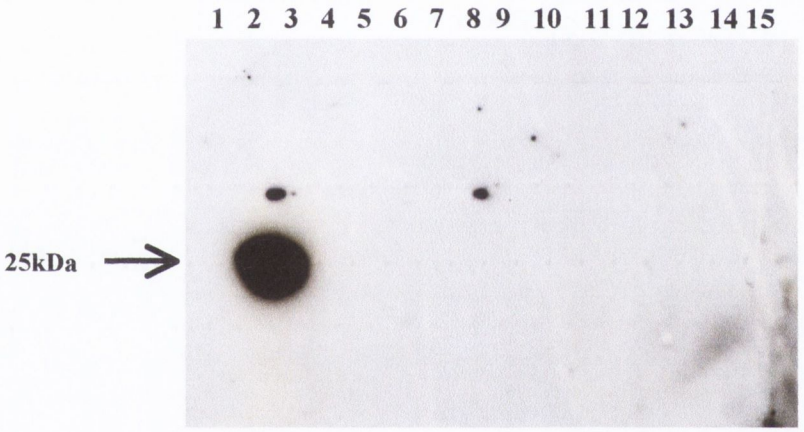
1 2 3 4 5 6 7 8 9 10 11 12 13 14 15
25kDa

In conclusion, the addition of the 6xHis-tag did not help overcome the lack of detection of recombinant HβD-3 in supernatant samples when grown in minimal media. Previous data obtained suggests that HβD-3 is heavily glycosylated, thus Endo-H treatment of these supernatant samples may help overcome this lack of detection by Western blotting.

4.3 Discussion

The overall aim of the research discussed in this chapter was to quantify expression levels of recombinant HβD-3 from the recombinant strains of the lager yeast CMBS-33, and to determine if recombinant HβD-3 is secreted from the cell.

Firstly semi-quantitative RT-PCR was performed on all yeast strains and results demonstrated that HβD-3 mRNA transcripts are synthesized in all HβD-3-encoding yeast strains (Fig. 4.1). However, this data does not clarify if these mRNA transcripts are fully functioning mature transcripts. Further analysis of the recombinant HβD-3 mature peptide will help to deduce if the non-specific 5'UTR modifications and various mutations discussed in chapter 3, had an affect on the translation of HβD-3 mRNA transcripts. Results depicted in Fig. 4.1, indicate that HβD-3 was efficiently expressed from all promoters. The *GAL1* and *AGT1* promoters were induced in the presence of galactose and maltose respectively and the *PGK1* and *TEF1* promoters appear to promote constitutive expression of recombinant HβD-3 in YEPMal. Previous studies have shown that the *AGT1* gene does not produce a functional Agt1p protein in *S. pastorianus* due to the presence of an inframe nonsense codon (Nakao et al., 2009; Vidgren et al., 2005). However, our results demonstrate that the *S. cerevisiae AGT1* promoter is fully functional in *S. pastorianus*. Furthermore, the truncated Mig1 binding site of the *AGT1* 500bp promoter does not affect the functioning of this promoter. According to the data in Fig. 4.1, the *TEF1* promoter appears to be extremely efficient at expressing high levels of recombinant HβD-3 over a 24hr period. Studies by Partow et al. (2010) confirmed that *TEF1* is one of the strongest constitutive promoters, compared to six different constitutive promoters (*PGK1, ADH1, TPI1, HXT1, TDH3* and *PYK1*) and shows the best levels of constitutive expression in YEPD or YEPGal *S. cerevisiae* fermentations after 24hrs (Partow et al., 2010). Our data is in agreement with data by Partow et al. (2010), and suggests that *TEF1* is one of the strongest constitutive promoters compared to $PGK1_{SC}$ and $PGK1_{SB}$. Additionally the results presented here indicate that the *TEF1* promoter is active in cells grown in YEPMal.

Due to the complexity of the *S. pastorianus* genome, the direct integration of the HβD-3 gene cassette into the chromosome of CMBS-33 may have caused disruption to the regions surrounding the site of integration (section 1.6). The synthesis of YPR159W and YPR160W mRNA transcripts was confirmed in CM-INT-37 and CM-INT-51 via

RT-PCR (Fig. 4.2). However, this data does not clarify if these mRNA transcripts are fully functioning mature transcripts. If the final functioning copy of *GPH1* was affected by the integration the HβD-3 gene cassette, this would subsequently affect the strains ability to survive in a fermentation due to stress intolerance. This topic will be examined further in chapter 5.

The literature indicates that β-defensins are extremely difficult to detect (Corrales-Garcia et al., 2011; Valore and Ganz, 1997). The HβD-3 gene has been introduced into various *E. coli* strains and soluble expression and antimicrobial activity have been achieved (Huang L, 2007; Si et al., 2007), however there is a lack of eukaryotic expression systems for β-defensins (Corrales-Garcia et al., 2011). To tackle both of these problems, the secretion of recombinant HβD-3 was analysed from various eukaryotic expression systems and various detection methods were used to detect secreted recombinant HβD-3.

ELISA results suggest that recombinant HβD-3 is present in the supernatants of CM-505hbd3GAL1 and CM-506hbd3GAL1, with slightly higher activity being observed in the supernatants of CM-505hbd3GAL1 (section 4.2.3.1). Furthermore, preliminary data suggests that recombinant HβD-3 is present in the supernatants of CM-505hbd3TEF1, CM-506hbd3AGT1, CM-INT-51 and CM-pRShbd3PGK1 (data not shown). While two negative controls were analysed during this study, CMBS-33 and CM-pRS, a third negative control, CM-505GAL1, should have been analysed also. However, it is important to note that the presence of the empty multi-copy plasmid did not affect the ELISA analysis of recombinant HβD-3, as only background values were obtained for CM-pRS (data not shown). However, further experiments are required to verify if the empty pGREG-505 vector affects the ELISA analysis of recombinant HβD-3. Overall, this data is preliminary and further experimentation is needed to quantify the true values of recombinant HβD-3 in each strain. Furthermore, as expression levels of recombinant HβD-3 were analysed in strains grown in rich media (YEP) and secretion levels of recombinant HβD-3 were analysed from strains grown in minimal media (SC), expression levels and peptide levels cannot be directly compared. Thus, further experimentation is required to compare the expression levels of recombinant HβD-3 to the secreted peptide levels.

To purify correctly folded recombinant HβD-3 and separate alternatively folded HβD-3 variants, 10X supernatant samples were separated via RP-HPLC. This process was performed on CM-505hbd3GAL1 supernatant (10X) and CM-506hbd3GAL1 supernatant (10X), as both of these strains appear to secret slightly higher levels of recombinant HβD-3 (section 4.2.3.1/4.2.3.2). Synthetic HβD-3 was shown to elute from the column between 3.7 – 5mins, with an average maximum elution of 4.1mins (Fig. 4.4). Recombinant HβD-3 produced by both CM-505hbd3GAL1 and CM-506hbd3GAL1, co-eluted with synthetic HβD-3 and displayed a maximum elution at 3.3mins (Fig. 4.5). As shown in Fig. 4.4, synthetic HβD-3 retention time varies slightly between each experiment, thus this minor variation between synthetic HβD-3 and supernatant samples may be irrelevant or may indicate a reduced hydrophobicity and/or variation in disulphide linkages, post-translational modifications or tertiary structure between the synthetic HβD-3 and the recombinant HβD-3. The presence of recombinant HβD-3 in fractions that produced peaks at 215nm was verified by ELISA analysis (Fig. 4.6 and 4.7). The overall results indicate that CM-506hbd3GAL1 produces slightly higher HβD-3 activity compared to CM-505hbd3GAL1. However, ELISA results also indicate that the accurate quantification of recombinant HβD-3 purified via RP-HPLC is difficult. While the levels of recombinant HβD-3 in RP-HPLC fractions appear higher than the levels obtained in crude concentrated supernatants (Fig. 4.6/4.7 and Fig. 4.3 respectively), this increase in activity could be due to high background levels. Furthermore, the increase observed in HβD-3 concentrations post fraction could be due to the removal of inhibitors that may affect detection via the ELISA method.

RP-HPLC was also performed on CM-INT-51 concentrated supernatant to analyse and purify recombinant HβD-3 encoded in the genome. The peak profile obtained for CM-INT-51 (+/- G418) concentrated supernatant was very different to that obtained for CM-505hbd3GAL1 and CM-506hbd3GAL1 concentrated supernatant (Fig. 4.8 and 4.5 respectively). This difference in peak profiles may be due to the production of different HβD-3 variants from each strain. Furthermore, the difference in peak profiles obtained for CM-INT-51 concentrated supernatant and CM-505hbd3GAL1 and CM-506hbd3GAL1 concentrated supernatant, may be analysed further using alternative RP-HPLC columns.

Recombinant HβD-3 secreted from CM-INT-51 cells (+/-G418) eluted from the column at three different times points, with small variations in the elution profiles between samples grown in the presence and absence of G418 (Fig. 4.8). As mentioned above, the maximum peak elutions of synthetic HβD-3 have been shown to vary from experiment to experiment (Fig. 4.4), thus this small disparity could represent variation between two independent cultures. Furthermore, the results show that HβD-3 variants with alternative tertiary structures are present in concentrated supernatants of CM-INT-51. Fractions containing the desired HβD-3 peptide were verified by ELISA analysis for CM-INT-51 (+G418) RP-HPLC fractions (Fig. 4.9), and the results indicate that recombinant HβD-3 was mainly detected in fractions 4 and 7. This suggests that some variant of recombinant HβD-3 is retained on the column longer than synthetic HβD-3. To determine background levels obtained during ELISA analysis, CMBS-33 supernatant should be analysed alongside CM-INT-51 (+G418) supernatant. However, recombinant HβD-3 concentration values for CM-INT-51 (+G418) would still be estimates, as the levels of HβD-3 retained on the column are undetermined.

Schroeder et al. (2011) state that when treated with a reducing agent, such as DTT, the reduced form of HβD-1 is retained on the column up to 3.5mins longer than an oxidized form (Schroeder et al., 2011). A variant of recombinant HβD-3 elutes from the column approximately 2mins later than synthetic HβD-3 (Fig. 4.8). To analyse if the reduction of HβD-3 leads to longer retention time, synthetic HβD-3 was treated with the reducing agent DTT (section 4.2.4.5). These experimental conditions did not lead to any major change in the elution time of synthetic HβD-3 (Fig. 4.10), but varying the experimental parameters may vary the RP-HPLC results. Further experiments would need to be performed to verify that a variant of recombinant HβD-3 secreted from CM-INT-51 is in fact a reduced form of the peptide.

Glycosylation is another possibility for the array of variants of recombinant HβD-3 detected in supernatants from CM-INT-51, as yeast cells are known to hyperglycosylate recombinant secretory proteins. Studies by Hsu et al. (2009) implied that a human α-defensin (HD-5) secreted by the yeast strain *Pichia pastoris* underwent O-glycosylation, as multiple HD-5 specific bands were obtained during Western immunoblot of supernatant samples (Hsu et al., 2009). HβD-3 contains two serine (S) and two threonine (T) residues along with one asparagine (N) residue (Fig. 1.4) indicating that

this peptide is susceptible to both O-glycosylation and N-glycosylation. The addition of glycans to the peptide during this post-translational modification process would result in a change in the surface area of the recombinant HβD-3 peptide, overall changing the hydrophobicity of the peptide. Thus, this change in hydrophobicity will be detected by RP-HPLC. To examine this hypothesis, CM-INT-51 (+/-G418) concentrated supernatant was treated with the enzyme Endoglycosidase H (Endo-β-N-acetylglucosaminidase H/ Endo H). Endo H is a highly specific endoglycosidase, it cleaves only asparagine-linked mannose rich oligosaccharides (N-glycosylation). Endo H treated samples were analysed by RP-HPLC. The elution profile of Endo H treated samples was different to that observed for untreated samples, indicating a certain degree of deglycosylation. Endo H treatment of CM-INT-51 (-G418) concentrated supernatant resulted in a distinct change in peak patterns for recombinant HβD-3. Three peaks with maximum peak elutions ranging from 3.3 – 6mins are produced by untreated concentrated supernatant (Fig. 4.11, blue peaks). Upon Endo H treatment two peaks are obtained with maximum peak elutions of 3.1 and 4.2mins (Fig. 4.11, pink peaks). This suggests that N-glycosylation of recombinant HβD-3 has occurred. Endo H treatment of CM-INT-51 (+G418) concentrated supernatant also shows a similar shift in elution peaks (Fig. 4.12). Three peaks with maximum peak elutions ranging from 3.4 – 6.3mins are produced by untreated concentrated supernatant (Fig. 4.12, blue peaks). Upon Endo H treatment three peaks are obtained with maximum peak elutions of 3.1, 4.4 and 5.9mins (Fig. 4.12, pink peaks). As described in section 4.2.3, supernatants were first concentrated via freeze-drying, followed by further concentration using 3kDa molecular weight cut-off filters. Thus, this second step should remove the majority of G418 as this antibiotic has a molecular weight of 692.70. One hypothesis is that each independent culture contains multiple isoforms of recombinant HβD-3, each differing in their degree of glycosylation. The minor differences in elution profiles of HβD-3 from cultures grown in the presence or absence of G418, most likely reflects different levels of deglycosylation, adding to the production of multiple intermediate forms of HβD-3 varying in their degree of glycosylation. Alternatively, residual G418 which may be present in the supernatant may affect the activity of Endo H, resulting in lower levels of deglycosylation overall. The results indicate that deglycosylation of recombinant HβD-3 from CM-INT-51 produces isoforms with elution profiles similar to recombinant HβD-3 from CM-505hbd3GAL1 and CM-506hbd3GAL1 and to synthetic HβD-3.

Western blot analysis of CM-INT-51 cell pellet samples detected specific bands at approximately 35kDa for CM-INT-51 cells cultured in the presence of G418 (Fig. 4.13), however no band was detected for CM-INT-51 cells cultured in the absence of G418. Since this was a single experiment, and the SDS-PAGE gel transferred to PVDF membrane for Western blotting was not subsequently stained, it is possible that less of the latter sample was loaded onto the gel. Based on the RP-HPLC analysis, it is possible that the increase in molecular mass of the peptide is a result of glycosylation. Given the different pattern of glycosylation observed in the +/-G418 treated samples, the lower level of detection of HβD-3 in the –G418 sample may result from masking of antibody binding sites by the additional N-glycans. Studies by Borsig et al. (1997) suggest that hyperglycosylation can adversly effect the detection of a His-tag. N-glycosylation that occured 69 amino acids away from the His-tag, caused steric hindrance of the His-tag (Borsig et al., 1997). HβD-3 contains five possible glycosylation sites. Glycosylation of any of these sites may directly impair the ability of the anti-HβD-3 antibody to bind to the peptide. The N-glycosylation of recombinant HβD-3 was further verified upon deglycosylation with Endo H which resulted in specific bands at approximately 15, 16 and 22kDa for both CM-INT-51 (+/-G418) (Fig. 4.14). As stated above, Endo H is a highly specific endoglycosidase that only cleaves N-linked oligosaccharides. Thus, these variants of HβD-3 may be a result of O-glycosylation of the recombinant peptide.

Recombinant HβD-3 was not detected by Western immunoblot, in the concentrated supernatant samples of any HβD-3 encoding strains under any experimental conditions. This may be due to low growth levels of strains when cultured in minimal media. Furthermore, we now know glycosylation is occuring thus, recombinant HβD-3 available in the supernatant may be hyperglycosylated which may make it difficult to detect the recombinant peptide via Western blot analysis. To try and overcome this problem, a 6xHis-tag was fused to the 3'end of HβD-3 and Western immunoblot was performed using His-tag specific antibodies (section 4.2.5.2). The nickel column purification results suggest that the 6xHis-tag was successfully fused to HβD-3 as this fusion peptide was purified during the nickel column purification step (Fig. 4.15). Furthermore, this result verifys that recombinant HβD-3 is secreted from the cell. However, this fusion peptide is not detected via Western immunoblot. As stated above, studies by Borsig et al. (1997) suggest that hyperglycosylation can adversly effect the

detection of a His-tag. HβD-3 contains glycosylation sites located 11, 12, 24, 41 and 42 amino acids upstream of the 6xHis-tag. Glycosylation of any of these sites may directly impair the ability of the anti-HIS antibody to bind to the 6xHis-tag.

RP-HPLC results indicate a 0.9mins difference in retention time of recombinant HβD-3 secreted from CM-505hbd3GAL1 and CM-506hbd3GAL1 compared to synthetic HβD-3. This difference may indicate slight glycosylation of recombinant HβD-3. This hypothesis is in agreement with the observed pattern of glycosylated HβD-3 secreted from CM-INT-51.

The data obtained during this research indicates that recombinant HβD-3 undergoes glycosylation in CMBS-33. Glycosylation of HβD-3 appears to affect the ability of antibodies to bind to the peptide, but this may also affect the antimicrobial activity of the secretory peptide. The level of antimicrobial activity of recombinant HβD-3 is crucial in this study, if the activity levels are too high the peptide may affect yeast, if they are too low they may not be be sufficient to eradicate bacterial contamination during fermentation. The antibacterial activity of secretory recombinant HβD-3 will be analysed in the next chapter.

Chapter 5:
Analysis of HβD-3 Antimicrobial Activity

5.1 Introduction

The research outlined in this chapter was carried out to examine the antimicrobial activity of synthetic and recombinant HβD-3, both *in vitro* and *in vivo* and to determine the ability of beer spoilage micro-organisms (BSMs) to survive and multiply in various fermentative conditions.

Fermentations were first carried out to examine the ability of the BSM, *Lb. brevis*, to grow in a fermentative environment. Furthermore, previous studies have reported the broad antimicrobial spectrum of HβD-3, which is active against Gram-positive bacteria, Gram-negative bacteria, fungi and viruses (Garcia et al., 2001; Harder et al., 2001; Hoover et al., 2003; Shelburne et al., 2005; Starner et al., 2005; Wu et al., 2003). To determine if the BSM, *Lb. brevis,* is susceptible to synthetic and recombinant HβD-3 *in vitro* bioassays were carried out.

The survival of Gram-positive, facultative anaerobic BSMs (*Lb. brevis*) and Gram-negative, strictly anaerobic BSMs (*P. frisingensis*) under a variety of fermentative conditions was initially analysed and the ability of recombinant HβD-3 to eliminate these BSMs was determined. Since lactic acid bacteria are deemed the most hazardous of beer spoiling micro-organisms (Ogden, 1986), *Lb. brevis* spoilage was examined in detail. To test the ability of expressed recombinant HβD-3 to eliminate the BSMs, *Lb. brevis* was seeded into fermentations carried out with both wild-type and HβD-3 expressing yeast in high and low specific gravity wort as well as into defined rich media (YEPGal), at both 11°C and 20°C.

The mechanism of action of the positively charged HβD-3 peptide involves electrostatic interactions with the negatively charged phospholipids of the bacterial membrane, leading to membrane disruption (Fig. 1.3) (Wiesner and Vilcinskas, 2010). When bacteria undergo cold-shock, homeoviscous adaption occurs (Sinensky, 1974). This complex process, involving an increase in unsaturated fatty acids and a reduction in chain length occurs to stabilize membrane fluidity. Such alterations in the bacterial membrane may make the bacteria more susceptible to HβD-3. Thus, to improve antimicrobial activity against BSMs, a novel "freeze treatment" was incorporated into the process. Additionally, alcohol can diffuse through the cell membrane and is an effective bacteriocidal agent against many bacterial species (Moorer, 2003). The

bacteriocidal efficiacy of alcohol can be increased when mixed with other chemicals/reagents, thus reducing the amount of alcohol required for killing. For example, 29.4% alcohol mixed with the wetting agent, dodecanoic soap, displays antimicrobial activity against a broad range of organisms (www.urthpro.com). Since yeast fermentations produce alcohol levels in the range of 3-5%, the presence of alcohol in combination with recombinant HβD-3 and a freeze-thaw cycle may provide a synergistic effect, resulting in increased antimicrobial activity against Gram-positive and Gram-negative bacteria.

5.2 Results

5.2.1 Analysis of BSM survival in fermentations

To test the viability of the BSM, *Lb. brevis*, under fermentation conditions, the yeast strain, CMBS-33, was inoculated at 1.5 x 10^7 cfu/mL, into eight separate flasks of brewer's wort (16°Bx) and incubated at 20°C (section 2.17). Triplicate cultures were seeded with *Lb. brevis* on day 7, at 10^4 and 10^6 cfu/mL respectively and duplicate control cultures were left unseeded (section 2.18). The decrease in Brix values during the fermentation was monitored as described in section 2.17 (Fig. 5.1 A). Brix values decreased as the fermentation proceeded and the production of CO_2 bubbles, characteristic of yeast fermentations, was observed. The fermentations attenuated at approximately 8°Bx, which is reflective of the relatively high °Bx starting point (Fig. 5.1 A). The Brix values decreased in all fermentations in a similar manner, indicating that the addition of *Lb. brevis* did not affect the fermentative capacity (Fig. 5.1 A). The percentage alcohol was calculated from the decreasing Brix values as described in section 2.17. The % alcohol values obtained for each fermentation are shown in Fig. 5.1 B. The final alcohol percentage of each fermentation was approximately 4%.

General contamination characteristics were observed in fermentations seeded with *Lb. brevis*. The brew became hazy and off odours developed. Samples were taken on day 13 (day 6 of seeding) and lawned onto MRS plates, with cycloheximide at 80μg/mL (section 2.18). Cycloheximide inhibits protein biosynthesis in eukaryotic organisms, preventing yeast growth, thus enabling the enumeration of bacteria. *Lb. brevis* seeded at 10^4 cfu/mL displayed an approximate 0.3 log increase, while *Lb. brevis* seeded at 10^6 cfu/mL resulted in a 4 log decrease after 6 days (Fig. 5.2). These results suggest that *Lb. brevis* can survive under fermentation conditions, where an acidic, anaerobic environment has already been created and the alcohol content is between 3.5 – 4% (Fig. 5.1 B). However when *Lb. brevis* is present in high concentrations in this stressful environment, its viability decreases significantly (Fig. 5.2).

FIG. 5.1 CMBS-33 fermentations with or without *Lb. brevis*

A) CMBS-33 fermentations in wort (16°Bx) at 20°C. Control fermentations in duplicate (blue) contain no *Lb. brevis*. Experimental fermentations in triplicate were seeded with 10^4 cfu/mL [red] and 10^6 cfu/mL [green] of *Lb. brevis*, on day 7. The error bars represent the standard error from two or three independent fermentations. **B)** % Alcohol of CMBS-33 fermentations as above.

A)

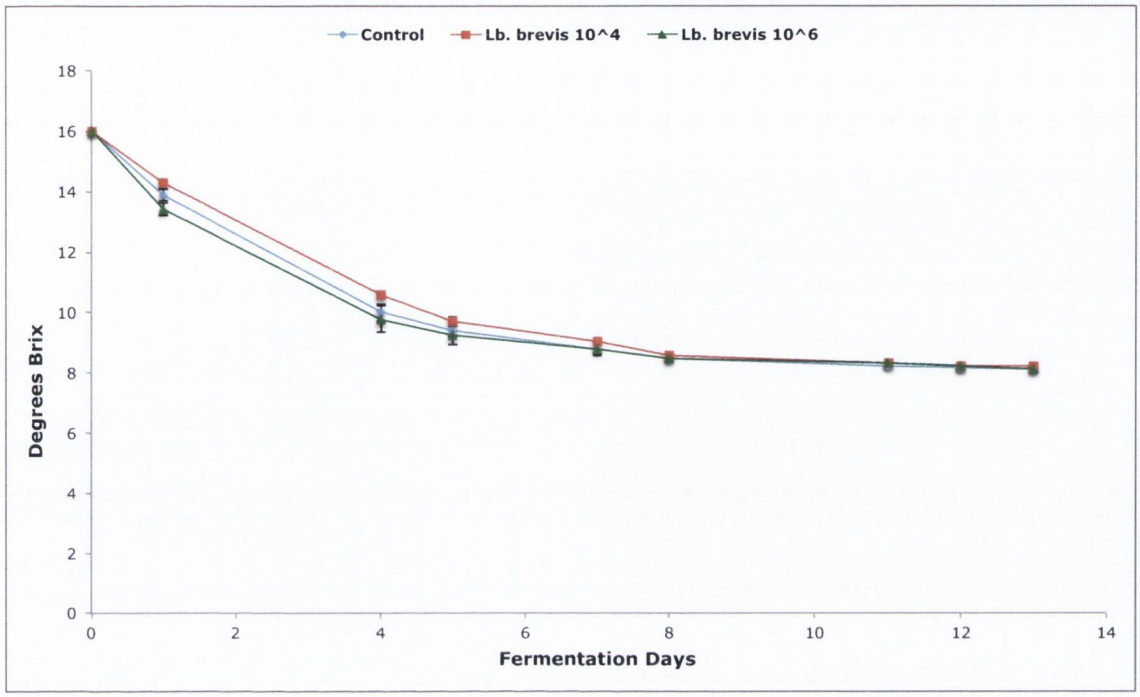
Control
Lb. brevis 10^4
Lb. brevis 10^6
Degrees Brix
Fermentation Days
0
2
4
6
8
10
12
14
16
18

B)

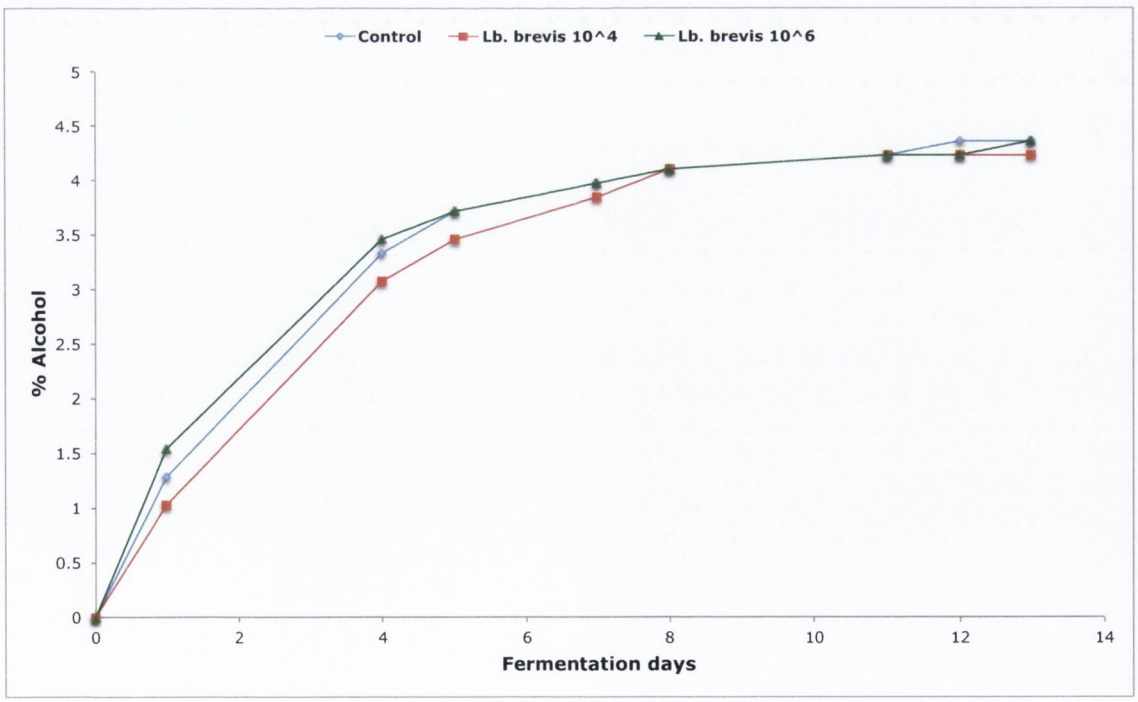
Control
Lb. brevis 10^4
Lb. brevis 10^6
% Alcohol
Fermentation days
0
0.5
1
1.5
2
2.5
3
3.5
4
4.5
5
0
2
4
6
8
10
12
14

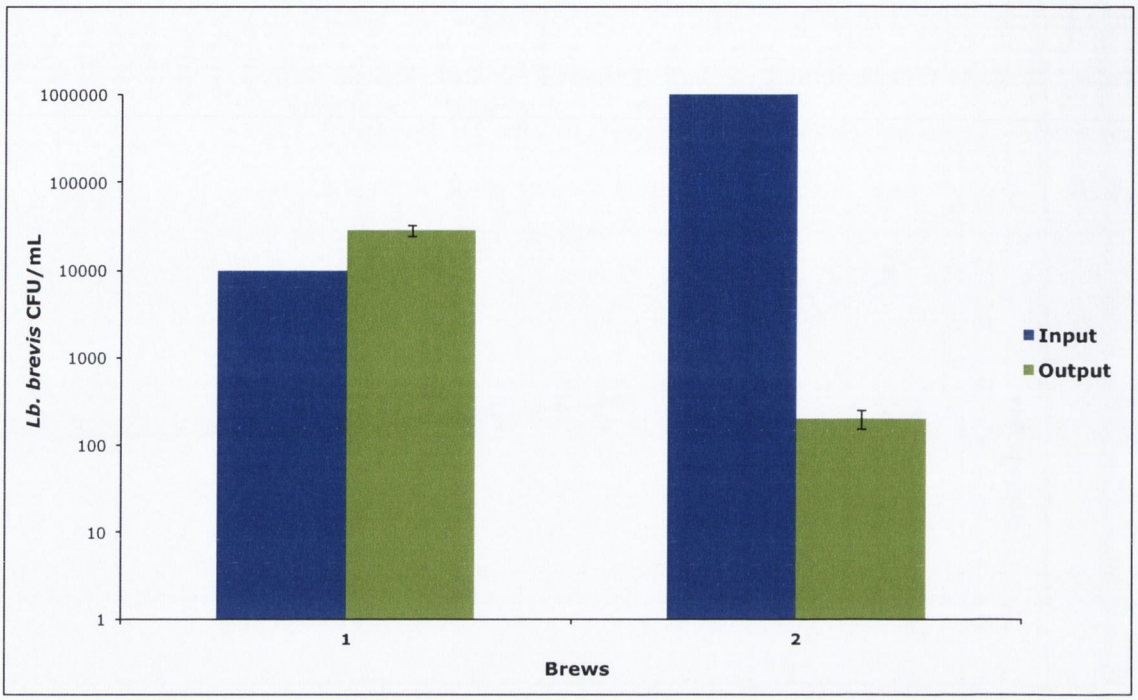

FIG. 5.2 Viability of *Lb. brevis* in CMBS-33 fermentations at 20°C

Triplicate cultures of CMBS-33 were seeded with 10^4 and 10^6 cfu/mL of *Lb. brevis* (brews 1 and 2 represent respectively). Blue columns show the input cfu/mL seeded into the brew, and green columns show the number of bacteria recovered from the fermentation after 6 days. The error bars represent the standard error from three independent brews.

5.2.2 Analysis of the antimicrobial activity of recombinant HβD-3 in concentrated supernatant samples

As outlined in chapter 3, a series of *S. pastorianus* strains expressing recombinant HβD-3 were generated. To test if the recombinant HβD-3, which is secreted from the cells, has antimicrobial activity, bioassays were performed on *Lb. brevis* using concentrated supernatant samples from the recombinant strains (section 2.24.1). The yeast strains CMBS-33, CM-505hbd3GAL1 and CM-506hbd3GAL1 were cultured in 400mL of SC-Gal media, with the addition of G418 where appropriate. The cells were pelleted and the supernatants were concentrated using Sep-Pak C18 columns as described in section 2.19.3. Any G418 present in the media should not bind to the column due to its hydrophilic nature. The final concentration of each supernatant sample varied slightly with CMBS-33, CM-505hbd3GAL1 and CM-506hbd3GAL1 being concentrated 6.25X, 7.5X and 5X respectively. *Lb. brevis* was cultured overnight at 37°C in MRS media and diluted to a cell density of approximately 10^3 cfu/mL as ascertained by measuring the optical density of the culture at OD_{600}. The culture was treated with aliquots (100µl) of concentrated supernatant samples and incubated at 37°C for 2 hrs (experiment 1) or 2.5 hrs (experiment 2), followed by duplicate plating onto MRS agar.

The data from experiment 1 is shown in Fig. 5.3. Based on viable counts on MRS agar plates, the density of the starting culture was approximately 4 x 10^3 cfu/mL (Fig. 5.3 A and B). This increase in starting inoculum may reflect an error in the estimation of the OD_{600} value or a burst of growth in SDW following incubation for 2hrs, however the latter is unlikely. The bactericidal activity of the supernatants, were compared to that of synthetic HβD-3 (Fig. 5.3 A). Synthetic HβD-3 exhibited antimicrobial activity against *Lb. brevis*, with an MBC value of 2µg/mL (Fig. 5.3 A). Previous work in the lab has demonstrated that HβD-3 at concentrations as high as 50-100µg/mL does not inhibit the growth of lager yeasts when pitched at densities used to initiate lager fermentations, i.e. 1.5 x 10^7 cfu/mL (Usher, James, Kavanagh and Bond, unpublished). Thus *Lb. brevis,* is killed by synthetic HβD-3 at concentrations that do not affect the lager strain, CMBS-33. No bactericidal activity was detected with supernatants from CMBS-33 cells, with *Lb. brevis* viability similar to the negative control (0µg/mL of synthetic HβD-3) (Fig. 5.3 A and B). Supernatants from CM-505hbd3GAL1 showed antimicrobial activity against *Lb. brevis*, reducing viability of the cells by 22% compared to CMBS-33 viability (Fig. 5.3 B). Statistical analysis was performed using a student T-test to

FIG. 5.3 Treatment of *Lb. brevis* with synthetic and recombinant HβD-3

Lb. brevis at a cell density of approximately 4 x 10^3 cfu/mL, was treated with concentrated supernatants of CMBS-33, CM-505hbd3GAL1 and CM-506hbd3GAL1 for 2hrs at 37°C. **A)** Standard curve of bactericidal activity of synthetic HβD-3 against *Lb. brevis*. The cultures were serially diluted and plated onto MRS agar and surviving bacteria were enumerated. **B)** Total colony forming units (CFU) of *Lb. brevis* after treatment with concentrated supernatant samples of CMBS-33, CM-505hbd3GAL1 and CM-506hbd3GAL1. Surviving bacteria were enumerated on MRS agar. The error bars represent the standard deviation from duplicate viable counts.

A.

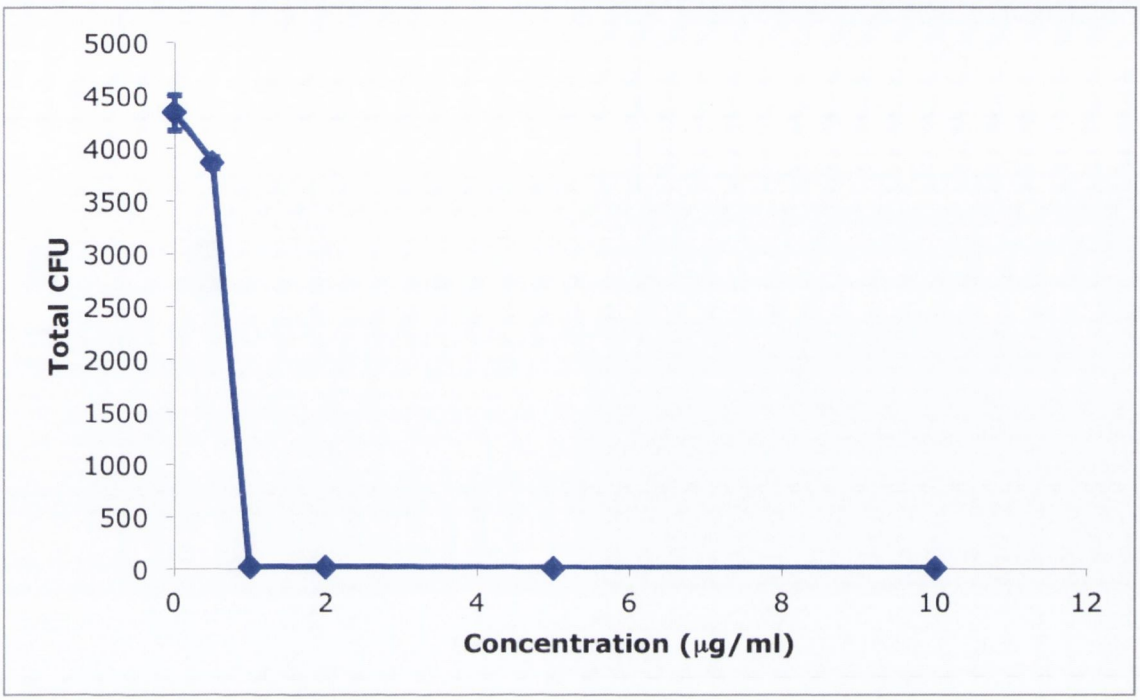
5000
4500
4000
3500
3000
2500
2000
1500
1000
500
0
Total CFU
0
2
4
6
8
10
12
Concentration (μg/ml)

B.

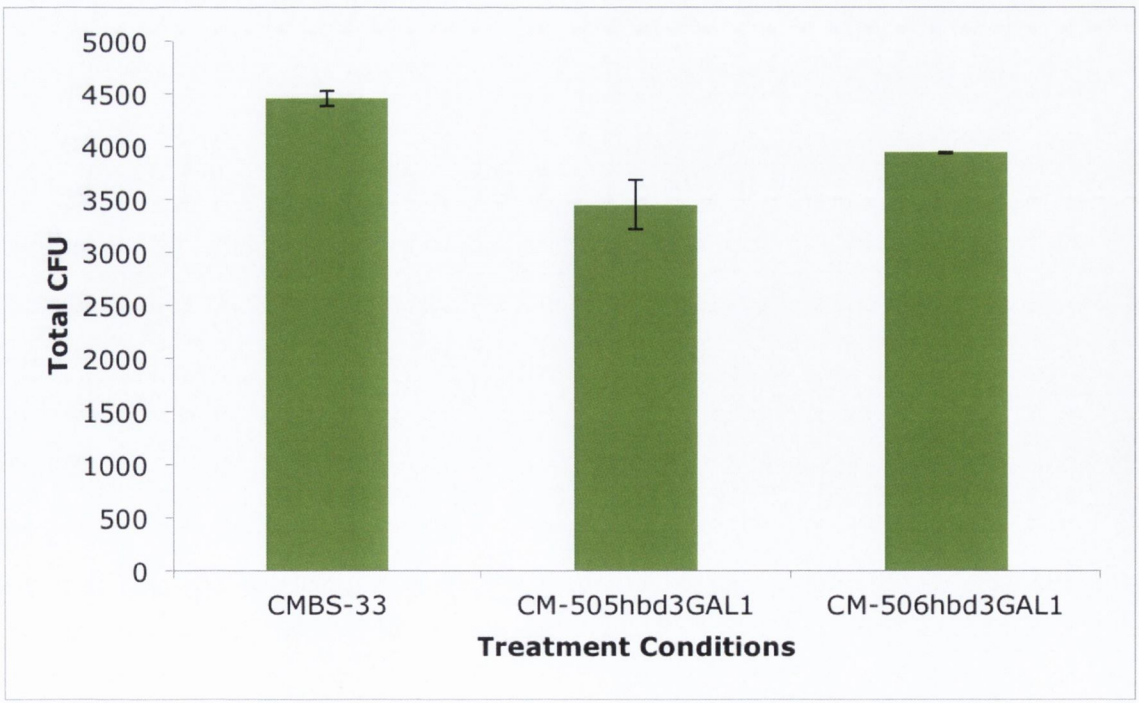
5000
4500
4000
3500
3000
2500
2000
1500
1000
500
0
Total CFU
CMBS-33
CM-505hbd3GAL1
CM-506hbd3GAL1
Treatment Conditions

compare viability of *Lb. brevis* following treatment with yeast culture supernatants. The threshold for statistical significance was set at 0.05. Thus, p values below 0.05 were deemed significant while those above 0.05 were deemed insignificant. Comparison of *Lb. brevis* viability in CM-505hbd3GAL1 and CMBS-33 supernatants revealed a p value of 0.028. Supernatants from CM-506hbd3GAL1 reduced the viability of *Lb. brevis* by approximately 11% with a p value of 0.009 (Fig. 5.3 B). The level of antimicrobial activity displayed by CM-506hbd3GAL1 supernatant (5X) was similar to that obtained by synthetic HβD-3 at 0.5μg/mL, which reduced viability of *Lb. brevis* by 13%, while CM-505hbd3GAL1 supernatant (7.5X) displayed a higher level of antimicrobial activity compared to 0.5μg/mL of synthetic HβD-3 (Fig. 5.3 A and B).

Thus, 100μl of concentrated supernatant appears to possess antimicrobial activity against *Lb. brevis*, equivalent to 50ng of synthetic HβD-3. Based on this comparison a minimum of 50ng of recombinant HβD-3 in 100μl of concentrated supernatant (7.5X), would indicate that CM-505hbd3GAL1 secretes active recombinant HβD-3 at a minimum concentration of 0.06μg/mL. Likewise, CM-506hbd3GAL1 secretes active recombinant HβD-3 at approximately 0.1μg/mL.

The bioassay was repeated except on this occasion the samples were incubated for 2.5hrs. The data revealed a similar trend of recombinant HβD-3 activity against *Lb. brevis*, with one exception. No bactericidal activity was detected with supernatants from CMBS-33 cells, with *Lb. brevis* viability similar to the negative control (0μg/mL of synthetic HβD-3). Supernatants from CM-505hbd3GAL1 displayed antimicrobial activity against *Lb. brevis*, reducing viability of the cells by 45% compared to CMBS-33 viability (p=0.044). Supernatants from CM-506hbd3GAL1 reduced the viability of *Lb. brevis* by approximately 6%, however this result is not statistically significant. In this experiment, the level of antimicrobial activity displayed by CM-505hbd3GAL1 supernatant (7.5X) was equivalent to that obtained by synthetic HβD-3 at 0.5μg/mL, which reduced viability of *Lb. brevis* by 46% (data not shown). This indicates that CM-505hbd3GAL1 secreted active recombinant HβD-3 at approximately 0.06μg/mL. This result is in agreement with the results obtained in experiment 1. However, in this experiment less HβD-3 was produced by CM-506hbd3GAL1, therefore this experiment would need to be repeated to verify the levels of recombinant HβD-3 in CM-506hbd3GAL1 supernatant.

ELISA analysis of crude concentrated supernatants indicated that CM-506hbd3GAL1 and CM-505hbd3GAL1 secrete recombinant HβD-3 in the range of 30ng/mL and 54ng/mL respectively (Fig. 4.3). However, ELISA analysis of RP-HPLC fractionated supernatants indicated that these strains secrete recombinant HβD-3 at a range of 1.59 - 1.66μg/mL and 0.84 - 1.49μg/mL respectively (Fig. 4.6 and 4.7). Thus the results from the bioassay are in agreement with ELISA results from crude concentrated supernatants. As this assay only allows limited antimicrobial activity to be observed for recombinant HβD-3 secreted into the supernatants, the antimicrobial activity levels of all remaining strains were examined *in vivo*.

5.2.3 Detection of antimicrobial activity of recombinant HβD-3 in vivo

The data compiled thus far indicates that synthetic HβD-3 is an appropriate antimicrobial peptide for the use of killing the BSM *Lb.brevis*, without significantly affecting lager yeast. Furthermore, recombinant HβD-3 secreted into the medium appears to display antimicrobial activity *in vitro*. Since both Gram-positive and Gram-negative bacteria can cause beer spoilage, the antimicrobial activity of recombinant HβD-3 against *Lb. brevis* (Gram-positive) and *P. frisingensis* (Gram-negative) was examined under a variety of fermentation conditions *in vivo*.

To examine the bactericidal activity of recombinant HβD-3 *in vivo*, CMBS-33, CM-505hbd3GAL1 and CM-506hbd3GAL1 were first inoculated into YEPD media, containing G418 where appropriate, and cultured at 30°C overnight. Yeast cells were washed twice in SDW to remove any traces of G418 and cells were inoculated at 1.5 x 10^7 cfu/mL into microbrews (10mL) of either wort (16°Bx) (four independent experiments) or YEP media containing 2% galactose (YEPGal) (three independent experiments), and incubated at 11°C (section 2.17). 2% galactose was added to wort fermentations to induce the GAL1 promoter of HβD-3. *Lb. brevis* or *P. frisingensis* were added to each set of fermentations on day 2 at 10^3 cfu/mL (section 2.24.2). Samples were then taken approximately 2hrs after seeding (day 0 of seeding) and 2 days later (day 2 of seeding, day 4 of the fermentation) and lawned onto MRS agar containing cycloheximide to enumerate bacterial levels (untreated). The antimicrobial activity of recombinant HβD-3 *in vivo* was also analysed after a "freeze-treatment". An aliquot of each sample taken 2 hrs after the initial seeding and 2 days later, was subjected to a freeze-thaw cycle, whereby cells in 20% glycerol were frozen at -70°C overnight and then thawed on ice before plating (freeze-treated).

All data was normalized relative to 100% growth/viability in CMBS-33 fermentations.

5.2.3.1 Analysis of recombinant HβD-3 bactericidal activity against Gram-positive bacteria, under various growth conditions

Fermentations were seeded with *Lb. brevis* at a concentration of 1 x 10^3 cfu/mL on day 2 of the fermentation. The starting inoculum was based on OD_{600} readings. However, analysis of viable counts after 2hrs indicated a more accurate inoculum of approximately 0.3 x 10^3 cfu/mL. This decrease in initial cfu's may reflect a decrease in

viability upon inoculation into media at 11°C and is observed in both wort and YEPGal (Fig. 5.4 A and B). After 4 days of fermentation (day 2 of seeding), the bacterial cell count increased approximately 2-fold in wort (Fig. 5.4 A). Statistical analysis of viable counts on day 4 indicate a significant difference ($p<0.05$). In the YEPGal fermentations the bacterial count increases by approximately 5-fold after 2 days as shown in Fig. 5.4 B ($p<0.05$).

Analysis of the antimicrobial activity in untreated samples revealed that within 2 hrs of the initial contamination (day 2 of the fermentation), *Lb. brevis* viability decreased in CM-505hbd3GAL1 fermentations (YEPGal) by an average of 18% (Fig. 5.5 A, red columns). This is compared to 100% *Lb. brevis* viability in the CMBS-33 fermentations (Fig. 5.5 A, blue columns). Statistical analysis of viable counts of the BSM in CM-505hbd3GAL1 fermentations compared to the CMBS-33 fermentations revealed a p value below 0.05. *Lb. brevis* viability was unaffected in CM-506hbd3GAL1 fermentations compared to viability in CMBS-33 fermentations on day 2, with $p>0.05$ (Fig. 5.5 A, green and blue columns respectively). On day 4 viable counts of *Lb. brevis* viability in CM-505hbd3GAL1 and CM-506hbd3GAL1 fermentations were similar to CMBS-33 fermentations as seen in Fig. 5.5 A ($p>0.05$). Upon freeze-treatment of these samples, *Lb. brevis* viability in CM-505hbd3GAL1 fermentations was similar to viability in CMBS-33 fermentations on day 2, $p>0.05$ (Fig. 5.5 B, red and blue columns respectively). Whereas, *Lb. brevis* viability was reduced by an average of 24% in CM-506hbd3GAL1 fermentations compared to CMBS-33 fermenations on day 2, however statistical analysis revealed a p value greater than 0.05 (Fig. 5.5 B, green and blue columns respectively). As *Lb. brevis* numbers increase on day 4 in YEPGal fermentations, the viability of *Lb. brevis* in CM-505hbd3GAL1 and CM-506hbd3GAL1 fermentations is unaffected compared to CMBS-33 fermentations, $p>0.05$ (Fig. 5.5 B).

The viability of *Lb. brevis* in wort (16°Bx) fermentations was also examined. Before freeze-treatment no killing is detected in CM-505hbd3GAL1 and CM-506hbd3GAL1 fermentations compared to CMBS-33 fermentations, on days 2 and 4 of the fermentations (Fig. 5.6 A). On day 4 *Lb. brevis* viability is higher in CM-505hbd3GAL1 and CM-506hbd3GAL1 fermentations compared the control (Fig. 5.6 A,

A.

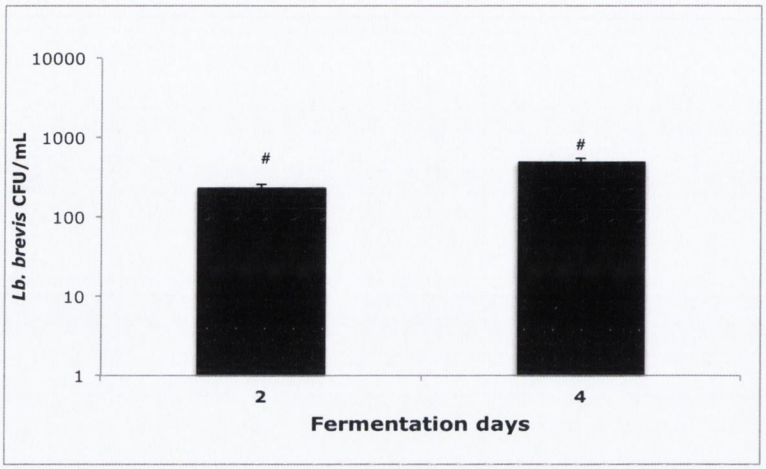

B.

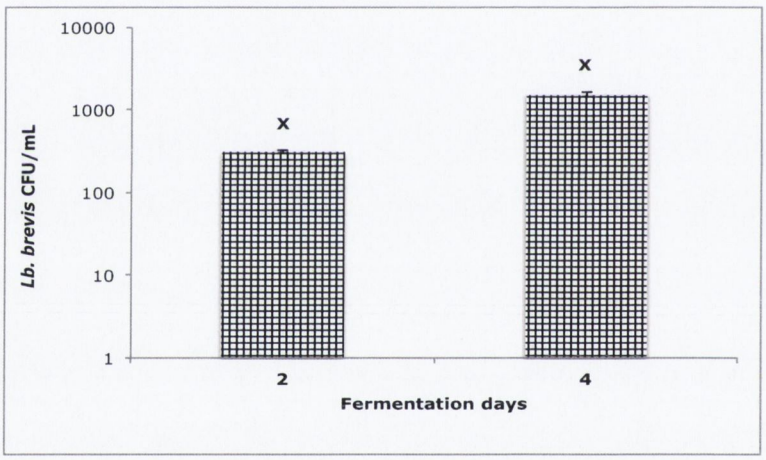

FIG. 5.4 *Lb. brevis* viability in various fermentative conditions

Lb. brevis viability in CMBS-33 fermentations at 11°C. Fermentations were inoculated at 10^3 cfu/mL of *Lb. brevis* on day 2. Bacterial cells were enumerated 2 hrs after the initial seeding (day 2) and 2 days later (day 4). **A)** *Lb. brevis* viability on days 2 and 4 in wort (16°Bx) fermentations. **B)** *Lb. brevis* viability on days 2 and 4 in YEPGal (2%) fermentations. The error bars represent the standard error of viable counts from four independent experiments (#) in wort or three independent experiments (x) in YEPGal. A minimum of duplicate viable counts were obtained for each independent experiment.

FIG. 5.5 Antimicrobial activity of recombinant HβD-3 against *Lb. brevis* in YEPGal fermentations

Lb. brevis viability in YEPGal fermentations at 11°C. Fermentations were seeded with 10^3 cfu/mL of *Lb. brevis* on day 2. Bacterial cells were enumerated 2 hrs after the initial seeding (day 2) and 2 days later (day 4). Bacterial counts for each culture were normalized relative to CMBS-33 which was set at 100% viability. CMBS-33: blue columns. CM-505hbd3GAL1: red columns. CM-506hbd3GAL1: green columns. **A)** *Lb. brevis* viability before freeze-treatment. **B)** *Lb. brevis* viability after freeze-treatment. The error bars represent the standard error from three independent experiments with a minimum of duplicate viable counts per experiment.

A.

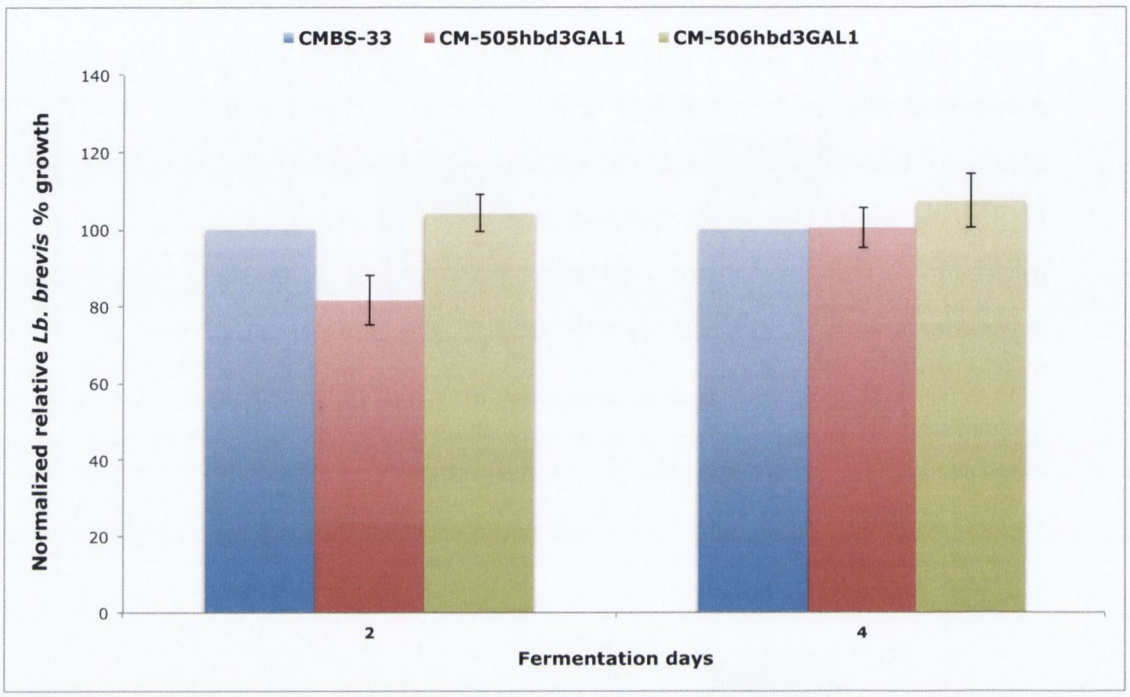
CMBS-33
CM-505hbd3GAL1
CM-506hbd3GAL1
Normalized relative Lb. brevis % growth
140
120
100
80
60
40
20
0
2
4
Fermentation days

B.

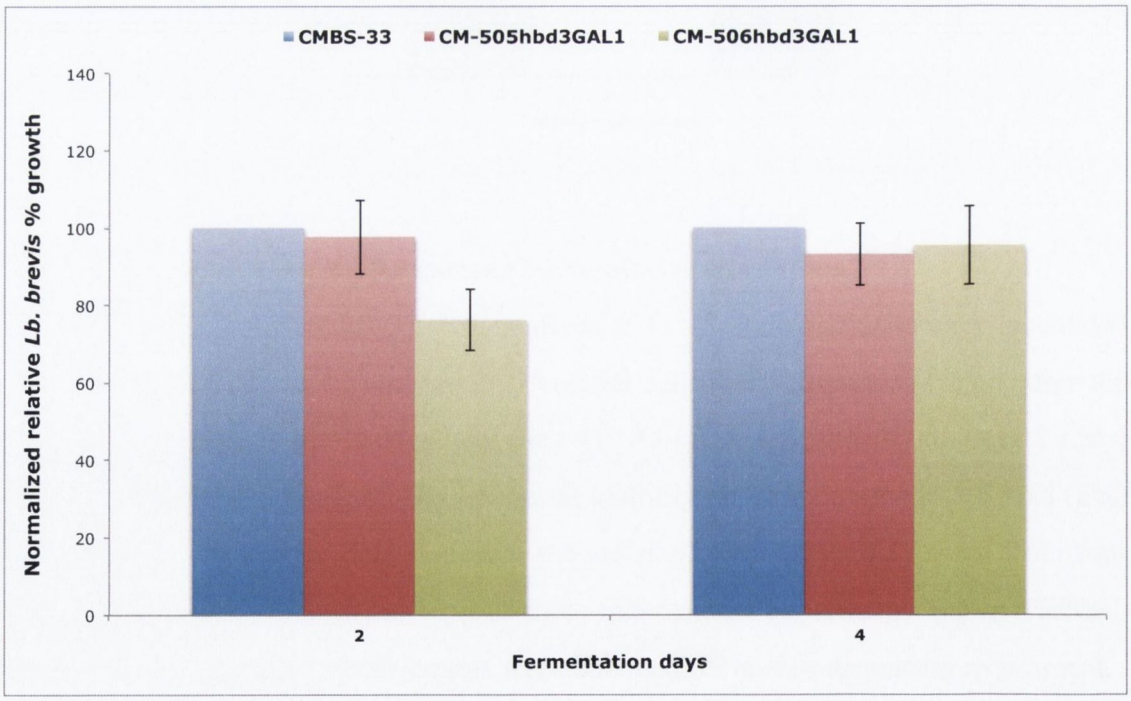
CMBS-33
CM-505hbd3GAL1
CM-506hbd3GAL1
Normalized relative Lb. brevis % growth
140
120
100
80
60
40
20
0
2
4
Fermentation days

FIG. 5.6 Antimicrobial activity of recombinant HβD-3 against *Lb. brevis* in wort fermentations

Lb. brevis viability in wort (16°Bx) fermentations at 11°C. Fermentations were seeded with 10^3 cfu/mL of *Lb. brevis* on day 2. Bacterial cells were enumerated 2 hrs after the initial seeding (day 2) and 2 days later (day 4). Bacterial counts for each culture were normalized relative to CMBS-33 which was set at 100% viability. CMBS-33: blue columns. CM-505hbd3GAL1: red columns. CM-506hbd3GAL1: green columns. **A)** *Lb. brevis* viability before freeze-treatment. **B)** *Lb. brevis* viability after freeze-treatment. The error bars represent the standard error from four independent experiments with a minimum of duplicate viable counts per experiment.

A.

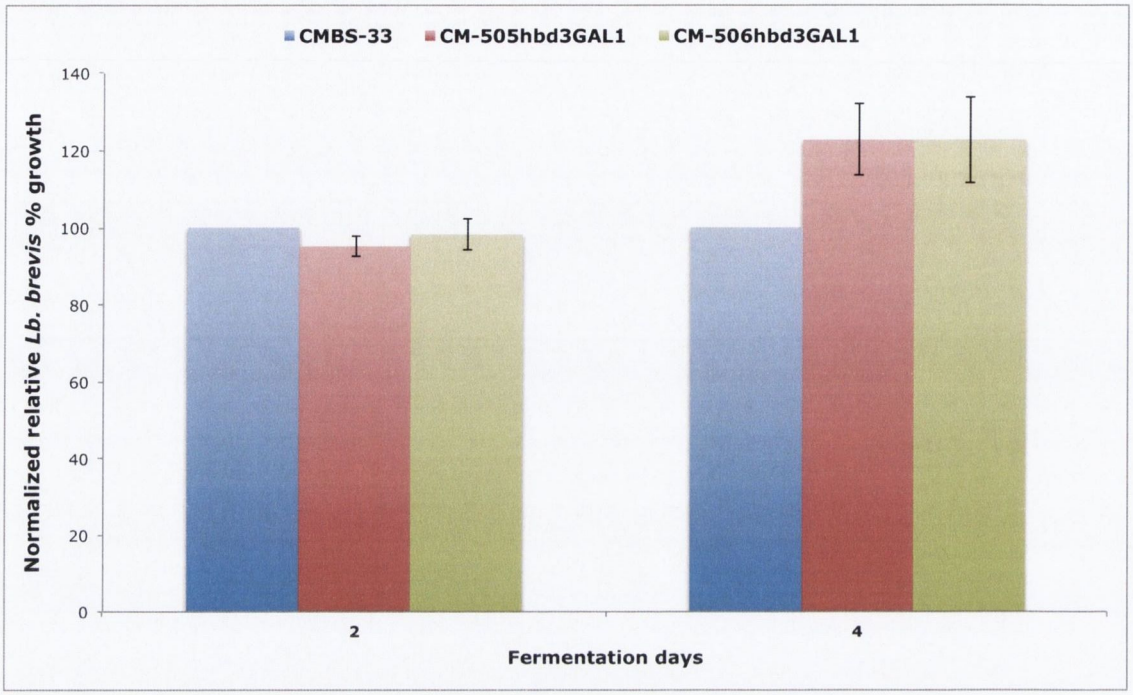
CMBS-33
CM-505hbd3GAL1
CM-506hbd3GAL1
Normalized relative Lb. brevis % growth
140
120
100
80
60
40
20
0
2
4
Fermentation days

B.

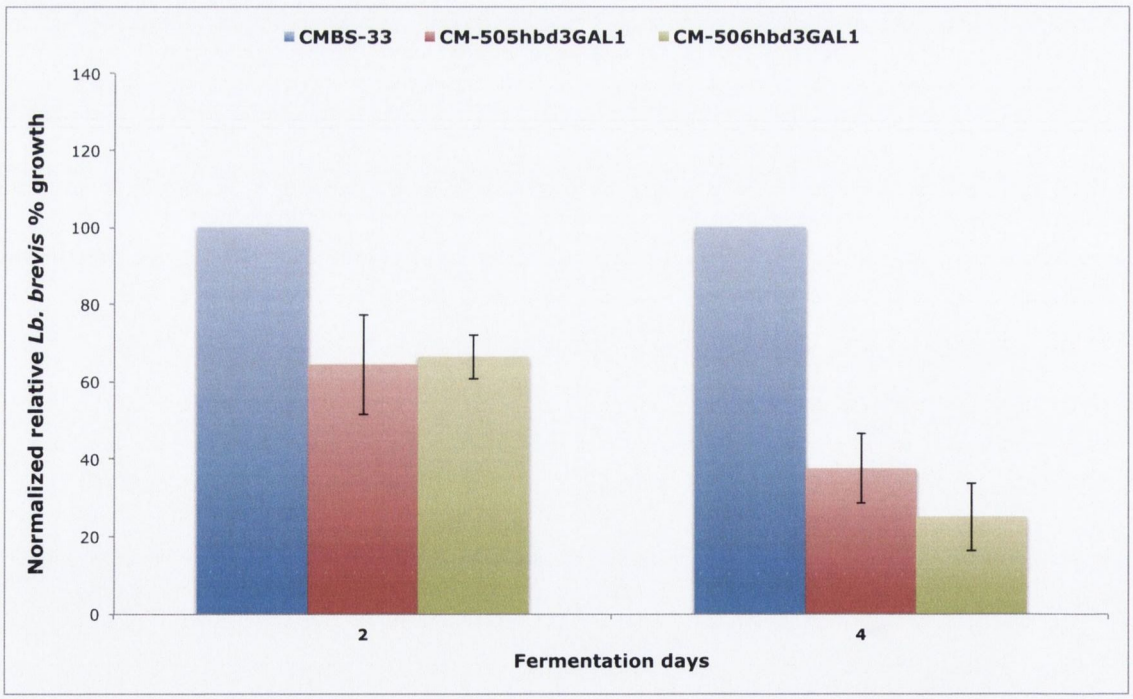
CMBS-33
CM-505hbd3GAL1
CM-506hbd3GAL1
Normalized relative Lb. brevis % growth
140
120
100
80
60
40
20
0
2
4
Fermentation days

red, green and blue columns respectively). Statistical analysis was performed on this data and T-tests revealed p values greater than 0.05 for CM-505hbd3GAL1 and CM-506hbd3GAL1 fermentations on days 2 and 4, thus this increase is not deemed statistically significant.

After freeze-treatment an average decrease of 34-36% was observed for *Lb. brevis* viability in CM-506hbd3GAL1 and CM-505hbd3GAL1 fermentations compared to CMBS-33 fermentations, on day 2 (Fig. 5.6 B, green, red and blue columns respectively). This decrease is deemed significant for CM-506hbd3GAL1 fermentations ($p<0.05$) and insignificant for CM-505hbd3GAL1 fermentations ($p>0.05$). Levels of *Lb. brevis* in CM-505hbd3GAL1 and CM-506hbd3GAL1 fermentations were further reduced by averages of 63 and 75% respectively when compared to viability in CMBS-33 fermentations on day 4, with $p<0.05$ for both CM-505hbd3GAL1 and CM-506hbd3GAL1 fermentations (Fig. 5.6 B, red, green and blue columns respectively). Thus, the decrease in *Lb. brevis* viability observed on day 4 of the fermentations is statistically significant.

This data collectively suggests that freeze-treatment contributes to a reduction in *Lb. brevis* viability in wort fermentations carried out with HβD-3-encoding lager strains compared to fermentations carried out with wild-type CMBS-33 and confirms that secretory recombinant HβD-3 retains antimicrobial activity under fermentation conditions. Overall a higher level of bactericidal activity was found in wort fermentations, compared to YEPGal fermentations in which activity was found on only one occasion.

5.2.3.2 Analysis of recombinant HβD-3 bactericidal activity against Gram-negative bacteria, under various growth conditions

The Gram-negative bacterium, *P. frisingensis*, was inoculated in either wort (16°Bx) or YEPGal at a concentration of 1×10^3 cfu/mL on day 2 of the fermentation. As before, the actual inoculum of *P. frisingensis*, as estimated by viability assays after 2hrs of incubation at 11°C, was lower than expected (Fig. 5.7). This decrease may reflect an initial decrease in viability upon inoculation and incubation at 11°C and is observed in both wort (16°Bx) and YEPGal fermentations (Fig. 5.7). An average 4-fold increase in viable counts is observed in wort (16°Bx) fermentations on day 4 compared to day 2

A.

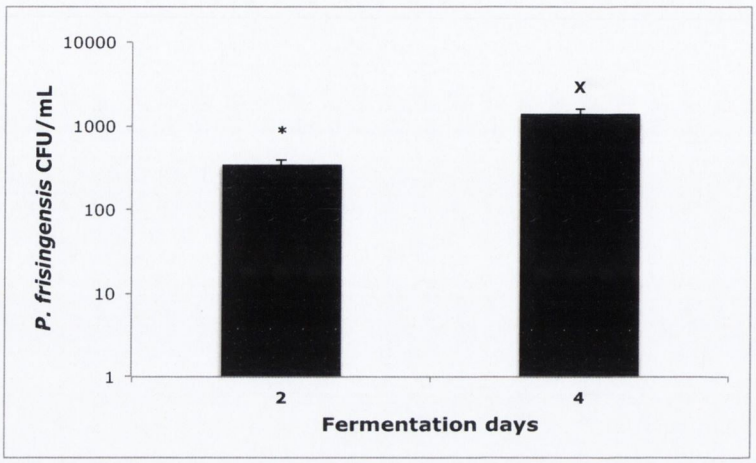

B.

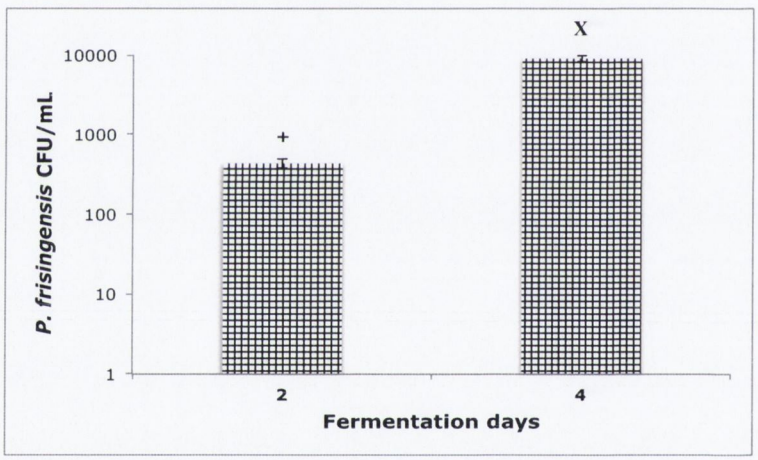

FIG. 5.7 *P. frisingensis* viability in various fermentative conditions

P. frisingensis viability in CMBS-33 fermentations at 11°C. Fermentations were inoculated with 10^3 cfu/mL of *P. frisingensis* on day 2. Bacterial cells were enumerated 2 hrs after the initial seeding (day 2) and 2 days later (day 4). **A)** *P. frisingensis* viability on days 2 and 4 in wort (16°Bx) fermentations. **B)** *P. frisingensis* viability on days 2 and 4 in YEPGal (2%) fermentations. The error bars represent either the standard error from two (*) or three (x) independent experiments, or the standard deviation from a single experiment (+). A minimum of duplicate viable counts were obtained for each experiment.

(Fig. 5.7 A). This increase is considered statistically significant ($p<0.05$). Viability of *P. frisingensis* in YEPGal fermentations increased by approximately 20-fold on day 4 of the fermentations, $p<0.05$ (Fig. 5.7 B). However, it should be noted that data from only a single experiment was available for day 2 analysis of YEPGal fermentations (Fig. 5.7 B).

The viability of *P. frisingensis* before treatment (untreated) and after freeze-treatment (freeze-treated) was examined. In untreated samples the viability of *P. frisingensis* in CM-505hbd3GAL1 and CM-506hbd3GAL1 (YEPGal) fermentations was similar to the viability in CMBS-33 fermentations on days 2 and 4 (Fig. 5.8 A, red, green and blue columns respectively). Statistical analysis revealed p values greater than 0.05 for both CM-505hbd3GAL1 and CM-506hbd3GAL1 fermentations on days 2 and 4.

Following freeze-treatment no decrease in *P. frisingensis* viability was observed in CM-505hbd3GAL1 and CM-506hbd3GAL1 fermentations compared to CMBS-33 viability (Fig. 5.8 B). As before, statistical analysis revealed p values greater than 0.05 for both CM-505hbd3GAL1 and CM-506hbd3GAL1 fermentations on days 2 and 4. However, it should be noted that data from only a single experiment was available for analysis of day 2 viable counts, thus the results should be deemed preliminary.

The viability of *P. frisingensis* in wort (16°Bx) fermentations differed to that observed in YEPGal fermentations. On day 2, an average decrease of 14% in *P. frisingensis* viability was observed in CM-505hbd3GAL1 fermentations compared to CMBS-33 fermentations, however this is deemed insignificant with $p>0.05$ (Fig. 5.9 A, red and blue columns respectively). *P. frisingensis* viability was similar on day 4 in CM-505hbd3GAL1 fermentations compared to CMBS-33 fermentations, $p>0.05$ (Fig. 5.9 A, red and blue columns respectively). Similar viable counts were observed in the CM-506hbd3GAL1 fermentations compared to CMBS-33 fermentations on day 2 and an increase in viable counts was observed on day 4, with $p>0.05$ on both days (Fig. 5.9 A, green and blue columns respectively).

Upon freeze-treatment, statistically significant decreases ($p<0.05$) were observed for *P. frisingensis* viability in CM-505hbd3GAL1 and CM-506hbd3GAL1 fermentations compared to CMBS-33 fermentations on days 2 and 4 (Fig. 5.9 B, red, green and blue columns respectively). An average decrease of 32% was observed for *P. frisingensis*

FIG. 5.8 Antimicrobial activity of recombinant HβD-3 against *P. frisingensis* in YEPGal fermentations

P. frisingensis viability in YEPGal fermentations at 11°C. Fermentations were seeded with 10^3 cfu/mL of *P. frisingensis* on day 2. Bacterial cells were enumerated 2 hrs after the initial seeding (day 2) and 2 days later (day 4). Bacterial counts for each culture were normalized relative to CMBS-33 which was set at 100% viability. CMBS-33: blue columns. CM-505hbd3GAL1: red columns. CM-506hbd3GAL1: green columns. **A)** *P. frisingensis* viability before freeze-treatment. **B)** *P. frisingensis* viability after freeze-treatment. The error bars represent either the standard error from three (x) independent experiments or the standard deviation from a single experiment (+). A minimum of duplicate viable counts were obtained for each experiment.

A.

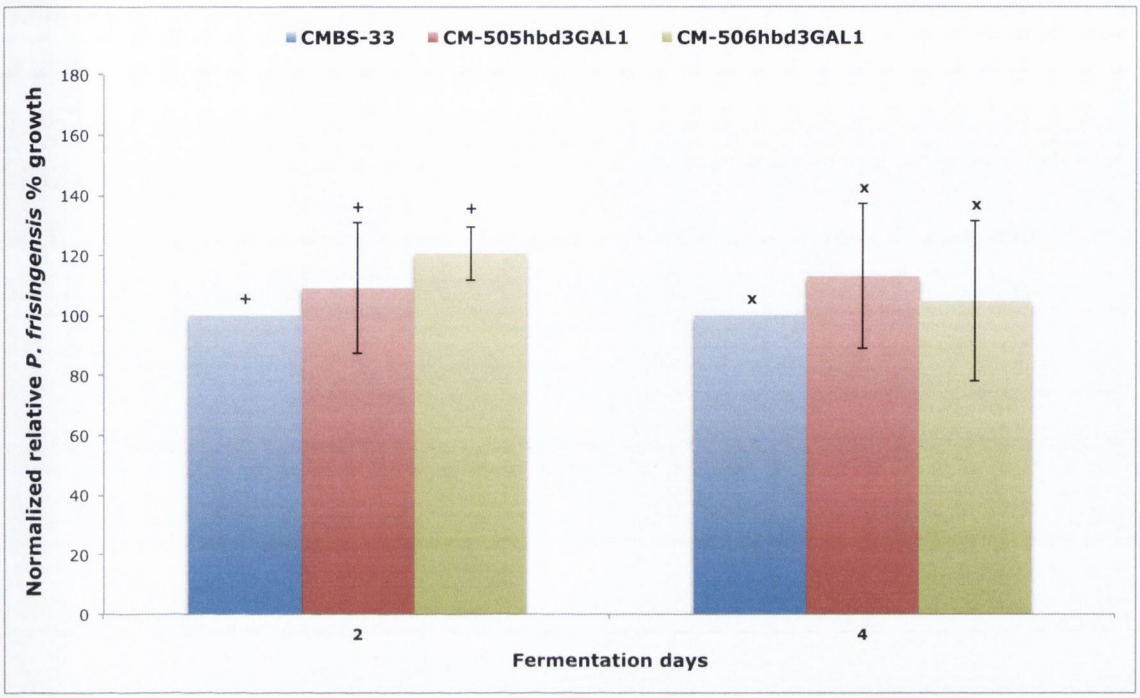
CMBS-33
CM-505hbd3GAL1
CM-506hbd3GAL1
Normalized relative P. frisingensis % growth
180
160
140
120
100
80
60
40
20
0
+
+
+
x
x
x
2
4
Fermentation days

B.

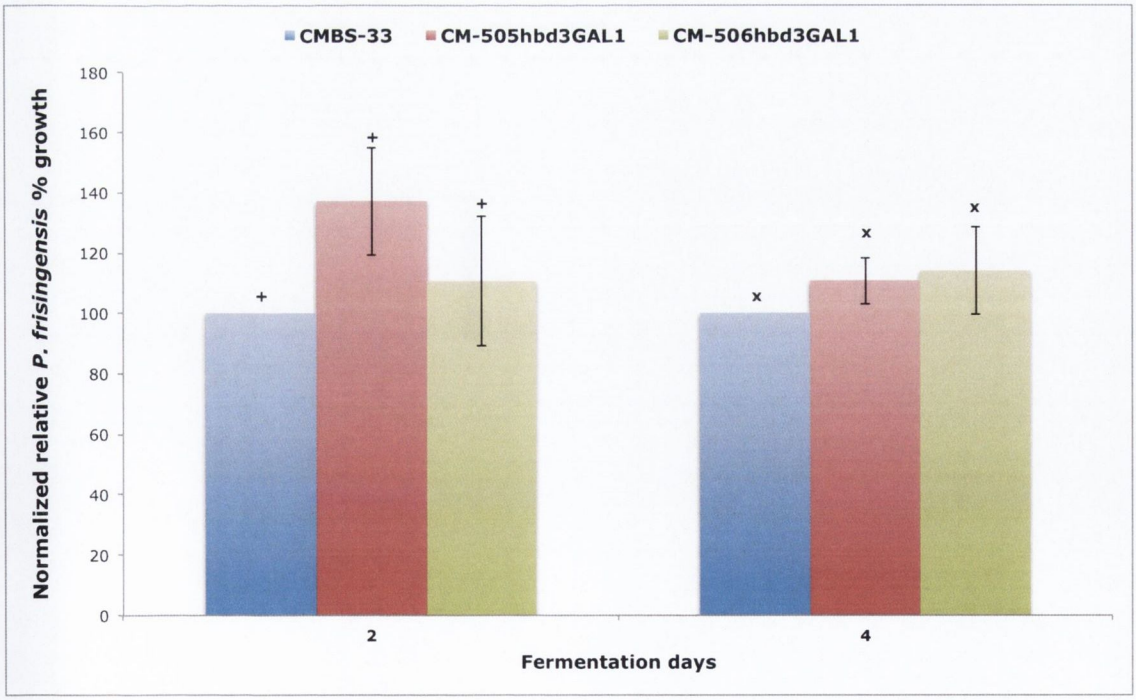
CMBS-33
CM-505hbd3GAL1
CM-506hbd3GAL1
Normalized relative P. frisingensis % growth
180
160
140
120
100
80
60
40
20
0
+
+
+
x
x
x
2
4
Fermentation days

FIG. 5.9 Antimicrobial activity of recombinant HβD-3 against *P. frisingensis* in wort fermentations

P. frisingensis viability in wort (16°Bx) fermentations at 11°C. Fermentations were seeded with 10^3 cfu/mL of *P. frisingensis* on day 2. Bacterial cells were enumerated 2 hrs after the initial seeding (day 2) and 2 days later (day 4). Bacterial counts for each culture were normalized relative to CMBS-33 which was set at 100% viability. CMBS-33: blue columns. CM-505hbd3GAL1: red columns. CM-506hbd3GAL1: green columns. **A)** *P. frisingensis* viability before freeze-treatment. **B)** *P. frisingensis* viability after freeze-treatment. The error bars represent either the standard error from two (*), three (x) or four (#) independent experiments. A minimum of duplicate viable counts were obtained for each experiment.

A.

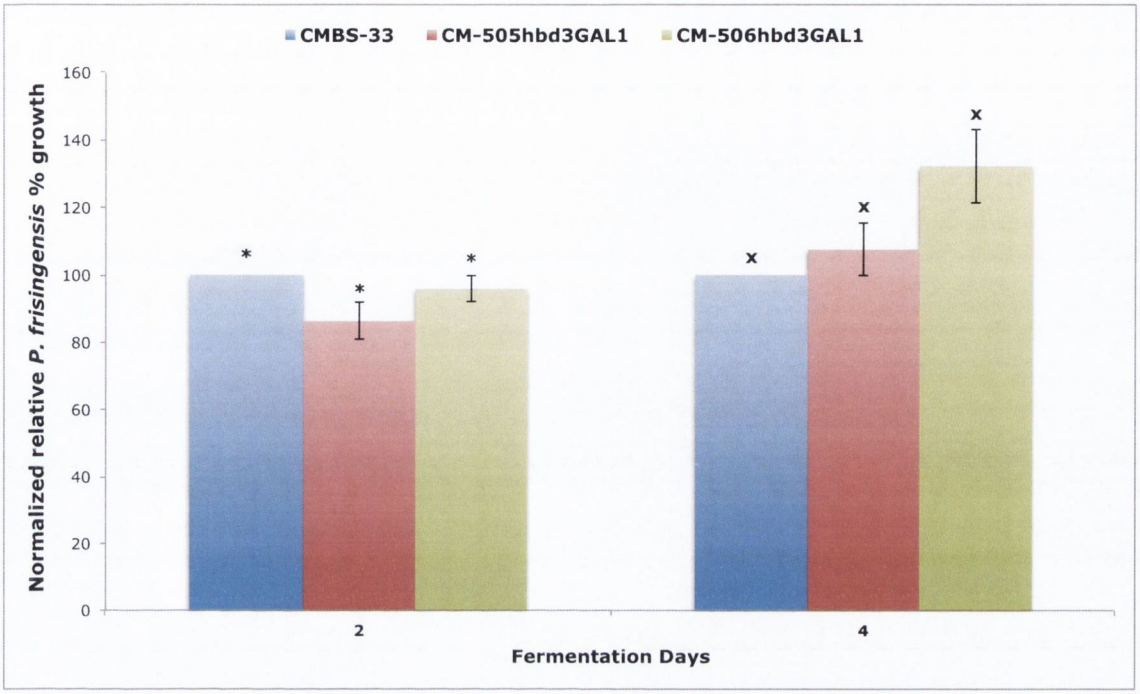
CMBS-33
CM-505hbd3GAL1
CM-506hbd3GAL1
Normalized relative P. frisingensis % growth
160
140
120
100
80
60
40
20
0
*
*
*
x
x
x
2
4
Fermentation Days

B.

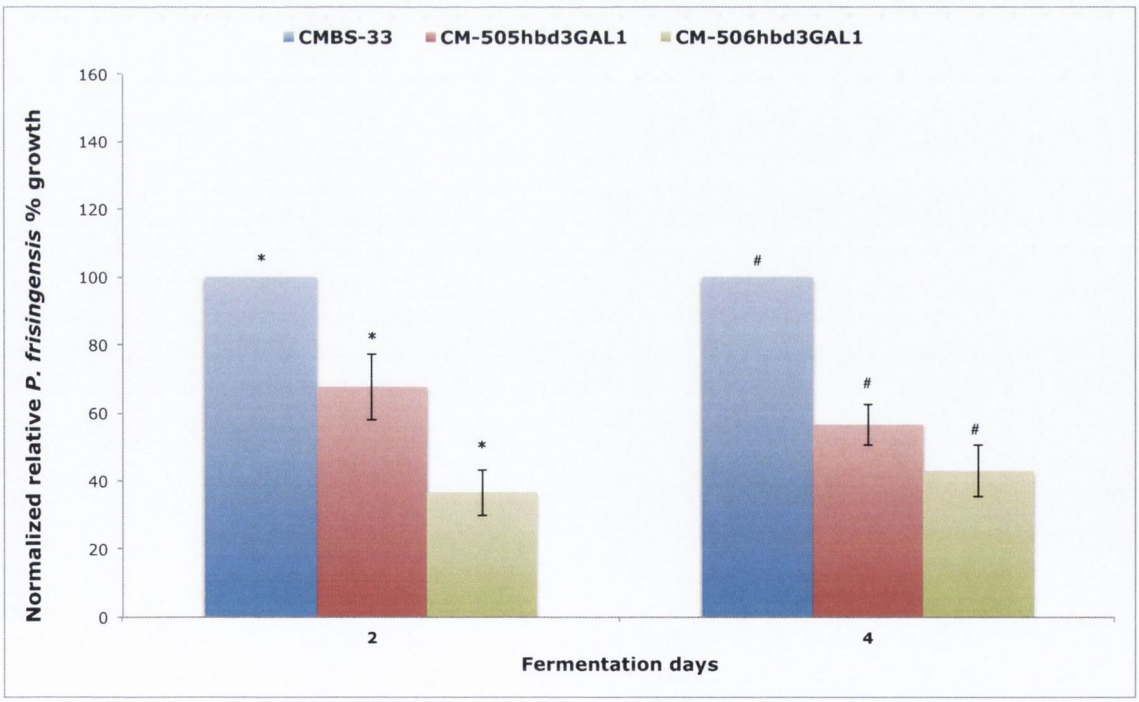
CMBS-33
CM-505hbd3GAL1
CM-506hbd3GAL1
Normalized relative P. frisingensis % growth
160
140
120
100
80
60
40
20
0
*
*
*
#
#
#
2
4
Fermentation days

viability in CM-505hbd3GAL1 fermentations compared to CMBS-33 fermentations on day 2 (Fig. 5.9 B, red and blue columns respectively). The viability of *P. frisingensis* in CM-505hbd3GAL1 fermentations decreased further by an average of 43% on day 4 (Fig. 5.9 B, red column). Furthermore, *P. frisingensis* viability in CM-506hbd3GAL1 fermentations decreased by averages of 63% and 57% on days 2 and 4 compared to CMBS-33 (Fig. 5.9 B, green and blue columns respectively). The above data suggests that freeze-treatment significantly contributes to a reduction in *P. frisingensis* viability in wort fermentations encoding HβD-3. However, in YEPGal fermentations, freeze-treament does not contribute to antimicrobial activity.

As mentioned in section 5.2.3.1, recombinant HβD-3 appears to retain antimicrobial activity in a fermentation, with *Lb. brevis* becoming more susceptible to the peptide after a freeze-thaw cycle. The results obtained for *P. frisingensis* are in agreement with this hypothesis. Overall higher bactericidal effects are seen in wort fermentations, compared to YEPGal fermentations.

5.2.4 Comparison of the antimicrobial activity of recombinant HβD-3, in vivo, expressed from various promoters and under varying fermentation temperatures

Thus far, secretory recombinant HβD-3 under the control of a *GAL1* promoter has been shown to display bactericidal activity towards various BSMs in a fermentation. Galactose is not normally present in wort thus yeast strains have been generated to encode HβD-3 under the control of a variety of inducible and constitutive promoters (chapter 3). The *in vivo* antimicrobial activity of HβD-3 was examined in numerous recombinant strains, namely the strains CM-505hbd3TEF1, CM-506hbd3AGT1, CM-506hbd3PGK1, CM-pRShbd3PGK1, CM-INT-37 and CM-INT-51. To further determine the ideal fermentative environment to achieve maximum levels of antimicrobial activity, fermentations were carried out at 11°C or 20°C.

HβD-3 encoding yeast strains and CMBS-33 were cultured in YEPD overnight at 30°C. Hygromycin and G418 antibiotics were added where appropriate. Yeast cells were centrifuged and washed twice in SDW to remove all traces of antibiotics. Cells were inoculated at 1.5 x 10^7 cfu/mL into microbrews (12mL) of brewer's wort (12°Bx) and incubated at either 11°C or 20°C (section 2.17). *Lb. brevis* at 10^3 cfu/mL was added to each fermentation on day 0 (section 2.24.2). The progress of the fermentation was followed by measuring the decrease in degrees Brix values of the wort (section 2.17). Samples were taken on days 1, 3, 5 and 7 for 11°C fermentations and days 1, 3, 5, 7 and 8 for 20°C fermentations. Bacterial counts were obtained following plating on MRS plates, with cycloheximide at 80μg/ml (untreated sample) (section 2.24.2). An aliquot of each sample was also subjected to a freeze-thaw cycle as described in section 5.2.3.

All data was normalized relative to 100% growth/viability in CMBS-33 fermentations.

5.2.4.1 *In vivo* antimicrobial activity of recombinant HβD-3 expressed from different promoters at a fermentation temperature of 11°C

As expected, brix values decreased as the fermentation progressed (Fig. 5.10 A). Fermentations attenuated on day 7 at 6°Bx, with the exception of CM-INT-37 (Fig. 5.10 A), which attenuated at 10.6°Bx (Fig. 5.10 A, green line). The % alcohol produced for each fermentation was determined as described in section 2.17. The concentration of alcohol on day 7 was approximately 3.2% for each fermentation with the exception of CM-INT-37 (Fig. 5.10 B). The final alcohol concentration in the CM-INT-37

FIG. 5.10 Brix values and percentage alcohol for fermentations at 11°C

Degrees Brix and percentage alcohol levels were measured throughout fermentations. CMBS-33: dark blue. CM-505hbd3TEF1: red. CM-INT-37: green. CM-INT-51: purple. CM-506hbd3AGT1: turquoise. CM-506hbd3PGK1: orange. CM-pRShbd3PGK1: light blue. CM-pRS42H: pink. **A)** Degrees brix values. **B)** Percentage alcohol levels. The error bars represent either the standard error from two (*) independent experiments or the standard deviation from a single experiment (+). A minimum of duplicate values were obtained for each experiment.

Note: Only single values for CM-pRShbd3PGK1 and CM-pRS42H fermentations on days 0, 1, 2 and 7.

A.

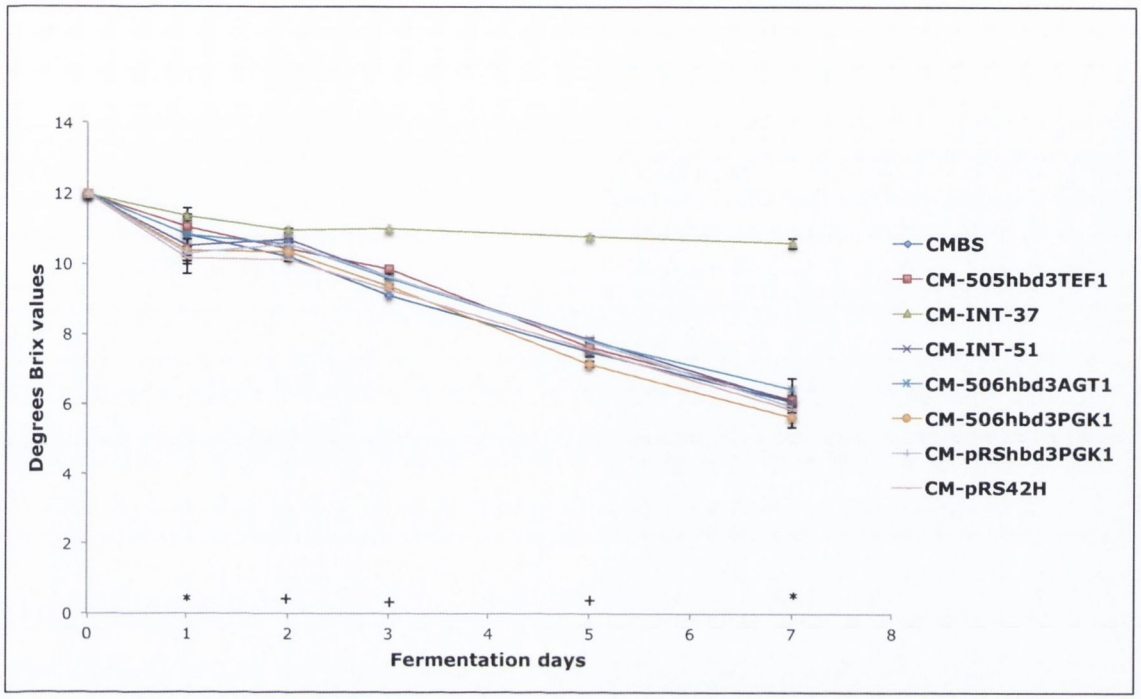
Degrees Brix values
Fermentation days
CMBS
CM-505hbd3TEF1
CM-INT-37
CM-INT-51
CM-506hbd3AGT1
CM-506hbd3PGK1
CM-pRShbd3PGK1
CM-pRS42H

B.

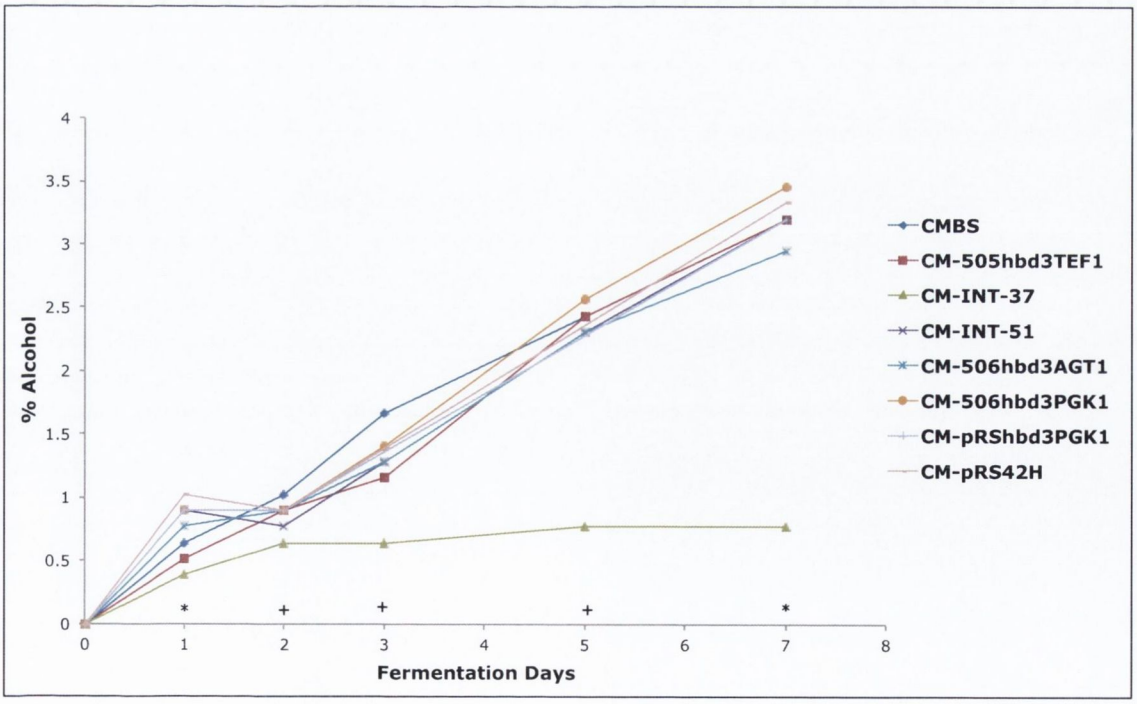
% Alcohol
Fermentation Days
CMBS
CM-505hbd3TEF1
CM-INT-37
CM-INT-51
CM-506hbd3AGT1
CM-506hbd3PGK1
CM-pRShbd3PGK1
CM-pRS42H

fermentation was 0.77% (Fig. 5.10 B, green line).

Antimicrobial activity was analysed before freeze-treatment. As observed in Fig. 5.4, an increase in bacterial growth was observed as the fermentations progressed at 11°C (data not shown). The viability of *Lb. brevis* in CM-505hbd3TEF1 and CM-INT-51 fermentations was similar to that observed in CMBS-33 fermentations, on days 1 and 3 (Fig. 5. 11 A, red, green and blue columns respectively). Statistical analysis revealed p values greater than 0.05 on day 1 for both CM-505hbd3TEF1 and CM-INT-51 fermentations, whereas on day 3 $p<0.05$ for one independent CM-505hbd3TEF1 fermentation, while $p<0.05$ for two independent CM-INT-51 fermentations. A 3.4 – 4-fold increase in *Lb. brevis* viability was observed on days 5 and 7 respectively, in CM-505hbd3TEF1 fermentations compared to CMBS-33 fermentations (Fig. 5.11 A, red and blue columns respectively). Statistical analysis performed on this data indicates that this increase is statistically significant, $p<0.05$ for all CM-505hbd3TEF1 fermentations on days 5 and 7. Since only one experimental data set was available for the day 5 sample, this result should be deemed preliminary. A 34% decrease in *Lb. brevis* viability was observed in the CM-INT-51 fermentation compared to CMBS-33 on day 5, however this decrease is not deemed significant, $p>0.05$ (Fig. 5.11, green and blue columns respectivley). As before, since only one experimental data set was available for the day 5 sample, this result should be deemed preliminary. An increase in *Lb. brevis* viability is observed in CM-INT-51 fermentations on day 7 (Fig. 5.11 A, red column), however as evident in Fig. 5.11 A, the standard error for these duplicate fermentations was extremely high. T-test analysis revealed a p value greater than 0.05 for one independent experiment.

Upon freeze-treatment an average decrease of 82% was observed for *Lb. brevis* viability on day 1 in CM-505hbd3TEF1 fermentations compared to CMBS-33 fermentations, $p<0.05$ for two independent fermentations (Fig. 5.11 B, red and blue columns respectively). No further significant killing of *Lb. brevis* was observed in the CM-505hbd3TEF1 fermentations as bacterial growth increased as the fermentation progressed. On day 3 similar viability is observed in CMBS-33 and CM-505hbd3TEF1 fermentations, $p>0.05$. A 1.5 - 2.6-fold increase was observed in *Lb. brevis* viability in CM-505hbd3TEF1 fermentations compared to CMBS-33 fermentations on days 5 and 7 (Fig. 5.11 B, red and blue columns respectively). The data obtained for both of these samples was only available for one individual experiment, however statistical analysis

FIG. 5.11 Antimicrobial activity of recombinant HβD-3 in fermentations at 11°C

Lb. brevis viability in wort (12°Bx) fermentations at 11°C. Fermentations were seeded with at 10^3 cfu/mL of *Lb. brevis* on day 0. Bacterial cells were enumerated on days 1, 3, 5 and 7. Bacterial counts for each culture were normalized relative to CMBS-33 which was set at 100% viability. CMBS-33: blue colums. CM-505hbd3TEF1: red columns. CM-INT-51: green columns. **A)** *Lb. brevis* viability before freeze-treatment. **B)** *Lb. brevis* viability after freeze-treatment. The error bars represent either the standard error from two (*) or three (x) independent experiments or the standard deviation from a single experiment (+). A minimum of duplicate viable counts were obtained for each experiment.

A.

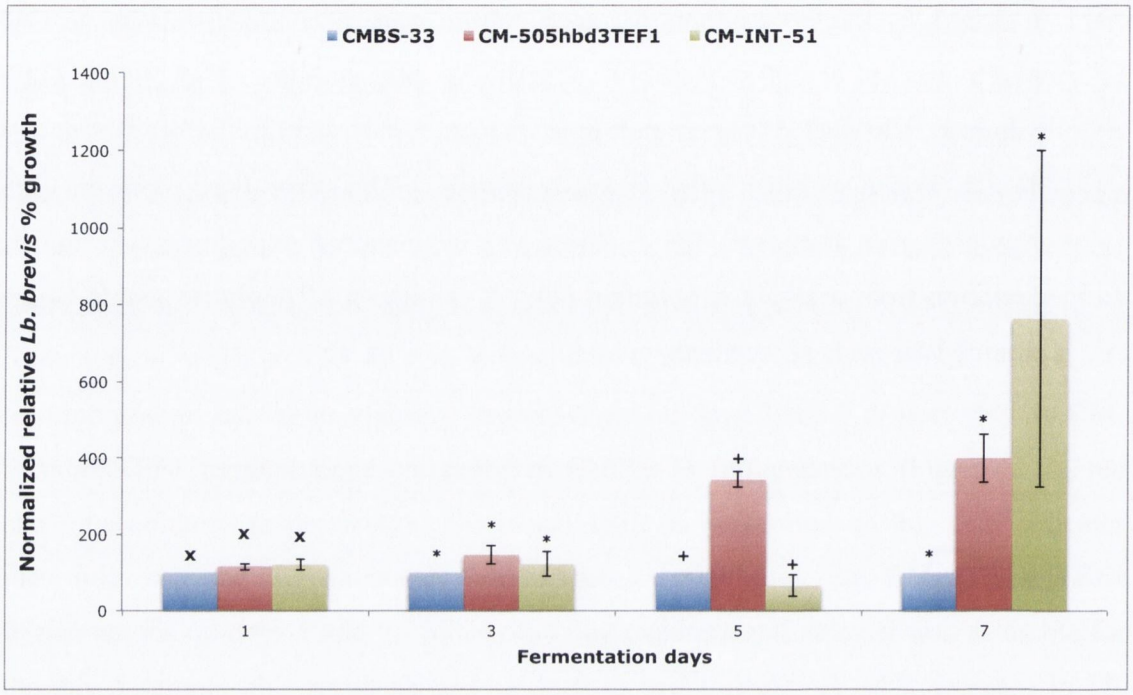
CMBS-33
CM-505hbd3TEF1
CM-INT-51
Normalized relative Lb. brevis % growth
1400
1200
1000
800
600
400
200
0
1
3
5
7
Fermentation days

B.

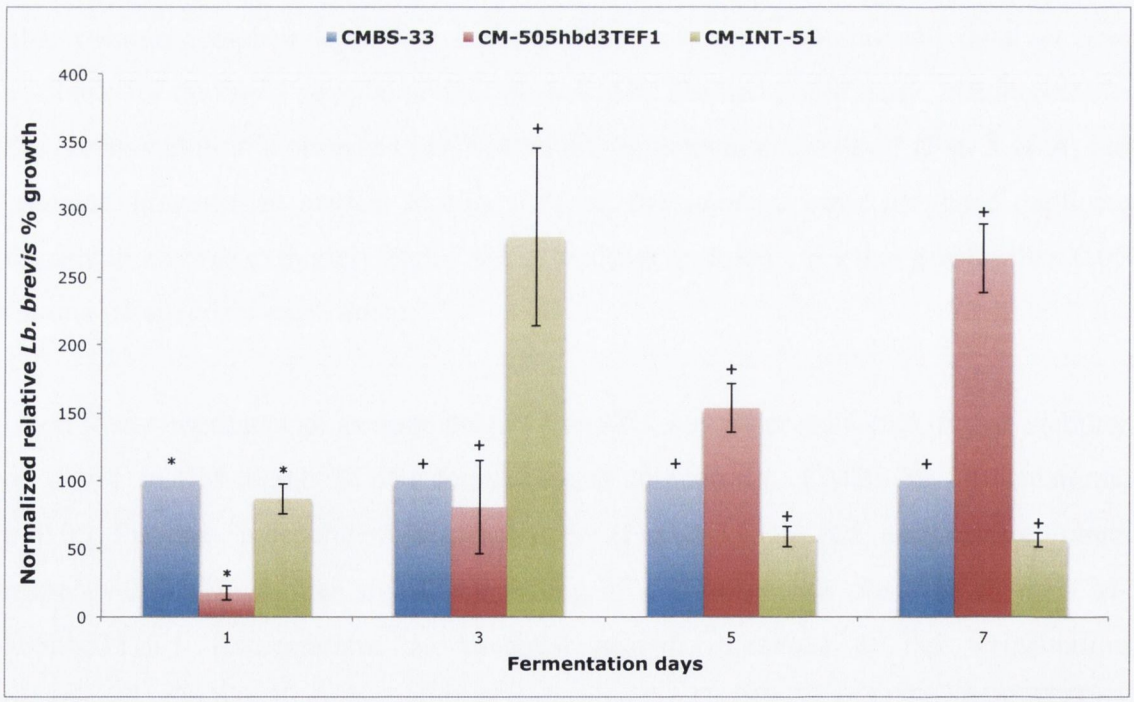
CMBS-33
CM-505hbd3TEF1
CM-INT-51
Normalized relative Lb. brevis % growth
400
350
300
250
200
150
100
50
0
1
3
5
7
Fermentation days

resulted in p values below 0.05 for days 5 and 7, thus this increase in *Lb. brevis* viability is deemed significant. An average 13% decrease in *Lb. brevis* viability was observed in CM-INT-51 fermentations compared to CMBS-33 fermentations on day 1, however $p>0.05$ for two independent fermentations thus this decrease is not deemed significant (Fig. 5.11 B, green and blue columns respectively). On day 3 a 2.8-fold increase was observed in CM-INT-51 fermentations compared to CMBS-33 fermentations, $p<0.05$ (Fig. 5.11 B, green and blue columns respectively). However, only one experimental data set was available for this time point and the error between the duplicate viable counts is high, thus this result is deemed preliminary. A further decrease in viable counts (41 – 43%) were observed for *Lb. brevis* viability in CM-INT-51 fermentations compared to CMBS-33 fermentations on days 5 and 7 respectively, $p<0.05$ for days 5 and 7 (Fig. 5.11 B, green and blue columns respectively). As for day 3, only a single independent data set was available for days 5 and 7, thus further experimentation is needed to verify this data.

Fermentations were also carried out for CM-INT-37, CM-506hbd3AGT1, CM-506hbd3PGK1, CM-pRShbd3PGK1 and CM-pRS42H. As shown in Fig. 5.10, CM-INT-37 does not ferment efficiently, compared to all other lager strains in this study, and produces very low levels of alcohol. Thus, an environment consisting of rich medium and a low alcohol percentage, provides a superior habitat for *Lb. brevis* growth. *Lb. brevis* growth in CM-INT-37 compared to CMBS-33, was 1.6 fold higher on day 1, increasing to 130-fold higher on day 7 (data not shown). This high increase in *Lb. brevis* growth was also observed in CM-506hbd3AGT1 and CM-506hbd3PGK1 fermentations compared to CMBS-33 fermentations (data not shown). Furthermore, within 3 independent experiments, no significant antimicrobial activity was observed in CM-pRShbd3PGK1 or CM-pRS fermentations compared to CMBS-33 fermentations (data not shown).

5.2.4.2 *In vivo* antimicrobial activity of recombinant HβD-3 expressed from different promoters at a fermentation temperature of 20°C

Traditionally, lager yeast fermentations are performed at temperatures of 7 - 11°C. The data gathered thus far suggests that recombinant HβD-3 produced from CM-INT-51 can exert antimicrobial activity against *Lb. brevis* immediately after seeding and for several days thereafter when fermentations are carried out at this low temperature, but for maximum effectiveness, a freeze-thaw cycle is required. Recombinant HβD-3 produced from CM-505hbd3TEF1 was less effective at this low temperature. While lager yeast fermentations are often carried out at temperatures between 7 - 14°C, other fermentations such as those used for the production of ales, spirits and non-potable alcohol are carried out at temperatures between 20 - 37°C, thus the antimicrobial activity of recombinant HβD-3 was examined in fermentations carried out at 20°C.

As described in section 5.4.2, CMBS-33, CM-505hbd3TEF1 and CM-INT-51 were inoculated into wort (12°Bx) at 1.5 x 10^7 cfu/mL and *Lb. brevis* was added to each fermentation at 10^3 cfu/mL on day 0 (section 2.24.2). As expected, Brix values decreased as the fermentation progressed (Fig. 5.12 A). Fermentations attenuated on day 8 at 5.5°Bx, with the exception of CM-INT-37 (Fig. 5.12 A), which attenuated at 10.45°Bx (Fig. 5.12 A, green line). The % alcohol produced for each fermentation was determined as described in section 2.17. The concentration of alcohol was approximately 3.36% on day 8 for each fermentation with the exception of CM-INT-37 (Fig. 5.12 B). The final alcohol concentration in the CM-INT-37 fermentation was 0.77% (Fig. 5.12 B, green line).

Antimicrobial activity was analysed before freeze-treatment. As observed in Fig. 5.4, an increase in bacterial growth was observed as the fermentations progressed at 20°C (data not shown). As the fermentations progressed and alcohol levels increased, the viable counts of *Lb. brevis* in CM-505hbd3TEF1 fermentations decreased compared to CMBS-33 fermentations (Fig. 5.13 A, red and blue columns respectively). On day 1, viable counts for CM-505hbd3TEF1 were similar to CMBS-33, whereas on days 3, 5 and 7, the viable counts decreased by an average of 65%, 67% and 85% respectively (Fig. 5.13 A, red columns). Statistical analysis revealed p values below 0.05 for two independent fermentations on day 1, while $p<0.05$ for all fermentations on days 3, 5 and

FIG. 5.12 Brix values and percentage alcohol for fermentations at 20°C

Degrees Brix and percentage alcohol levels were measured throughout fermentations. CMBS-33: dark blue. CM-505hbd3TEF1: red. CM-INT-37: green. CM-INT-51: purple. CM-506hbd3AGT1: turquoise. CM-506hbd3PGK1: orange. CM-pRShbd3PGK1: light blue. CM-pRS42H: pink. **A)** Degrees brix values. **B)** Percentage alcohol levels. The error bars represent either the standard error from two (*) independent experiments or the standard deviation from a single experiment (+). A minimum of duplicate values were taken for each experiment.

A.

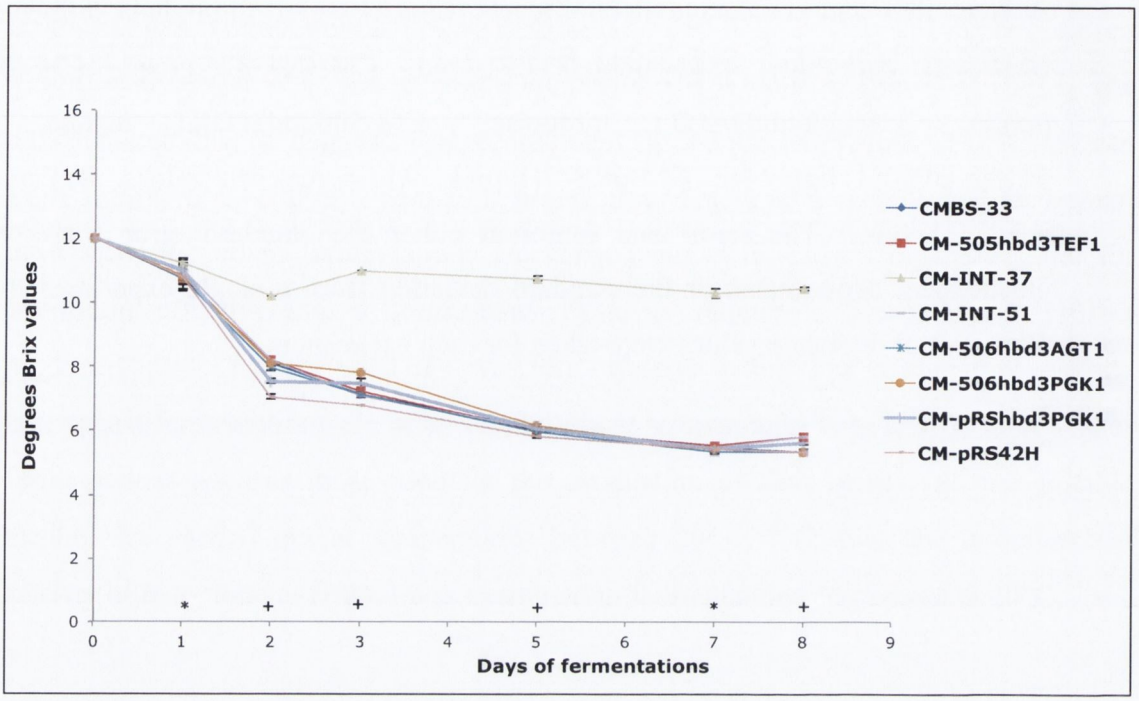
Degrees Brix values
16
14
12
10
8
6
4
2
0
0 1 2 3 4 5 6 7 8 9
Days of fermentations
CMBS-33
CM-505hbd3TEF1
CM-INT-37
CM-INT-51
CM-506hbd3AGT1
CM-506hbd3PGK1
CM-pRShbd3PGK1
CM-pRS42H

B.

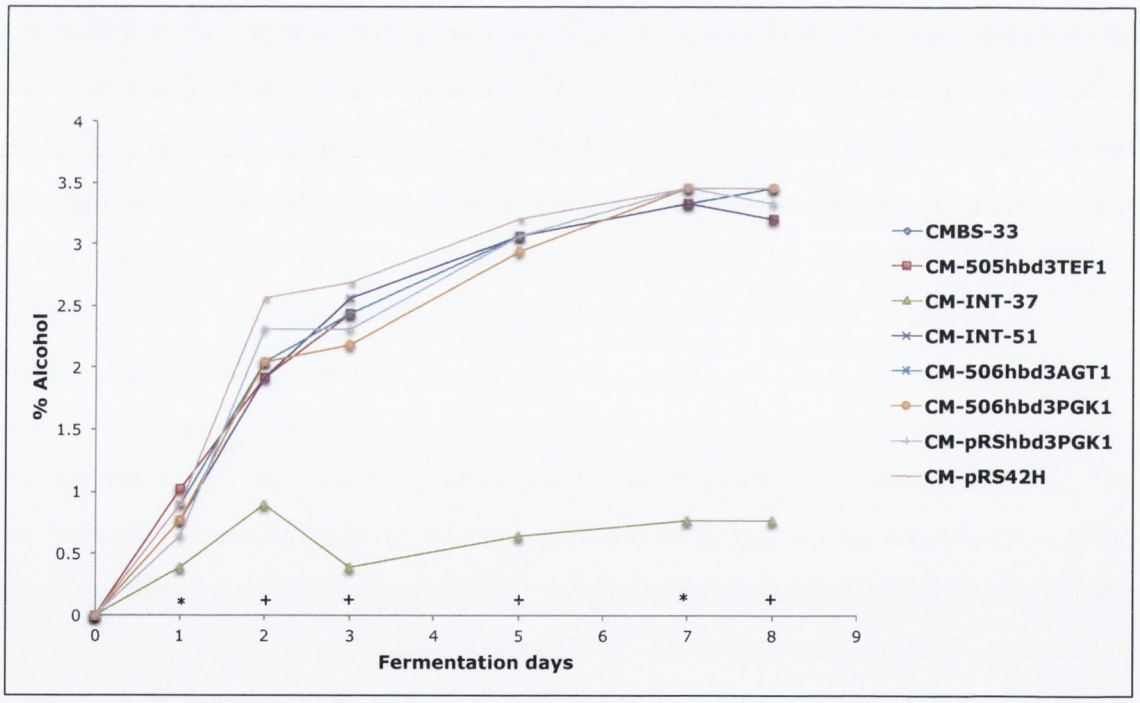
% Alcohol
4
3.5
3
2.5
2
1.5
1
0.5
0
0 1 2 3 4 5 6 7 8 9
Fermentation days
CMBS-33
CM-505hbd3TEF1
CM-INT-37
CM-INT-51
CM-506hbd3AGT1
CM-506hbd3PGK1
CM-pRShbd3PGK1
CM-pRS42H

FIG. 5.13 Antimicrobial activity of recombinant HβD-3 in fermentations at 20°C

Lb. brevis viability in wort (12°Bx) fermentations at 20°C. Fermentations were seeded with at 10^3 cfu/mL of *Lb. brevis* on day 0. Bacterial cells were enumerated on days 1, 3, 5, 7 and 8. Bacterial counts for each culture were normalized relative to CMBS-33 which was set at 100% viability. CMBS-33: blue colums. CM-505hbd3TEF1: red columns. CM-INT-51: green columns. **A)** *Lb. brevis* viability before freeze-treatment. **B)** *Lb. brevis* viability after freeze-treatment. The error bars represent either the standard error from two (*) or three (x) independent experiments or the standard deviation from a single experiment (+). A minimum of duplicate viable counts were taken for each experiment.

Note: there is no CM-505hbd3TEF1 untreated sample for day 8.

A.

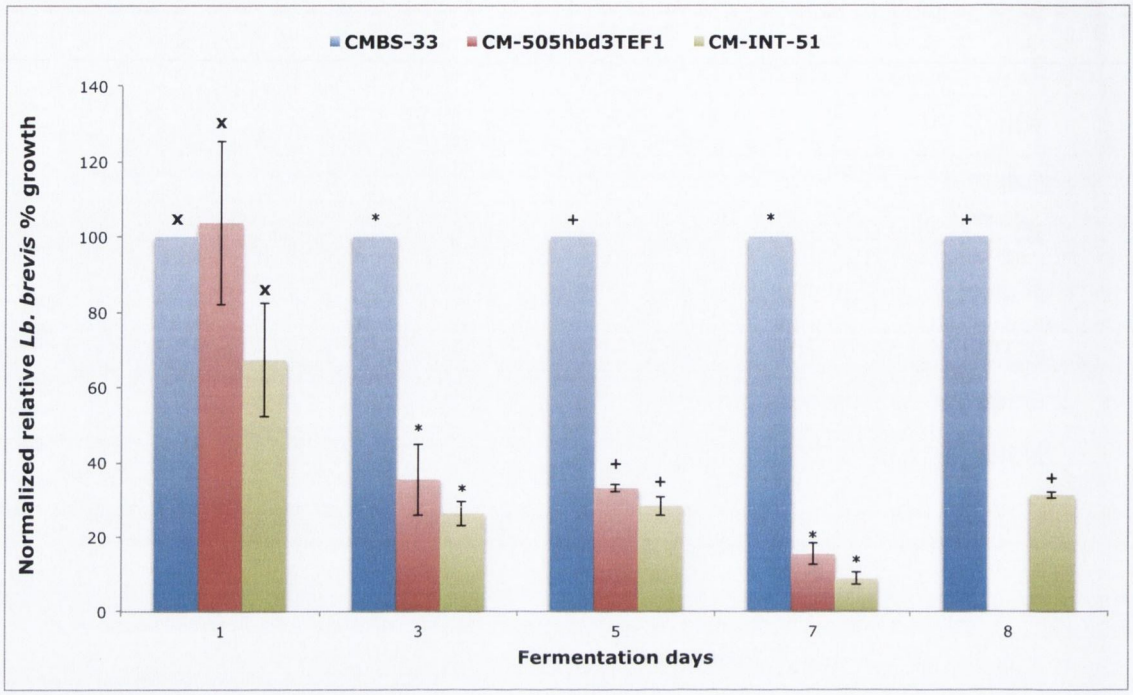
CMBS-33
CM-505hbd3TEF1
CM-INT-51
Normalized relative Lb. brevis % growth
140
120
100
80
60
40
20
0
1
3
5
7
8
Fermentation days

B.

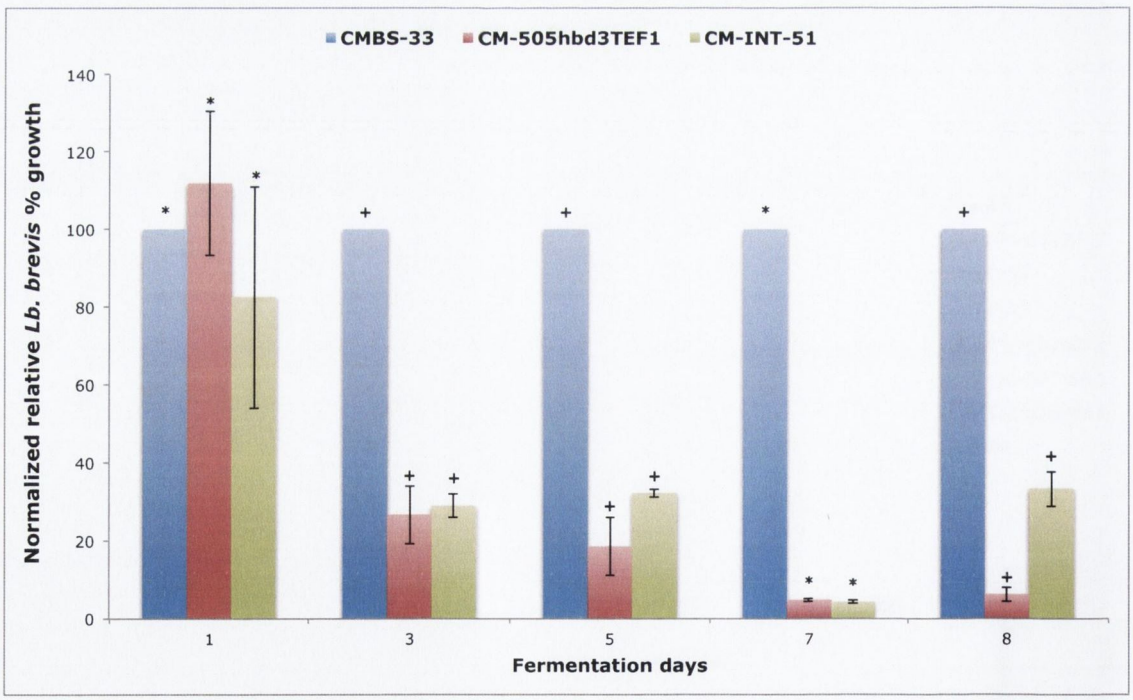
CMBS-33
CM-505hbd3TEF1
CM-INT-51
Normalized relative Lb. brevis % growth
140
120
100
80
60
40
20
0
1
3
5
7
8
Fermentation days

7. With the exception of day 5 in which data from a single experiment was available, the decrease in viability is reproduced in two independent experiments. Thus, the increase in killing of *Lb. brevis* observed throughout the CM-505hbd3TEF1 fermentations is deemed statistically significant. A similar trend is observed for CM-INT-51 fermentations. On days 1, 3 and 7 an average decrease of 33, 74 and 91% for *Lb. brevis* viability is observed in CM-INT-51 fermentations compared to CMBS-33 fermentations, $p<0.05$ for all fermentations with the exception of one independent fermentation on day 1 (Fig. 5.13 A, green and blue columns respectively). On days 5 and 8, single data sets were obtained and a decrease in *Lb. brevis* viability of 72% and 69% respectively, was observed. P values less than 0.05 for days 5 and 8 indicate that the decrease in *Lb. brevis* viability observed in CM-INT-51 fermentations compared to CMBS-33 fermentations is statistically significant.

Upon freeze-treament, slightly higher antimicrobial activity is observed for both CM-505hbd3TEF1 and CM-INT-51 fermentations, thus as observed in other experiments freeze-treatment did improve the antimicrobial activity. On day 1, no significant decrease in *Lb. brevis* viability was observed in CM-505hbd3TEF1 and CM-INT-51 fermentations compared to CMBS-33 fermentations, $p>0.05$ for CM-505hbd3TEF1 fermentations and $p>0.05$ for one independent CM-INT-51 fermentation (Fig. 5.13 B, red, green and blue columns respectively). On days 3, 5, 7 and 8, a decrease of 73, 81, 95 and 94% is observed in *Lb. brevis* viability in CM-505hbd3TEF1 fermentations compared to CMBS-33 fermentations (Fig. 5.13 B, red and blue columns respectively). This consistant decrease in *Lb. brevis* viability is statistically significant with $p<0.05$ for all CM-505hbd3TEF1 fermentations on days 3, 5, 7 and 8. Furthermore, a decrease of 71, 68, 96 and 67% in *Lb. brevis* viability is observed in CM-INT-51 fermentations on days 3, 5, 7 and 8 respectively (Fig. 5.13 B, green and blue columns respectively). The decrease in *Lb. brevis* viability is statistically significant, $p<0.05$ for all CM-INT-51 fermentations on days 3, 5, 7 and 8. As shown in Fig. 5.13 B, only one data set is available for day 8, thus further experimentation is needed to verify these results.

Fermentations at 20°C were also carried out for CM-INT-37, CM-506hbd3AGT1, CM-506hbd3PGK1, CM-pRShbd3PGK1 and CM-pRS42H. CM-INT-37 shows the same fermention pattern at 11°C and 20°C, whereby fermentation efficiency is extremely low, compared to all other lager strains (Fig. 5.12 A & B). On day 1, *Lb. brevis* growth in CM-INT-37 was at least 2 fold higher than that observed in CMBS-33 (data not

shown). Colony counts were unobtainable on days 3 and 7, as *Lb. brevis* growth was so high (data not shown). This high increase in *Lb. brevis* growth was also observed in CM-506hbd3AGT1 and CM-506hbd3PGK1 fermentations compared to CMBS-33 fermentations (data not shown). Preliminary results indicate that CM-pRShbd3PGK1 displays antimicrobial activity compared to CMBS-33 fermentations carried out at 20°C (data not shown). However these results are preliminary and further experimentation is needed to verify these results.

5.3 Discussion

Synthetic HβD-3 has been shown to have a wide variety of antimicrobial activities against many pathogens (Harder et al., 2001; Hoover et al., 2003; Shelburne et al., 2005; Starner et al., 2005; Wu et al., 2003). Previous results from Dr. Bond's laboratory have demonstrated that HβD-3 at concentrations as high as 50 - 100μg/mL does not inhibit the growth of lager yeasts when pitched at cell densities of 1.5 x 10^7 cfu/mL (Usher, James, Kavanagh and Bond, unpublished). Thus the expression of HβD-3 in yeast strains should not affect the ability of these yeasts to ferment sugars to alcohol. Comparison of fermentations carried out with CMBS-33 wild-type and HβD-3-encoding yeast strains have indicated that the presence of recombinant HβD-3 does not affect the fermentation process (Fig. 5.10 and 5.12).

In this chapter, the antimicrobial activity of both synthetic and recombinant HβD-3 against both Gram-positive and Gram-negative beer spoiling bacteria was examined. Two different approaches were tested. Firstly, *in vitro* bioassays were used to examine the antimicrobial activity of HβD-3 secreted from cells grown in SC-Gal. The supernatants were concentrated using C18 Sep-pak columns, which are highly hydrophobic. As HβD-3 contains hydrophobic regions the peptide binds efficiently to C18 columns. On the other hand G418 is a hydrophilic compound and should not bind to the C18 column, removing G418 from the concentrated supernatant. Concentrated supernatant of CM-505hbd3GAL1 and CM-506hbd3GAL1 displayed antimicrobial activity against *Lb. brevis*. An average reduction of 33% in viable counts was observed in CM-505hbd3GAL1 (7.5X), while an average 8% reduction was observed in CM-506hbd3GAL1 (5X). The decrease in viable counts for CM-505hbd3GAL1 was statistically significant in both experiments, while the reduced effect in CM-506hbd3GAL1 was only statistically significant for one experiment. However, in both experiments, the antimicrobial activity of CM-506hbd3GAL1 was less than that observed for CM-505hbd3GAL1. Further experimentation is necessary to verify whether levels of HβD-3 activity observed in CM-506hbd3GAL1 supernatants are reproducible. Previous quantitation of HβD-3 in concentrated supernatant samples of CM-505hbd3GAL1 by ELISA (section 4.2.3.1), indicated that recombinant HβD-3 is secreted into the supernatant at concentrations up to 0.06 μg/mL. The *in vitro* bioassays carried out in this chapter (section 5.2.2) indicate that CM-505hbd3GAL1 secretes active HβD-3 into the supernatant at approximately 0.06 μg/mL, thus these results are

in agreement. RP-HPLC fractionation of the supernatants and subsequent ELISA analysis suggests that recombinant HβD-3 is present at an approximate concentration range of 0.84 - 1.49μg/mL in CM-505hbd3GAL1 (Fig. 4.6 and 4.7). Thus, the latter results are conflicting with *in vitro* bioassay results.

Lb. brevis was shown to retain viability in wort fermentations carried out at 20°C, when inoculated at the late stages of fermentation at lower cell densities (Fig. 5.2). The presence of bacteria did not affect fermentation efficiency as the same final alcohol percentage was produced in each brew (Fig. 5.1 B). Likewise, *Lb. brevis* viability was retained in wort and YEPGal fermentations at 11°C (Fig. 5.4). The Gram-negative, strictly anaerobic *P. frisingensis* also survived and propagated in various fermentative environments (Fig. 5.7). An initial reduction in bacterial viability was observed on all occasions indicating that seeding of bacteria into fresh medium and immediate incubation at 11°C resulted in an initial decrease in bacterial viability. Furthermore, bacterial growth was higher in YEPGal fermentations compared to wort fermentations. This may be due to the sugar concentrations and thus lower alcohol levels in YEPGal fermentations. Thus bacterial growth is influenced by the physiological conditions of the cultures.

The antimicrobial activity produced by CM-505hbd3GAL1 and CM-506hbd3GAL1 was assessed by seeding both YEPGal and wort fermentations with cultures of *Lb. brevis* and *P. frisingensis*. Additionally, the effectiveness of introducing a freeze-thaw step was also examined to analyse if bacterial membranes become more susceptible to HβD-3 following cold-shock. A decrease in viable counts of *Lb. brevis* was observed in CM-505hbd3GAL1 YEPGal fermentations compared to CMBS-33 fermentations on one occasion before freeze-treatment (Fig. 5.5 A). Furthermore, freeze-treatment of these samples did not result in a further decrease in *Lb. brevis* viability in all samples analysed (Fig. 5.5 B). Thus, no consistent antimicrobial activity was observed in YEPGal fermentations (Fig. 5.5). *P. frisingensis* viability was unaffected in all CM-505hbd3GAL1 and CM-506hbd3GAL1 YEPGal fermentations (Fig. 5.8). However, upon analysis of the viability of these BSMs in wort fermentations, the results obtained indicated that the viability of both BSMs is significantly reduced in CM-505hbd3GAL1 and CM-506hbd3GAL1 wort fermentations compared to CMBS-33 wort fermentations after freeze-treatment (Fig. 5.6 and 5.9). As explained in section 5.2.4, yeast cells were washed twice in SDW before inoculation into wort, thus one can assume that G418 is

not responsible for the decrease in viability. One hypothesis is that a synergistic effect is occurring whereby the combination of recombinant HβD-3, high alcohol levels, a freeze-thaw cycle and low bacterial growth results in a significant decrease in *Lb. brevis* viability in the CM-505hbd3GAL1 and CM-506hbd3GAL1 fermentations. This hypothesis supports the reduced antimicrobial activity observed in YEPGal fermentations, where 2% galactose would result in very little or no alcohol production due to the low level of fermentable sugars and BSM growth is higher (Fig. 5.5 and 5.7). Further experimentation is needed to compare the antibacterial effects of synthetic and recombinant HβD-3 in fermentations and analyse if BSMs are more susceptible to synthetic HβD-3 following a freeze-thaw cycle.

CM-505hbd3TEF1 and CM-INT-51 produced the highest levels of antimicrobial activity against *Lb. brevis* in this study, with *Lb. brevis* viability decreasing by 65 – 85% and 33 – 91% before freeze-treatment for each strain respectively in fermentations carried out at 20°C (Fig. 5.13). Antimicrobial activity was further increased by freeze-treatment of these samples. CM-505hbd3TEF1 and CM-INT-51 fermentations carried out at 11°C, did not exhibit any significant affect on the viability of *Lb. brevis* before freeze-treatment. This result is similar to results obtained for CM-505hbd3GAL1 and CM-506hbd3GAL1 (Fig. 5.6 A). After freeze-treatment, *Lb. brevis* viability is reduced in CM-505hbd3TEF1 fermentations on day 1 and CM-INT-51 fermentations on days 5 and 7. Thus, this data clearly indicates that freeze-treatment increases the susceptibility of *Lb. brevis* to recombinant HβD-3. As the mechanism of action of HβD-3 is known to involve membrane disruption (section 1.5.4.2), this increase in susceptibility may be due to alterations in the bacterial membrane that occur during homeoviscous adaption in response to cold-shock (Sinensky, 1974). It is possible that due to lower metabolism of yeast cells at 11°C, less HβD-3 is produced at this temperature. Furthermore, these results suggest that continual growth of *Lb. brevis* is required to promote antimicrobial activity of HβD-3.

CM-INT-51 has the HβD-3 gene stability integrated into chromosome XVI. Additionally CM-INT-51 contains a kanMX cassette. As a further control and to ensure that this cassette does not promote antimicrobial activity, further experiments can be carried out with CM-INT-51 minus the kanMX cassette. A strain in which the kanMX cassette has been deleted has been constructed (James, T. C., unpublished).

Unlike CM-INT-51, no antimicrobial activity was detected in CM-INT-37 fermentations. The CM-INT-37 strain appears to possess a loss-of-function phenotype and cannot ferment efficiently when grown in wort (Fig. 5.10 and 5.12). This may be due a lower *S. cerevisiae* copy number in the region YPR159C-A to YPR160W (section 1.6). The lack of ethanol production creates a very sugar rich medium for growth of contaminants. Therefore, as described in sections 5.2.4.1 and 5.2.4.2, bacterial growth in CM-INT-37 fermentations were always extremely higher than that observed in CMBS-33 fermentations. While recombinant HβD-3 was expressed in this strain, further analysis is needed to analyse secreted recombinant HβD-3 from CM-INT-37.

Unlike CM-505hbd3GAL1, CM-506hbd3GAL1 and CM-505hbd3TEF1, no antimicrobial activity was detected in CM-506hbd3AGT1 and CM-506hbd3PGK1 fermentations. Bacterial growth appeared higher in these fermentations compared to CM-505hbd3GAL1, CM-506hbd3GAL1 and CM-505hbd3TEF1 fermentations. The reason for this increase in bacterial growth is unclear as these strains ferment as efficiently as CMBS-33 (Fig. 5.10 and 5.12) and produce similar levels of alcohol. Furthermore, the reason for this lack of HβD-3 activity is also unclear, as HβD-3 appears to be synthesized in each strain (section 4.2.3.1/4.2.3.2). This anomaly may be due to numerous factors. It is possible that a different isoform of recombinant HβD-3 is produced in these strains that is less effective at reducing bacterial growth. Alternatively, the half-life of the peptide may be different in each of the strains. Thus, it will be important to compare the HβD-3 peptide levels in each strain throughout the course of the fermentation. An in depth analysis of CM-506hbd3AGT1 and CM-506hbd3PGK1 is required to investigate this anomaly further. Since activity was observed in the strains CM-505hbd3GAL1, CM-506hbd3GAL1 and CM-505hbd3TEF1 which all carry the HβD-3 gene on the pGREG vector, it is unlikely that the lack of expression in CM-506hbd3AGT1 and CM-506hbd3PGK1 is due to selective plasmid loss, however this should also be investigated.

Preliminary results indicate that CM-pRShbd3PGK1 displays antimicrobial activity at 20°C, while no activity is detected at 11°C. However, as these results were deemed preliminary further experimentation is needed to verify the levels of antimicrobial activity produced by this strain at 20°C.

The higher levels of antimicrobial activity displayed in CM-505hbd3TEF1 and CM-INT-51 compared to CM-505hbd3GAL1 and CM-506hbd3GAL1 may be accounted for by differences in experimental design. For CM-505hbd3TEF1 and CM-INT-51 fermentations were seeded on day 0, while the CM-505hbd3GAL1 and CM-506hbd3GAL1 fermentations were seeded on day 2. The lower activity in the latter fermentations may be a consequence of the fact that the majority of galactose will have been consumed on day 2. Since expression of HβD-3 is dependent on galactose the levels after day 2 may be quite low or may not be expressed at all. Thus, examining these strains with earlier bacterial inocula will determine if higher levels are observed at the earlier stages of the fermentation.

CM-INT-51 and CM-505hbd3TEF1 display higher levels of activity at 20°C compared to 11°C, thus the HβD-3 peptide appears to be more active at this higher temperature. Therefore, experiments should be carried out with CM-505hbd3GAL1 and CM-506hbd3GAL1 at 20°C, to examine if antimicrobial activity can be increased. Furthermore, RP-HPLC results discussed in Chapter 4, indicate that secretory recombinant HβD-3 from CM-INT-51 and CM-505hbd3GAL1 and CM-506hbd3GAL1 is structurally different, with CM-INT-51 appearing to be heavily glycosylated. The structure of the β-defensin changes the peptides mode of action towards microbial and host cells, and furthermore dimerizartion appears to increase antimicrobial activity (Antcheva, 2009). Thus, the structural differences of recombinant HβD-3, observed between each strain, may influence the activity of this peptide. As similar experiments were not carried out on secretory recombinant HβD-3 from CM-505hbd3TEF1, one cannot yet decipher if this peptide structure is altered. However, as activity levels are similar to that observed for CM-INT-51 recombinant HβD-3, it can be hypothesized that similar structures of recombinant HβD-3 are produced by CM-505hbd3TEF1. The use of constitutive promoters appears to result in antimicrobial activity being produced throughout the fermentation.

Overall, results obtained during this research indicate that higher levels of antimicrobial activity were observed in fermentations carried at 20°C compared to 11°C (Fig. 5.13 & 5.11). This is indicative of the optimal temperature for HβD-3 activity. This peptide is a human antimicrobial that is active in the body at 37°C, thus, observing higher activity levels nearer to this optimal temperature is expected. Lager yeasts ferment best at 7 –

14°C, yet an increase in approximately 10°C does not appear to affect the fermentative capacity of CMBS-33 and HβD-3-encoding lager strains (Fig. 5.10 & 5.12). Fermentations were seeded with relatively high amounts of bacteria, and a maximum reduction of 96% in *Lb. brevis* viability was achieved in CM-INT-51 after 7 days of fermentations at 20°C and including a freeze-treatment. Modification of the experimental parameters may lead to 100% killing. Furthermore, alternative treatments, for example flash pasteurisation, may reveal increased susceptibility of bacteria towards HβD-3.

Chapter 6: General Discussion

6.1 General Discussion

Industrial yeast strains involved in brewing have adapted to grow in extremely harsh conditions, while maintaining the ability to efficiently convert available carbohydrates to ethanol and further by-products. Despite restrictive growth conditions, as described in section 1.3.1 microbial contamination remains a major problem in the brewing industry. The overall aim of the research presented in this thesis was to generate a series of *Saccharomyces* strains that produce an antimicrobial peptide, which would be capable of eliminating or minimizing bacterial contamination in a fermentation, without affecting the fermentation process. To date, various approaches have been carried out to help eradicate bacterial contamination, these include the addition of bacteriocins such as nisin and polysaccharides such as chitosan to the brew. Nisin has been shown to successfully kill beer spoilage micro-organisms (BSMs) within a fermentation, but has also been shown to have a minor affect on *S. cerevisiae* growth (Galvagno et al., 2007). Chitosan effectively kills BSMs within a fermentation while having no affect on *S. cerevisiae* (Galvagno et al., 2007). The caveat with both of these methods is that these antimicrobials are sourced externally and addition of these to the fermentation may be cost prohibitive to the brewer. The expression of antimicrobial peptides in yeast strains would eliminate this problem, producing the AMP within the fermentation.

Various human defensins have previously been expressed in both yeast and bacterial strains. HβD-1 has been successfully produced and secreted from a *S. cerevisiae* strain (Cipáková, 2005). This study was carried out to create an expression system that could rapidly produce functional peptide and the secreted peptide displayed antimicrobial activity towards *E. coli*. Studies by Hsu et al. (2009) produced a *P. pastoris* strain that secretes bioactive HD-5. This active peptide showed selective killing against *S. typhimurium* and *S. aureus*, but did not display activity against the most prominent BSMs, Lactobacilli. HβD-3 is a well characterised defensin that possesses a broad spectrum of activity and unlike some defensins, its activity is salt independent. While Huang et al. (2006) have successfully expressed HβD-3 from *E. coli*, to my knowledge HβD-3 has never been expressed from a yeast strain. In this study we have generated a series of yeast strains that have the ability to express and secrete active HβD-3. HβD-3 was chosen as it is expressed in the oral cavity, thus certifying biosafety of the final beverage (Diamond et al. 2008). We have innovatively achieved the generation of HβD-3 encoding yeast by direct integration into the chromosome, thus eliminating the need for a carrier plasmid and creating novel HβD-3-encoding yeast strains.

The first major aim of this research was to generate a series of yeast strains that encode HβD-3. As discussed in Chapter 3, HβD-3 was placed under the control of various promoters. Semi-quantitative RT-PCR analysis indicated that each promoter produces an mRNA HβD-3 transcript (Fig. 4.1). Furthermore, these results suggest that *TEF1* is the strongest constitutive promoter and CM-INT-51 produces higher levels of HβD-3 mRNA compared to CM-INT-37 (Fig. 4.1 F and J). Secretion studies indicate that recombinant HβD-3 could be detected by ELISA analysis in all crude concentrated supernatants with the exception of CM-506hbd3PGK1 (section 4.2.3.1/4.2.3.2). However, ELISA experiments performed on RP-HPLC fractions throughout this research, indicate that when the peptide is fractionated, the detectable levels of secretory recombinant HβD-3 increase by approximately 20- to 50-fold. These high concentration levels may be indicative of high background levels during ELISA analysis of RP-HPLC fractions, thus ELISA analysis of crude concentrated supernatants may provide more accurate estimations of recombinant HβD-3 concentrations.

CM-505hbd3GAL1 and CM-506hbd3GAL1 were both analysed thoroughly throughout this study. Initial ELISA analysis indicated that both strains secrete recombinant HβD-3 (section 4.2.3.1). Furthermore, *in vitro* bioassays indicate that CM-505hbd3GAL1 secretes active recombinant HβD-3 at 0.06μg/mL (Fig. 5.3). This result validates the initial ELISA analysis, which indicated that recombinant HβD-3 is produced by CM-505hbd3GAL1 at approximately 0.06μg/mL. While previous studies by Huang et al. (2007) indicated that *E. coli* produces recombinant HβD-3 at ~1mg/mL, these levels of recombinant HβD-3 produced by *S. pastorianus* are comparable to salivary levels of HβD-3 (0.1-0.3μg/mL) (Forte et al., 2010; Tao et al., 2005). The level of antimicrobial activity produced by CM-505hbd3GAL1 at 0.06μg/mL was equivalent to that obtained by 0.5μg/mL of synthetic HβD-3. This suggests that recombinant HβD-3 is more potent than synthetic HβD-3. Furthermore, RP-HPLC results obtained for CM-505hbd3GAL1 and CM-506hbd3GAL1 were slightly different to that obtained for synthetic HβD-3 (Fig. 4.6), suggesting the structures of recombinant and synthetic HβD-3 differ. Further *in vivo* bioassays indicate that CM-505hbd3GAL1 and CM-506hbd3GAL1 exhibit antimicrobial activity against the Gram-positive bacteria, *Lb. brevis,* and the Gram-negative bacteria, *P. frisingensis*, when the presence of recombinant HβD-3 is combined with high alcohol levels and a freeze-treatment (Fig. 5.6 and 5.9 respectively). Studies by Schroeder et al. (2011) suggest that reducing the

disulphide bonds of HβD-1 increases the antimicrobial activity of this peptide. In this particular study, the addition of the reducing agent DTT, decreased antimicrobial activity of HβD-3. This data suggests that the tertiary structure of β-defensins determines the potency of the peptide. This agrees with various studies that suggest that HβD-3 activity is influenced by the structure of the peptide and the charged residues and hydrophobicity are responible for electrostatic interactions and disruption of the lipid bilayer, respectively (Brogden, 2005; White et al., 1995). Antcheva et al. (2009) have carried out studies to determine the structure-activity relationship of β-defensins using a chemically synthesized artificial β-defensin molecule. These studies showed that altering the structure of the artificial β-defensin changed the peptides mode of action towards microbial and host cells, and furthermore dimerization appears to increase antimicrobial activity (Antcheva, 2009). Thus, the levels of activity observed during bioassays may not be directly related to the concentration of HβD-3 and may instead be influenced by the structure of the peptide. Furthermore, studies by Wilmes et al. (2011) suggest that defensins primarily act on patches of negatively charged lipids, this initial attraction is followed by stresses on cell wall synthesis and energy conservation. Added stress such as very high levels of peptide or extra environmental stress leads to physical disruption of the lipid bilayer resulting in cell death. This hypothesis is in agreement with our findings, whereby the added stress of incubation at -70°C results in increased killing of the bacteria (chapter 5). Future work should be carried out in this area to determine if -70°C freeze-treatment of fermentation samples, has a major impact on the final beverage.

The strains CM-505hbd3TEF1 and the integrative strain CM-INT-51 produced similar results throughout this study. Both strains produced low levels of secretory recombinant HβD-3 when crude concentrated supernatant samples were analysed by ELISA analysis (section 4.2.3.2), yet the activity levels seen in *in vivo* bioassays indicate that recombinant HβD-3 secreted from these strains may be at a much higher concentration than first anticipated. The integrated strain, CM-INT-51, was analysed by RP-HPLC and subsequent ELISA analysis indicates that recombinant HβD-3 is secreted from this strain in the μg/mL range. However, taking the ELISA results of CM-505hb3GAL1 and CM-506hbd3GAL1 into consideration, this concentration is more than likely overestimated. Further ELISA analysis of CM-INT-51 crude concentrated supernatants will verify the true concentrations of recombinant HβD-3 secreted from

this strain. Semi-quantitative RT-PCR results indicate that CM-INT-51 and CM-505hbd3TEF1 are the most efficient at expressing HβD-3, thus *in vivo* bioassay results correlate with RT-PCR results. Furthermore, both strains display high levels of antibacterial activity against *Lb. brevis* at room temperature both before and after freeze-treatment (Fig. 5.13). Further RP-HPLC and ELISA analysis of CM-505hbd3TEF1 would indicate if this strain secretes similar isoforms of recombinant HβD-3 as CM-INT-51. The very high level of activity observed in CM-INT-51 may be due to very high levels of peptide or a different peptide structure or a combination of both. In this study, the additional freeze-treatment of CM-INT-51 and CM-505hbd3TEF1 samples resulted in a minor further decrease in bacterial viability. This may indicate a certain level of saturation for the antimicrobial activity of recombinant HβD-3 at high bacterial growth.

Overall, antimicrobial activity could only be detected for certain yeast strains encoding HβD-3. The non-specific 5'UTRs of CM-505hbd3GAL1, CM-506hbd3GAL1 and CM-505hbd3TEF1 are different in length and sequence, yet all strains display antimicrobial activity, thus modifying the non-specific 5'UTR did not have a negative affect on the overall translation of mature HβD-3. Furthermore, the activity levels displayed by CM-INT-51 were similar to that of CM-505hbd3TEF1. As CM-INT-51 does not posses a non-specific 5'UTR, this verifys that the non-specific 5'UTR does not affect the translation of recombinant HβD-3. Activity analysis of CM-506hbd3PGK1 and CM-506hbd3AGT1 revealed an unusual phenomenon, whereby these fermentations provide an environment in which bacteria thrive and bacterial viability increases significantly in these fermentations compared to CMBS-33 fermentations (section 5.2.4). Thus, HβD-3 activity levels of CM-506hbd3AGT1 and CM-506hbd3PGK1 were undetectable in this study. Further *in vivo* analysis of both of these strains, with the inclusion of a pGREG empty vector as a negative control, will provide more information regarding the HβD-3 activity produced by CM-506hbd3AGT1 and CM-506hbd3PGK1. Thus, the increase in bacterial viability observed in CM-506hbd3AGT1 and CM-506hbd3PGK1 fermentations is unusual, as these strains do not possess any novel features. However, the presence of a plasmid may promote bacterial growth due to the expression of other genes such as *URA3*, *LEU2* or *KAN*. Since antimicrobial activity was detected in CM-505hbd3GAL1, CM-506hbd3GAL1 and CM-505hbd3TEF1 and these strains contain the same backbone of the pGREG plasmids, it is unlikely that genes expressed from the

plasmids could influence bacterial growth. It is also possible that CM-506hbd3AGT1 and CM-506hbd3PGK1 produce a variant of HβD-3 that somehow promotes bacterial growth, however this is highly unlikely. Further experimentation is needed to verify the structure of recombinant HβD-3 produced by these strains and to analyse the antimicrobial activity of these strains compared to the empty vector pGREG-506.

RP-HPLC results showed that HβD-3 produced from the vector strains was significantly different from that produced from the integrated strain (Fig. 4.6 and 4.9 respectively). The latter strain produced a RP-HPLC profile that differed from both synthetic and recombinant HβD-3 produced from plasmids (Fig. 4.9). A dedicated column was used throughout this study, which may have resulted in experimental limitations, thus further work should be carried out with various different RP-HPLC columns. However, both RP-HPLC (Fig. 4.12 and 4.13) and Western immunoblot analysis (Fig. 4.14 and 4.15) verify that recombinant HβD-3 produced from CM-INT-51 is glycosylated. This is in agreement with previous findings of the glycosylation of human defensins secreted from yeast strains (Hsu et al., 2009). Glycosylation of a peptide ultimately changes the overall structure of the peptide as N and O-linked glycans are added to the peptide. Glycosylation of HβD-3 resulted in detection problems throughout this study. As described in section 4.2.5.2, Western immunoblot detection of a 6xHis-tag fused to HβD-3 was not possible and it can be hypothesized that this is due to glycosylation of HβD-3 inhibiting the interaction of the peptide with the anti-His antibody. For future work, the above sample can be treated with Endo-H, this will result in a deglycosylated form of fused HβD-3, which may enable detection via Western blotting. To detect secretory recombinant HβD-3, cells were grown in minimal media, as this is readily concentrated. Growth in minimal media is low. Thus, together with glycosylation this was an added complication when attemping to detect HβD-3 in spent media by Western blotting. As mentioned in section 4.2.5.1, concentrated supernatant samples were treated with Endo-H, which did not result in detection by Western blotting. This may be due to the fact that Endo-H only removes N-glycans, while O-glycans may still be present preventing the detection of low amounts of secreted recombinant HβD-3. However as mentioned above low levels of secreted peptide were detected by ELISA anaylsis. This method detects the native form, thus these results are not encumbered by glycosylation. In future work, yeast strains could be cultured in richer minimal media, supplemented with up to 10% galactose or maltose, to promote higher growth levels,

overcoming one obstacle. As only N-glycans have been removed by Endo H treatment, removal of O-glycans by further enzymatic treatment of concentrated supernatant samples may promote the interaction of recombinant HβD-3 with anti-HβD-3 antibody, overcoming another obstacle. Furthermore, glycosylation does not appear to affect the antimicrobial activity of recombinant HβD-3 (chapter 5), which agrees with the literature that states that hyperglycosylated enzymes secreted from *S. cerevisiae* are still active (Cummings and Fowler, 1996; Penttila et al., 1988).

Another integrated strain, created during this study, is CM-INT-37. Interestingly this strain did not ferment efficiently compared to CM-INT-51 (Fig. 5.10 and 5.12). As mentioned in section 1.6, CM-INT-37 and CM-INT-51 were generated in a similar manner, however microarray analysis of this strain revealed that the region YPR159C-A to YPR190W of chromosome XVI in CM-INT-37 has a lower copy number of the *S. bayanus* complement, compared to CM-INT-51 and CMBS-33. Thus the integration of the HβD-3 cassette appears to have disrupted this region of the genome and also altered the copy number composition of *S. cerevisiae* and *S.eubayanus* in this particular strain. DNA sequencing results indicate that the HβD-3 gene cassette has been integrated in CM-INT-37 and CM-INT-51, into a hybrid copy of chromosome XVI (section 1.6). RT-PCR analysis indicates that YPR160W mRNA transcripts are synthesized by CM-INT-37 and CM-INT-51 (Fig. 4.2), however further work should be carried out to determine if these transcripts are translated to mature functioning proteins. As discussed in section 4.1, previous studies by Favre et al. (2008) have shown that the deletion of *GPH1* leads to stress intolerance and decreased survival in stationary phase. The loss-of-function phenotype observed for CM-INT-37 is not seen in CM-INT-51, thus the copy number variation of the YPR159C-A to YPR190W region observed between the two strains may have resulted in an adverse effect on *GPH1* protein expression and the fermentative capacity of CM-INT-37. Integrating the HβD-3 gene cassette into a recombination hot-spot may result in adverse effects on the genomes of CM-INT-37 and CM-INT-51. Furthermore, other areas of this chromosome may also have been affected by the integration of the HβD-3 gene cassette, thus further genome analysis of CM-INT-51 and CM-INT-37 may be required to gain a better understanding of these strains. Similar to CM-506hbd3AGT1 and CM-506hbd3PGK1, *in vivo* bioassays of CM-INT-37 indicate that *Lb. brevis* thrives in these fermentations compared to CMBS-33 fermentations. It can be hypothesized for CM-INT-37, in which

fermentation levels are extremely low (Fig. 5.10 and 5.12), that *Lb. brevis* thrives due to rich media containing minimal levels of alcohol.

Recombinant HβD-3 was shown to be active under fermentation conditions. Furthermore, higher antimicrobial activity is achieved at room temperature compared to 11°C. This most likely results from the overall decreased metabolism at 11°C. However, HβD-3, like other AMPs, is active within the human body, thus the optimal temperature of this peptide will be approximately 37°C. This resulted in limitations throughout this study as lager fermentations are normally carried out between 7 - 14°C. During this study it has been shown that lager fermentations carried out with CMBS-33 strains, perform just as well at room temperature compared to 11°C (Fig. 5.10 and 5.12). As stated in Chapter 2 (Table 2.4), HβD-3 was also introduced into *S. cerevisiae* strains. *S. cerevisiae* strains are commonly used for ale fermentations which are normally carried out at approximately 20°C. HβD-3 could also show activity in these strains when fermentations are carried out at 20°C, and this temperature may be increased to promote higher levels of activity without affecting the fermentation process. Time constraints did not allow for the analysis of these strains, thus for future studies HβD-3 activity in ale fermentations should be examined. This fortuitous development can be applied to various yeast strains promoting HβD-3 expression in many industrial applications such as wine fermentations as well as for bioethanol production. Furthermore, a novel finding revealed during this study indicated that the BSMs *Lb. brevis* and *P. frisingensis* were found to be more susceptible to recombinant HβD-3 upon freeze-treatment of wort fermentation samples. This may be due to a combination of the change in the bacterial membrane in response to cold shock, the presence of low levels of alcohol along with the presence of HβD-3, which appears to have resulted in a synergistic effect. This novel approach could also be applied to various other fermentations such as those used for the production of ales, wines and spirits.

While recombinant HβD-3 showed lower levels of antimicrobial activity at 11°C, altering extrinsic factors may result in an increase in activity at this ideal fermentation temperature. In commercial brewery conditions, contamination will commonly start with very low levels of bacteria, thus reducing the amount of bacteria initially seeded into each fermentation may result in higher activity levels. Furthermore, the addition of hops in combination with low bacterial numbers and the presence of HβD-3 may result

in higher levels of killing overall. CM-505hbd3TEF1 and CM-INT-51 inhibit the growth of *Lb. brevis* by 85 – 91% respectively, in fermentations carried out at room temperature. The addition of hop-extracts and a lower starter inoculum of bacteria may result in increased activity towards *Lb. brevis*, which could eradicate the need for freeze-treatment of fermentation samples. Furthermore, a common trend seen during CM-INT-51 and CM-505hbd3TEF1 room temperature fermentations, is that the activity increases as the fermentation progresses. This study only analysed bacterial counts up to day 7/8 of a fermentation, if further analysis was carried out on days 10, 12, 14 etc., would higher levels of activity be seen, eliminating all bacterial contamination? Future work should be carried out in this area to analyse this hypothesis. Furthermore, these strains have the potential to prevent the growth of wort spoilage organisms also, thus future experiments could be carried out to examine this also. Finally, the use of alternative AMPs should also be examined, as these may provide higher levels of antimicrobial activity in lager fermentations carried out at 11°C.

As described in section 1.1, James et al. (2008) carried out studies whereby a series of "stress-tolerant" lager strains were produced. Further studies in the lab suggest that the lager strain, CM-51, grows best under high stress conditions compared to the wild-type strain CMBS-33 and various other "stress-tolerant" strains generated during this study (Kricka, W. and Bond, U., unpublished). Incorporating HβD-3 into CM-51 may result in the generation of a "super-strain" that exhibits antimicrobial activity during fermentation while withstanding very high stress conditions.

In conclusion, the data presented in this thesis reports the expression of HβD-3 from *S. pastorianus* for the first time. While numerous advantages may be obtained from the use of yeast strains expressing AMPs, the negative attitude of consumers towards genetically modified foods would need to be overcome. Yeast have ultimately been provided with their own innate immune system. Antimicrobial activity is retained during the fermentation process with no apparent affect on the overall process. Future studies can be carried out to improve antimicrobial activity, while further fermentation analysis will determine if flavour has been affected by the presence of the HβD-3 gene cassette. Furthermore, the final beverage may be used as a therapeutic agent, containing low levels of HβD-3, which may be used to treat various oral/dental infections. Similarly, the spent yeast with antimicrobial properties may be used as a nutraceutical

product, which could be added to animal feed providing nutritional value along with antimicrobial and preservation properties.

Bibliography

Abiko, Y., Nishimura, M., and Kaku, T. (2003). Defensins in saliva and the salivary glands. Med Electron Microsc *36*, 247-252.

Agerberth, B., Charo, J., Werr, J., Olsson, B., Idali, F., Lindbom, L., Kiessling, R., Jornvall, H., Wigzell, H., and Gudmundsson, G.H. (2000). The human antimicrobial and chemotactic peptides LL-37 and alpha-defensins are expressed by specific lymphocyte and monocyte populations. Blood *96*, 3086-3093.

Agerberth, B., Gunne, H., Odeberg, J., Kogner, P., Boman, H.G., and Gudmundsson, G.H. (1995). FALL-39, a putative human peptide antibiotic, is cysteine-free and expressed in bone marrow and testis. Proc Natl Acad Sci U S A *92*, 195-199.

Albrethsen, J., Bogebo, R., Gammeltoft, S., Olsen, J., Winther, B., and Raskov, H. (2005). Upregulated expression of human neutrophil peptides 1, 2 and 3 (HNP 1-3) in colon cancer serum and tumours: a biomarker study. BMC Cancer *5*, 8.

Alves, S.L., Jr., Herberts, R.A., Hollatz, C., Trichez, D., Miletti, L.C., de Araujo, P.S., and Stambuk, B.U. (2008). Molecular analysis of maltotriose active transport and fermentation by Saccharomyces cerevisiae reveals a determinant role for the AGT1 permease. Appl Environ Microbiol *74*, 1494-1501.

Antcheva, N., Morgera, F., Creatti, L., Vaccari, L., Pag, U., Pacor, S., Shai, Y., Sahl, H.G., and Tossi, A. (2009). Artificial beta defensin based on a minimal defensin template Biochemical Journal *421*, 435-447.

Attfield, P.V. (1997). Stress tolerance: the key to effective strains of industrial baker's yeast. Nat Biotechnol *15*, 1351-1357.

Back, W. (1981). Bedeutung der Mikrokokken als Bierschaedlinge. Brauwissenschaft *34*, 109-114.

Back, W. (1994). Sekundarkontaminationen im Abfullereich. Brauwelt *16*, 686-695.

Bals, R., Wang, X., Wu, Z., Freeman, T., Bafna, V., Zasloff, M., and Wilson, J.M. (1998). Human beta-defensin 2 is a salt-sensitive peptide antibiotic expressed in human lung. J Clin Invest *102*, 874-880.

Banerjee, S., and Hansen, J.N. (1988). Structure and expression of a gene encoding the precursor of subtilin, a small protein antibiotic. The Journal of Biological Chemistry *263*, 9508-9514.

Barnett, J.A. (1981). The utilization of disaccharides and some sugars by yeasts. Advances in Carbohydrate Chemistry and Biochemistry *39*, 347-404.

Barney, M., and Kot, E. (1992). A comparison of rapid microbiological methods for detecting beer spoilage microorganisms. Master Brewers Association of the Americas Technical Quarterly *29*, 91-95.

Barth, S.J. (2011). The barth report hops 2010/2011, http://www.barthhaasgroup.com.

Basanta, A., Carmen, H., Gutierrez, J., Criado, R., Hernandez, P.E., and Cintas, L. (2009). Development of Bacteriocinogenic Strains of Saccharomyces cerevisiae Heterologously Expressing and Secreting the Leaderless Enterocin L50 Peptides L50A and L50B from Enterococcus faecium L50. Appl Environ Microbiol *75*, 2382-2392.

Basanta, A., Sanchez, J., Gomez-Sala, B., Herranz, C., Hernandez, P.E., and Cintas, L.M. (2008). Antimicrobial activity of Enterococcus faecium L50, a strain producing enterocins L50 (L50A and L50B), P and Q, against beer-spoilage lactic acid bacteria in broth, wort (hopped and unhopped), and alcoholic and non-alcoholic lager beers. International Journal of Food Microbiology *125*, 293-307.

Bateman, A., Singh, A., Jothy, S., Fraser, R., Esch, F., and Solomon, S. (1992). The levels and biologic action of the human neutrophil granule peptide HP-1 in lung tumors. Peptides *13*, 133-139.

Bauer, F., Schweimer, K., Kluver, E., Conejo-Garcia, J.R., Forssmann, W.G., Rosch, P., Adermann, K., and Sticht, H. (2001). Structure determination of human and murine

beta-defensins reveals structural conservation in the absence of significant sequence similarity. Protein Sci *10*, 2470-2479.

Belloch, C., Perez-Torrado, R., Gonzalez, S.S., Perez-Ortin, J.E., Garcia-Martinez, J., Querol, A., and Barrio, E. (2009). Chimeric genomes of natural hybrids of Saccharomyces cerevisiae and Saccharomyces kudriavzevii. Appl Environ Microbiol *75*, 2534-2544.

Bensch, K.W., Raida, M., Magert, H.J., Schulz-Knappe, P., and Forssmann, W.G. (1995). hBD-1: a novel beta-defensin from human plasma. FEBS Lett *368*, 331-335.

Bond, U., and A. Blomberg (2006). Principles and applications of genomics and proteomics in the analysis of industrial yeast strains. Yeast in Food and Beverages. Springer-Verlag, Heidleberg *In Querol, A. & Fleet, G. (ed) The Yeast Handbook*, 175-213.

Bond, U., Neal, C., Donnelly, D., and James, T.C. (2004). Aneuploidy and copy number breakpoints in the genome of lager yeasts mapped by microarray hybridisation. Current Genetics *45*, 360-370.

Boniotto, M., Antcheva, N., Zelezetsky, I., Tossi, A., Palumbo, V., Verga Falzacappa, M.V., Sgubin, S., Braida, L., Amoroso, A., and Crovella, S. (2003). A study of host defence peptide beta-defensin 3 in primates. Biochem J *374*, 707-714.

Borsig, L., Berger, E.G., and Malissard, M. (1997). Expression and purification of His-tagged beta-1,4-galactosyltransferase in yeast and in COS cells. Biochem Biophys Res Commun *240*, 586-589.

Bose, S.K., Gibson, W., Bullard, R.S., and Donald, C.D. (2009). PAX2 oncogene negatively regulates the expression of the host defense peptide human beta defensin-1 in prostate cancer. Molecular Immunology *46*, 1140-1148.

Boulton, C.A. (1991). Developments in brewery fermentation. Biotechnol Genet Eng Rev *9*, 127-181.

Brogden, K.A. (2005). Antimicrobial peptides: pore formers or metabolic inhibitors in bacteria? Nat Rev Microbiol *3*, 238-250.

Brosnan, M.P., Donnelly, D., James, T.C., and Bond, U. (2000). The stress response is repressed during fermentation in brewery strains of yeast. J Appl Microbiol *88*, 746-755.

Bulet, P., Stocklin, R., and Menin, L. (2004). Anti-microbial peptides: from invertebrates to vertebrates. Immunol Rev *198*, 169-184.

Caesar, R., Palmfeldt, J., Gustafsson, J.S., Pettersson, E., Hashemi, S.H., and Blomberg, A. (2007). Comparative proteomics of industrial lager yeast reveals differential expression of the cerevisiae and non-cerevisiae parts of their genomes. Proteomics *7*, 4135-4147.

Campbell, I. and Priest, F.G. (2003). Brewing Microbiology, 3 edn.

Campbell, I. (1996). Wild yeast in brewing and distilling (London: Chapman and Hall).

Campbell, I., and Msongo, H.S. (1991). Growth of aerobic wild yeast The Journal of the The Institute of Brewing and Distilling, 279-282.

Carrasco, P., Querol, A., and del Olmo, M. (2001). Analysis of the stress resistance of commercial wine yeast strains. Arch Microbiol *175*, 450-457.

Casey, G.P. (1996). Practical applications of pulsed field electrophoresis and yeast chromosome fingerprinting in brewing. Techincal Quaterly Master Brewers Association of the Americas *33*, 1-10.

Castagnola, M., Inzitari, R., Rossetti, D.V., Olmi, C., Cabras, T., Piras, V., Nicolussi, P., Sanna, M.T., Pellegrini, M., Giardina, B., and Messana, I. (2004). A cascade of 24 histatins (histatin 3 fragments) in human saliva. Suggestions for a pre-secretory sequential cleavage pathway. The Journal of Biological Chemistry *279*, 41436-41443.

Cederlund, A., Gudmundsson, G.H., and Agerberth, B. (2011). Antimicrobial peptides important in innate immunity. Febs J.

Chadwick, L.R., Pauli, G.F., and Farnsworth, N.R. (2006). The pharmacognosy of Humulus lupulus L. (hops) with an emphasis on estrogenic properties. Phytomedicine *13*, 119-131.

Chang, W.K., Wimley, W.C., Searson, P.C., Hristova, K., and Merzlyakov, M. (2008). Characterization of antimicrobial peptide activity by electrochemical impedance spectroscopy. Biochimica et biophysica acta *1778*, 2430-2436.

Chang, Y.S., Dubin, R.A., Perkins, E., Michels, C.A., and Needleman, R.B. (1989). Identification and characterization of the maltose permease in genetically defined Saccharomyces strain. Journal of Bacteriology *171*, 6148-6154.

Charron, M.J., and Michels, C.A. (1988). The naturally occurring alleles of MAL1 in Saccharomyces species evolved by various mutagenic processes including chromosomal rearrangement. Genetics *120*, 83-93.

Charron, M.J., Read, E., Haut, S.R., and Michels, C.A. (1989). Molecular evolution of the telomere-associated MAL loci of Saccharomyces. Genetics *122*, 307-316.

Chaudhuri, B., Steube, K., and Stephan, C. (1992). The pro-region of the yeast prepro-alpha-factor is essential for membrane translocation of human insulin-like growth factor 1 in vivo. Eur J Biochem *206*, 793-800.

Chen, C.I., Schaller-Bals, S., Paul, K.P., Wahn, U., and Bals, R. (2004). Beta-defensins and LL-37 in bronchoalveolar lavage fluid of patients with cystic fibrosis. J Cyst Fibros *3*, 45-50.

Cheng, Q.a.M., C. A. (1990). MAL11 and MAL61 Encode the Inducible High-Affinity Maltose Transporter of Saccharomyces cerevisiae. Journal of Bacteriology, 1817-1820.

Christianson, T.W., Sikorski, R.S., Dante, M., Shero, J.H., and Hieter, P. (1992). Multifunctional yeast high-copy-number shuttle vectors. Gene *110*, 119-122.

Cintas, L.M., Casaus, P., Herranz, C., Nes, I.F., and Hernandez, P.E. (2001). Bacteriocins of lactic acid bacteria. Food Science and Technology International *7*, 281-305.

Cipáková, I.a.H., E. (2005). Production of the human-beta-defensin using Saccharomyces cerevisiae as a host. Protein and Peptide Letters *6*, 551-554.

Claro, F.B., Rijsbrack, K., and Soares, E.V. (2007). Flocculation onset in Saccharomyces cerevisiae: effect of ethanol, heat and osmotic stress. J Appl Microbiol *102*, 693-700.

Cleveland, J., Montville, T.J., Nes, I.F., and Chikindas, M.L. (2001). Bacteriocins: safe, natural antimicrobials for food preservation. International Journal of Food Microbiology *71*, 1-20.

Cole, A.M., Hong, T., Boo, L.M., Nguyen, T., Zhao, C., Bristol, G., Zack, J.A., Waring, A.J., Yang, O.O., and Lehrer, R.I. (2002). Retrocyclin: a primate peptide that protects cells from infection by T- and M-tropic strains of HIV-1. Proc Natl Acad Sci U S A *99*, 1813-1818.

Corrales-Garcia, L.L., Possani, L.D., and Corzo, G. (2011). Expression systems of human beta-defensins: vectors, purification and biological activities. Amino Acids *40*, 5-13.

Corran, H.S. (1975). A History of Brewing (London, UK).

Cotter, P.D., Hill, C., and Ross, R.P. (2005). Bacteriocins: developing innate immunity for food. Nat Rev Microbiol *3*, 777-788.

Cummings, C., and Fowler, T. (1996). Secretion of Trichoderma reesei beta-glucosidase by Saccharomyces cerevisiae. Current Genetics *29*, 227-233.

Dale, B.A., and Krisanaprakornkit, S. (2001). Defensin antimicrobial peptides in the oral cavity. J Oral Pathol Med *30*, 321-327.

David, L., Huber, W., Granovskaia, M., Toedling, J., Palm, C.J., Bofkin, L., Jones, T., Davis, R.W., and Steinmetz, L.M. (2006). A high-resolution map of transcription in the yeast genome. Proc Natl Acad Sci U S A *103*, 5320-5325.

Day, R.E., Rogers, P.J., Dawes, I.W., and Higgins, V.J. (2002). Molecular analysis of maltotriose transport and utilization by Saccharomyces cerevisiae. Appl Environ Microbiol *68*, 5326-5335.

de Angelo, J., and Siebert, K.J. (1987). A new medium for the detection of wild yeast in brewing culture yeast. Journal of the American Society of Brewing Chemists.

de Barros Lopes, M., Bellon, J.R., Shirley, N.J., and Ganter, P.F. (2002). Evidence for multiple interspecific hybridization in Saccharomyces sensu stricto species. FEMS Yeast Res *1*, 323-331.

de Leeuw, E., Li, C., Zeng, P., Diepeveen-de Buin, M., Lu, W.Y., Breukink, E., and Lu, W. (2010). Functional interaction of human neutrophil peptide-1 with the cell wall precursor lipid II. FEBS Lett *584*, 1543-1548.

De Smet, K., and Contreras, R. (2005). Human antimicrobial peptides: defensins, cathelicidins and histatins. Biotechnology Letters *27*, 1337-1347.

De, Y., Chen, Q., Schmidt, A.P., Anderson, G.M., Wang, J.M., Wooters, J., Oppenheim, J.J., and Chertov, O. (2000). LL-37, the neutrophil granule- and epithelial cell-derived cathelicidin, utilizes formyl peptide receptor-like 1 (FPRL1) as a receptor to chemoattract human peripheral blood neutrophils, monocytes, and T cells. J Exp Med *192*, 1069-1074.

Deinzer, M.L. (2006). Chemistry of hop polyphenols (Corvallis, Oregon).

Delves-Broughton, J., Blackburn, P., Evans, R.J., and Hugenholtz, J. (1996). Applications of the bacteriocin, nisin. Antonie Van Leeuwenhoek *69*, 193-202.

DeMan, J.D., Rogosa, M., and Sharpe, M.E. (1960). A Medium for the Cultivation of Lactobacilli. J. Appl. Bacteriol. *23*, 130-135.

Dhople, V., Krukemeyer, A., and Ramamoorthy, A. (2006). The human beta-defensin-3, an antibacterial peptide with multiple biological functions. Biochim Biophys Acta *1758*, 1499-1512.

Diamond, G., Beckloff, N., and Ryan, L.K. (2008). Host defense peptides in the oral cavity and the lung: similarities and differences. Journal of Dental Research *87*, 915-927.

Diamond, G., Zasloff, M., Eck, H., Brasseur, M., Maloy, W.L., and Bevins, C.L. (1991). Tracheal antimicrobial peptide, a cysteine-rich peptide from mammalian tracheal mucosa: peptide isolation and cloning of a cDNA. Proc Natl Acad Sci U S A *88*, 3952-3956.

Dielbandhoesing, S.K., Zhang, H., Caro, L.H., van der Vaart, J.M., Klis, F.M., Verrips, C.T., and Brul, S. (1998). Specific cell wall proteins confer resistance to nisin upon yeast cells. Appl Environ Microbiol *64*, 4047-4052.

Diep, D.B., and Nes, I.F. (2002). Ribosomally synthesized antibacterial peptides in Gram positive bacteria. Curr Drug Targets *3*, 107-122.

DiMichele, L.J., and Lewis, M.J. (1993). Rapid, species-specific detection of lactic acid bacteria from beer using the polymerase chain reaction. Journal of the American Society of Brewing Chemists *51*, 63-66.

Donalies, U.E., Nguyen, H.T., Stahl, U., and Nevoigt, E. (2008). Improvement of Saccharomyces yeast strains used in brewing, wine making and baking. Advances in Biochemical Engineering/Biotechnology *111*, 67-98.

Douglas, P., Meneses, F.J., and Jiranek, V. (2006). Filtration, haze and foam characteristics of fermented wort mediated by yeast strain. J Appl Microbiol *100*, 58-64.

Dowhanick, T.M., Sobczak, J., Presente, E., and Russell, I. (1995). Trial studies on the rapid quantitative detection of brewery microorganisms using a prototype ATP bioluminescence system In EBC Congress, pp. 645-651.

Dunn, B., and Sherlock, G. (2008). Reconstruction of the genome origins and evolution of the hybrid lager yeast Saccharomyces pastorianus. Genome Research *18*, 1610-1623.

Dunsche, A., Acil, Y., Siebert, R., Harder, J., Schroder, J.M., and Jepsen, S. (2001). Expression profile of human defensins and antimicrobial proteins in oral tissues. J. Oral. Pathol. Med. *30*, 154-158.

Dworkin, M and Falkow, S. (2006). The Prokaryotes: a handbook on the biology of bacteria. Proteobacteria: Alpha and Beta Subclasses, Volume 5 (Springer).

Favre, C., Aguilar, P.S., and Carrillo, M.C. (2008). Oxidative stress and chronological aging in glycogen-phosphorylase-deleted yeast. Free Radic Biol Med *45*, 1446-1456.

Fernandez, J.L., and Simpson, W.J. (1994). Cyclic growth of lactobacilli in beer. Journal of Applied Bacteriology *77*, 635-638.

Fleming, A. (1922). On a remarkable bacteriolytic element found in tissues and secretions Proceedings of the Royal Society *93*, 306-317.

Forster, A., Beck, B., Massinger, S., and Schmidt, R. (2003). The formation of low-molecular polyphenols during the growth of hops. In Proceedings of the Scientific Commision of International Hop Growers Convention, pp. 50-57.

Forte, L.F., Cortelli, S.C., Cortelli, J.R., Aquin, D.R., de Campos, M.V., Cogo, K., Costa, F.O., and Franco, G.C. (2010). Psychological stress has no association with salivary levels of β-defensin 2 and β-defensin 3. J. Oral. Pathol. Med. *39*, 765-769.

Franz, C.M., van Belkum, M.J., Holzapfel, W.H., Abriouel, H., and Galvez, A. (2007). Diversity of enterococcal bacteriocins and their grouping in a new classification scheme. FEMS Microbiol Rev *31*, 293-310.

Frohm, M., Agerberth, B., Ahangari, G., Stahle-Backdahl, M., Liden, S., Wigzell, H., and Gudmundsson, G.H. (1997). The expression of the gene coding for the antibacterial peptide LL-37 is induced in human keratinocytes during inflammatory disorders. The Journal of Biological Chemistry *272*, 15258-15263.

Frye, M., Bargon, J., Lembcke, B., Wagner, T.O., and Gropp, R. (2000). Differential expression of human alpha- and beta-defensins mRNA in gastrointestinal epithelia. Eur J Clin Invest *30*, 695-701.

Fujii, T., Nakashima, K., and Hayashi, N. (2005). Random amplified polymorphic DNA-PCR based cloning of markers to identify the beer-spoilage strains of Lactobacillus brevis, Pediococcus damnosus, Lactobacillus collinoides and Lactobacillus coryniformis. J Appl Microbiol *98*, 1209-1220.

Galvagno, M.A., Gil, G.R., Iannone, L.J., and Cerrutti, P. (2007). Exploring the use of natural antimicrobial agents and pulsed electric fields to control spoilage bacteria during a beer production process. Rev Argent Microbiol *39*, 170-176.

Ganz, T. (1999). Defensins and host defense. Science *286*, 420-421.

Ganz, T., Liu, L., Valore, E.V., and Oren, A. (1993). Posttranslational processing and targeting of transgenic human defensin in murine granulocyte, macrophage, fibroblast, and pituitary adenoma cell lines. Blood *82*, 641-650.

Ganz, T., Selsted, M. E., and Lehrer, R. I. (1990). Defensins. European Journal of Haematology *44*, 1-8.

Garcia, J.R., Jaumann, F., Schulz, S., Krause, A., Rodriguez-Jimenez, J., Forssmann, U., Adermann, K., Kluver, E., Vogelmeier, C., Becker, D., *et al.* (2001). Identification of a novel, multifunctional beta-defensin (human beta-defensin 3) with specific antimicrobial activity. Its interaction with plasma membranes of Xenopus oocytes and the induction of macrophage chemoattraction. Cell Tissue Res *306*, 257-264.

Gatignol, A., Dassain, M., and Tiraby, G. (1990). Cloning of Saccharomyces cerevisiae promoters using a probe vector based on phleomycin resistance. Gene *91*, 35-41.

Gazit, E., Miller, I.R., Biggin, P.C., Sansom, M.S.P., and Shai, Y. (1996). Structure and Orientation of the Mammalian Antibacterial Peptide Cecropin P1 within Phospholipid Membranes. J Mol Biol *258*, 860-870.

Gibson, B.R., Lawrence, S.J., Boulton, C.A., Box, W.G., Graham, N.S., Linforth, R.S., and Smart, K.A. (2008). The oxidative stress response of a lager brewing yeast strain during industrial propagation and fermentation. FEMS Yeast Res *8*, 574-585.

Gil, G., del Monaco, S., Cerrutti, P., and Galvagno, M. (2004). Selective antimicrobial activity of chitosan on beer spoilage bacteria and brewing yeasts. Biotechnol Lett *26*, 569-574.

Goldenthal, M.J., Vanoni, M., Buchferer, B., and Marmur, J. (1987). Regulation of MAL gene expression in yeast: gene dosage effects. Mol Gen Genet *209*, 508-517.

Goldman, M.J., Anderson, G.M., Stolzenberg, E.D., Kari, U.P., Zasloff, M., and Wilson, J.M. (1997). Human beta-defensin-1 is a salt-sensitive antibiotic in lung that is inactivated in cystic fibrosis. Cell *88*, 553-560.

Gonzalez, S.S., Barrio, E., and Querol, A. (2008). Molecular characterization of new natural hybrids of Saccharomyces cerevisiae and S. kudriavzevii in brewing. Appl Environ Microbiol *74*, 2314-2320.

Gonzalez, S.S., Gallo, L., Climent, M.A., Barrio, E. and Querol, A. (2007). Enological characterization of natural hybrids from Saccharomyces cerevisiae and S. kudriavzevii. International Journal of Food Microbiology *116*, 11-18.

Groth, C., Hansen, J., and Piskur, J. (1999). A natural chimeric yeast containing genetic material from three species. International Journal of Systematic Bacteriology *49*, 1933-1938.

Haakensen, M., Dobson, C.M., Hill, J.E., and Ziola, B. (2009). Reclassification of Pediococcus dextrinicus (Coster and White 1964) back 1978 (Approved Lists 1980) as Lactobacillus dextrinicus comb. nov., and emended description of the genus Lactobacillus. Int J Syst Evol Microbiol *59*, 615-621.

Haikara, A., and Lounatmaa, K. (1987). Characterization of Megasphaera sp., a new anaerobic beer spoilage coccus. In European Brewey Convention, Proceedings of the 21st Congress (Madrid, Spain, IRL Press, Oxford), pp. 473-480.

Halme, A., Bumgarner, S., Styles, C., and Fink, G.R. (2004). Genetic and epigenetic regulation of the FLO gene family generates cell-surface variation in yeast. Cell *116*, 405-415.

Han, E.K., Cotty, F., Sottas, C., Jiang, H., and Michels, C.A. (1995). Characterization of AGT1 encoding a general alpha-glucoside transporter from Saccharomyces. Mol Microbiol *17*, 1093-1107.

Hansen, E.C. (1883). Recherches sur la physiologie et la morphologie des ferments alcooliques V. Methodes pour obtenir des cultures pures de Saccharomyces et de mikroorganismes analogues. C.R. Trav. Lab. Carlsberg *2*, 92–105.

Harder, J., Bartels, J., Christophers, E., and Schroder, J.M. (1997). A peptide antibiotic from human skin. Nature *387*, 861.

Harder, J., Bartels, J., Christophers, E., and Schroder, J.M. (2001). Isolation and characterization of human beta-defensin-3, a novel human inducible peptide antibiotic. The Journal of Biological Chemistry *276*, 5707-5713.

Harder, J., Meyer-Hoffert, U., Wehkamp, K., Schwichtenberg, L., and Schroder, J. M. (2004). Differential gene induction of human beta-defensins (hBD-1, -2, -3, and -4) in keratinocytes is inhibited by retinoic acid. The Journal of Investigative Dermatology *123*, 522-529.

Hayashi, N., Ito, M., Horiike, S., and Taguchi, H. (2001). Molecular cloning of a putative divalent-cation transporter gene as a new genetic marker for the identification of Lactobacillus brevis strains capable of growing in beer. Applied Microbiology and Biotechnology *55*, 596-603.

Henning, S., Metz, R., and Hammes, W.P. (1986). New aspects for the application of nisin to foods based on its mode of action. International Journal of Food Microbiology *3*.

Hitzeman, R.A., Clarke, L., and Carbon, J. (1980). Isolation and characterization of the yeast 3-phosphoglycerokinase gene (PGK) by an immunological screening technique. The Journal of Biological Chemistry *255*, 12073-12080.

Hoffmann, J.A., Kafatos, F.C., Janeway, C.A., and Ezekowitz, R.A. (1999). Phylogenetic perspectives in innate immunity. Science *284*, 1313-1318.

Hong, S.H., and Marmur, J. (1987). Upstream regulatory regions controlling the expression of the yeast maltase gene. Mol Cell Biol *7*, 2477-2483.

Hoover, D.M., Boulegue, C., Yang, D., Oppenheim, J.J., Tucker, K., Lu, W. and Lubkowski, J. (2002). The structure of human macrophage inflammatory protein-3alpha /CCL20. Linking antimicrobial and CC chemokine receptor-6-binding activities with human beta-defensins. The Journal of Biological Chemistry *277*, 37647-37654.

Hoover, D.M., Chertov, O., and Lubkowski, J. (2001). The structure of human beta-defensin-1: new insights into structural properties of beta-defensins. The Journal of Biological Chemistry *276*, 39021-39026.

Hoover, D.M., Rajashankar, K.R., Blumenthal, R., Puri, A., Oppenheim, J.J., Chertov, O., and Lubkowski, J. (2000). The structure of human beta-defensin-2 shows evidence of higher order oligomerization. The Journal of Biological Chemistry *275*, 32911-32918.

Hoover, D.M., Wu, Z., Tucker, K., Lu, W., and Lubkowski, J. (2003). Antimicrobial characterization of human beta-defensin 3 derivatives. Antimicrob Agents Chemother *47*, 2804-2809.

Hough, J.S., Briggs, D.E., Stevens, R., and Young, T.W. (1982). Malting and Brewing Science, Vol 2 (London).

Hornsey, I. (2003). A history of beer and brewing. RSC Paperbacks, Cambride, UK.

Hsu, K.H., Pei, C., Yeh, J.Y., Shih, C.H., Chung, Y.C., Hung, L.T., and Ou, B.R. (2009). Production of bioactive human alpha-defensin 5 in Pichia pastoris. J Gen Appl Microbiol *55*, 395-401.

Huang, L., Wang, J., Zhong, Z., Peng, L., Chen, H., Xu, Z., and Cen, P. (2006). Production of bioactive human beta-defensin-3 in Escherichia coli by soluble fusion expression. Biotechnology Letters *28*, 627-632.

Huang L, X.Z., Zhong Z, Peng L, Chen H, Cen P (2007). Enhanced expression and primary purification of soluble HBD3 in Escherichia coli. Applied Biochemistry and Biotechnology *142*, 139-147.

Hughes, A.L., and Yeager, M. (1997). Coordinated amino acid changes in the evolution of mammalian defensins. Journal of Molecular Evolution *44*, 675-682.

Hwang, P.K., Tugendreich, S., and Fletterick, R.J. (1989). Molecular analysis of GPH1, the gene encoding glycogen phosphorylase in Saccharomyces cerevisiae. Mol Cell Biol *9*, 1659-1666.

Ilett, D.R. (1995). Aspects of the analysis, role, and fate of sulphur dioxide in beer – a review. Techincal Quaterly Master Brewers Association of the Americas *32*, 213-221.

Ingledew, W.M., and Casey, G.P. (1982). The use and understanding of media used in brewing microbiology. Brewers Digest *57*, 18-22.

Jack, R.W., Tagg, J.R., and Ray, B. (1995). Bacteriocins of gram-positive bacteria. Microbiol Rev *59*, 171-200.

James, T.C., Campbell, S., Donnelly, D., and Bond, U. (2003). Transcription profile of brewery yeast under fermentation conditions. J Appl Microbiol *94*, 432-448.

James, T.C., Usher, J., Campbell, S., and Bond, U. (2008). Lager yeasts possess dynamic genomes that undergo rearrangements and gene amplification in response to stress. Curr Genet *53*, 139-152.

Jang, B.C., Lim, K.J., Paik, J.H., Kwon, Y.K., Shin, S.W., Kim, S.C., Jung, T.Y., Kwon, T.K., Cho, J.W., Baek, W.K., Kim, S.P., Suh, M.H., and Suh, S.I. (2004). Up-regulation of human beta-defensin 2 by interleukin-1beta in A549 cells: involvement of PI3K, PKC, p38 MAPK, JNK, and NF-kappaB. Biochemical and Biophysical Research Communications *320*, 1026-1033.

Jansen, G., Wu, C., Schade, B., Thomas, D.Y., and Whiteway, M. (2005). Drag&Drop cloning in yeast. Gene *344*, 43-51.

Jenssen, H., Hamill, P., and Hancock, R.E. (2006). Peptide antimicrobial agents. Clin Microbiol Rev *19*, 491-511.

Jespersen, L., and Jakobsen, M. (1996). Specific spoilage organisms in breweries and laboratory media for their detection. Int J Food Microbiol *33*, 139-155.

Jespersen, L., Lassen, S., and Jakobsen, M. (1993). Flow cytometric detection of wild yeast in lager breweries. International Journal of Food Microbiology *17*, 321-328.

Ji, S., Shin, J.E., Kim, Y.S., Oh, J.E., Min, B.M., and Choi, Y. (2009). Toll-like receptor 2 and NALP2 mediate induction of human beta-defensins by fusobacterium nucleatum in gingival epithelial cells. Infect Immun *77*, 1044-1052.

Jia, H.P., Schutte, B.C., Schudy, A., Linzmeier, R., Guthmiller, J.M., Johnson, G.K., Tack, B.F., Mitros, J.P., Rosenthal, A., Ganz, T., and McCray, P.B., Jr. (2001). Discovery of new human beta-defensins using a genomics-based approach. Gene *263*, 211-218.

Jin, G., Kawsar, H.I., Hirsch, S.A., Zeng, C., Jia, X., Feng, Z., Ghosh, S.K., Zheng, Q.Y., Zhou, A., McIntyre, T.M., and Weinberg, A. (2010). An antimicrobial peptide regulates tumor-associated macrophage trafficking via the chemokine receptor CCR2, a model for tumorigenesis. PLoS One *5*, e10993.

Johnston, M., and Davis, R.W. (1984). Sequences that regulate the divergent GAL1-GAL10 promoter in Saccharomyces cerevisiae. Mol Cell Biol *4*, 1440-1448.

Kai-Larsen, Y., and Agerberth, B. (2008). The role of the multifunctional peptide LL-37 in host defense. Front Biosci *13*, 3760-3767.

Kaneda, H., Tsuchiya, Y., Takashio, M., Tamaki, T., and Shinotsuka, K. (1998). New techniques for rapid and sensitive detection and identification of beer spoilage organisms. Recent Research Developments in Fermentation and Bioengineering *1*, 115-128.

Kavalier, A.R., Litt, A., Ma, C., Pitra, N.J., Coles, M.C., Kennelly, E.J., and Matthews, P.D. (2011). Phytochemical and morphological characterization of hop (Humulus lupulus L.) cones over five developmental stages using high performance liquid chromatography coupled to time-of-flight mass spectrometry, ultrahigh performance liquid chromatography photodiode array detection, and light microscopy techniques. J Agric Food Chem *59*, 4783-4793.

Kielland-Brandt, M.C., T. Nillson-Tillgren, C. Gjermansen, S. Holmberg, and M. B. Pedersen (1995). Genetics of brewing yeasts. The Yeasts *6, Academic Press Ltd, London.*, 223-254.

Klaenhammer, T.R. (1993). Genetics of bacteriocins produced by lactic acid bacteria. FEMS Microbiol Rev *12*, 39-85.

Kluver, E., Schulz-Maronde, S., Scheid, S., Meyer, B., Forssmann, W.G., and Adermann, K. (2005). Structure-activity relation of human beta-defensin 3: influence of disulfide bonds and cysteine substitution on antimicrobial activity and cytotoxicity. Biochemistry *44*, 9804-9816.

Krieg, P. (1996). A laboratory guide to RNA: Isolation, analysis and synthesis. (New York: John Wiley).

Kumar, A., Harrison, P.M., Cheung, K.H., Lan, N., Echols, N., Bertone, P., Miller, P., Gerstein, M.B., and Snyder, M. (2002). An integrated approach for finding overlooked genes in yeast. Nat Biotechnol *20*, 58-63.

Lawrence, D.R. (1988). Spoilage organisms in beer (London: Elsevier).

Lawrence, S.J., Gibson, B.R. and Smart, K.A. (2009). Expression of the cell wall mannoprotein genes CWP and DAN during industrial-scale lager fermentations. Journal of the American Society of Brewing Chemists *67*, 58-62.

Lawrence, S.J.a.S., K.A (2007). Impact of CO2-induced anaerobiosis on the assessment of brewing yeast flocculation. Journal of the American Society of Brewing Chemists, 208-213.

Lay, F.T., and Anderson, M.A. (2005). Defensins--components of the innate immune system in plants. Curr Protein Pept Sci *6*, 85-101.

Lay, F.T., Brugliera, F., and Anderson, M.A. (2003). Isolation and properties of floral defensins from ornamental tobacco and petunia. Plant Physiol *131*, 1283-1293.

Le Jeune, C., Lollier, M., Demuyter, C., Erny, C., Legras, J.L., Aigle, M., and Masneuf-Pomarede, I. (2007). Characterization of natural hybrids of Saccharomyces cerevisiae and Saccharomyces bayanus var. uvarum. FEMS Yeast Res *7*, 540-549.

Legras, J.L., Merdinoglu, D., Cornuet, J.M., and Karst, F. (2007). Bread, beer and wine: Saccharomyces cerevisiae diversity reflects human history. Mol Ecol *16*, 2091-2102.

Lehmann, J., Retz, M., Harder, J., Krams, M., Kellner, U., Hartmann, J., Hohgrawe, K., Raffenberg, U., Gerber, M., Loch, T., *et al.* (2002). Expression of human beta-defensins 1 and 2 in kidneys with chronic bacterial infection. BMC Infect Dis *2*, 20.

Lehrer, R.I., Barton, A., Daher, K.A., Harwig, S.S., Ganz, T., and Selsted, M.E. (1989). Interaction of human defensins with Escherichia coli. Mechanism of bactericidal activity. J Clin Invest *84*, 553-561.

Lehrer, R.I., and Ganz, T. (2002). Defensins of vertebrate animals. Curr Opin Immunol *14*, 96-102.

Libkind, D., Hittinger, C.T., Valerio, E., Goncalves, C., Dover, J., Johnston, M., Goncalves, P., and Sampaio, J.P. (2011). Microbe domestication and the identification of the wild genetic stock of lager-brewing yeast. Proc Natl Acad Sci U S A *108*, 14539-14544.

Linzmeier, R., Ho, C.H., Hoang, B.V., and Ganz, T. (1999). A 450-kb contig of defensin genes on human chromosome 8p23. Gene *233*, 205-211.

Liti, G., Peruffo, A., James, S.A., Roberts, I.N., and Louis, E.J. (2005). Inferences of evolutionary relationships from a population survey of LTR-retrotransposons and telomeric-associated sequences in the Saccharomyces sensu stricto complex. Yeast *22*, 177–192.

Liu, L., Zhao, C., Heng, H.H., and Ganz, T. (1997). The human beta-defensin-1 and alpha-defensins are encoded by adjacent genes: two peptide families with differing disulfide topology share a common ancestry. Genomics *43*, 316-320.

Lopandic, K., Gangl, H., Wallner, E., Tscheik, G., Leitner, G., Querol, A., Borth, N., Breitenbach, M., Prillinger, H., and Tiefenbrunner, W. (2007). Genetically different wine yeasts isolated from Austrian vine-growing regions influence wine aroma differently and contain putative hybrids between Saccharomyces cerevisiae and Saccharomyces kudriavzevii. FEMS Yeast Research *7*, 953-965.

Lundin, M., Nehlin, J.O., and Ronne, H. (1994). Importance of a flanking AT-rich region in target site recognition by the GC box-binding zinc finger protein MIG1. Mol Cell Biol *14*, 1979-1985.

Lynn, D.J., Lloyd, A.T., Fares, M.A., and O'Farrelly, C. (2004). Evidence of positively selected sites in mammalian alpha-defensins. Molecular Biology and Evolution *21*, 819-827.

Mable, B.K., and Otto, S.P. (2001). Masking and purging mutations following EMS treatment in haploid, diploid and tetraploid yeast (Saccharomyces cerevisiae). Genet Res *77*, 9-26.

MacKay, B.J., Pollock, J.J., Iacono, V.J., and Baum, B.J. (1984). Isolation of milligram quantities of a group of histidine-rich polypeptides from human parotid saliva. Infection and Immunity *44*, 688-694.

Maget-Dana, R., and Peypoux, F. (1994). Iturins, a special class of pore-forming lipopeptides: biological and physicochemical properties. Toxicology *87*, 151-174.

Maisetta, G., Batoni, G., Esin, S., Florio, W., Bottai, D., Favilli, F., and Campa, M. (2006). In vitro bactericidal activity of human beta-defensin 3 against multidrug-resistant nosocomial strains. Antimicrob Agents Chemother *50*, 806-809.

Mandel, I.D. (1987). The functions of saliva. J Dent Res *66 Spec No*, 623-627.

Masneuf, I., Hansen, J., Groth, C., Piskur, J., and Dubourdieu, D. (1998). New hybrids between Saccharomyces sensu stricto yeast species found among wine and cider production strains. Appl Environ Microbiol *64*, 3887-3892.

Martini, A.V., and Kurztman, C.P. (1985). Deoxyribonucleic acid relatedness among species of the genus Saccharomyces sensu stricto. Int. J. Syst. Bacteriol. *35*, 508–511.

Martini, A.V., and Martini, A. (1987). Three newly delimited species of Saccharomyces sensu stricto. Antonie van Leeuwenhoek *53*, 77-84.

Masuko, M., Kataoka, T., Sugiyama, N., Uchiyama, S., Sugiyama, H., Tarui, K., Kamiya, K., and Kawai, S. (1992). A photon counting TV camera equipped with an image guide for rapid detection and counting of single bacteria in a wide field. Photochemistry and Photobiology *56*, 107-111.

Mattick, A.T.R., and Hirsch, A. (1947). Further observations on an inhibitory substance (nisin) from lactic streptococci. Lancet *2*, 5-7.

Menz, G., Andrighetto, C., Lombardi, A., Corich, V., Aldred, P., and Vriesekoop, F. (2010). Isolation, Identification, and Characterisation of Beer-Spoilage Lactic Acid Bacteria from Microbrewed Beer from Victoria, Australia. J. Inst. Brew. *116*, 14-22.

Miller, R., and Galston, G. (1989). Rapid methods for the detection of yeast and lactobacillus by ATP bioluminescence The Journal of the The Institute of Brewing and Distilling *95*, 317-319.

Miller, T.L., and Wolin, M.J. (1974). A serum bottle modification of the Hungate technique for cultivating obligate anaerobes. Appl Microbiol *27*, 985-987.

Miura, F., Kawaguchi, N., Sese, J., Toyoda, A., Hattori, M., Morishita, S., and Ito, T. (2006). A large-scale full-length cDNA analysis to explore the budding yeast transcriptome. Proc Natl Acad Sci U S A *103*, 17846-17851.

Mizukawa, N., Sugiyama, K., Kamio, M., Yamachika, E., Ueno, T., Fukunaga, J., Takagi, S., and Sugahara, T. (2000). Immunohistochemical staining of human alpha-defensin-1 (HNP-1), in the submandibular glands of patients with oral carcinomas. Anticancer Res *20*, 1125-1127.

Moon, S.K., Lee, H.Y., Li, J.D., Nagura, M., Kang, S.H., Chun, Y.M., Linthicum, F.H., Ganz, T., Andalibi, A., and Lim, D.J. (2002). Activation of a Src-dependent Raf-MEK1/2-ERK signaling pathway is required for IL-1alpha-induced upregulation of beta-defensin 2 in human middle ear epithelial cells. Biochimica et biophysica acta *1590*, 41-51.

Moorer, W.R. (2003). Antiviral activity of alcohol for surface disinfection. Int J Dent Hyg *1*, 138-142.

Morgera, F., Antcheva, N., Pacor, S., Quaroni, L., Berti, F., Vaccari, L., and Tossi, A. (2008). Structuring and interactions of human beta defensin 2 and 3 with model membranes. Journal of Peptide Science *14*, 518-523.

Morton, C.O., Dos Santos, S.C., and Coote, P. (2007a). An amphibian-derived, cationic, alpha-helical antimicrobial peptide kills yeast by caspase-independent but AIF-dependent programmed cell death. Mol Microbiol *65*, 494-507.

Morton, C.O., Hayes, A., Wilson, M., Rash, B.M., Oliver, S.G., and Coote, P. (2007b). Global phenotype screening and transcript analysis outlines the inhibitory mode(s) of action of two amphibian-derived, alpha-helical, cationic peptides on Saccharomyces cerevisiae. Antimicrob Agents Chemother *51*, 3948-3959.

Moyne, A.L., Shelby, R., Cleveland, T.E., and Tuzun, S. (2001). Bacillomycin D: an iturin with antifungal activity against Aspergillus flavus. J Appl Microbiol *90*, 622-629.

Munk, C., Wei, G., Yang, O.O., Waring, A.J., Wang, W., Hong, T., Lehrer, R.I., Landau, N.R., and Cole, A.M. (2003). The theta-defensin, retrocyclin, inhibits HIV-1 entry. AIDS Res Hum Retroviruses *19*, 875-881.

Nakao, Y., Kanamori, T., Itoh, T., Kodama, Y., Rainieri, S., Nakamura, N., Shimonaga, T., Hattori, M., and Ashikari, T. (2009). Genome sequence of the lager brewing yeast, an interspecies hybrid. DNA Res *16*, 115-129.

Naumov, G.I., James, S.A., Naumova, E.S., Louis, E.J., and Roberts, I.N. (2000). Three new species in the Saccharomyces sensu stricto complex: Saccharomyces cariocanus, Saccharomyces kudriavzevii and Saccharomyces mikatae. Int J Syst Evol Microbiol *50 Pt 5*, 1931-1942.

Nes, I.F., Diep, D.B., Havarstein, L.S., Brurberg, M.B., Eijsink, V., and Holo, H. (1996). Biosynthesis of bacteriocins in lactic acid bacteria. Antonie Van Leeuwenhoek *70*, 113-128.

Nes, I.F., Diep, D.B., and Holo, H. (2007). Bacteriocin diversity in Streptococcus and Enterococcus. Journal of Bacteriology *189*, 1189-1198.

Neve, R.A. (1991). Hops (London, England: Chapman and Hall).

Nissen-Meyer, J., and Nes, I.F. (1997). Ribosomally synthesized antimicrobial peptides: their function, structure, biogenesis, and mechanism of action. Arch Microbiol *167*, 67-77.

Nuding, S., Zabel, L.T., Enders, C., Porter, E., Fellermann, K., Wehkamp, J., Mueller, H.A., and Stange, E.F. (2009). Antibacterial activity of human defensins on anaerobic intestinal bacterial species: a major role of HBD-3. Microbes Infect *11*, 384-393.

Odgen, K., and Tubb, R.S. (1985). Inhibition of beer-spoilage lactic acid bacteria by nisin The Journal of the The Institute of Brewing and Distilling *91*.

Odgen, K., Waites, M.J., and Hammond, J.R.M. (1988). Nisin and brewing. The Journal of the The Institute of Brewing and Distilling *94*.

Ogden, K. (1986). Nisin: a bacteriocin with potential use in brewing The Journal of the The Institute of Brewing and Distilling *92*, 379-383.

Oppenheim, J.J., Biragyn, A., Kwak, L.W., and Yang, D. (2003). Roles of antimicrobial peptides such as defensins in innate and adaptive immunity. Ann Rheum Dis *62 Suppl 2*, ii17-21.

Ouellette, A.J. (1999). IV. Paneth cell antimicrobial peptides and the biology of the mucosal barrier. Am J Physiol *277*, G257-261.

Overk, C.R., Yao, P., Chadwick, L.R., Nikolic, D., Sun, Y., Cuendet, M.A., Deng, Y., Hedayat, A.S., Pauli, G.F., Farnsworth, N.R., *et al.* (2005). Comparison of the in vitro estrogenic activities of compounds from hops (Humulus lupulus) and red clover (Trifolium pratense). J Agric Food Chem *53*, 6246-6253.

Pag, U., Oedenkoven, M., Papo, N., Oren, Z., Shai, Y., and Sahl, H.G. (2004). In vitro activity and mode of action of diastereomeric antimicrobial peptides against bacterial clinical isolates. J Antimicrob Chemother *53*, 230-239.

Papagianni, M. (2003). Ribosomally synthesized peptides with antimicrobial properties: biosynthesis, structure, function, and applications. Biotechnol Adv *21*, 465-499.

Paquette, D.W., Simpson, D.M., Friden, P., Braman, V., and Williams, R.C. (2002). Safety and clinical effects of topical histatin gels in humans with experimental gingivitis. J Clin Periodontol *29*, 1051-1058.

Partow, S., Siewers, V., Bjorn, S., Nielsen, J., and Maury, J. (2010). Characterization of different promoters for designing a new expression vector in Saccharomyces cerevisiae. Yeast *27*, 955-964.

Pazgier, M., Hoover, D.M., Yang, D., Lu, W., and Lubkowski, J. (2006). Human beta-defensins. Cell Mol Life Sci *63*, 1294-1313.

Pazgier, M., Li, X., Lu, W., and Lubkowski, J. (2007a). Human defensins: synthesis and structural properties. Curr Pharm Des *13*, 3096-3118.

Pazgier, M., Prahl, A., Hoover, D.M., and Lubkowski, J. (2007b). Studies of the biological properties of human beta-defensin 1. The Journal of Biological Chemistry *282*, 1819-1829.

Penttila, M.E., Andre, L., Lehtovaara, P., Bailey, M., Teeri, T.T., and Knowles, J.K. (1988). Efficient secretion of two fungal cellobiohydrolases by Saccharomyces cerevisiae. Gene *63*, 103-112.

Perez-Canadillas, J.M., Zaballos, A., Gutierrez, J., Varona, R., Roncal, F., Albar, J.P., Marquez, G., and Bruix, M. (2001). NMR solution structure of murine CCL20/MIP-3alpha, a chemokine that specifically chemoattracts immature dendritic cells and lymphocytes through its highly specific interaction with the beta-chemokine receptor CCR6. The Journal of Biological Chemistry *276*, 28372-28379.

Peterson S.W., and Kurtzman C.P. (1991). Ribosomal RNA sequence divergence among sibling species of yeasts. Syst. Appl. Microbiol. *14*, 124–129

Powell, C.D., Quain, D.E., and Smart, K.A. (2003). The impact of brewing yeast cell age on fermentation performance, attenuation and flocculation. FEMS Yeast Res *3*, 149-157.

Powell, C.D.a.D., A.N. (2007). Long term serial repitching and the genetic and phenotypic stability of brewer's yeast. Journal of the Institute of Brewing *113*.

Priest, F.G. (1981). Contamination (London: The Institute of Brewing).

Querol, A., and Bond, U. (2009). The complex and dynamic genomes of industrial yeasts. FEMS Microbiol Lett *293*, 1-10.

Radler, F. (1990a). Possible use of nisin in winemaking I. Action of nisin against lactic acid bacteria and wine yeasts in solid and liquid media. American Journal of Enology and Viticulture *41*, 1-6.

Radler, F. (1990b). Possible use of nisin in winemaking II. Experiments to control lactic acid bacteria in production of wine. American Journal of Enology and Viticulture *41*, 7-11.

Rainbow, C. (1981). Beer Spoilage Microorganisms. In Brewing Science, J.R.A. Pollock., ed. (London).

Rainieri, S., Kodama, Y., Kaneko, Y., Mikata, K., Nakao, Y., and Ashikari, T. (2006). Pure and mixed genetic lines of Saccharomyces bayanus and Saccharomyces pastorianus and their contribution to the lager brewing strain genome. Appl Environ Microbiol *72*, 3968-3974.

Raj, P.A., Marcus, E., and Sukumaran, D.K. (1998). Structure of human salivary histatin 5 in aqueous and nonaqueous solutions. Biopolymers *45*, 51-67.

Roemer, T., and Bussey, H. (1991). Yeast beta-glucan synthesis: KRE6 encodes a predicted type II membrane protein required for glucan synthesis in vivo and for glucan synthase activity in vitro. Proc Natl Acad Sci U S A *88*, 11295-11299.

Rothstein, D.M., Spacciapoli, P., Tran, L.T., Xu, T., Roberts, F.D., Dalla Serra, M., Buxton, D.K., Oppenheim, F.G., and Friden, P. (2001). Anticandida activity is retained in P-113, a 12-amino-acid fragment of histatin 5. Antimicrob Agents Chemother *45*, 1367-1373.

Rouxhet, P.B.D.a.P.G. (1997). Surface properties of Top- and Bottom-Fermenting Yeast. Yeast *13*, 931-943.

Sabatini, L.M., Ota, T., and Azen, E.A. (1993). Nucleotide sequence analysis of the human salivary protein genes HIS1 and HIS2, and evolution of the STATH/HIS gene family. Mol Biol Evol *10*, 497-511.

Saerens, S.M., Verbelen, P.J., Vanbeneden, N., Thevelein, J.M., and Delvaux, F.R. (2008). Monitoring the influence of high-gravity brewing and fermentation temperature on flavour formation by analysis of gene expression levels in brewing yeast. Applied Microbiology and Biotechnology *80*, 1039-1051.

Sahl, H.G. (1994). Gene-encoded antibiotics made in bacteria (New York: Wiley).

Sakamoto, K., and Konings, W.N. (2003). Beer spoilage bacteria and hop resistance. International Journal of Food Microbiology *89*, 105-124.

Sakamoto, K., Margolles, A., van Veen, H.W., and Konings, W.N. (2001). Hop resistance in the beer spoilage bacterium Lactobacillus brevis is mediated by the ATP-binding cassette multidrug transporter HorA. Journal of Bacteriology *183*, 5371-5375.

Sakamoto, K., Van Veen, H.W., Saito, H., Kobayashi, H., and Konings, W.N. (2002). Membrane-bound ATPase contributes to hop resistance of Lactobacillus brevis. Appl Environ Microbiol *68*, 5374-5378.

Salema-Oom, M., Valadao Pinto, V., Goncalves, P., and Spencer-Martins, I. (2005). Maltotriose utilization by industrial Saccharomyces strains: characterization of a new member of the alpha-glucoside transporter family. Appl Environ Microbiol *71*, 5044-5049.

Sami, M., and Yamashita, H. (1997). A new and rapid method for determination of beer-spoilage ability of Lactobacilli. Journal of the American Society of Brewing Chemists *55*, 137-140.

Sami, M., Yamashita, H., Hirono, T., Kadokura, H., Kitamoto, K., Yoda, K., and Yamasaki, M. (1997). Hop-resistant Lactobacillus brevis contains a novel plasmid harboring a multidrug resistance-like gene. Journal of Fermentation and Bioengineering, 1-6.

Sampaio, J.P., and Goncalves, P. (2008). Natural populations of Saccharomyces kudriavzevii in Portugal are associated with oak bark and are sympatric with S. cerevisiae and S. paradoxus. Appl Environ Microbiol *74*, 2144-2152.

Sampermans, S., Mortier, J., and Soares, E.V. (2005). Flocculation onset in Saccharomyces cerevisiae: the role of nutrients. J Appl Microbiol *98*, 525-531.

Sass, V., Pag, U., Tossi, A., Bierbaum, G., and Sahl, H.G. (2008). Mode of action of human beta-defensin 3 against Staphylococcus aureus and transcriptional analysis of responses to defensin challenge. Int J Med Microbiol *298*, 619-633.

Sato, M., Kishimoto, M., Watari, J., and Takashio, M. (2002). Breeding of brewer's yeast by hybridization between a top-fermenting yeast Saccharomyces cerevisiae and a cryophilic yeast Saccharomyces bayanus. Journal of Bioscience and Bioengineering *93*, 509-511.

Sawai, M.V., Jia, H.P., Liu, L., Aseyev, V., Wiencek, J.M., McCray, P.B., Jr., Ganz, T., Kearney, W.R., and Tack, B.F. (2001). The NMR structure of human beta-defensin-2 reveals a novel alpha-helical segment. Biochemistry *40*, 3810-3816.

Scharf, S., Vardarova, K., Lang, F., Schmeck, B., Opitz, B., Flieger, A., Heuner, K., Hippenstiel, S., Suttorp, N., and N'Guessan, P.D. (2010). Legionella pneumophila induces human beta defensin-3 in pulmonary cells. Respiratory Research *11*, 93.

Schibli, D.J., Hunter, H.N., Aseyev, V., Starner, T.D., Wiencek, J.M., McCray, P.B., Jr., Tack, B.F., and Vogel, H.J. (2002). The solution structures of the human beta-defensins lead to a better understanding of the potent bactericidal activity of HBD3 against Staphylococcus aureus. J Biol Chem *277*, 8279-8289.

Schiller, M., and Busch, Jim. (1993). Reinheitsgebot and the Fifth Ingrediant. Brewing Techniques.

Schleifer, K.H., Kraus, J., Dvorak, C., Kilpper-Balz, R., Collins, M.D., and Fischer, W. (1985). Transfer of Streptococcus lactis and related streptococci to the genus Lactococcus gen. nov. Systematic and Applied Microbiology *6*, 183-195.

Schleifer, K.H., Leuteritz, M., Weiss, N., Ludwig, W., Kirchhof, G., and Seidel-Rufer, H. (1990). Taxonomic study of anaerobic, gram-negative, rod-shaped bacteria from breweries: emended description of Pectinatus cerevisiiphilus and description of Pectinatus frisingensis sp. nov., Selenomonas lacticifex sp. nov., Zymophilus raffinosivorans gen. nov., sp. nov., and Zymophilus paucivorans sp. nov. Int J Syst Bacteriol *40*, 19-27.

Schoeman, H., Vivier, M.A., Toit, M.D., Dicks, L.M.T., and Pretorius, I.S. (1999). The Development of Bactericidal Yeast Strains by Expressing the Pediococcus acidilactici Pediocin Gene (pedA) in Saccharomyces cerevisiae. Yeast *15*, 647-656.

Schroder, J.M., and Harder, J. (1999). Human-defensins-2. The International Journal of Biochemistry & Cell Biology *31*, 645-651.

Schroeder, B.O., Wu, Z., Nuding, S., Groscurth, S., Marcinowski, M., Beisner, J., Buchner, J., Schaller, M., Stange, E.F., and Wehkamp, J. (2011). Reduction of disulphide bonds unmasks potent antimicrobial activity of human beta-defensin 1. Nature *469*, 419-423.

Schulz, A., Kluver, E., Schulz-Maronde, S., and Adermann, K. (2005). Engineering disulfide bonds of the novel human beta-defensins hBD-27 and hBD-28: differences in disulfide formation and biological activity among human beta-defensins. Biopolymers *80*, 34-49.

Schutte, B.C., Mitros, J.P., Bartlett, J.A., Walters, J.D., Jia, H.P., Welsh, M.J., Casavant, T.L., and McCray, P.B., Jr. (2002). Discovery of five conserved beta -defensin gene clusters using a computational search strategy. Proc Natl Acad Sci U S A *99*, 2129-2133.

Seeboth, P.G., and Heim, J. (1991). In-vitro processing of yeast alpha-factor leader fusion proteins using a soluble yscF (Kex2) variant. Applied Microbiology and Biotechnology *35*, 771-776.

Seidel, A., Ye, Y., de Armas, L.R., Soto, M., Yarosh, W., Marcsisin, R.A., Tran, D., Selsted, M.E., and Camerini, D. (2010). Cyclic and acyclic defensins inhibit human immunodeficiency virus type-1 replication by different mechanisms. PLoS One *5*, e9737.

Shelburne, C.E., Coulter, W.A., Olguin, D., Lantz, M.S., and Lopatin, D.E. (2005). Induction of {beta}-defensin resistance in the oral anaerobe Porphyromonas gingivalis. Antimicrob Agents Chemother *49*, 183-187.

Sherman, H., Chapnik, N., and Froy, O. (2006). Albumin and amino acids upregulate the expression of human beta-defensin 1. Molecular Immunology *43*, 1617-1623.

Si, L.G., Liu, X.C., Lu, Y.Y., Wang, G.Y., and Li, W.M. (2007). Soluble expression of active human beta-defensin-3 in Escherichia coli and its effects on the growth of host cells. Chinese Medical Journal *120*, 708-713.

Si Li-gang, L.X.-c., LU You-yong, WANG Gen-yu and LI Wen-mei (2007). Soluble expression of active human β-defensin-3 in *Escherichia coli* and its effects on the growth of host cells Chinese Medical Journal *120*, 708-713.

Sikorski, R.S., and Hieter, P. (1989). A system of shuttle vectors and yeast host strains designed for efficient manipulation of DNA in Saccharomyces cerevisiae. Genetics *122*, 19-27.

Simpson, W. (1993). Cambridge prize lecture, studies on the sensitivity of lactic acid bacteria to hop bitter acids. Journal of the Institute of Brewing *99*, 405-411.

Simpson, W., and Hughes, P.S. (1993). Cooperative binding of potassium ions to trans-isohumulone in the presence of divalent and trivalent cations. Bioorganic and Medicinal Chemistry Letters *3*, 769-772.

Simpson, W., and Smith, A. (1992). Factors affecting antibacterial activity of hop compounds and their derivatives. Journal of Applied Bacteriology, 327-334.

Simpson, W.J., and Fernandez, J.L. (1994). Mechanism of the resistance of lactic acid bacteriato trans-isohumulone. Journal of the American Society of Brewing Chemists *52*, 9-11.

Sinensky, M. (1974). Homeoviscous adaptation--a homeostatic process that regulates the viscosity of membrane lipids in Escherichia coli. Proc Natl Acad Sci U S A *71*, 522-525.

Smart, K.A.a.W., S (1996). Effect of serial repitching on the fermentation properties and condition of brewing yeast. Journal of the American Society of Brewing Chemists *54*, 41-44.

Smukalla, S., Caldara, M., Pochet, N., Beauvais, A., Guadagnini, S., Yan, C., Vinces, M.D., Jansen, A., Prevost, M.C., Latge, J.P., *et al.* (2008). FLO1 is a variable green beard gene that drives biofilm-like cooperation in budding yeast. Cell *135*, 726-737.

Sniegowski, P.D., Dombrowski, P.G., and Fingerman, E. (2002). Saccharomyces cerevisiae and Saccharomyces paradoxus coexist in a natural woodland site in North America and display different levels of reproductive isolation from European conspecifics. FEMS *1*, 299-306.

Sperandio, B., Regnault, B., Guo, J., Zhang, Z., Stanley, S.L., Jr., Sansonetti, P.J., and Pedron, T. (2008). Virulent Shigella flexneri subverts the host innate immune response through manipulation of antimicrobial peptide gene expression. The Journal of Experimental Medicine *205*, 1121-1132.

Starner, T.D., Agerberth, B., Gudmundsson, G.H., and McCray, P.B., Jr. (2005). Expression and activity of beta-defensins and LL-37 in the developing human lung. J Immunol *174*, 1608-1615.

Steiner, H., Hultmark, D., Engstrom, A., Bennich, H., and Boman, H.G. (1981). Sequence and specificity of two antibacterial proteins involved in insect immunity. Nature *292*, 246-248.

Steinmetz, E.J., Warren, C.L., Kuehner, J.N., Panbehi, B., Ansari, A.Z., and Brow, D.A. (2006). Genome-wide distribution of yeast RNA polymerase II and its control by Sen1 helicase. Mol Cell *24*, 735-746.

Steubesand, N., Kiehne, K., Brunke, G., Pahl, R., Reiss, K., Herzig, K.H., Schubert, S., Schreiber, S., Folsch, U.R., Rosenstiel, P., and Arlt, A. (2009). The expression of the beta-defensins hBD-2 and hBD-3 is differentially regulated by NF-kappaB and MAPK/AP-1 pathways in an in vitro model of Candida esophagitis. BMC Immunol *10*, 36.

Stevens, J.F., Ivancic, M., Hsu, V.L., and Deinzer, M.L. (1997). Prenylflavonoids from Humulus lupulus. Phytochemistry *44*, 1575-1585.

Storm, D.R., Rosenthal, K.S., and Swanson, P.E. (1977). Polymyxin and related peptide antibiotics. Annu Rev Biochem *46*, 723-763.

Tao, R., Jurevic, R.J., Coulton, K.K., Tsutsui, M.T., Roberts, M.C., Kimball, J.R., Wells, N., Berndt, J., and Dale, B.A. (2005). Salivary Antimicrobial Peptide Expression and Dental Caries experience in Children. Antimicrobial Agents and Chemotherapy *49*, 3883-3888.

Taxis, C., and Knop, M. (2006). System of centromeric, episomal, and integrative vectors based on drug resistance markers for Saccharomyces cerevisiae. Biotechniques *40*, 73-78.

Taylor, A.W., Barofsky, E., Kennedy, J.A., and Deinzer, M.L. (2003). Hop (Humulus lupulus L.) proanthocyanidins characterized by mass spectrometry, acid catalysis, and gel permeation chromatography. J Agric Food Chem *51*, 4101-4110.

Territo, M.C., Ganz, T., Selsted, M.E., and Lehrer, R. (1989). Monocyte-chemotactic activity of defensins from human neutrophils. J Clin Invest *84*, 2017-2020.

Thastum, S., and Jakobsen, M. (1981). Psychotrophic bacteria as spoilage organisms in lager breweries In Proceedings of the 11th International Symposium on Food Microbiology (London, Academic Press), pp. 322-325.

Thorpe, P.H., Gonzalez-Barrera, S., and Rothstein, R. (2007). More is not always better: the genetic constraints of polyploidy. Trends Genet *23*, 263-266.

Thurston, P.A. (1986). Detection and control of contaminants in pitching yeast. In Symposium on Brewers' Yeast, Monograph XII (European Brewer's Convention), pp. 84-92.

Timke, M., Wang-Lieu, N.Q., Altendorf, K., and Lipski, A. (2005). Fatty acid analysis and spoilage potential of biofilms from two breweries. J Appl Microbiol *99*, 1108-1122.

Timke, M., Wolking, D., Wang-Lieu, N.Q., Altendorf, K., and Lipski, A. (2004). Microbial composition of biofilms in a brewery investigated by fatty acid analysis, fluorescence in situ hybridisation and isolation techniques. Applied Microbiology and Biotechnology *66*, 100-107.

Tsai, H., and Bobek, L.A. (1997). Human salivary histatin-5 exerts potent fungicidal activity against Cryptococcus neoformans. Biochimica et biophysica acta *1336*, 367-369.

Tsuchiya, Y., Kaneda, H., Kano, Y., and Koshino, S. (1992). Detection of beer spoilage organisms by polymerase chain reaction technology. Journal of the American Society of Brewing Chemists *50*, 64-67.

Tsuchiya, Y., Kano, Y., and Koshino, S. (1993). Detection of Lactobacillus brevis in beer using polymerase chain reaction technology Journal of the American Society of Brewing Chemists *51*, 40-41.

Tsuchiya, Y., Kano, Y., and Koshino, S. (1994). Identification of lactic acid bacteria using temperature gradient gel electrophoresis for DNA fragment amplified by

polymerase chain reaction Journal of the American Society of Brewing Chemists *52*, 95-99.

Usher, J., and Bond, U. (2009). Recombination between homoeologous chromosomes of lager yeasts leads to loss of function of the hybrid GPH1 gene. Appl Environ Microbiol *75*, 4573-4579.

Valore, E.V., and Ganz, T. (1997). Laboratory production of antimicrobial peptides in native conformation. Methods Mol Biol *78*, 115-131.

van der Aa Kuhle, A., and Jespersen, L. (1998). Detection and identification of wild yeasts in lager breweries. International Journal of Food Microbiology *43*, 205-213.

van der Weerden, N.L., Hancock, R.E., and Anderson, M.A. (2010). Permeabilization of fungal hyphae by the plant defensin NaD1 occurs through a cell wall-dependent process. The Journal of Biological Chemistry *285*, 37513-37520.

Van Holle, A., Machado, M.D., and Soares, E.V. (2011). Flocculation in ale brewing strains of Saccharomyces cerevisiae: re-evaluation of the role of cell surface charge and hydrophobicity. Applied Microbiology and Biotechnology.

Van Reenen, C.A., Chikindas, M.L., Van Zyl, W.H., and Dicks, L.M. (2003). Characterization and heterologous expression of a class IIa bacteriocin, plantaricin 423 from Lactobacillus plantarum 423, in Saccharomyces cerevisiae. International Journal of Food Microbiology *81*, 29-40.

van Vuuren, H.J.J. (1996). Gram-negative spoilage bacteria (London: Elsevier).

vanderSpek, J.C., Wyandt, H.E., Skare, J.C., Milunsky, A., Oppenheim, F.G., and Troxler, R.F. (1989). Localization of the genes for histatins to human chromosome 4q13 and tissue distribution of the mRNAs. Am J Hum Genet *45*, 381-387.

Varoga, D., Wruck, C.J., Tohidnezhad, M., Brandenburg, L., Paulsen, F., Mentlein, R., Seekamp, A., Besch, L., and Pufe, T. (2009). Osteoblasts participate in the innate

immunity of the bone by producing human beta defensin-3. Histochem Cell Biol *131*, 207-218.

Vaughan, A., OSullivan, T., and van Sinderen, D. (2005). Enhancing the microbiological stability of malt and beer—a review. Journal of the Institute of Brewing *111*, 355-371.

Vaughan, A., Rouse, S., and van Sinderen, D. (2004). Investigating the antimicrobial efficacy of a lactococcal bacteriocin for the development of microbiologically stable beer. Journal of the Institute of Brewing *110*, 181-188.

Vaughan-Martini, A., and Martini, A. (1995). Facts, myths and legends on the prime industrial microorganism. J Ind Microbiol *14*, 514-522.

Venkataraman, N., Cole, A.L., Ruchala, P., Waring, A.J., Lehrer, R.I., Stuchlik, O., Pohl, J., and Cole, A.M. (2009). Reawakening retrocyclins: ancestral human defensins active against HIV-1. PLoS Biol *7*, e95.

Verstrepen, K.J., Derdelinckx, G., Verachtert, H., and Delvaux, F.R. (2003). Yeast flocculation: what brewers should know. Applied Microbiology and Biotechnology *61*, 197-205.

Vidgren, V., Kankainen, M., Londesborough, J., and Ruohonen, L. (2011). Identification of regulatory elements in the AGT1 promoter of ale and lager strains of brewer's yeast. Yeast *28*, 579-594.

Vidgren, V., Ruohonen, L., and Londesborough, J. (2005). Characterization and functional analysis of the MAL and MPH Loci for maltose utilization in some ale and lager yeast strains. Appl Environ Microbiol *71*, 7846-7857.

Wan, M., Godson, C., Guiry, P.J., Agerberth, B., and Haeggstrom, J.Z. (2011). Leukotriene B4/antimicrobial peptide LL-37 proinflammatory circuits are mediated by BLT1 and FPR2/ALX and are counterregulated by lipoxin A4 and resolvin E1. Faseb J *25*, 1697-1705.

Wang, S.A., and Bai, F.Y. (2008). Saccharomyces arboricolus sp. nov., a yeast species from tree bark. Int J Syst Evol Microbiol *58*, 510-514.

Weghuber, J., Aichinger, M.C., Brameshuber, M., Wieser, S., Ruprecht, V., Plochberger, B., Madl, J., Horner, A., Reipert, S., Lohner, K., *et al.* (2011). Cationic amphipathic peptides accumulate sialylated proteins and lipids in the plasma membrane of eukaryotic host cells. Biochimica et biophysica acta *1808*, 2581-2590.

Wehkamp, J., Harder, J., Wehkamp, K., Wehkamp-von Meissner, B., Schlee, M., Enders, C., Sonnenborn, U., Nuding, S., Bengmark, S., Fellermann, K., Schroder, J.M., and Stange, E.F. (2004). NF-kappaB- and AP-1-mediated induction of human beta defensin-2 in intestinal epithelial cells by Escherichia coli Nissle 1917: a novel effect of a probiotic bacterium. Infection and Immunity 72, 5750-5758.

Wehkamp, J., Harder, J., Weichenthal, M., Schwab, M., Schaffeler, E., Schlee, M., Herrlinger, K.R., Stallmach, A., Noack, F., Fritz, P., *et al.* (2004). NOD2 (CARD15) mutations in Crohn's disease are associated with diminished mucosal alpha-defensin expression. Gut *53*, 1658-1664.

Wehkamp, K., Schwichtenberg, L., Schroder, J.M. and Harder, J. (2006). Pseudomonas aeruginosa- and IL-1beta-mediated induction of human beta-defensin-2 in keratinocytes is controlled by NF-kappaB and AP-1. The Journal of Investigative Dermatology *126*, 121-127.

Weinberg, A., Krisanaprakornkit, S., and Dale, B.A. (1998). Epithelial antimicrobial peptides: review and significance for oral applications. Crit Rev Oral Biol Med *9*, 399-414.

White, S.H., Wimley, W.C., and Selsted, M.E. (1995). Structure, function, and membrane integration of defensins. Curr Opin Struct Biol *5*, 521-527.

Wiesner, J., and Vilcinskas, A. (2010). Antimicrobial peptides: the ancient arm of the human immune system. Virulence *1*, 440-464.

Wilmes, M., Cammue, B.P., Sahl, H.G., and Thevissen, K. (2011). Antibiotic activities of host defense peptides: more to it than lipid bilayer perturbation. Nat Prod Rep *28*, 1350-1358.

Wolfe, K. (2004). Evolutionary genomics: yeasts accelerate beyond BLAST. Current Biology *14*, 392-394.

Wolfe, K. (2000). Robustness--it's not where you think it is. Natural Genetics *25*, 3-4.

Wolfe, K.H., and Shields, D.C. (1997). Molecular evidence for an ancient duplication of the entire yeast genome. Nature *387*, 708-713.

Wu, Z., Hoover, D.M., Yang, D., Boulegue, C., Santamaria, F., Oppenheim, J.J., Lubkowski, J., and Lu, W. (2003). Engineering disulfide bridges to dissect antimicrobial and chemotactic activities of human beta-defensin 3. Proc Natl Acad Sci U S A *100*, 8880-8885.

Xiao, Y., Hughes, A.L., Ando, J., Matsuda, Y., Cheng, J.F., Skinner-Noble, D., and Zhang, G. (2004). A genome-wide screen identifies a single beta-defensin gene cluster in the chicken: implications for the origin and evolution of mammalian defensins. BMC Genomics *5*, 56.

Xie, C., Prahl, A., Ericksen, B., Wu, Z., Zeng, P., Li, X., Lu, W.Y., Lubkowski, J., and Lu, W. (2005). Reconstruction of the conserved beta-bulge in mammalian defensins using D-amino acids. The Journal of Biological Chemistry *280*, 32921-32929.

Yang, D., Biragyn, A., Kwak, L.W., and Oppenheim, J.J. (2002). Mammalian defensins in immunity: more than just microbicidal. Trends Immunol *23*, 291-296.

Yang, D., Chertov, O., Bykovskaia, S.N., Chen, Q., Buffo, M.J., Shogan, J., Anderson, M., Schroder, J.M., Wang, J.M., Howard, O.M., and Oppenheim, J.J. (1999). Beta-defensins: linking innate and adaptive immunity through dendritic and T cell CCR6. Science *286*, 525-528.

Yasui, T. (1996). Recent advance in rapid detection and identification methods for beer spoilage lactic acid bacteria. In 24th Convention of the Institute of Brewing (March/AP section) (Singapore), pp. 228-231.

Yu, H., Braun, P., Yildirim, M.A., Lemmens, I., Venkatesan, K., Sahalie, J., Hirozane-Kishikawa, T., Gebreab, F., Li, N., Simonis, N., *et al.* (2008). High-quality binary protein interaction map of the yeast interactome network. Science *322*, 104-110.

Zasloff, M. (2002). Antimicrobial peptides of multicellular organisms. Nature *415*, 389-395.

Zastrow, C.R., Hollatz, C., de Araujo, P.S. and Stambuk, B.U. (2001). Maltotriose fermentation by Saccharomyces cerevisiae. Journal of Industrial Microbiology and Biotechnology *27*, 34-38.

Zhang, Y., Doherty, T., Li, J., Lu, W., Barinka, C., Lubkowski, J., and Hong, M. (2010). Resonance Assignment and Three-Dimensional Structure Determination of a Human Alpha-Defensin, HNP-1, by Solid-State NMR. J Mol Biol *397*, 408-422.

Zuzuarregui, A., Carrasco, P., Palacios, A., Julien, A., and del Olmo, M. (2005). Analysis of the expression of some stress induced genes in several commercial wine yeast strains at the beginning of vinification. J Appl Microbiol *98*, 299-307.

Zuzuarregui, A., and del Olmo, M.L. (2004). Expression of stress response genes in wine strains with different fermentative behavior. FEMS Yeast Res *4*, 699-710.